DESIGN AND SYNTHESIS OF HETEROLEPTIC AND HETEROMETALLIC METALLO-SUPRAMOLECULAR TERPYRIDINE ARCHITECTURES

A Dissertation

Presented to

The Graduate Faculty of The University of Akron

In Partial Fulfillment

of the Requirements for the Degree

Doctor of Philosophy

Rajarshi Sarkar

December, 2015

DESIGN AND SYNTHESIS OF HETEROLEPTIC AND HETEROMETALLIC METALLO-SUPRAMOLECULAR TERPYRIDINE ARCHITECTURES

Rajarshi Sarkar

Dissertation

Approved:	Accepted:
_____	_____
Advisor Dr. George R. Newkome	Department Chair Dr. Kim Calvo
_____	_____
Committee Member Dr. Wiley J. Youngs	Interim Dean of the College Dr. John Green
_____	_____
Committee Member Dr. Christopher J. Ziegler	Dean of the Graduate School Dr. Chand Midha
_____	_____
Committee Member Dr. David A. Modarelli	Date
_____	
Committee Member Dr. Sadhan C. Jana	

ABSTRACT

Inspiration from biological assemblies in Nature has produced an extraordinary amount of research in supramolecular chemistry. Various non-covalent interactions have been employed to design and synthesize numerous sophisticated architectures with unique structural and functional properties.

Metallo-supramolecular constructs are primarily synthesized in a homoleptic assembly; whereas, a preprogrammed monomer is reacted with a suitable metal ion to produce the desired, highly symmetric architectures. On the other hand, structural variance in the supramolecular materials is instilled mainly by step-wise or dynamic assembly protocols. Owing to the unavailability of suitable building blocks and lack of control over the outcome of the assembly, study of these assembly methods has been limited.

Two novel terpyridine-based bimetallic triangles were synthesized *via* a less explored supramolecular fusion approach. Syntheses of two homometallic cyclic trimer and two metallo-squares were achieved, and they were characterized by NMR and MS techniques. Mixing of triangular and the tetrameric units produced the desired bimetallic triangular complexes in quantitative yield. The multinuclear structures were characterized by ^{1}H, 2D-COSY, 2D-NOESY, ESI- and TWIM-MS data. Tandem MS data provided information on the stability of these triangles. UV-vis and luminiscence data indicated metal-ligand charge transfer.

Three bimetallic triangles were constructed by a step-wise directed assembly method. An oligomeric trimer was synthesized from a 60º-directed *bis*terpyridine ligand and was characterized by NMR and MS techniques. Three heterobimetallic triangular architectures were obtained by reacting the oligomeric trimer with Zn(II), Cd(II), and Fe(II). ^{1}H, 2D-COSY, and 2D-NOESY NMR, ESI- and TWIM-MS data confirmed the proposed structures. Luminescence data showed the emission intensities of the triangles are lower than the linear trimer indicating quenching effect of Zn(II), Cd(II), and Fe(II) centers.

Synthesis of a structural mimic of first-generation Sierpiński triangle was achieved *via* dynamic supramolecular assembly. The two required *bis*- and tetra*kis*-terpyridine ligands were synthesized and characterized. The ligands were reacted with Cd(II) in precise 1:1:3 molar ratio to obtain the desired complex in near quantitative yield. ^{1}H, 2D-COSY, and 2D-NOESY NMR, ESI- TWIM-MS, and collision cross-section data confirmed the presence of a Sierpiński triangle as the sole product of the reaction. TEM provided the visualization of the desired architecture, shape, and size of the observed molecules, which fit perfectly the simulated parameters.

DEDICATION

I would like to dedicate this dissertation to my parents *Manjusree* and *Sagar Sarkar*, my elder brother *Saptarshi Sarkar* and my lovely wife *Dripta*. Without their unconditional love, support, and sacrifice I would not be here.

"*Research is to see what everybody else has seen, and to think what nobody else has thought"* – Albert Szent-Gyorgyi

"*History may forget you, or misinterpret your accomplishments, or what you stood for. The ripples you leave behind may get redirected but the universe will never be able to forget the entropy you add. That's the law. The Second Law of Thermodynamics*." –
Michael Stevens

ACKNOWLEDGMENTS

I would like to express my gratitude to my advisor Prof. George R. Newkome, for all his ideas, advice and guidance. It was a pleasure and honor to work for him. I am also thankful to Dr. Charles N. Moorefield for all his help and advice over the years. Special thanks to all my present and past colleagues for their help and fruitful scientific discussions. I would also like to thank The University of Akron for providing me with all the wonderful facilities.

I greatly appreciate my committee members Prof. Wiley J. Youngs, Prof. Christopher J. Ziegler, Prof. David A. Modarelli, and Prof. Sadhan C. Jana for their valuable input and for spending their precious time reading and revising my dissertation.

TABLE OF CONTENTS

Page

LIST OF TABLES

LIST OF FIGURES

LIST OF SCHEMES

CHAPTER I

RECENT ADVANCEMENT IN HETEROLEPTIC AND HETEROMETALLIC SUPRAMOLECULAR ARCHITECTURES

1.1 Introduction

In 1953, Watson and Crick described the double-helical structure of DNA,[1] formed by hydrogen-bonding between complimentary base-pairs. Since then, a tremendous amount of research has been dedicated to exploring, developing, and understanding biomimetic or bioinspired materials.[2-4] The discovery of "Cryptands," "Crown ethers," and "Spherands" by J.-M. Lehn, C. J. Pedersen, and D. J. Cram, respectively, (Figure 1.1) in 1970s led to the understanding that small, pre-programmed molecules can be made to recognize each other to form supramolecules with different physical and chemical properties compared to their precursor building blocks.[5-7] Lehn defined supramolecular chemistry as "chemistry beyond the molecule," where simple chemical species are held together by various intermolecular non-covalent interactions, such as van der Waals forces, π-π interactions, hydrogen bonding, ionic and coordinative interactions to engineer well-defined intricate architectures.[5] As a consequence, the interdisciplinary supramolecular science has drawn substantial attention from the scientific community and has provided essential principles for the design and synthesis of novel functional materials and

architectures with potential applications in gas storage,[8,9] catalysis,[10] molecular electronics,[11] drug delivery,[12] *etc*.

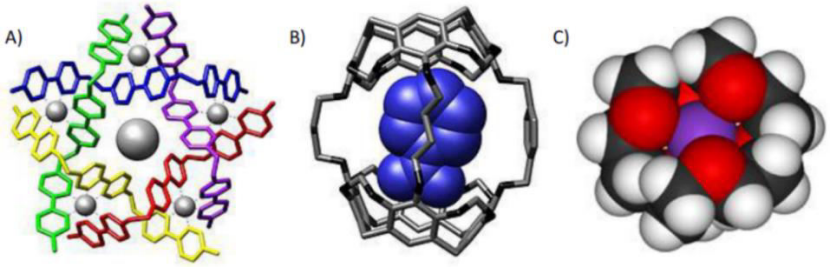

Figure 1.1: Examples of early work in supramolecular Chemistry by a) Lehn, b) Cram, and c) Pederson.

The design and synthesis of supramolecular architectures *via* the assembly of pre-programmed constituents have made considerable progress in the past three decades. Introductory works of Lehn,[7,13-17] followed by contribution from Stang,[18-23] Newkome,[24-29] Fujita,[30-32] Schmittel,[33,34] and many others[35-42] have successfully integrated different weak-interactions into complex supramolecular architectures. Among all the available weak-interactions, coordination-driven assembly has emerged as the most successful and versatile method due to the synthetic ease to instill premeditated construction algorithms in the ligand systems and availability of large number of metal ions.[43,44] Thus, extensive research in metallosupramolecular assembly has produced a large assortment of riveting two- and three-dimensional structures.[45,46]

Most of the metallosupramolecular architectures are constructed by using a highly symmetric building block in a homoleptic assembly.[46] Although these highly symmetric supramolecular constructs are aesthetically pleasing, they often lack structural and functional diversity. In contrast, the potential of heteroleptic assembly, where two or more ligands are assembled to form a single, discrete moiety, has not been explored extensively

due to their inherent tendency to form self-organized product.[16,47] Hence, the introduction of higher structural complexity into the supramolecular structures accompanies the challenge to produce a single molecule in a multi-component reaction. To address this issue supramolecular materials with two or more different ligands (heteroleptic) or metal ions (heterometallic) are constructed either *via* directed step-wise assembly[20] or dynamic assembly methods.[48] In this review, the methods used to prepare both heteroleptic and heterometallic metallomacrocycles will be discussed in detail.

1.2 Directed Step-wise Assembly Approach

The directed step-wise approach is a high-yielding method, which produces a plethora of 2D and 3D supramolecular architectures.[49,18] Since the seminal works of Stang[50] and Fujita,[51] numerous metallomacrocycles and metallocages have been synthesized by using the directed assembly design protocol. The basic design strategy to assemble different metallomacrocycles by this approach is to use complementary ligand systems with precise bite-angles in an appropriate stoichiometric ratio. This logical approach allows structural dissection of any geometrical architectures and provides the required building-blocks to assemble them. For this review, we will only focus on those constructs, which are either heteroleptic or heterometallic in nature.

1.2.1 Two-Dimensional Constructs

Following the reports of the design and syntheses of metallosupramolecular squares by Fujita[51] and Stang,[50] a large number of 2D metallomacrocycles with different

geometrics has been reported. The design protocol used to synthesize these 2D architectures is summarized in Figure 1.2, as described by Stang[20] *et al*.

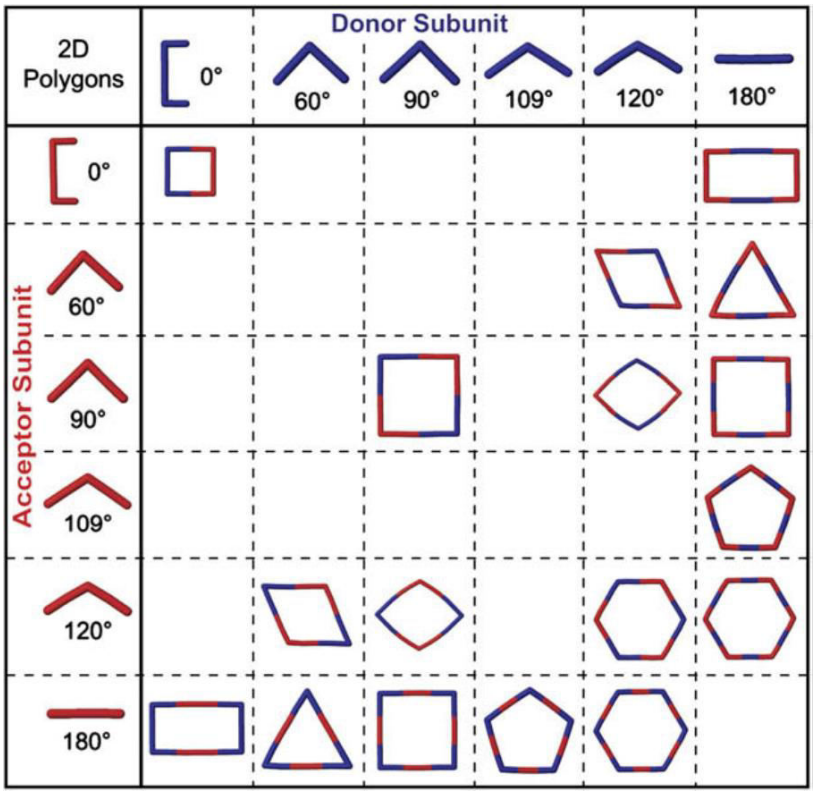

Figure 1.2: Assembly of different building-blocks to generate various 2D architectures.[20] Reprinted with permission from *Tetrahedron*, **2008**, *50*, 11495. Copyright (2008) Elsevier.

1.2.1.1 Molecular Triangles

Numerous coordination-driven metallotriangles have been synthesized and reviewed.[52] As illustrated in Figure 1.3 by Stang and co-workers,[20] metallomacrocyclic trimers can be synthesized by the assembly of building-blocks with a 60º bite angle or by the combination of an angular 60º ligand with a 180º linear motif. Most of the reported triangular structures are homometallic or homoleptic in nature; however, there are several examples of heterometallic and heteroleptic constructs in the literature.

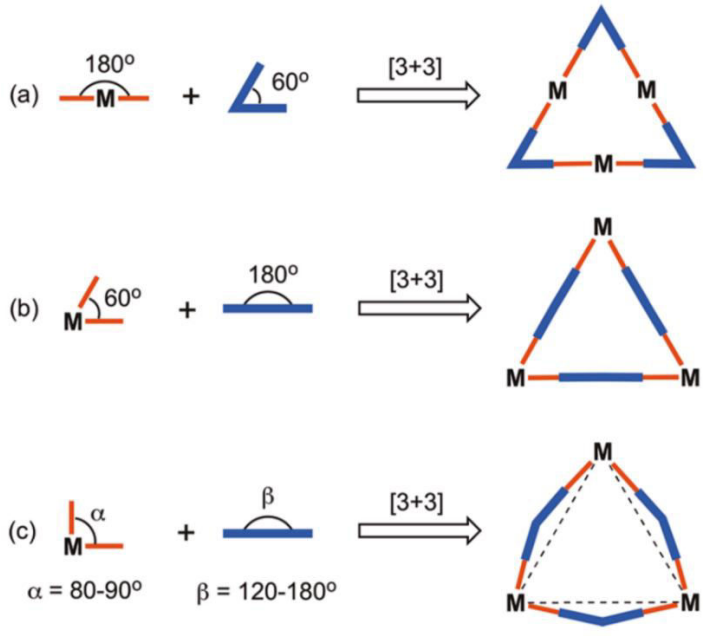

Figure 1.3: General design protocol to construct molecular triangles.[20] Reprinted with permission from *Chem. Rev.*, **2011**, *111*, 6810. Copyright (2011) American Chemical Society.

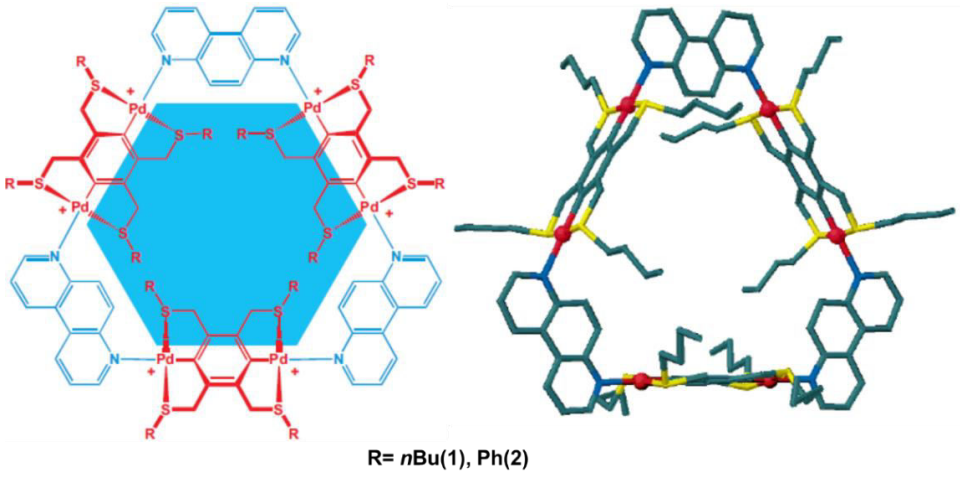

Figure 1.4: Chemical and crystal structures of 4,7-phenanthroline-based trinuclear complexes **1** and **2**. Reprinted with permission from *Angew. Chem. Int. Ed.*, **1998**, *37*, 121. Copyright (1998) WILEY-VCH.

Loeb and co-workers have reported the assembly of two rigid heteroleptic [3+3] triangular moieties **1** and **2** (Figure 1.4) by combining a rigid 60º 4,7-phenanthroline ligand with two linear organopalladium complexes.[53] Both of these triangular cyclic arrays were

obtained in near quantitative yield and were characterized by ^{1}H NMR spectroscopy, where the phenanthroline protons showed significant downfield shift upon coordination. Macrocycle **2** was also characterized by X-ray crystallography. The width of triangle **2** is around 2 nm and the diameter of the cavity was found to be about 1.2 nm.

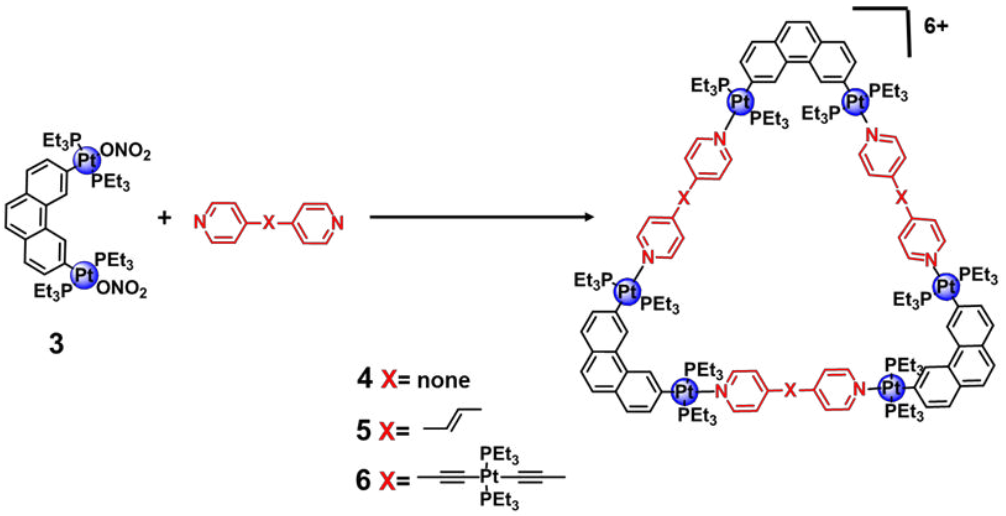

Scheme 1.1: Synthesis of phenanthrene and *bis*pyridyl-based heteroleptic triangles **4**, **5** and **6**. Reproduced with permission from *J. Am. Chem. Soc.*, **2003**,*125*, 5193. Copyright (2003) American Chemical Society.

Step-wise constructions of various multi-component triangular architectures by assembling ditopic phenanthrene-Pt complex with different bipyridine derivatives (Scheme 1.1), such as 4,4'-bipyridine, *trans*-1,2-*bis*(4-pyridyl)ethylene, *trans*-[*bis*(4-pyridylethynyl)*bis*(triphenylphosphine)]platinum(II) were reported by Stang *et al*.[54] Linear tectons allowed the formation of strain-free hexacationic triangles. The ^{31}P NMR data of **4**, **5**, and **6** showed a sharp singlet along with ^{195}Pt satellite, indicating the presence of a single, discrete structure. The crystal structure of complex **4** showed a partially distorted triangular structure, in which each is *ca*. 2.7 nm in length and the cavity size is *ca*. 1.4 nm. The same research group also assembled carborane-based heteronuclear metallotrimer by

employing similar synthetic techniques. Phenanthrene-Pt complex **3** was reacted with linear carborane unit to obtain hexametallic construct **7** in high yield (Figure 1.5).[55]

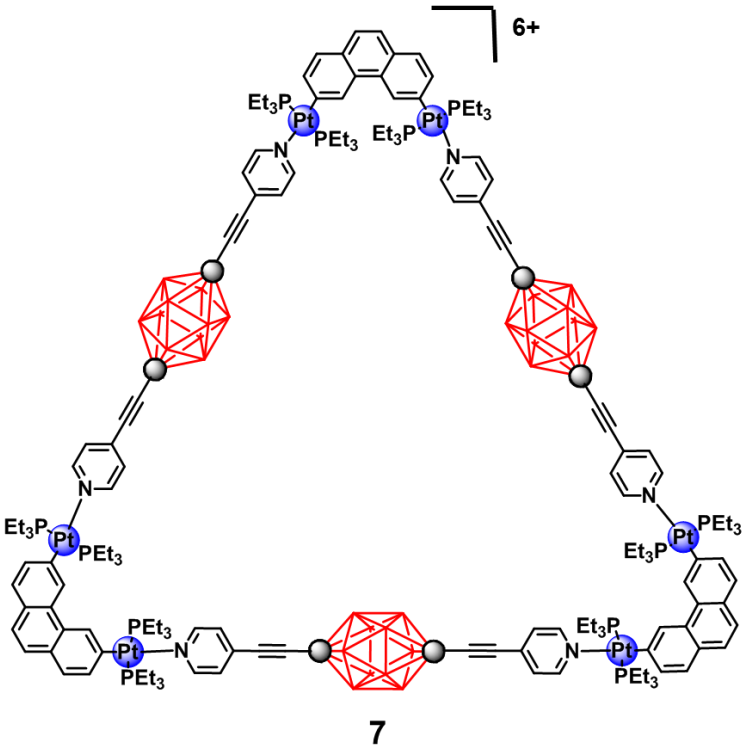

Figure 1.5: Phenanthrene and carborane-based triangle **7**. Reproduced with permission from *J. Am. Chem. Soc.*, **2005**, *127*, 12131. Copyright (2005) American Chemical Society.

Newkome and co-workers reported a step-wise preparation of the terpyridine-based heteronuclear triangle involving two Ru(II) centers and one Fe(II) center. First a *bis*Ru(III)-adduct of a terpyridine-based 60º-ligand was reacted with two additional equivalent of initial monomer to obtain oligomeric trimer **8**, which was subsequently cyclized with Fe(II) to generate the heterometallic triangle **9**.[56] Presence of two types of metal-terpyridine coordination in the metallocycle was confirmed by ^{1}H NMR and ESI-MS data.

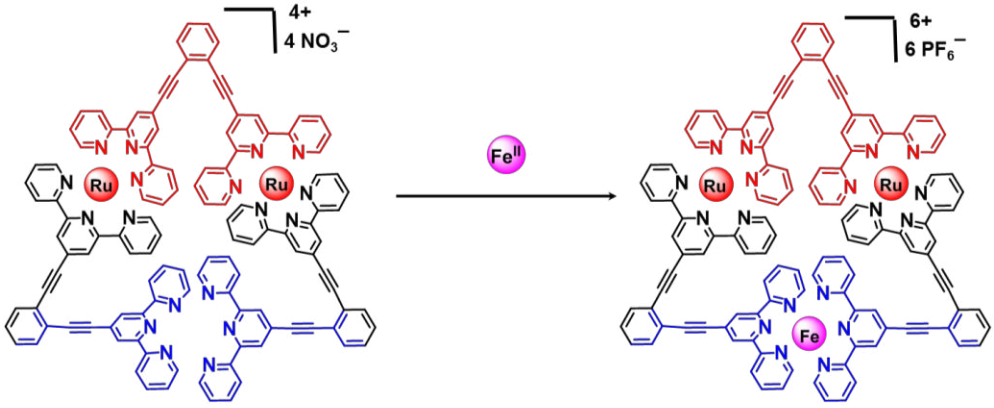

Scheme 1.2: Synthesis of terpyridine-based heterometallic triangle **9**. Reproduced with permission from *Chem. Commun.*, **2005**, 713. Copyright (2005) Royal Society of Chemistry.

Puddephatt *et al*. have investigated the assembly of *cis*-blocked square planar palladium(II) ($[Pd(bu_2bpy)\text{-}(THF)_2][BF_4]_2$) or platinum(II) ($[Pt(bu_2bpy)(O_3SCF_3)_2]$) ($bu_2bpy$ = 4,4'-di*tert*-butyl-2,2'-bipyridine) units with various linear bridging amidopyridine ligands such as *N*-(pyridin-4-yl)isonicotinamide, *N*,*N*′-*bis*(pyridin-3-yl)pyridine-2,6-dicarboxamide, *N*,*N*′-*bis*(pyridin-4-yl)pyridine-2,6-dicarboxamide, *N*,*N*′-*bis*(pyridin-3-yl)benzene-1,3-dicarboxamide, and *N*,*N*′-*bis*(pyridin-4-yl)benzene-1,3-dicarboxamide.[57,58] However, only the ligand *N*-(pyridin-4-yl)isonicotinamide produced a metallotriangle with both the Pd(II) and Pt(II) precursors. The Pt(II)-macrocycle was characterized by X-ray crystallography, which revealed that the triangle has a C_5 symmetry.

Stang and co-workers used a similar protocol to synthesize the phenanthrene-based charge neutral heteroleptic trinuclear complexes using different dicarboxylate anions (Scheme 1.3) in near quantitative yield.[59] The triangles were characterized by ^{31}P, ^{1}H NMR, IR, and ESI-MS data. Both ^{31}P and ^{1}H spectra indicated the presence of a highly symmetric

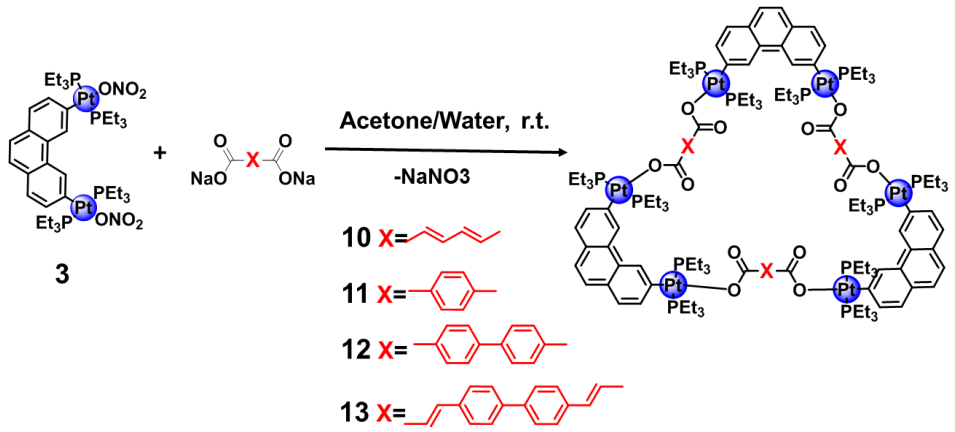

Scheme 1.3: Synthesis of phenanthrene and carboxylate-based triangles **10**-**13**. Reproduced with permission from *J. Am. Chem. Soc.*, **2004**, *126*, 2464. Copyright (2004) American Chemical Society.

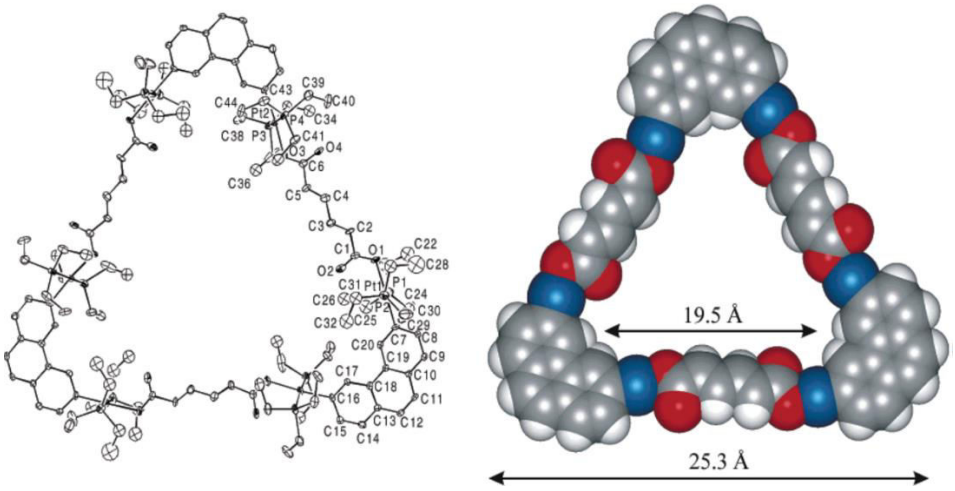

Figure 1.6: Crystal structure and CPK model of phenanthrene and carboxylate-based triangle **10**. Reprinted with permission from *J. Am. Chem. Soc.*, **2004**, *126*, 2464. Copyright (2004) American Chemical Society.

structure with a significant spectroscopic difference compared to the building blocks. The IR frequency corresponding to the carboxylate group showed a shift to higher wave number upon complexation as expected. Macrocycles **10** and **11** were characterized by X-ray crystallography; the sides and cavity diameter of the **10** (Figure 1.6) were 2.53 nm and 1.95 nm, respectively.

1.2.1.2 Molecular Squares

Metallosquares are discrete cyclic assemblies formed by the combination of a 90º corner unit with a linear bridging moiety. Numerous supramolecular squares have been synthesized *via* a directed assembly method.[60] As proposed by Stang *et al*., there are two primary ways to synthesize metallomacrocyclic squares: a) by combining a 90º-corner unit containing metal ions and a linear 180º-ligand, b) by using a linear building block containing metal ion and a ligand with a bite-angle of 90º (Figure 1.7[20]). Because of the constraints inflicted by the binding ligands, the molecular squares are known to exhibit significant conformational rigidity.

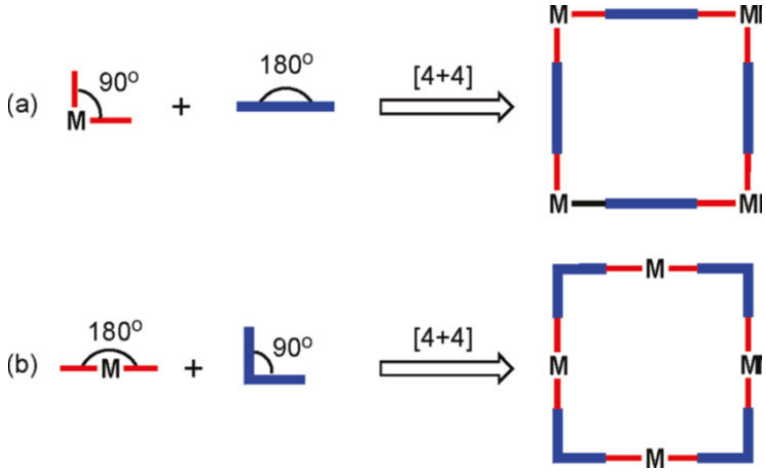

Figure 1.7: General design protocol to construct molecular squares.[20] Reprinted with permission from *Chem. Rev.*, **2011**, *111*, 6810. Copyright (2011) American Chemical Society.

Transition metal ions with a square-planar, trigonal-bipyramidal or octahedral geometry can be used as a corner unit to synthesize molecular squares; however, metal ions possessing square-planar geometry are extensively utilized. The *cis*-protected 90º metal corners are derived very easily by coordinating two adjacent sites of a square-planar metal ion by strong chelating ligands and leaving the other two sites for further complexation.

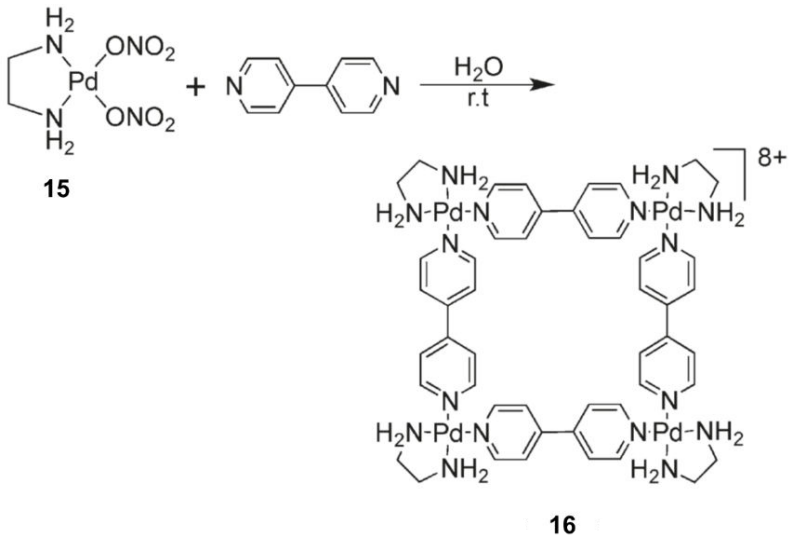

Scheme 1.4: Synthesis of metallo-square **16**. Reprinted with permission from *J. Am. Chem. Soc.*, **1990**, *112*, 5645. Copyright (1990) American Chemical Society.

Fujita and co-workers have reported the first supramolecular square **16**, by reacting a 90º *cis*-protected Pd(II) precursor, **15**, with bidentate bridging ligand 4,4'-bipyridine, in near quantitative yield (91%) (Scheme 1.4).[51] The proposed structure was characterized by elemental analysis and multinuclear NMR spectroscopy. ^{1}H NMR data showed two clean doublets, which eliminates the presence of any oligomers and confirms the presence of a single, discrete component. But interestingly, the Pt(II) analogue of metallosquare **16** was obtained only after heating a *cis*-protected Platinum(II) motif with 4,4'-bipyridine at 100 ºC for 4 weeks.[61] This can be attributed to the kinetic inertness of the Pt-N bond compared to the Pd-N bond, and as a result, Pt(II)-square is considerably more stable than the corresponding Pd(II) macrocycle. A noteworthy feature of the metallosquare **16** is its ability to incorporate 1,3,5-trimethoxybenzene in aqueous media. The host-guest complex was confirmed by the ^{1}H NMR studies, where the aromatic protons of 1,3,5-trimethoxybenzene exhibited an expected upfield shift upon complexation.

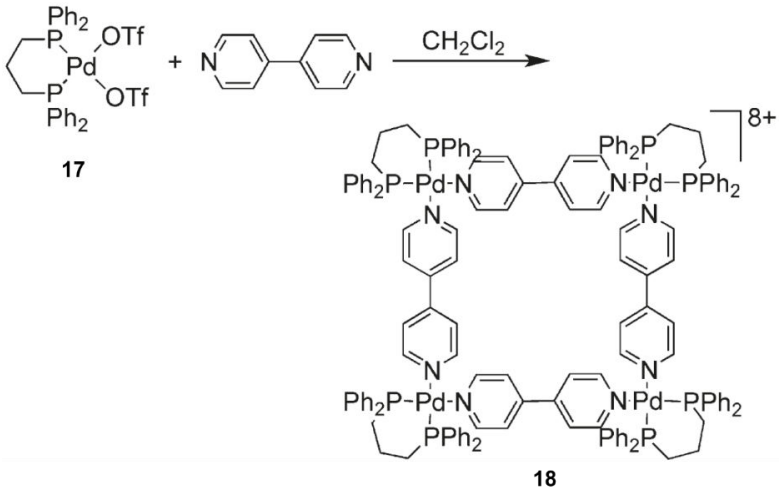

Scheme 1.5: Synthesis of metallo-square **18**. Reprinted with permission from *J. Am. Chem. Soc.*, **1994**, *116*, 4981. Copyright (1994) American Chemical Society.

Stang *et al.* have utilized diphosphine *cis*-blocked for Pd(II) and Pt(II) complexes extensively to synthesize a large variety of molecular squares.[62,63] They reaction of 90º *cis*-[Pd(dppp) $(OTf)_2$] (dppp = 1,3-*bis*(diphenylphosphino)propane) (**17**) and bridging unit 4,4'-bipyridine in CH_2Cl_2 (Scheme 1.5) yielded the phosphino analogue of Fujita's square (**18**) in near quantitative yield.[50]

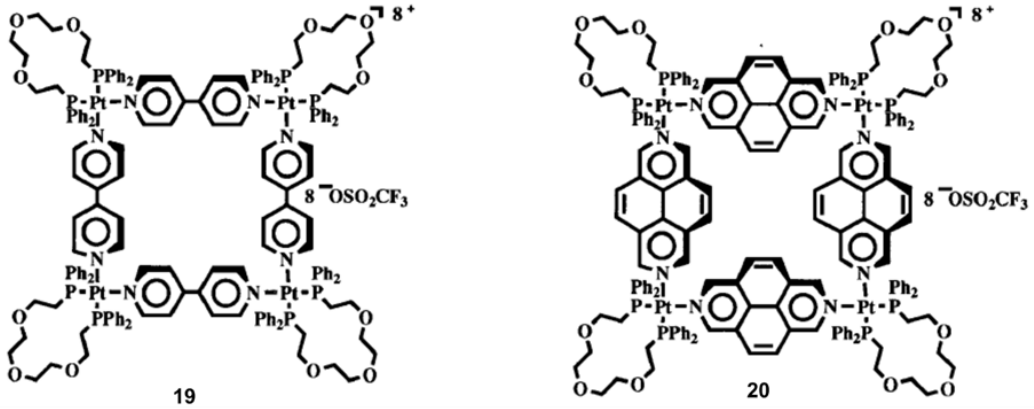

Figure 1.8: Crown-ether based molecular square **19** and **20**. Reprinted with permission from *J. Am. Chem. Soc.*, **1997**, *119*, 5163. Copyright (1997) American Chemical Society.

Various other metallo-squares were prepared *via* similar synthetic strategies by using 4,4'-dicyano-1,1'-biphenyl, 1,4-dicyanobenzene, diazapyrene, and diazaperylene as linear building blocks, in combination with both chelated and non-chelated biphosphines, as the 90º corner unit.[64,65] This method was also extended to prepare a series of molecular squares containing crown ethers (Figure 1.8, **19** and **20**) or calixarenes (Figure 1.9, **21** and **22**) as the corner motif[66] or squares with porphyrins, as the linear linkages.[67] Metallo-squares **19-22** were characterized by ^{31}P, ^{1}H NMR spectroscopy, ESI-FTICR spectrometry, and elemental analysis. All metallo-squares showed an affinity to incorporate a high number of water molecules in the solid state, which was confirmed by ESI-FTICR data. Complex **19** and **20** held onto water molecules even after being heated at 100 ºC or even after treatment in high vacuum for a week. It was postulated that the water molecules were simultaneously bonded with cationic Pt(II) *via* the lone pair electrons on oxygen atom and hydrogen bonded with the crown ether moiety.

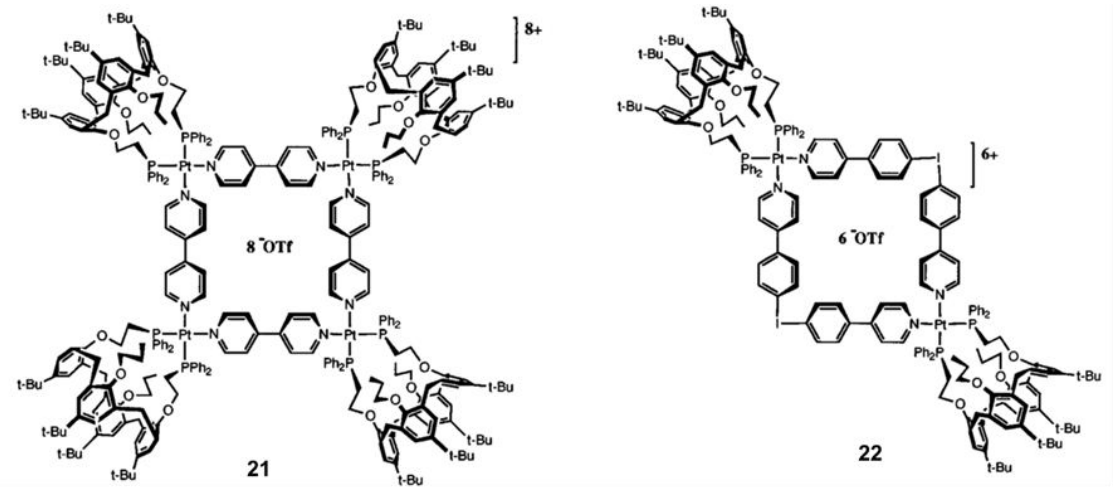

Figure 1.9: Calixarene-based molecular square **21** and **22**. Reprinted with permission from *J. Am. Chem. Soc.*, **1997**, *119*, 5163. Copyright (1997) American Chemical Society.

Lees *et al.* have synthesized a series of terpyridine-based octanuclear heterometallic squares *fac*-$Re(CO)_3Br[\mu$-$(pytpy)_2M](PF_6)_8$, (Scheme 1.6, **23-25**) (where M = Fe(II), Ru(II) and Os(II), and $[(dppf)Pd[\mu$-$(pytpy)_2Ru]]_4(PF_6)_8(OTf)_8$ (Scheme 1.7, **29**) (pytpy is 4'-(4'''-pyridyl)-[2,2':6',2'']-terpyridine, and dppf is 1,1'-*bis*(diphenyl-phosphino)ferrocene).[68] $Re(CO)_5Br$ was reacted with $(pyterpy)_2M(PF_6)_2$ to obtain the metallosquares **23-25**. On the other hand, the reaction of $Re(CO)_5Br$ with $(dppf)Pd(H_2O)_2(OTf)_2$ produced square **29** (Scheme 1.7). All of the metallocycles were characterized by NMR, IR, ESI-MS, and elemental analysis. Photoluminescence data revealed that the photophysical property of square **23-25**, and **29** are dominated by the bridging metal-complex moiety, while the corner units contribute minimally towards the overall absorption or emission.

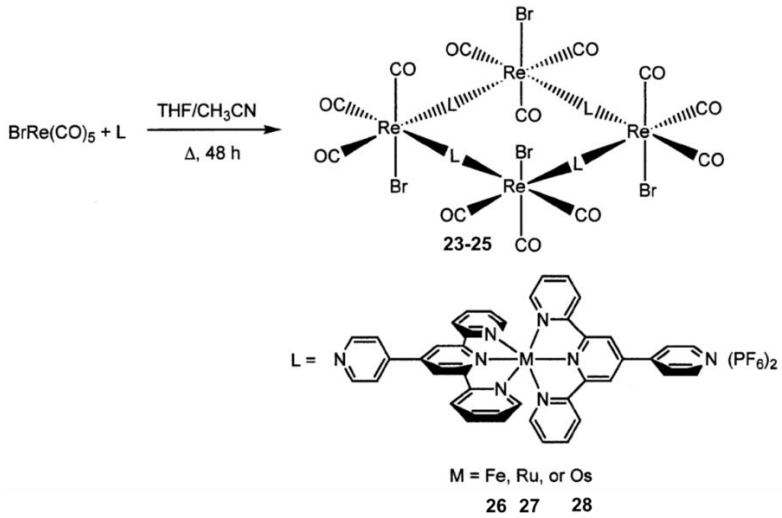

Scheme 1.6: Synthesis of heterometallic squares **23**-**25**. Reprinted with permission from *Inorg. Chem.*, **2001**, *40*, 3154. Copyright (2001) American Chemical Society.

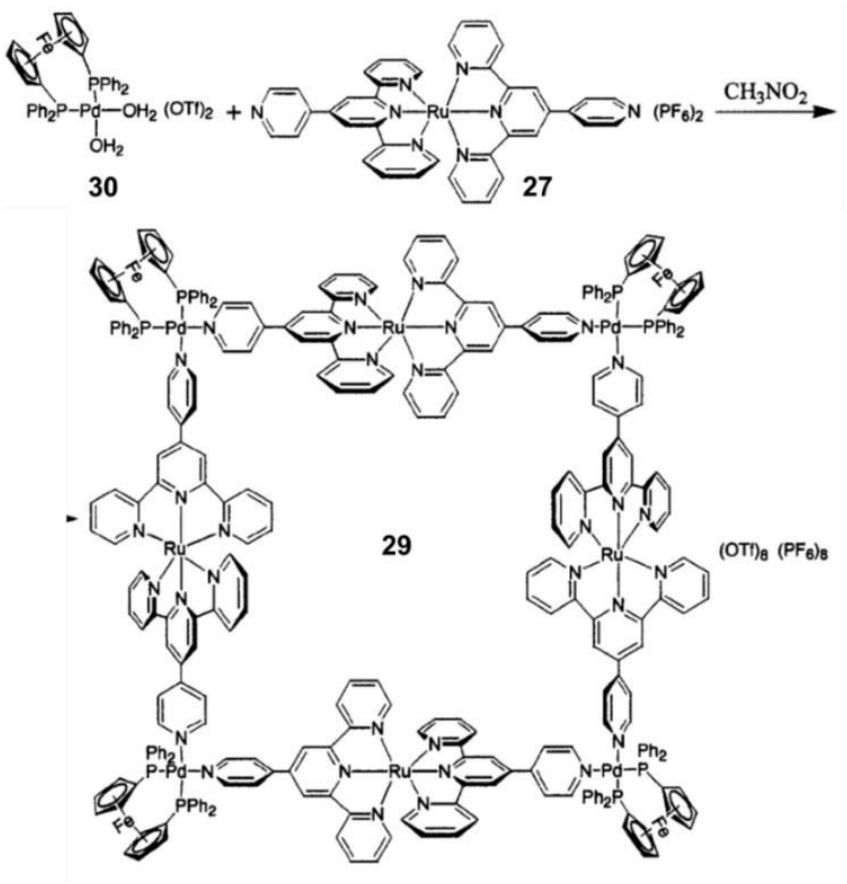

Scheme 1.7: Synthesis of heterometallic square **29**. Reprinted with permission from *Inorg. Chem.*, **2001**, *40*, 3154. Copyright (2001) American Chemical Society.

Newkome and co-workers have reported terpyridine-based binuclear "Dondorff rings".[69] The 60º-directed *bis*terpyridine ligand was dimerized with Ru(II) and was allowed to further cyclize with other transition metal ions, such as: Zn(II), Cd(II), and Fe(II), to obtain heterometallic squares **31-34** (Figure 1.10) in high yield. The metallo-squares were characterized by ^{1}H NMR and ESI- and TWIM-MS data. ^{1}H NMR data confirmed the presence of two different metal-terpyridine bonds, while ESI and TWIM-MS data substantiated the metallo-squares as the only product. Molecular simulation revealed the complexes possess a cavity of size *ca*. 9 Å.

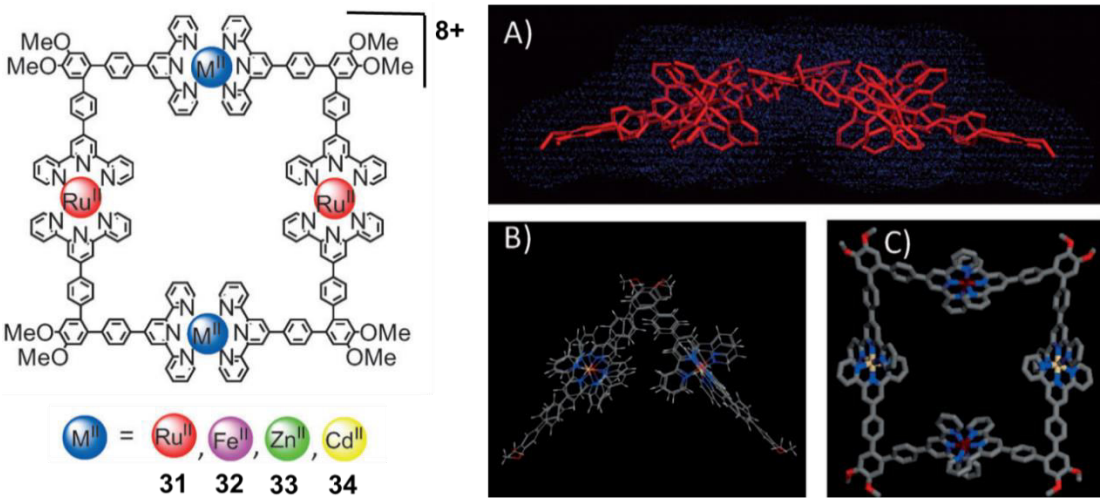

Figure 1.10: Terpyridine-based binuclear molecular square **31-34** and the computer simulation of square **34**: A) side view, B) lowest energy conformer, and C) stick model of the flattened higher energy conformer. Reprinted with permission from *Chem. Eur. J.*, **2012**, *18*, 11569. Copyright (2012) WILEY-VCH.

A series of [2+2] molecular squares was assembled by Mukherjee *et al.* by utilizing a Pt-based shape-selective linker 3,6-*bis*[*trans*-platinum (triethylphosphine)$_2$-(nitrate)(ethynyl)]carbazole and different flexible ditopic pyridyl derivatives namely, 1,3-*bis*(4-pyridyl)isophthalamide, 1,3-*bis*(3-pyridyl)-isophthalamide, and 1,2-*bis*(4-pyridyl)ethane.[70] The macrocycles were characterized by ^{1}H, ^{31}P NMR and ESI-MS data. The heteroleptic square (**35a**, Figure 1.11) prepared from 3,6-*bis*[*trans*-platinum (triethylphosphine)$_2$(nitrate)(ethynyl)]carbazole and 3-*bis*(4-pyridyl)-isophthalamide was also characterized its X-ray structure. Luminescence studies revealed that square **35a**, can selectively sense pyrophosphate ($P_2O_7^{4-}$) anions.

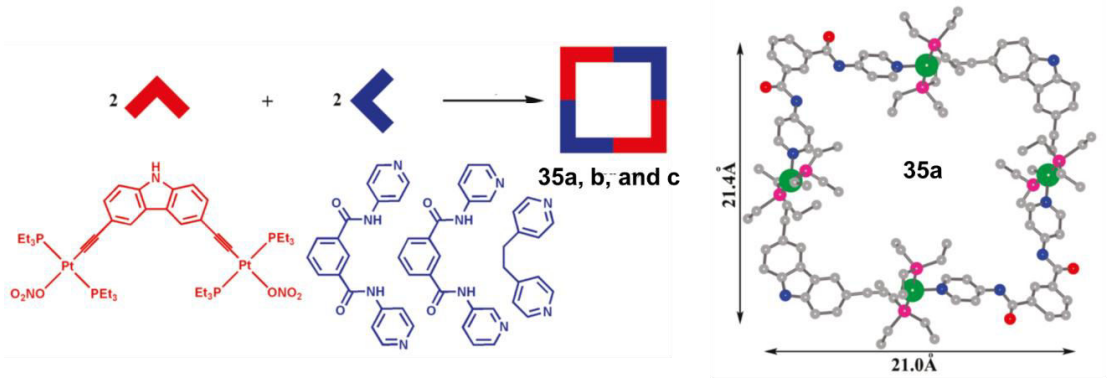

Figure 1.11: Assembly of metallo-square **35a**, **b** and **c** and the crystal structure of **35a**. (Green = Pt, Magenta = P, Blue = N, Black = C, Red = O). Reprinted with permission from *Organometallics*, **2010**, *29*, 2971. Copyright (2010) American Chemical Society.

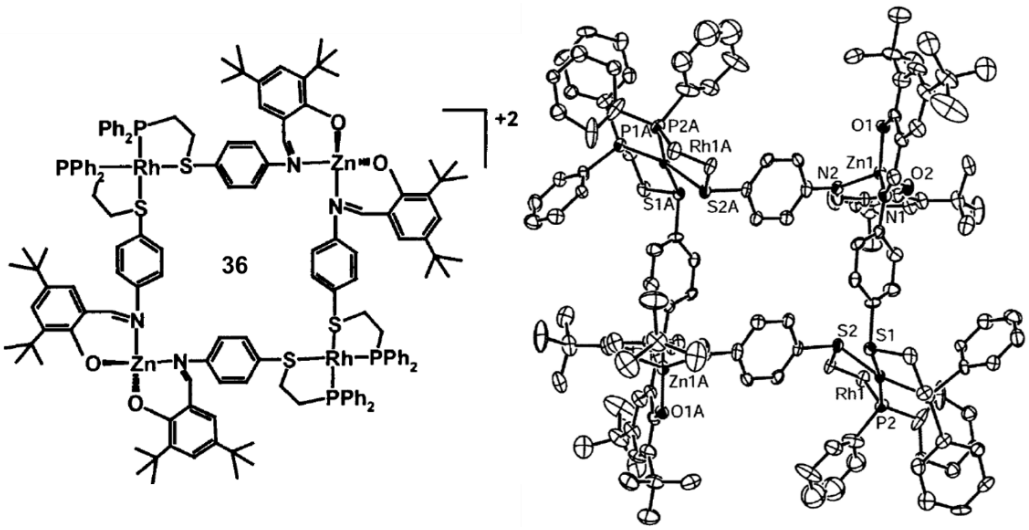

Figure 1.12: Structure and the crystal structure of heterometallic square **36**. Reprinted with permission from *Inorg. Chem.*, **2002**, *41*, 5326. Copyright (2002) American Chemical Society.

Mirkin and co-workers have synthesized a heterobimetallic square **36** by the reaction of mutually cooperating metal centers Rh(I) and Zn(II) with a ligand containing salicylaldiminato and thioether-phosphine moieties (Figure 1.12).[71] The crystal structure of **36** shows a slightly distorted square with two square planar Rh(I) centers and two distorted tetrahedral Zn(II) centers, bound by four ligands.

Severin *et al.* reported the construction of a neutral metallosquare by reacting a chloro-bridged Pd-based acceptor unit $[(PEt_3)PdCl_2]_2$ with 2,3-dihydroxypyridine in MeOH using Cs_2CO_3, as base.[72] The molecular square was characterized by X-ray crystallography and the average cavity diameter was found to be *ca*. 0.69 Å.

1.2.1.3 Triangle-Square Equilibrium

The composition of a multi-component assembly is often governed by "*self-correction*," which produces the most thermodynamically stable product over the other possible combinations. However, a single discrete product is produced in a thermodynamic control reaction only when there is a significant energy advantage of one combination over the other structural possibilities. There are several examples of metallomacrocyclic assemblies where two species co-exist in solution due to an absence of a clear thermodynamic preference of one over the other.

According to the design hypothesis, the self-assembly of a 90º corner with a linear 180º fragment should result in a molecular square; however, it often results in an equilibrium mixture of molecular square and triangle. This phenomenon was first observed by Fujita and co-workers in 1996,[73] when they reported the self-assembly of $[Pd(en)(ONO_2)_2]$ with the rigid-linker, 4,4'-bipyridine, exclusively produced the molecular square. But, the assemblies involving longer and more flexible linear fragment such as, py-X-py (X = CH=CH-, -C≡C-, -C≡C-C≡C-) produce equilibrium mixtures of both molecular squares and triangles (Scheme 1.8).

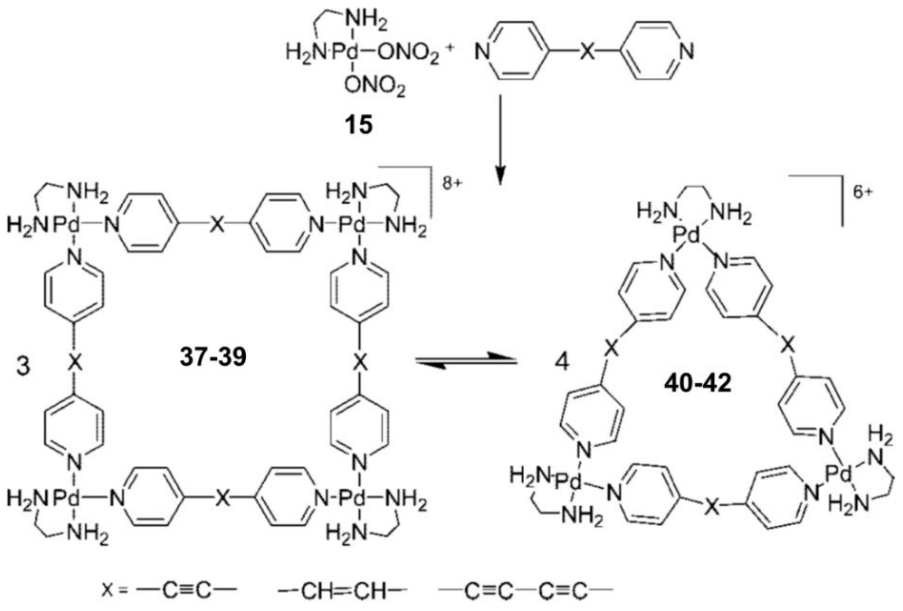

Scheme 1.8: An equilibrium between metallo-squares (**37-39**) and metallo-triangles (**40-42**). Reprinted with permission from *Chem. Commun.*, **1996**, 1535. Copyright (1996) Royal Society of Chemistry.

The equilibrium between a metallosquare and a metallotriangle can be explained by the thermodynamic parameters enthalpy and entropy. Formation of a molecular square is favored by enthalpy due to a smaller conformational strain compared to that of the related triangle. On a contrary, a molecular triangle is favored by entropy; since they are assembled from a smaller number of components, their formation results in more species in solution.

Hence, the relative concentration of square and triangle is regulated by a very delicate balance of entropy and enthalpy. The equilibrium between triangle and square is depicted in Scheme 1.8. Thus, according to Le Chatelier's principle an increase in concentration would favor the formation of square and an increase in temperature would lead the equilibrium towards the triangle.

Hong *et al.* have also described a triangle/square equilibrium from the assembly of [Pd(en)(ONO_2)$_2$ and a sigmoidal linker 1,2-*bis*(4-pyridyl)ethylene (**56**, BPE).[74] They found

that the equilibrium besides being concentration-dependent was also influenced by the hydrophobic interactions with guest in aqueous solution. Hence, the molecular triangle was the prevalent product either under low concentration or in presence of a guest, *e.g.*, *p*-dimethoxybenzene, which binds better to the triangular cavity than to the square cavity.

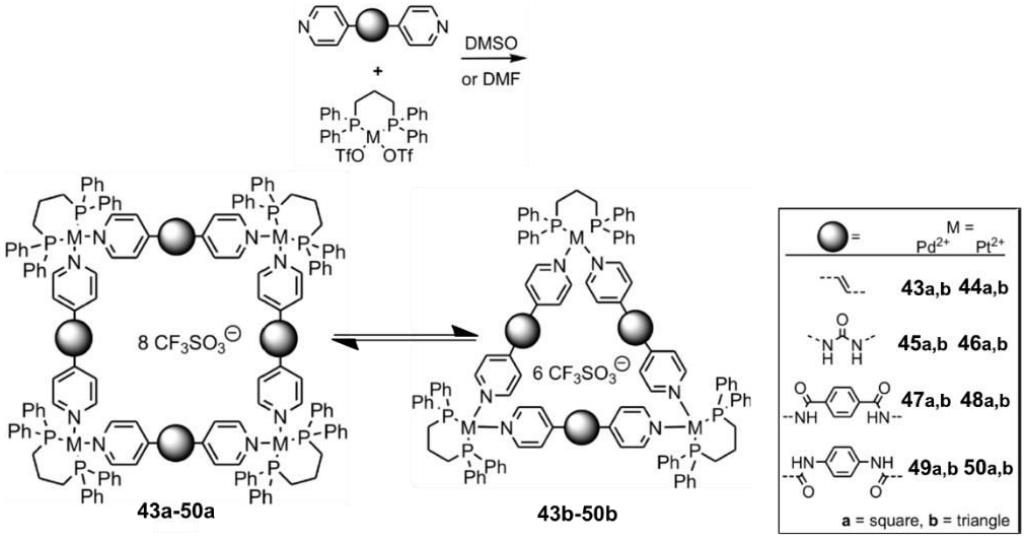

Scheme 1.9: Assembly of interconverting metallo-squares and metallo-triangles with flexible *bis*pyridyl linear linkage. Reprinted with permission from *Inorg. Chem.*, **2008**, *47*, 7588. Copyright (2008) American Chemical Society.

Schalley *et al.* have employed a series of extended and flexible *bis*pyridyl linear linkage with *cis*-blocked [M(dppp)$(OTf)_2$] (M = Pd^{II}, Pt^{II}), as the corner motifs, to demonstrate the triangle-square equilibrium in solution.[75] Scheme 1.9 shows the equilibrium for Pd(II) squares (**43a-50a**) with triangles (**43b-50b**), respectively, in the reaction of [Pd(dppp)$(OTf)_2$] and various bipyridine derivatives. Concentration, temperature, and solvent type significantly influence the equilibrium. The variable temperature NMR data indicated that the square-triangle equilibrium is significantly faster at higher temperature, as expected. Their study also revealed that the ligand exchange process is considerably slower with Pt(II) complexes compared to their Pd(II) analogue,

due to greater kinetic stability of Pt(II) ion. It was also observed that the increasing amount of nonpolar solvents promote the exchange process, which in turn shifts the equilibrium to favor the triangles.

Würthner and co-workers also reported an equilibrium between molecular triangles **51** and squares **52** by assembling *cis*-protected square-planar protectors [M(dppp)$(OTf)_2$] (M = Pd^{II}, Pt^{II}) with the phenoxy-substituted diazadibenzoperylene bridging unit (Scheme 1.10).[76] Characterization of the equilibria was accomplished by ^1H and $^{31}P[^1H]$ NMR spectroscopy. Also, concentration dependent UV-Vis and fluorescence spectroscopy revealed the dynamic nature of these assemblies.

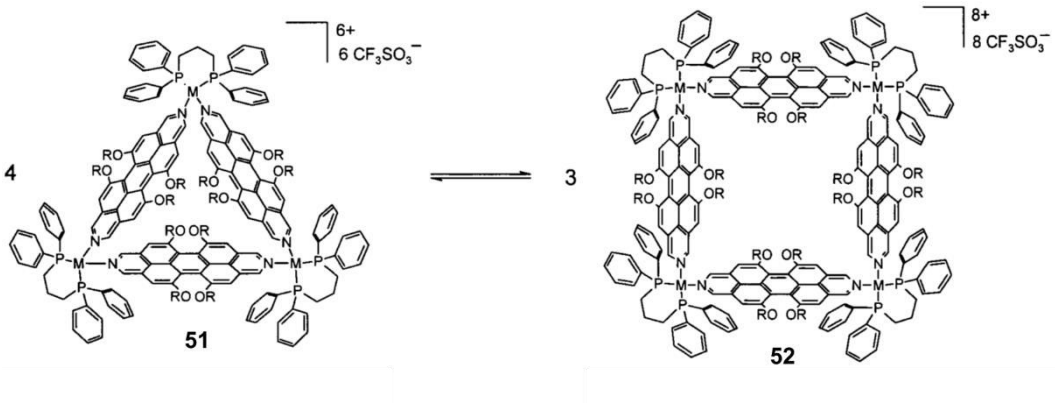

Scheme 1.10: Equilibrium between perylene-based metallo-squares **52** and metallo-triangles **51**. Reprinted with permission from *J. Am. Chem. Soc.*, **2001**, *123*, 5424. Copyright (2001) American Chemical Society.

Unfortunately, isolation of both assemblies in a triangle-square equilibrium still remains challenging. In 2002, Stang and co-workers investigated the equilibrium mixture of triangular and square metallomacrocycles assembled by a 90º acceptor [*cis*-$Pt(PMe_3)_2(OTf)_2$] (**55**) and a flexible ditopic donor *trans*-*bis*(4-pyridyl)ethylene (BPE, **56**) (Scheme 1.11).[77] Both the assemblies were characterized by multinuclear NMR spectroscopy in solution. They were also successful to selectively crystallize and

characterize both cationic constructs by the judicious choice of counter ions. The molecular square **53**, [*cis*-Pt(PMe_3)$_4$(μ-BPE)$_4$] (OTf)$_8$) was crystallized, as a triflate salt, while the triangular complex **54**, ([*cis*-Pt(PMe_3)$_3$(μ-BPE)$_3$] (OTf)$_4$($CoB_{18}C_4H_{22}$)$_2$) was crystallized as a mixed triflate/cobalticarborane ($CoB_{18}C_4H_{22}^-$) salt (Figure 1.13). Their work also concluded that the most prevalent species in the solution and solid state are not always consistent.

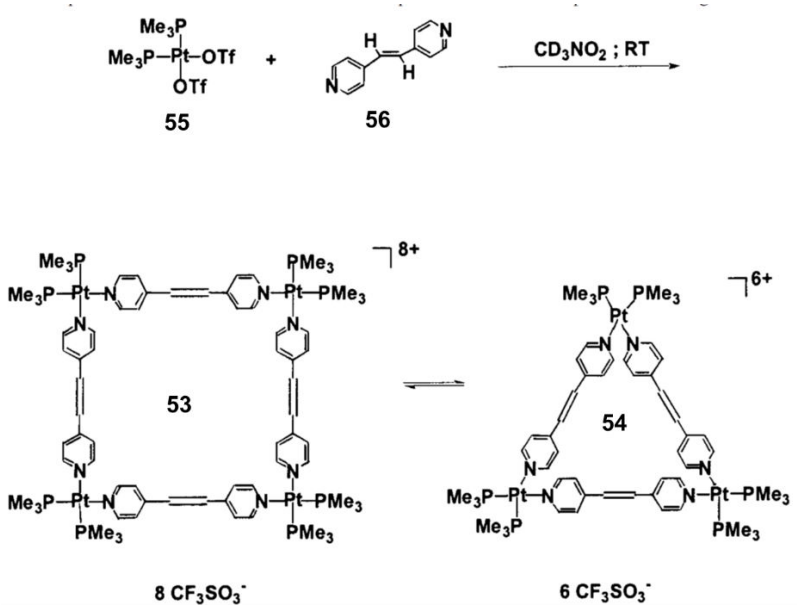

Scheme 1.11: Equilibrium mixture of square **53** and triangle **54**. Reprinted with permission from *Inorg. Chem.*, **2002**, *41*, 2556. Copyright (2002) American Chemical Society.

Mizuno and co-workers also studied a similar equilibrium mixture of triangle [Pd(tmeda)(4,4'-bpy)$_3$] (NO_3)$_6$ and square [Pd(tmeda)(4,4'-bipy)$_4$] (NO_3)$_8$ and successfully crystallized both components from different solvents (tmeda = *N*,*N*,*N*′,*N*′-tetramethylethylenediamine).[78] The X-ray structural determination revealed that in the triangular complex **53**, N_{py}-Pd-N_{py} angles (82.4º-86.0º) are only slightly smaller than the square **54** (86.8º-87.3º). The torsion angle between the pyridyl rings are considerably larger

in the metallosquare (21.89º-32.02º) than in the triangle (16.36º-20.89º). It was found that the macrocycle $[Pd(tmeda)(4,4'\text{-bpy})_4](NO_3)_8$, can selectively encapsulate polyoxometalate (POM) $[W_6O_{19}]^{2-}$ and $[W_{10}O_{32}]^{4-}$ over Keggin POM $[\alpha\text{-}SiW_{12}O_{40}]^{4-}$.

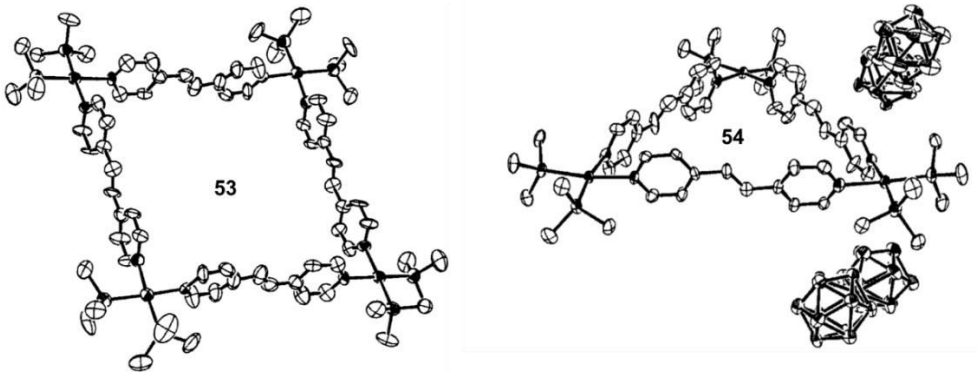

Figure 1.13: Crystal structure of **53** and **54**. Reprinted with permission from *Inorg. Chem.*, **2002**, *41*, 2556. Copyright (2002) American Chemical Society.

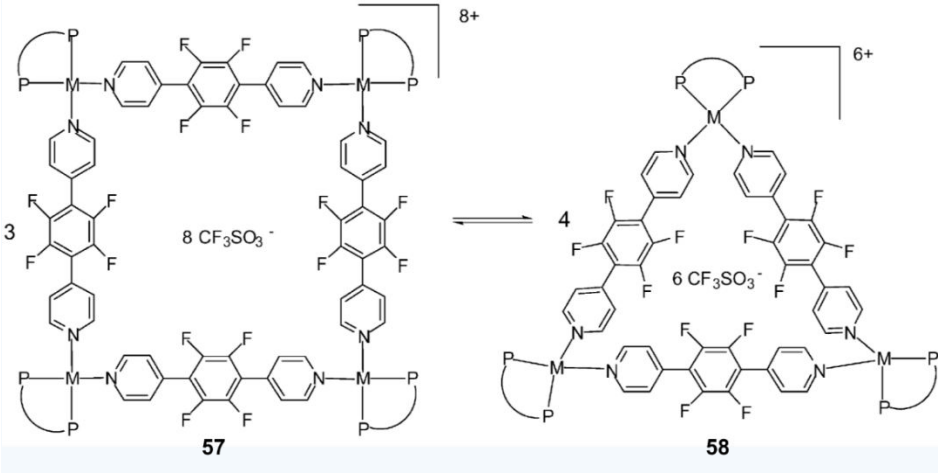

Scheme 1.12: Equilibrium between 1,4-*bis*(4-pyridyl)tetrafluorobenzene-based squares **57** and triangles **58**. Reprinted with permission from *Inorg. Chem.*, **2003**, *42*, 5890. Copyright (2003) American Chemical Society.

Ferrer *et al.* have investigated the assembly of a variety of $[M(P\text{-}P)(OTf)_2$ precursors ($M = Pd^{II}$, Pt^{II}; P-P = dppp, dppf, depe [1,2-*bis*(diethylphosphino)ethane], dppbz [1,2-*bis*(diphenylphosphino)benzene] with the linear bridging unit 1,4-*bis*(4-pyridyl)butadiyne and 1,4-*bis*(4-pyridyl)tetrafluorobenzene (Scheme 1.12).[79] The triangle-

square equilibria were characterized by ^{1}H, $^{31}P[^{1}H]$, ^{19}F, and $^{195}Pt[^{1}H]$ NMR and ESI-MS data. The triangle/square ratio was found to be dependent on the nature of the metal ions in the corner unit, concentration, and solvent. The same research group has also investigated the assembly using the linear motif 1,4-*bis*(4-pyridyl)tetrafluorobenzene and Pt(II) and Pd(II) complexes with *cis*-protecting nitrogen-chelating ligands: [M(N-N)$(OTf)_2$] (N-N = ethylenediamine, 4,4'-R_2bpy, R = H, Me, ^{t}Bu).[80] Their result further supported Fujita's conclusion that the nature of the ancillary ligands on the metal corners plays a crucial role in the outcome of a triangle-square equilibrium. Molecular squares were found to be the predominant product when a less sterically hindered and more flexible ethylenediamine was used as the end-capping ligand in the metal corners. Whereas, a triangle-square dynamic equilibrium was observed when the more sterically demanding 4,4'-R_2bpy was used as ancillary ligands. Besenyei *et al.* also made similar conclusion in their systematic study of the reaction of 4,4'-bpy with a series of square-planar complexes [Pd(N-N)$(ONO_2)_2$] that differ in the bulkiness on the diamine chelating ligand N-N = en, tmeda, *N,N,N′,N′*-tetraethylethylenediamine (teeda), 1,3-diaminopropane (dap), *N′,N′*-dimethylpiperazine (dmpip), and homopiperazine (hpip).[81] The reaction mixtures were investigated using NMR and DOSY spectroscopy and wide-angle X-ray diffraction. Although, a triangle-square equilibrium was observed in all cases, the triangular architecture was obtained as the major product in case of bulkier chelating ligands.

1.2.1.4 Triangles and Squares Non-equilibrium Mixtures

Diederich and co-workers reported an oxidative cyclization of $[Co_2(CO)_4$(dppm)$(C\text{-}C\equiv CH)_2]$ (dppm = *bis*(diphenylphosphino)methane), which gave a nonequilibrium mixture of a cyclic trimer and tetramer, where the diacetylide groups are

bridging the corner $Co_2(CO)_4$ units.[82] Two macrocycles were separated by thin-layer chromatography and the metallotriangle was found to be the major product, which was characterized by X-ray crystallography.

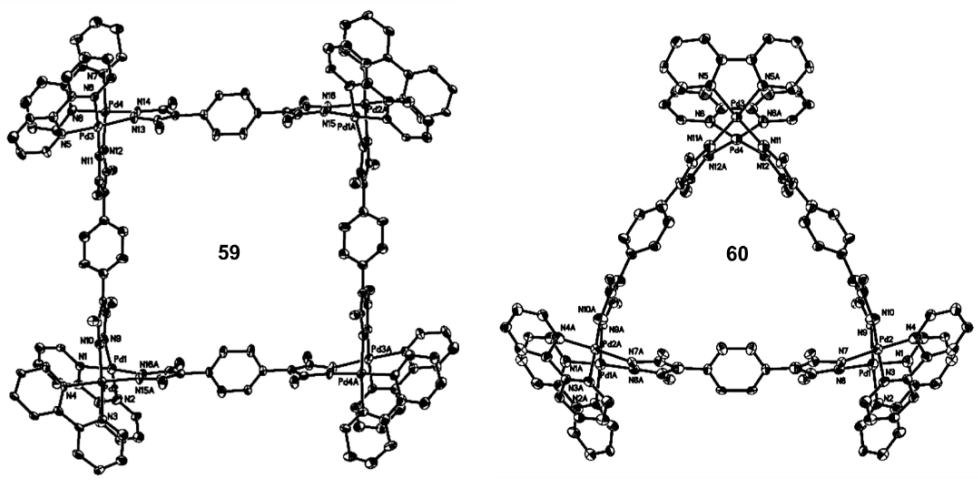

Figure 1.14: Crystal structure of square **59** and triangle **60**. Reprinted with permission from *Inorg. Chem.*, **2005**, *44*, 9471. Copyright (2005) American Chemical Society.

Jones *et al.* reported a nonequilibrium mixture of triangle and square from the reaction of $[M(NO)(Tp)I_2]$ (M = Mo, W; Tp^- = hydro*tris*(3,5-dimethylpyrazol-1-yl)borate) with 1,4-dihydroxybenzene.[83] Yu and co-workers reported that treatment of [Pd(bipy)-$(ONO_2)_2$ with the bipyrazole ligand [1,4-*bis*-4'-(3',5'-dimethyl)-pyrazolylbenzene] produced a mixture of a molecular triangle (**60**) $[(Pd_2(bipy)_2$-(μ-1,4-*bis*-4'-(3',5'-dimethyl)-pyrazolylbenzene))$_3](NO_3)_6$ in 20% yield and a molecular square (**59**) $[(Pd_2(bipy)_2$-(μ-1,4-*bis*-4'-(3',5'-dimethyl)-pyrazolylbenzene)$_4)](NO_3)_8$ in 80% yield.[84] Both the products were found to be stable in solution and no interconversion was observed. They were both characterized by X-ray crystallography (Figure 1.14).

1.2.1.5 Triangles or Squares

In various cases it is observed that the combination of 90º metal corners with 180º linkers selectively produce molecular triangles or squares depending on the reaction conditions or the nature of the reactants.

Cotton and co-workers reported that the reaction of the "paddlewheel", a metal-metal-linked binuclear precursor, $[Rh_2(DArF)_2(MeCN)_4][BF_4]_2$ (DArF = *N,N′*-diarylformamide) with $[Bu_4N]_2[C_2O_4]$ produced molecular triangle, $[Rh_2(DArF)_2(\mu,\eta^4\text{-}C_2O_4)_3]$, in quantitative yield; whereas, the corresponding molybdenum precursor, under the same reaction condition, produced a molecular square $[Mo_2(DArF)_2(\mu,\eta^4\text{-}C_2O_4)_4]$.[85] It was also observed that when the rhodium precursor is reacted with 10-fold excess of oxalate salt, the reaction exclusively generated molecular square $[Rh_2(DArF)_2(\mu,\eta^4\text{-}C_2O_4)_4]$. The same group has also reported a dirhenium(II) building-block $[cis\text{-}Re_2(\mu\text{-}O_2CCH_3)_2Cl_2(\mu\text{-}dppm_2)]$ with two adjacent labile acetato ligands and two bridging dppm ligands, reacts with terephthalic acid to produce the molecular triangle $[cis\text{-}Re_2Cl_2(\mu\text{-}dppm)_2(\mu,\eta^4\text{-}O_2CC_6H_4CO_2)_3]$, as the sole product.[86]

Recently, Long *et al.* have reported the reaction of a Ru(II) precursor, [Ru(cyclen)Cl(DMSO)]Cl, (cyclen = 1,4,7,10-tetraazacyclododecane) with 4,4'-bipy gave a molecular triangle (**61**), $[Ru(cyclen)(\mu\text{-}4,4'\text{-}bipy)_3]Cl_6$, exclusively.[87] But when the same Ru(II) precursor was reacted with pyrazine under similar reaction condition, a mixed Ru(II)/Ru(III) molecular square **56**, $[Ru(cyclen)(\mu\text{-}4,4'\text{-}pyrazine)_4]Cl_9$, was produced.[88] Both triangle **61** and square **62** were characterized by X-ray crystallography.

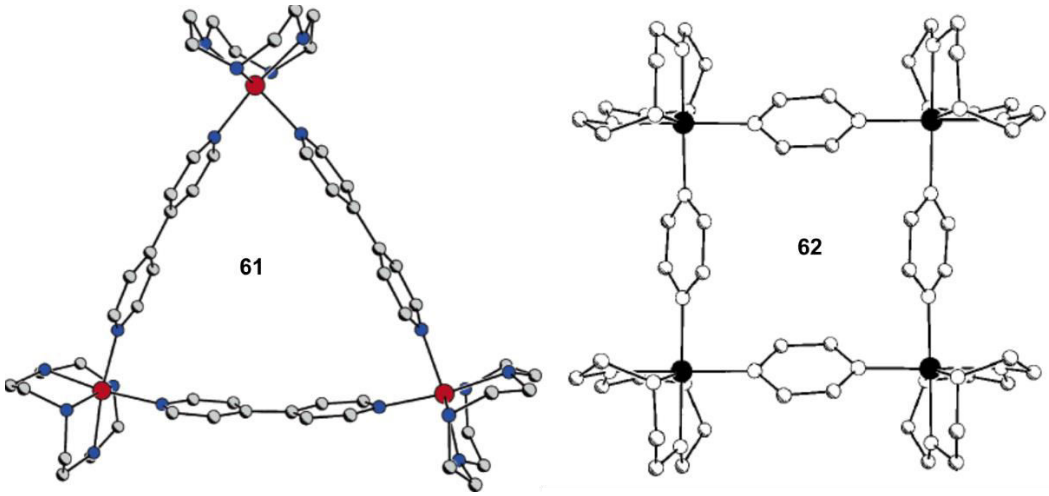

Figure 1.15: Crystal structure of metallo-triangle **61** and metallo-square **62**. Reproduced with permission from *Inorg. Chem.*, **2006**, *45*, 6378. Copyright (2006) American Chemical Society.

1.2.1.6 Molecular Rectangles

Despite their topological simplicity, construction of supramolecular rectangles has remained challenging to the greater scientific community. It is hypothesized that an assembly of a 90º metal precursor with two 180º rigid linkers of different length in absence of any "*self-sorting*" should produce a molecular rectangle;[20] however, without any selective recognition, two molecular squares with different size are detected instead of a rectangle. As a result, however, a considerable amount of effort has been devoted to attempted synthesis of molecular rectangles.

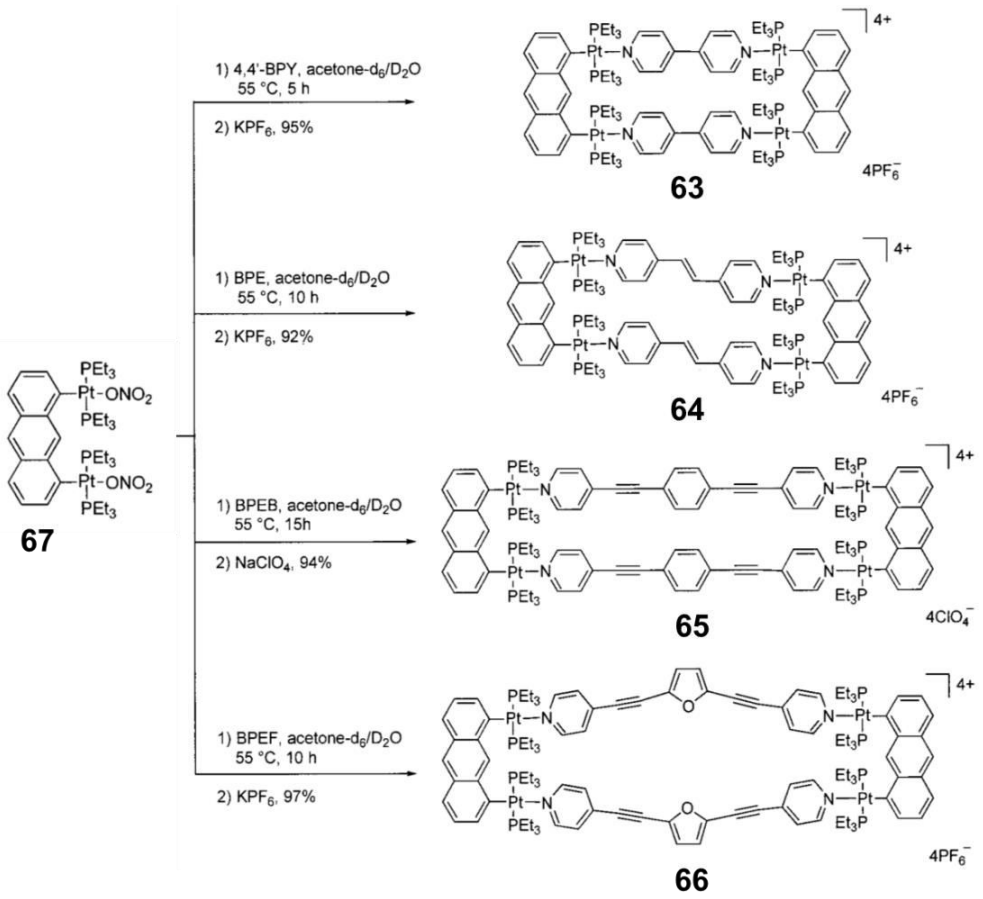

Scheme 1.13: Synthesis of different Pt- and *bis*pyridyl-based molecular rectangles **63-66**. Reprinted with permission from *J. Am. Chem. Soc.*, **2001**, *123*, 9634. Copyright (2001) American Chemical Society.

Stang and co-workers have developed a synthetic strategy where a platinum-based, shape-defining molecular "clip" possessing two parallel donor sites was reacted with various linear ditopic ligands to successfully synthesize metallomacrocyclic rectangles (Scheme 1.13).[89] The acceptor unit 1,8-*bis*[*trans*-Pt(PEt_3)$_2$(NO_3)]anthracene **67**, was treated with different *bis*pyridyl ligands, such as: 4,4'-bipyridine, *trans*-1,2-*bis*(4-pyridyl)ethylene (BPE), 1,4-*bis*(4'-pyridylethynyl)benzene (BPEB), 2,5-*bis*(4'-pyridylethynyl)furan (BPEF), to obtain cationic molecular rectangles **63-66** in excellent

overall yields. All of the tetranuclear macrocycles were characterized by multinuclear NMR, FAB-MS, and X-ray crystallography.

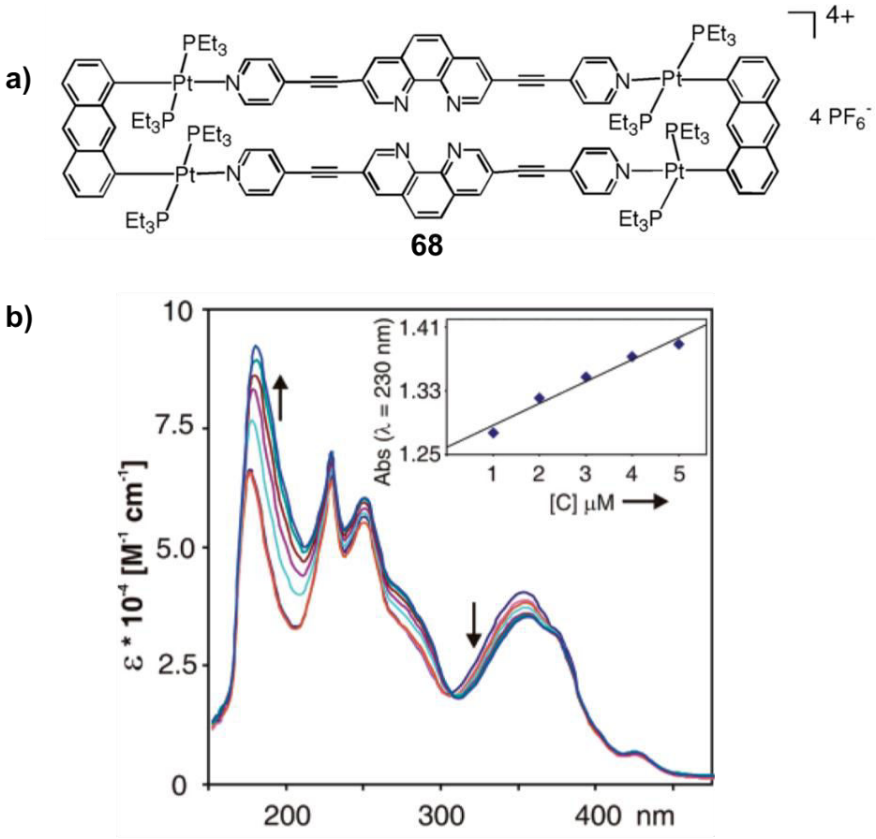

Figure 1.16: a) Structure of rectangle **68**, b) absorption spectra of **68** upon titration with $Ni(NO_3)_2 \cdot 6H_2O$. Reprinted with permission from *Org. Lett.*, **2004**, *6*, 651. Copyright (2004) American Chemical Society.

A mechanistic study revealed that an exchange of the counterions from the nucleophilic nitrate to non-nucleophilic tetrafluoroborate (BF_4^-) or hexafluorophosphate (PF_6^-) resulted in enhance stability of the rectangles. The 3,8-*bis*(pyridin-4-yl-ethynyl)[1,10]phenanthroline-functionalized rectangle (**68**) possesses selective optical sensing ability for Ni(II), Cd(II), and Cr(III) ions (Figure 1.16).[90] The addition of $Ni(NO_3)_2 \cdot 6H_2O$ into a methanolic solution of (**68**) causes a dramatic change in its

absorption spectra, as illustrated in Figure 1.16. Spectrochemical studies (UV-Vis, Near-IR, EPR) revealed that rectangles **63** and **64** can undergo a two electron reversible oxidation at the anthracene "clips", while two electron reversible reduction occurs at the neutral *bis*pyridyl acceptors.[91]

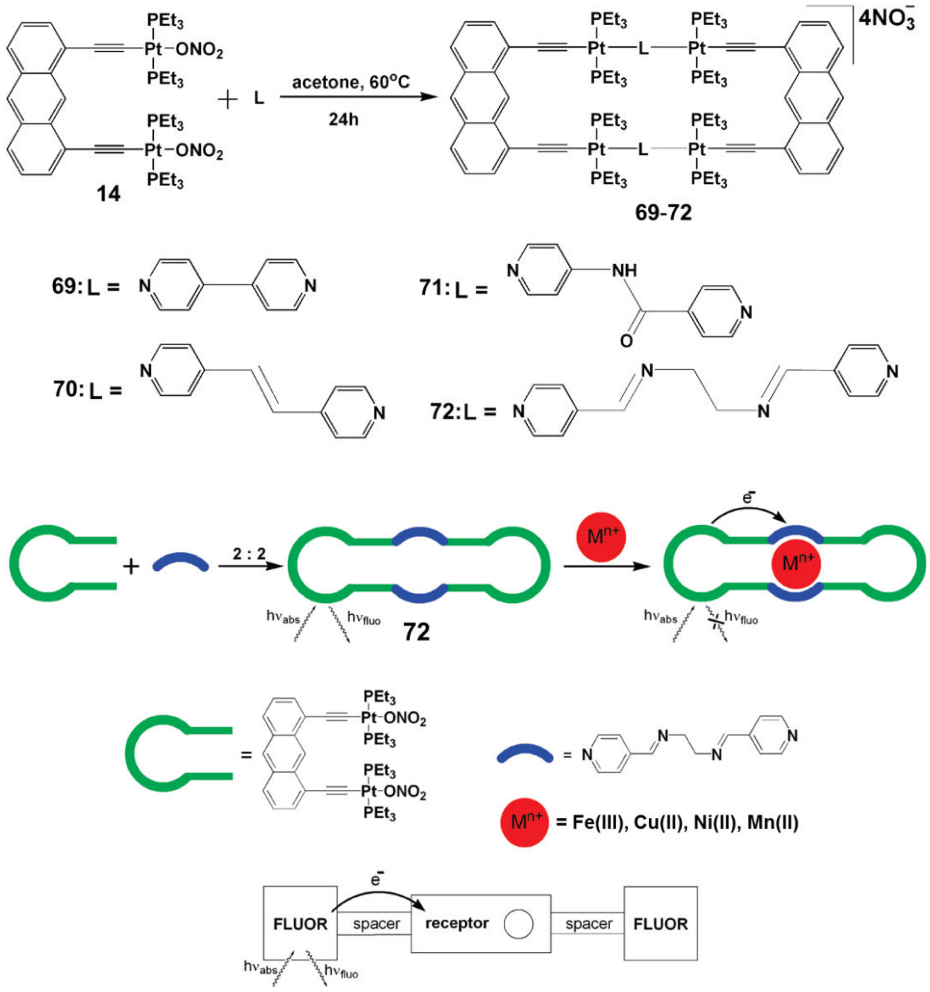

Scheme1.14: Assembly of different Pt-based molecular rectangles **69-72** and mechanism of action of molecular switch **72**. Reprinted with permission from *Inorg. Chem.*, **2009**, *48*, 549. Copyright (2009) American Chemical Society.

Mukherjee *et al.* have reported another series of cationic rectangles by extending the similar synthetic strategy (Scheme 1.14). Rectangles **69-72** were synthesized by using

a di-Pt(II) molecular "clip" **14**, with a triple bond functionality and *bis*pyridyl linear linkers, such as: 4,4-bipyridine, *trans*-1,2-*bis*(4-pyridyl)ethylene, *N*-(4-pyridyl)-isonicotinamide, and *N,N*-*bis*(4-pyridylidene)ethylenediamine.[92] Due to the presence of ethynyl groups, rectangle **72** exhibits luminescence, however, quenching was observed upon the binding of hard transition metal ions, such as: Fe(III), Cu(II), Ni(II), and Mn(II) into the N_4 pocket. The luminescent intensity of the Ni(II) bound complex was regained upon removal of the metal ion by a stronger chelating ligand e.g., 2,2'-*bis*pyridine.

Bosnich and co-workers have reported that a molecular co-facial di-palladium "clip" was formed upon reacting Pd(II) with a symmetrical terpyridine ligand (Figure 1.17). Reaction of this di-palladium complex with the linear linker 4,4'-bipyridine readily forms the molecular rectangle **73**.[93] The rectangle **73** was shown to possess the interesting capability of hosting 9-methylanthracene.

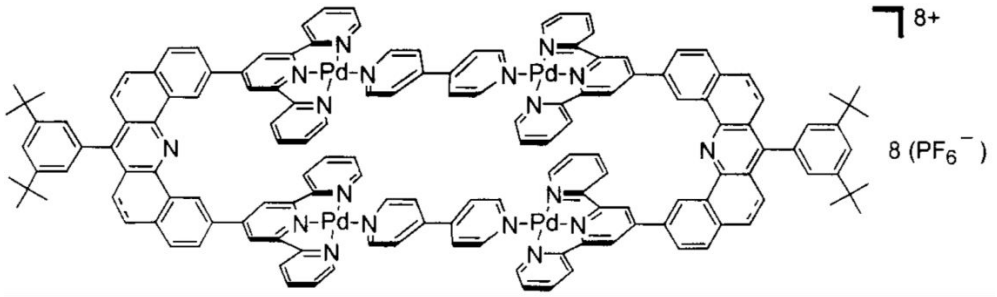

73

Figure 1.17: Terpyridine and bipyridine-based rectangle **73**. Reprinted with permission from *J. Am. Chem. Soc.*, **2001**, *123*, 3940. Copyright (2001) American Chemical Society.

Süss-Fink *et al*. have prepared a rectangular complex $[Ru_4(p\text{-cymene})_4(\mu\text{-}C_2O_4)_2]^{4+}$ (Figure 1.18, **74**) by reacting a diruthenium(II) molecular edge and the ditopic linear ligand 4,4'-bipyridne.[94] Therrien's group employed this synthetic strategy to prepare various ruthenium-based rectangles possessing large cavities. Dinuclear arene ruthenium

complexes such as $[Ru_2(\eta^6\text{-}p\text{-cymene})_2(\mu\text{-}OO\cap OO)_2Cl_2$ (μ-*OO*∩*OO* = 2,5-dihydroxy-1,4-benzoquinato,[95] 2,5-dichloro-3,6-dihydroxy-1,4-benzoquinato,[96] 5,8-dihydroxy-1,4-naphthoquinato,[97] 9,10-dihydroxy-1,4-anthraquinato,[98] or 6,11-dihydroxynaphthacene-5,12-dionato[98]) were reacted with pyrazine, bipyridine or 1,2-*bis*(4-pyridyl)ethylene ligands in presence of AgOTf to obtain rectangles $[Ru_4(\eta^6\text{-}p\text{-cymene})_4$ $(\mu\text{-N}\cap\text{N})_2(\mu\text{-}OO\cap OO)_2]^{4+}$. These molecular rectangles were characterized by multinuclear NMR, ESI-MS, X-ray crystallography, and cyclic voltammetry. Host-guest studies using polyaromatic compounds on these complexes gave interesting results.

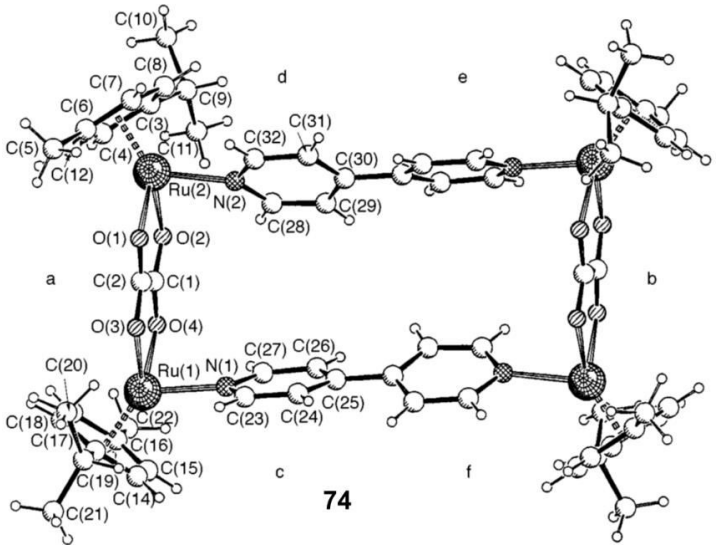

Figure 1.18: Crystal structure of rectangle $[Ru_4(p\text{-cymene})_4(\mu\text{-}C_2O_4)_2]^{4+}$ (**74**). Reprinted with permission from *J. Chem. Soc. Dalton Trans.*, **1997**, 4345. Copyright (1997) Royal Society of Chemistry.

The rectangle with 1,2-*bis*(4-pyridyl)ethylene linker was able to host pyrene, anthracene, perylene, and cornene within its cavity. On the other hand, the rectangle with 4,4'-bipyridine linker was shown to host only anthracene, and the rectangle with pyrazine linker was devoid of all host-guest property. Jin and co-workers have also used a similar

approach to synthesize a series of molecular rectangles (Scheme 1.15, **75-82**) by reacting unsaturated dinuclear arene ruthenium, iridium, and rhodium clips with various linear bridging ligands such as: 4,4'-bipyridine, pyrazine, 1,2-*bis*(4-pyridyl)ethylene, and 4-[5-(4-pyridyl)-1,3,4-oxadiazol-2-yl]pyridine.[99,100]

Lindner and co-workers have reported the preparation of various ferrocene-based rectangles.[101] The redox-active rectangular complex $[\eta^5\text{-}C_5H_4C_2\text{-}3\text{-}py)_2Fe]_2Pd_2Cl_4$ was prepared by reacting $PdCl_2(COD)$ with $(\eta^5\text{-}C_5H_4C_2\text{-}3\text{-}Py)_2Fe$. While the same donor moiety $(\eta^5\text{-}C_5H_4C_2\text{-}3\text{-}py)_2Fe$, was reacted respectively with $AgClO_4$ and $[Ni(H_2O)_6](NO_3)_2$ to obtain Ag(I)- and Ni(II)-based rectangles.

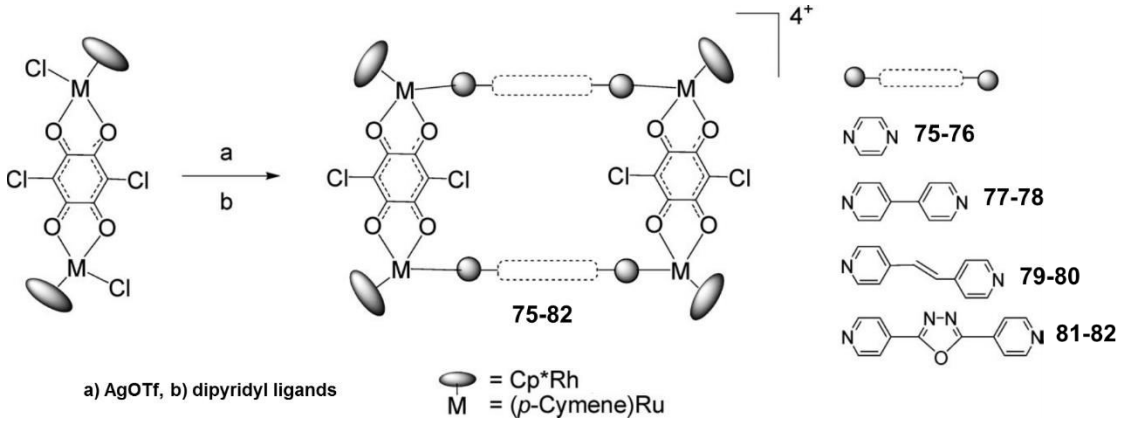

Scheme 1.15: Assembly of Rh- and Ag-based metallorectangles **75-82**. Reprinted with permission from *Organometallics*, **2008**, *27*, 5002. Copyright (2008) American Chemical Society.

1.2.1.7 Molecular Rhomboids

From structural complexity view point, molecular rhomboids are the simplest among the metallomacrocycles. Assembly of a 120º corner unit with a flexible linker motif readily yields molecular-rhomboids.

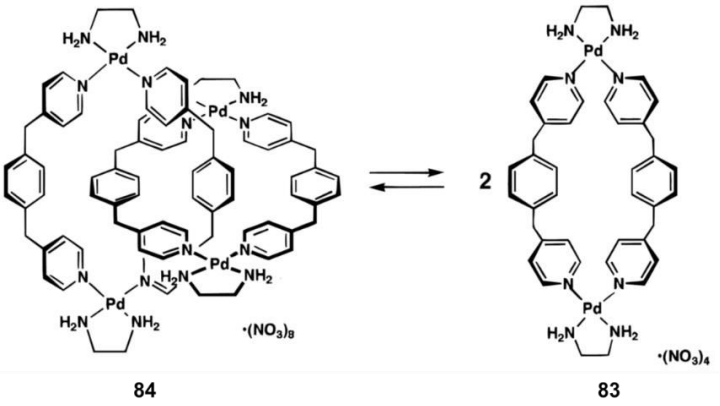

Scheme 1.16: Equilibrium between the rhomboidal **83** and a [2]catenane structure **84**. Reprinted with permission from *Nature*, **1994**, *367*, 720. Copyright (1994) Nature Publishing Group.

The first few examples of molecular rhomboids[102-105] were reported by Fujita and co-workers. All the rhomboids were prepared by a combination of a 90º *cis*-blocked $[Pd(en)(NO_3)_2]$ moiety with different *bis*(pyridine)-based linkers. Introduction of a the flexible, non-linear spacer $CH_2(p\text{-}C_6H_4)CH_2$- into a *bis*(pyridine) moiety resulted in an interesting equilibrium between the rhomboidal **83** and a [2]catenane structure **84** (Scheme 1.16).[102,104]

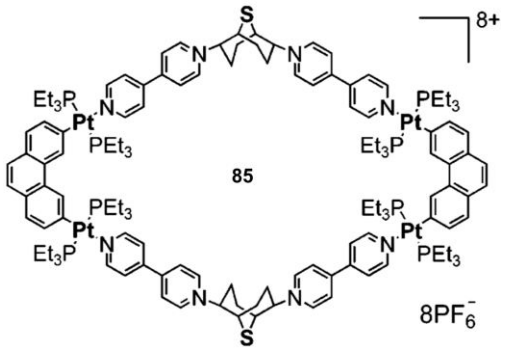

Figure 1.19: Structure of thiabicyclo[3.3.1]nonane-based rhombus **85**. Reprinted with permission from *J. Org. Chem.*, **2006**, *71*, 6644. Copyright (2006) American Chemical Society.

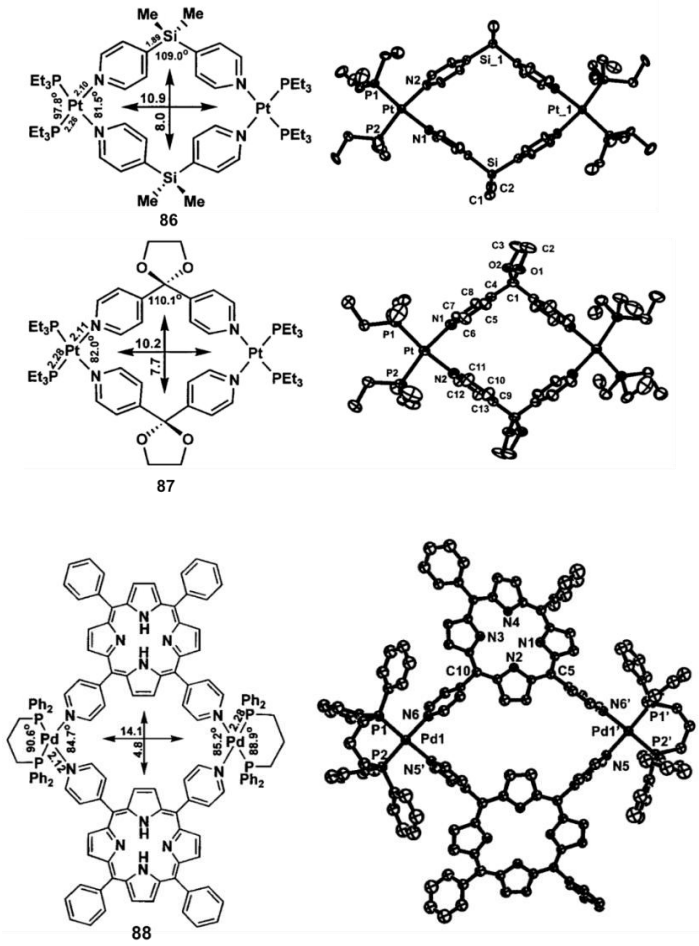

Figure 1.20: Structure and ORTEP diagram of molecular rhombuses **86-88**. Reprinted with permission from *Organometallics*, **1999**, *18*, 4718. Copyright (1999) American Chemical Society.

Pt(II)- and Pd(II)-based cationic dinuclear rhomboids were reported by Stang *et al*.[106] Treatment of the corner units *cis*-[$Pt(PEt_3)_2(OTf)_2$] and *cis*-[$Pd(dppp)(OTf)_2$] with *bis*(4-pyridyl) derivatives in an exact 1:1 ratio produced the desired metallo-rhomboids (Figure 1.20, **86-88**). All the macrocycles were confirmed by ^{1}H NMR, FAB-MS, and X-ray crystallographic data. The crystallographic data also revealed that the cavity diameter of these constructs are *ca*. 1 nm × 0.8 nm. The same group has also prepared other

molecular rhomboidal structures (Figure 1.19, **85**) by using bent Pt(II)-based phenanthrene corners with the rigid 120º linker, 2,6-di(4,4'-dipyridyl)-9-thiabicyclo[3.3.1]nonane.[107]

1.2.1.8 Higher Order Polygons

Various higher order polygons have been synthesized using the directional bonding approach. Although, most of the higher order polygons are homoleptic as well as homometallic in nature, there are several examples of heteroleptic or heterometallic larger polygons. Stang *et al*. have reported the assembly of a molecular hexagon *via* the combination of a nitrogen-containing motif with 120º bite angle and a linear organometallic linking unit. The angular ligand (4-pyridyl)ketone was reacted with linear diplatinum(II) "clip" in CH_2Cl_2 to obtain hexamer **89** (Figure 1.21) in near quantitative yield.[108] In the same work, they reported a complementary approach, where a 120º diplatinum(II) corner moiety was treated with a bridging 4,4'-bipyridine unit to produce a complimentary [6+6] hexagonal metallomacrocycle **90** (Figure 1.21).

Lehn *et al.* have synthesized a *circular double helix* by using a *tris*bipyridyl ligand.[109] When the ligand *tris*(2,2'-bipyridine) **91** was reacted with $FeCl_2 \cdot 4H_2O$ in ethylene glycol at 170º C, the formation of a pentanuclear helicate **92** was observed. The structure was confirmed by NMR and ESI-MS data along with X-ray crystallography. X-ray data revealed that the neighboring Fe(II) ions are coordinated by two intercrossing strands of *tris*(2,2'-bipyridine) ligand, which produces the novel helical complex. ESI-MS and X-ray data also confirmed the presence of a Cl^- ion within the cavity, which is perhaps responsible for the exclusive formation of this pentanuclear complex. It is also worth

mentioning that the same ligand *tris*(2,2'-bipyridine) **91** afforded a hexanuclear helicate when it was treated with $FeSO_4$ under the same reaction conditions.

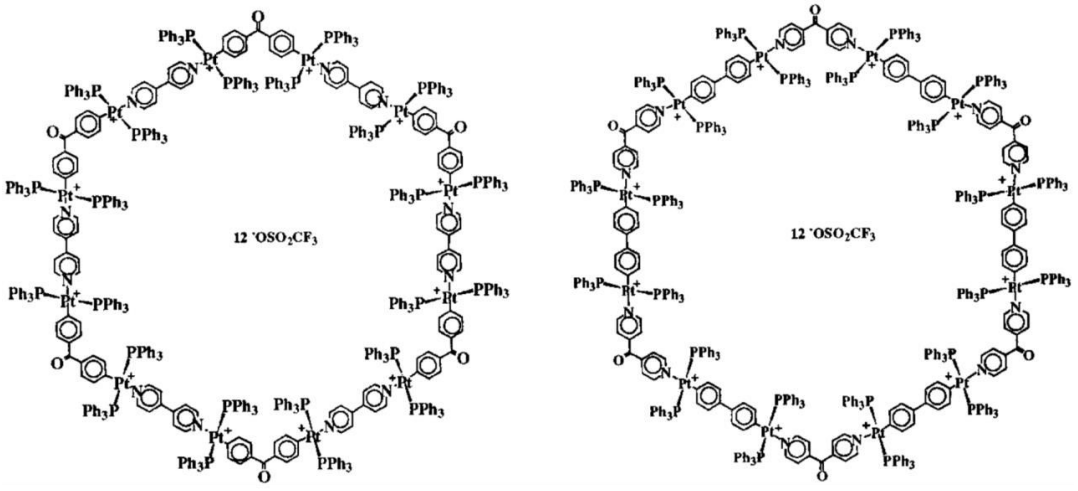

89 **90**

Figure 1.21: Structure of Pt-based molecular hexagons **89** and **90**. Reprinted with permission from *J. Am. Chem. Soc.*, **1997**, *119*, 4777. Copyright (1997) American Chemical Society.

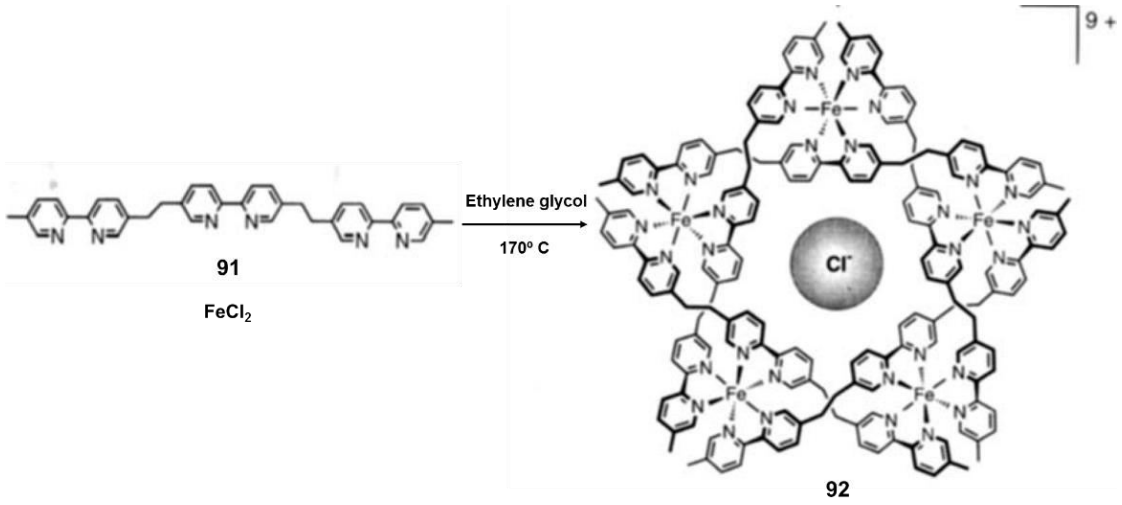

91

$FeCl_2$

92

Scheme 1.17: Self-assembly of molecular helicate **92**. Reprinted with permission from *Angew. Chem. Int. Ed.*, **1996**, *35*, 1838. Copyright (1996) WILEY-VCH.

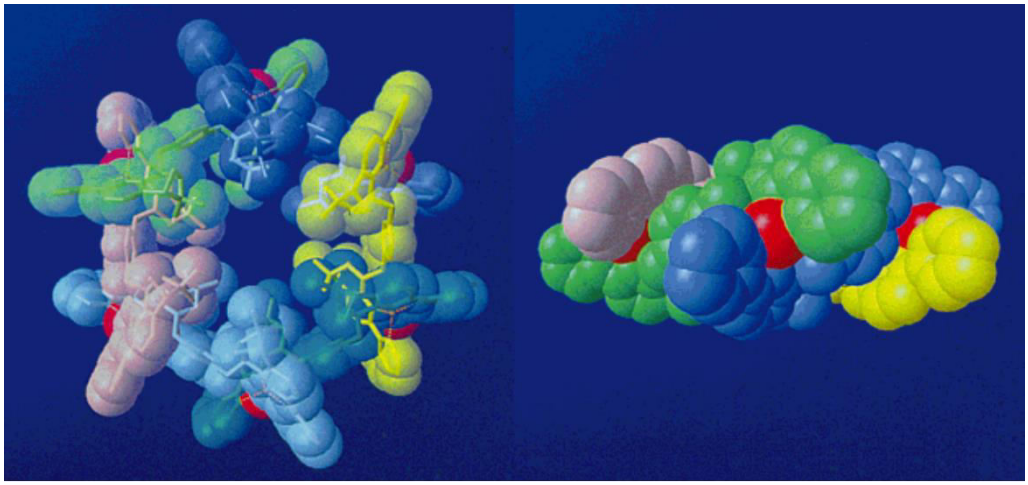

93

Figure 1.22: Crystal structure of **93**. Left: top view with superimposed stick model, Right: side view of the molecule. Reprinted with permission from *Angew. Chem. Int. Ed.*, **1998**, *37*, 289. Copyright (1998) WILEY-VCH.

Zelewsky *et al.* have synthesized an interwoven hexagonal construct **93**, by reacting α,α'-*bis*(pinene-2,2'-bipyridyl)-*p*-xylene with $AgPF_6$.[110] The hexameric architecture was readily characterized by NMR, ESI-MS, CD, and X-ray crystallographic data (Figure 1.22). The X-ray data confirmed the circular, single-stranded helicate structure of **93**. The outside diameter of the hexagon is *ca*. 3 nm and the cavity size is *ca*. 0.84 nm.

Newkome and co-workers have reported the synthesis of various terpyridine-based higher order polygons. Initially, a *bis*terpyridine ligand with 120º bite angle was trimerized with $RuCl_3 \cdot xH_2O$, then the trimer was subsequently reacted with Fe(II) to obtain bimetallic hexagonal metallomacrocycle.[111] Building upon this design protocol, the same group has synthesized a molecular "Sierpiński Hexagonal Gasket" **94**[24] in very high yield. The gasket was characterized by NMR, ESI-MS, TEM data, but because the high degree of molecular symmetry, it was definitively proven by low temperature UHV-STM, which precisely showed its complete molecular structure Newkome and co-workers have also prepared

terpyridine-based heteronuclear nonameric,[112] octameric and decameric[113] metallomacrocycles by using similar synthetic strategy.

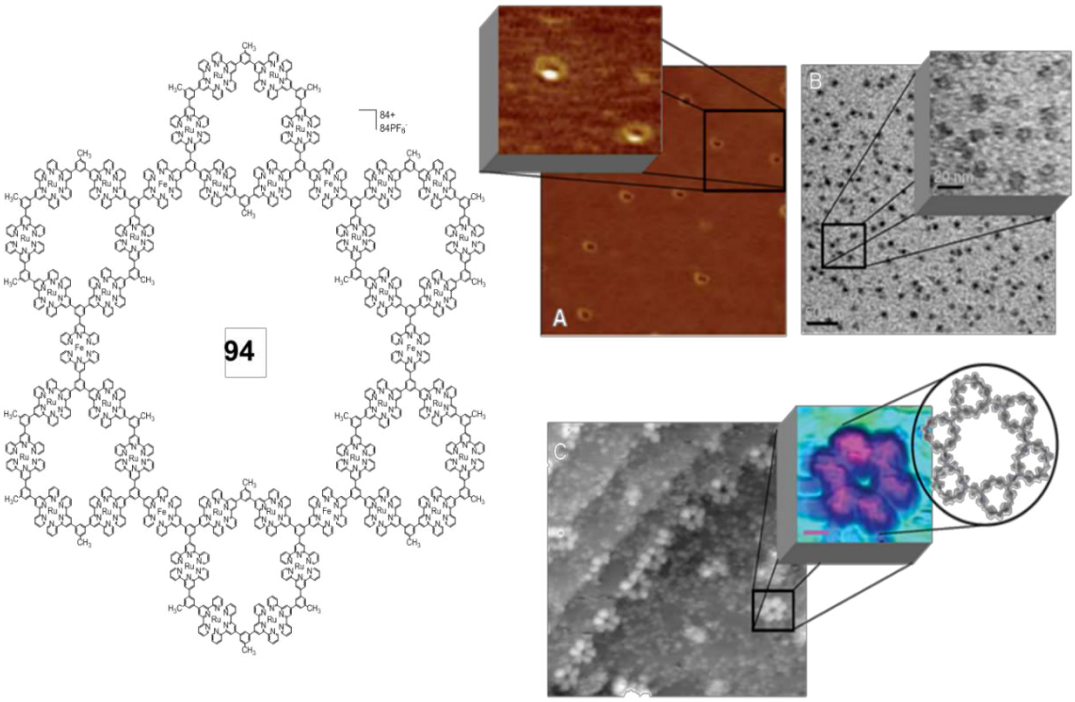

Figure 1.23. Sierpiński hexagonal gasket **94**. Images of **94**: (A) AFM images at 1.12 × 1.12 μm and 100 × 100 nm on a mica surface, (B) TEM images, and (C) ultrahigh-vacuum scanning tunneling microscopy (UHV-STM) images on a Au (111) surface at 6 K (scale bar, 3 nm). Reprinted with permission from *Science*, **2006**, *312*, 1782. Copyright (2006) The American Association for the Advancement of Science.

1.2.2 Three-Dimensional Constructs

Nature regularly uses self-assembly to form various three-dimensional (3D) constructs such as icosahedron or dodecahedron architectures of the viral capsids; however, abiological preparation of such complex structures remained challenging due to unavailability of suitable ligand systems. Development of various design protocols, synthetic strategies, and assorted building-blocks over last two decades has resulted in the synthesis of variety of high-symmetry supramolecular cages, such as: tetrahedron,

octahedron, cube, dodecahedron, icosahedron and other 3D metallomacrocycles, as illustrated in Figure 1.24.[63] For the purpose of this mini-review, we will only discuss those structures with heteroleptic coordination or heterometallic composition.

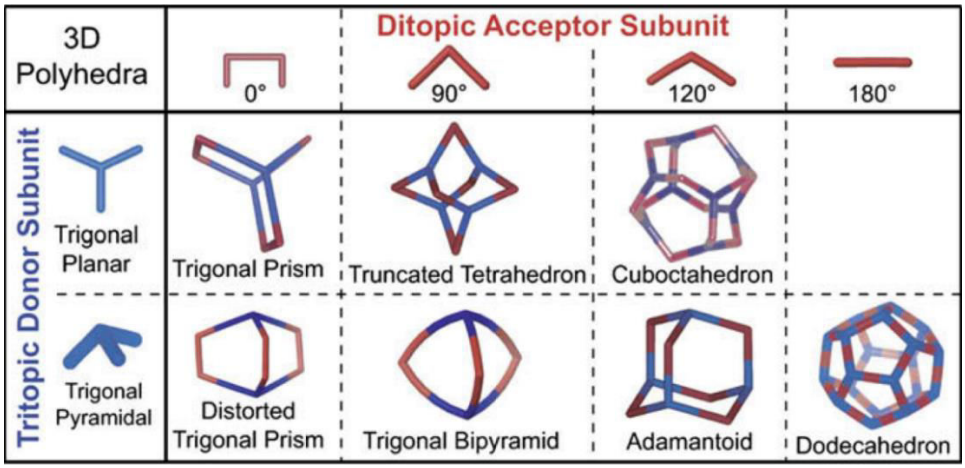

Figure 1.24. The directional bonding approach to assemble various 3D polyhedra.[63] Reprinted with permission from *Tetrahedron*, **2008**, *50*, 11495. Copyright (2008) Elsevier.

1.2.2.1 Tetrahedron

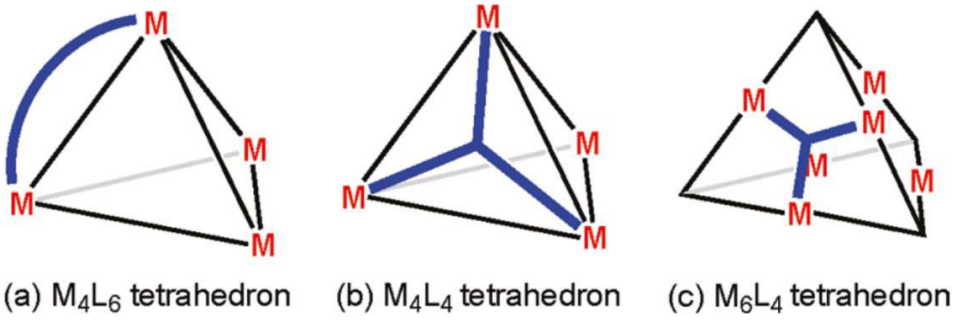

Figure 1.25: Schematic representation of different ways of constructing molecular tetrahedron.[20] Reprinted with permission from *Chem. Rev.*, **2011**, *111*, 6810. Copyright (2011) American Chemical Society.

A tetrahedron is the simplest of the platonic solids with four triangular faces. Structural dissection revealed that molecular tetrahedrons can be assembled predominantly *via* three different metal-ligand stoichiometries: (a) M_4L_6 tetrahedrons, where four vertices

are occupied by four metal ions and ligands act as the edges, (b) M_4L_4 tetrahedrons, where metal ions occupy four vertices and vertices are occupied by the ligands with 3-fold symmetry, and (c) M_6L_4 tetrahedron, where ligands occupy the four faces and are connected by the metal ions in the middle of the edges (Figure 1.25[20]).

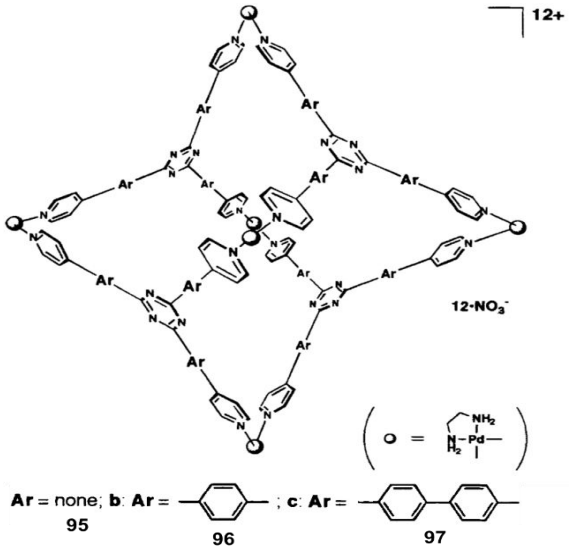

Figure 1.26: Pd- and triazine-based tetrahedrons **95-97**. Reprinted with permission from *Nature*, **1995**, *378*, 469. Copyright (1995) Nature Publishing Group.

The first reported synthesis of a metallo-tetrahedron was in 1988 by Saalfrank and co-workers.[114] In their effort to synthesize substituted allenes, they isolated a tetraanionic assembly resembling a distorted tetrahedron consisting of four Mg(II) ions. Fujita *et al*. have reported the synthesis of first truncated tetrahedrons[115] in which tetrahedrons **95-97** (Figure 1.26) and **98** (Scheme 1.18) were quantitatively assembled from the reaction of *cis*-capped metal hinges with 2,4,6-tri(4-pyridyl)-1,3,5-triazine[116] by following a similar synthetic strategy.[114] X-ray crystallographic data of **98** revealed three different inclusion geometries of the host-guest interactions for these cages.

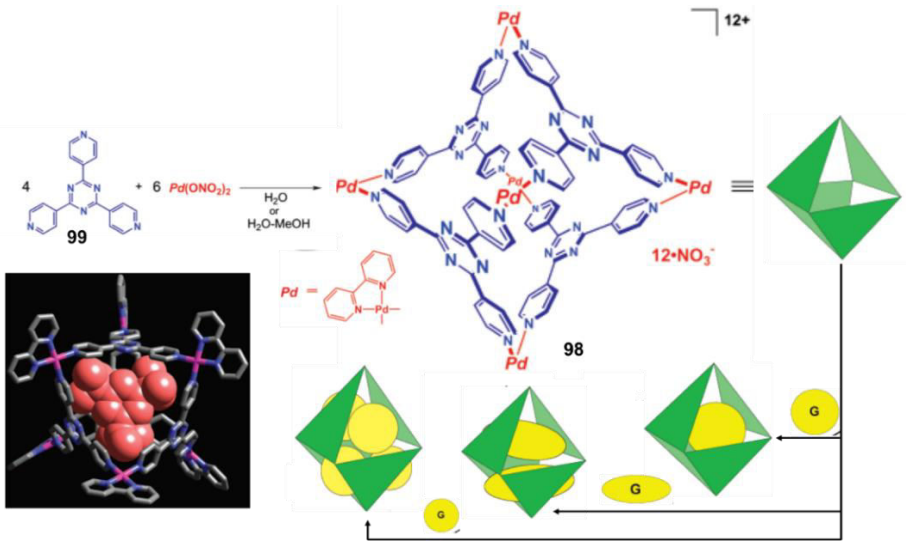

Scheme 1.18: Synthesis, crystal structure and inclusion mechanism of Pd- and triazine-based tetrahedron **98**. Reprinted with permission from *J. Am. Chem. Soc.*, **2012**, *124*, 13576. Copyright (2012) American Chemical Society.

Use of $[Ru_9[12])\text{-}aneS_4)(H_2O)(DMSO)](NO_3)_2$ under similar reaction condition afforded the truncated tetrahedron **100**, (Scheme 1.19) which was shown host different small organic molecules.[117]

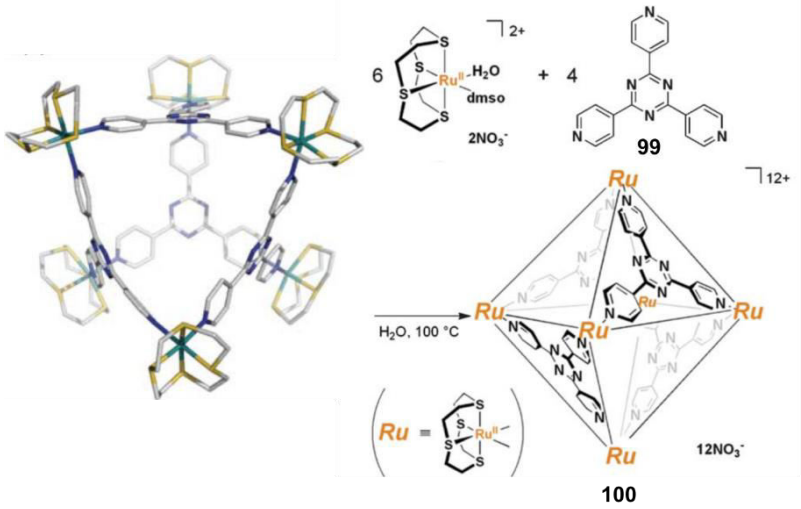

Scheme 1.19: Assembly Ru-based tetrahedron **100** and its crystal structure. Reprinted with permission from *Chem. Commun.*, **2007**, 4102. Copyright (2007) Royal Society of Chemistry.

Truncated tetrahedrons were prepared by assembling a tritopic 120º building-block with an angular ditopic 90º corner unit by Stang and co-workers. Reaction of 1,3,5-*tris*(4-pyridylethynyl)benzene and *cis*-[M-(dppf)$(OTf)_2$] (M = Pd, Pt) produced cationic M_6L_4 constructs **101-106** (Scheme 1.20).[118] Use of other angular moieties, such as [M-(*R*-BINAP)$(OTf)_2$][119] (M = Pd or Pt) or *cis*-[$Pt(PMe_3)_2(OTf)_2$][120] afforded similar truncated architectures. All of these tetrahedrons were characterized by (^{31}P and ^{1}H) NMR spectroscopy, ESI-MS, and X-ray crystallography and they can encapsulate up to three molecules of 1,3,5-triphenylbenzene.

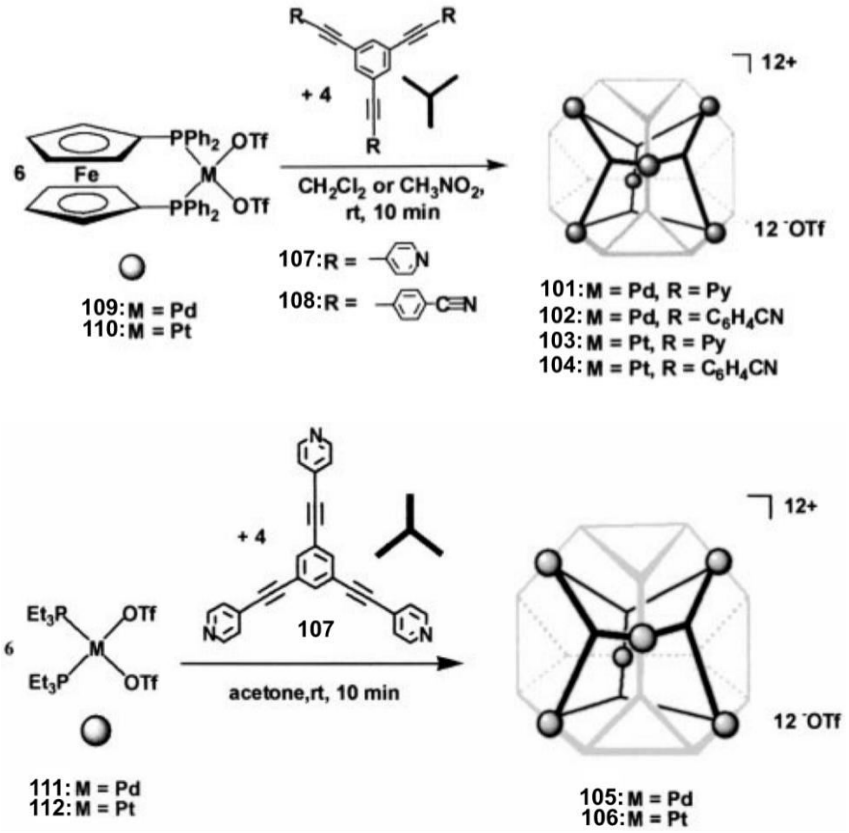

Scheme 1.20: Assembly of various Pd- and Pt-based tetrahedron **101-106**. Reprinted with permission from *Proc. Natl. Acad. Sci.*, **2000**, *97*, 1380. Copyright (2000) National Academy of Science.

1.2.2.2 Cube

Metallosupramolecular cubes are usually synthesized using two distinct procedures: (a) edge-directed and (b) face-directed assembly. So, a cube can be constructed *via* an edge-directed method by utilizing 8 tritopic 90º corner moieties and 12 ditopic linear bridging units. On the other hand in the face-directed method, ligands occupy the faces/sides of the cube hence to assemble a cube *via* this route 6 tetratopic, planar 90º subunits and 12 ditopic linkers are required.

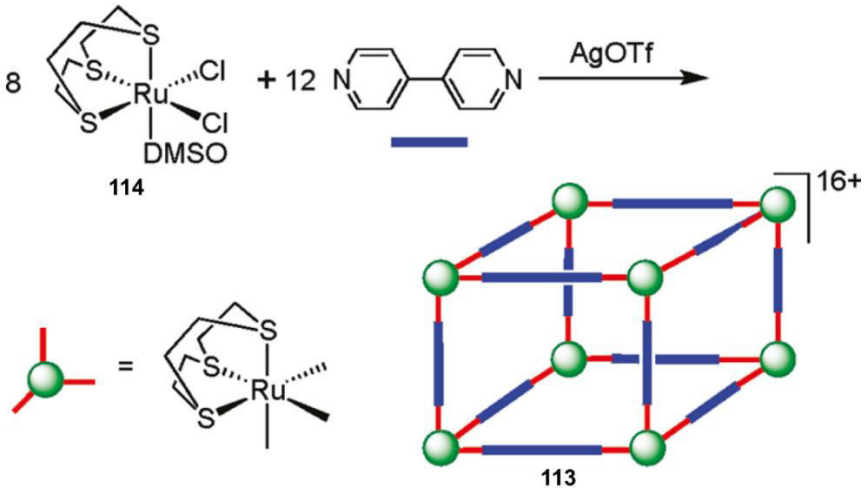

Scheme 1.21: Synthesis of Ru-based molecular cube **113**. Reprinted with permission from *Chem. Rev.*, **2011**, *111*, 6810. Copyright (2011) American Chemical Society.

.

Thomas *et al*. have described an edge-directed synthesis of molecular cube M_8L_{12}, from 8 tritopic 90º corner subunits and 12 ditopic linear linkers.[121] The reaction of ([9]aneS_3)Ru(DMSO)Cl_2] **114** and 4,4'-bipyridine in exact 8:12 molar ratio afforded the supramolecular cube **113**, which was confirmed by NMR and ESI-MS data. Whereas, Brisbois and co-workers have reported a $M_{12}L_6$ supramolecular cube by reacting 12 ditopic 90º metal corner units with 6 tritopic bridging ligands through directional bonding

approach.[122] The reaction of an (en)Pd(II) hinge **15** with tetrapyridyl derivative **115** in MeOH- water mixed solvent produced complex **116**.

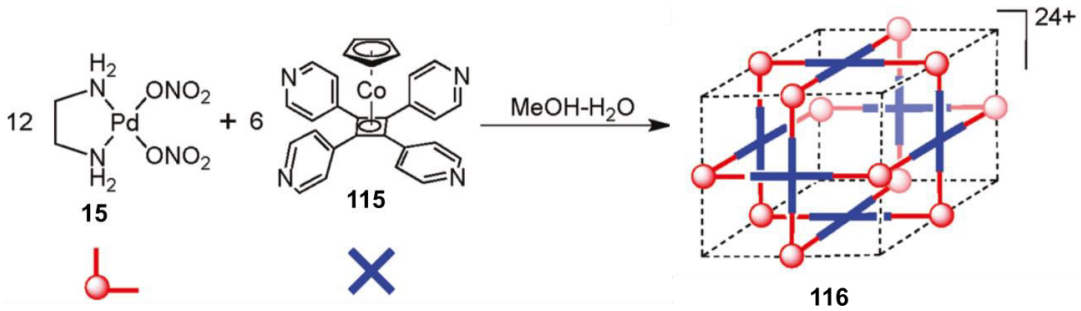

Scheme 1.22: Assembly of Pd- and Co-based molecular cube **116**. Reprinted with permission from *J. Am. Chem. Soc.*, **2001**, *123*, 3818. Copyright (2001) American Chemical Society.

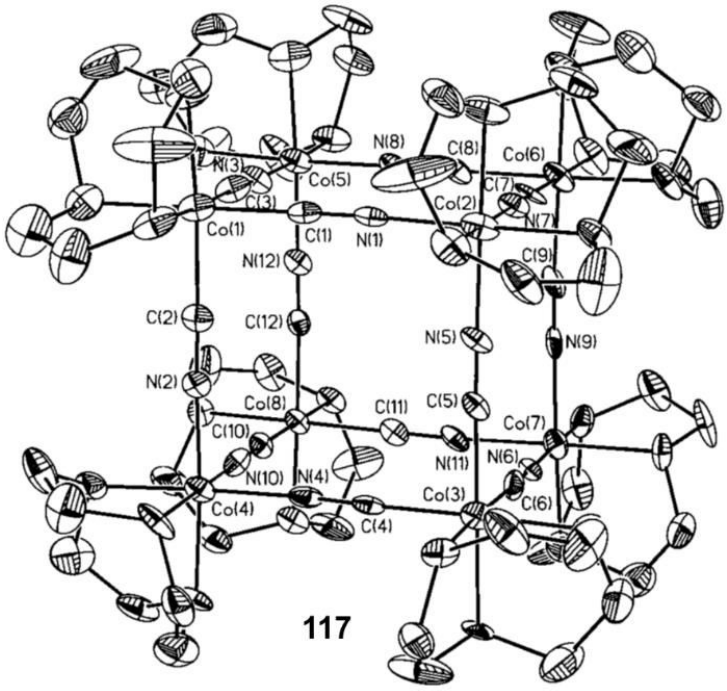

Figure 1.27: Molecular structure of cube **117**, reminiscent of Prussian Blue. Reprinted with permission from *Chem. Commun.*, **1998**, 1231. Copyright (1998) Royal Society of Chemistry.

Several cubic clusters with structure analogous to Prussian blue, were prepared by using cyanides as bridging ligands by Long *et al.*[123] Reaction of $[M(H_2O)_3(tacn)]^{3+}$ (M = Cr(III), Co(III); tacn = 1,4,7-triazacyclononane) with $[Co(CN)_3(tacn)]$ produced molecular box clusters $[Cr_4Co_4(CN)_{12}(tacn)_8]^{12+}$ and $[Co_8(CN)_{12}(tacn)_8]^{12+}$ **117**. X-ray crystallography confirmed that $[Co_8(CN)_{12}(tacn)_8]^{12+}$ moiety holds the 8 Co(III) at the corner locations (Figure 1.27).

1.2.2.3 Octahedron

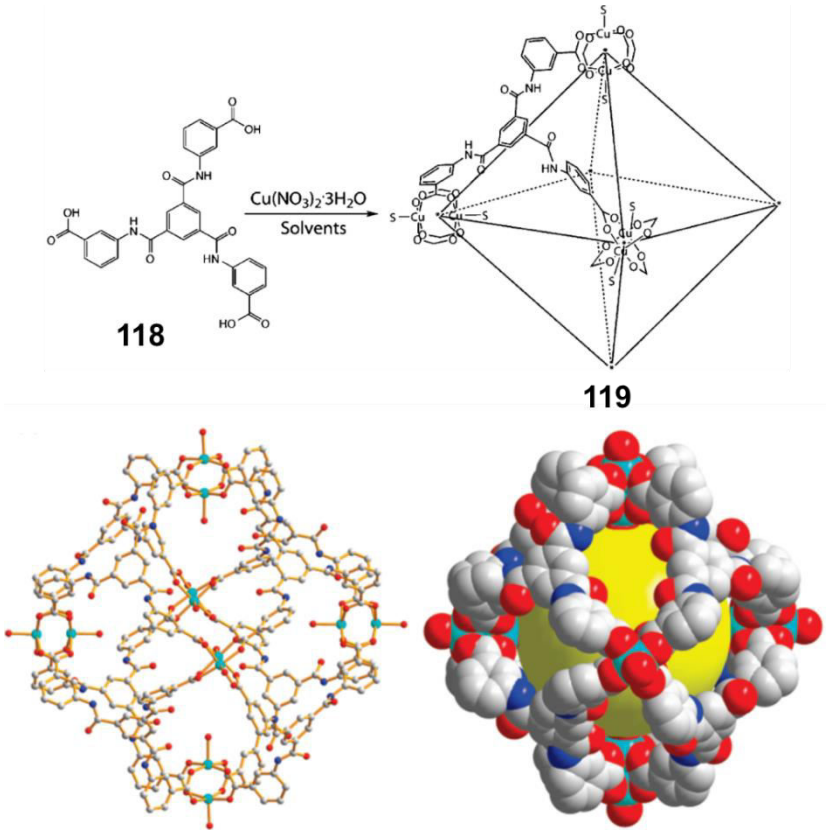

Scheme 1.23: Synthesis and crystal structure of Cu-based octahedron **119**. Reprinted with permission from *Inorg. Chem.*, **2009**, *48*, 1281. Copyright (2009) American Chemical Society.

There are only a handful of examples of a coordination-driven assembly of a supramolecular octahedron yet reported in the literature. Examples of heteroleptic or heterometallic octahedron constructs are even rarer. Lah and co-workers have assembled an octahedron **119** (Scheme 1.23) *via* the face-directed assembly of the tritopic ligand 3,3',3''-[1,3,5-benzenenetriyl*tris*(carbonylimino)]*tris*benzoate with a "paddlewheel"-like component $Cu_2(COO)_4$, as the corner.[124]

1.2.2.4 Cuboctahedron

Cuboctahedron is a semi-regular Archimedean type polyhedron, which consists of triangular and square faces.

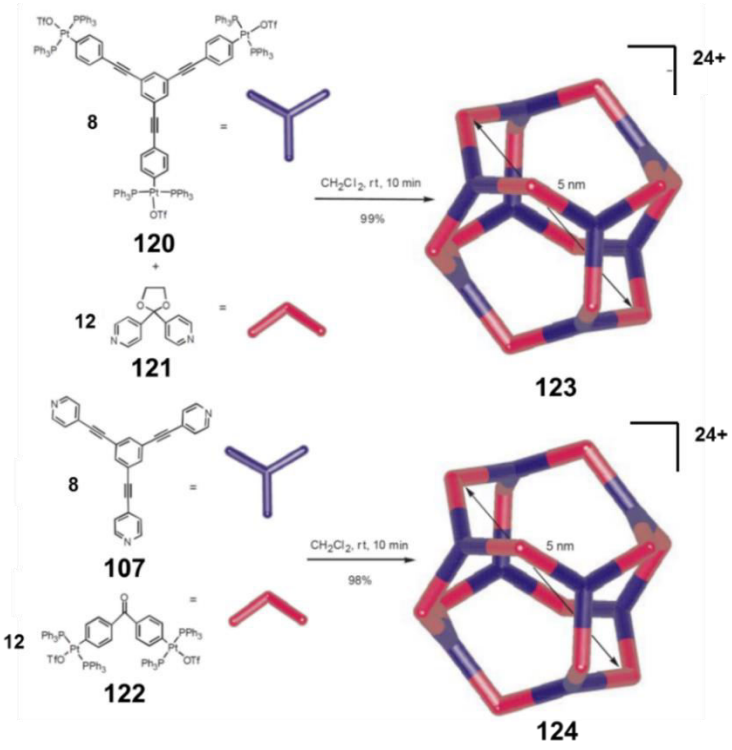

Scheme 1.24: Preparation of metallomacrocyclic cuboctahedrons **123** and **124**. Reprinted with permission from *Nature*, **1999**, *398*, 796. Copyright (1999) Nature Publishing Group.

Stang *et al.* prepared the first supramolecular cuboctahedron **123**[125] (Scheme 1.24) by assembling 12 tritopic Pt_3 acceptors with 8 bidentate 4,4'-bipyridylacetal linkers. In an alternative approach, 1,3,5-*tris*(4-pyridylethynyl)benzene was reacted with *bis*(4-[*trans*-$Pt(PPh_3)_3OTf$]phenyl)ketone to generate a structurally similar cuboctahedron **124**. Both the cuboctahedrons were characterized by ^1H and DOSY NMR and ESI-MS data.

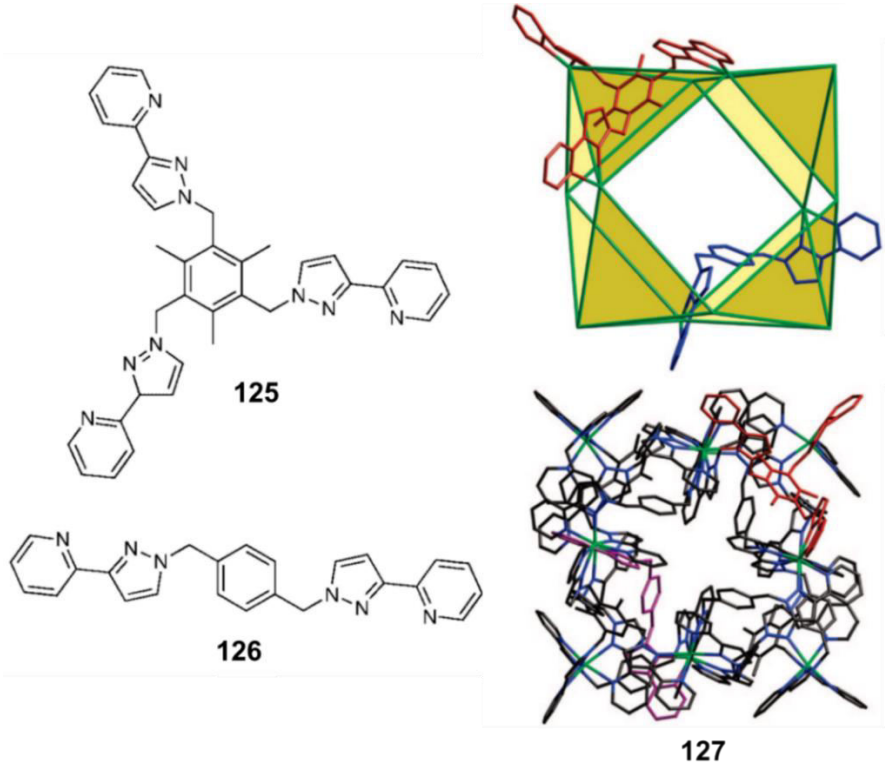

Figure 1.28: Structure of the ligands **125** and **126** and the crystal structure of **127**. Reprinted with permission from *J. Am. Chem. Soc.*, **2008**, *130*, 11641. Copyright (2008) American Chemical Society.

Ward and co-workers have reported the formation of a cuboctahedral cage by combining ligands with different coordination modes.[126,127] Reaction of the *tris*-bidentate ligand **125**, which caps the triangular faces, and a *bis*-bidentate ligand **126** with different transition metal ions, such as: Co(II), Cu(II), and Cd(II), in a precise 3:1:3 molar ratio

results in the formation of mixed-ligand cuboctahedron (Figure 1.28). The X-ray crystallographic data of macrocycle **127** showed a dodecanuclear cuboctahedral framework with eight triangular and six square faces. The ESI-MS data confirmed an intact heteroleptic cage with no peaks corresponding to homoleptic cages.

1.2.2.5 Trigonal Bipyramids and Double Squares

In principle, a trigonal bipyramid can be assembled from two tritopic and three ditopic 90º units *via* an edge-directed assembly. A large number of trigonal bipyramidal constructs have been designed and subsequently synthesized by following this simple design protocol.

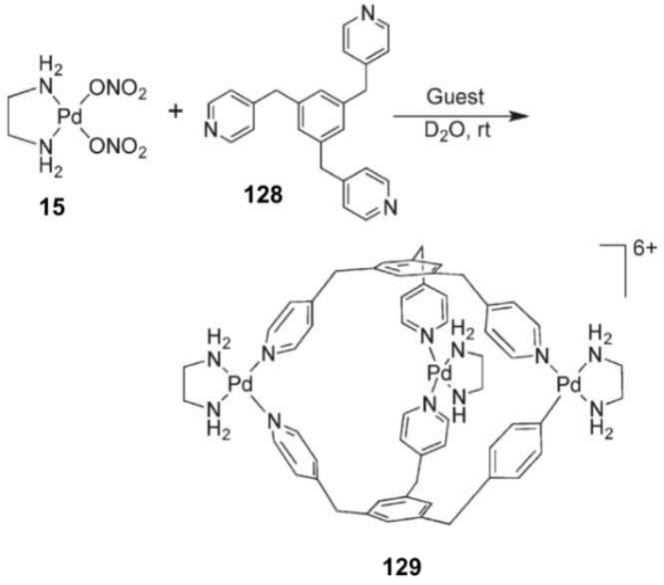

15 **128** **129**

Scheme 1.25: Assembly of trigonal-bipyramid **129**. Reprinted with permission from *J. Am. Chem. Soc.*, **1995**, *117*, 1649. Copyright (1995) American Chemical Society.

Fujita and co-workers have prepared one of the first supramolecular trigonal bipyramids (**129**), by reacting 2 equivalent of the tritopic ligand 1,3,5-*tris*(4-

pyridylmethyl)benzene **128** with 3 equivalent ditopic palladium-corner **15**, in presence of sodium 4-methoxyphenyl acetate.[128] It is worth mentioning that in absence of sodium 4-methoxyphenyl acetate the reaction only generated oligomeric products.

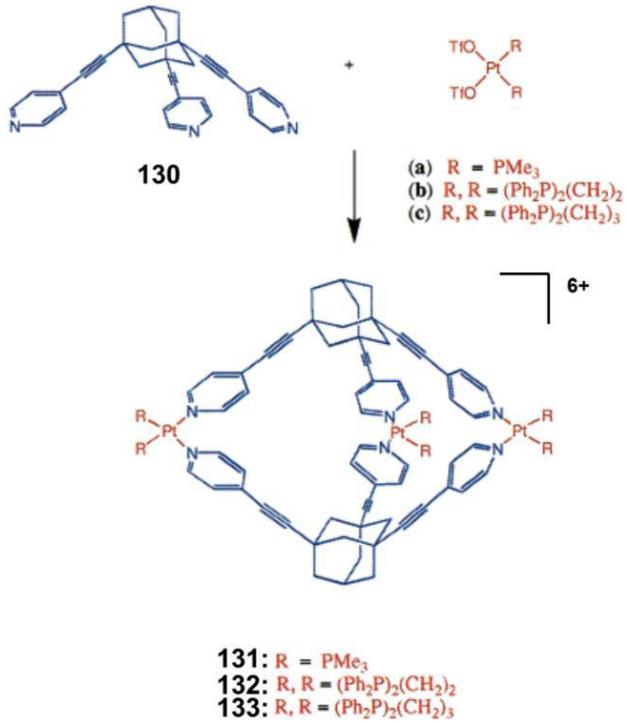

Scheme 1.26: Synthesis of trigonal bipyramidal cages **131-133**. Reprinted with permission from *J. Org. Chem.*, **2004**, *69*, 3526. Copyright (2004) American Chemical Society.

Stang *et al*. have prepared a numerous of M_3L_2 type trigonal bipyramidal cages using tritopic 109º linkers.[129,130] A [2+3] assembly of the 109º tritopic angular unit **130** with various 90º components such as: *cis*-[Pt(PMe$_3$)$_2$(OTf)$_2$], *cis*-[Pt(dppp)(OTf)$_2$] or *cis*-[Pt(dppe)(OTf)$_2$] (dppe = 1,2-*bis*(diphenylphosphino)ethane) (Scheme 1.26) afforded three different trigonal-bipyramidal cages (**131-133**). All the cages were characterized by multi-nuclear NMR and ESI-MS data.

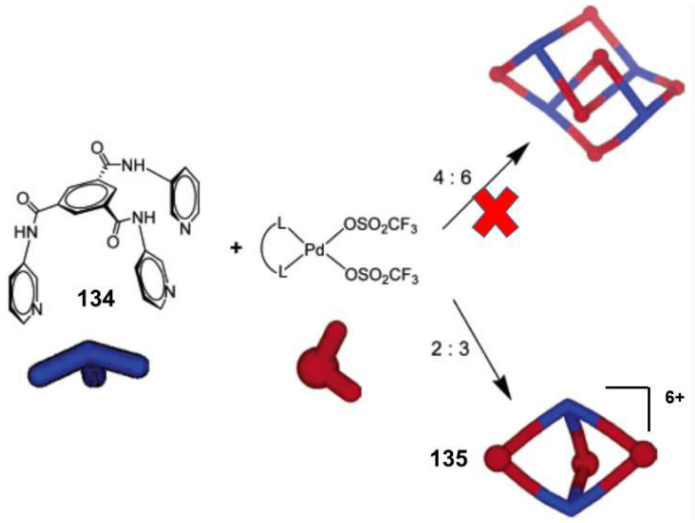

Scheme 1.27: Exclusive formation of trigonal bipyramidal **135**. Reprinted with permission from *Angew. Chem. Int. Ed.*, **1998**, *37*, 2082. Copyright (1998) WILEY-VCH.

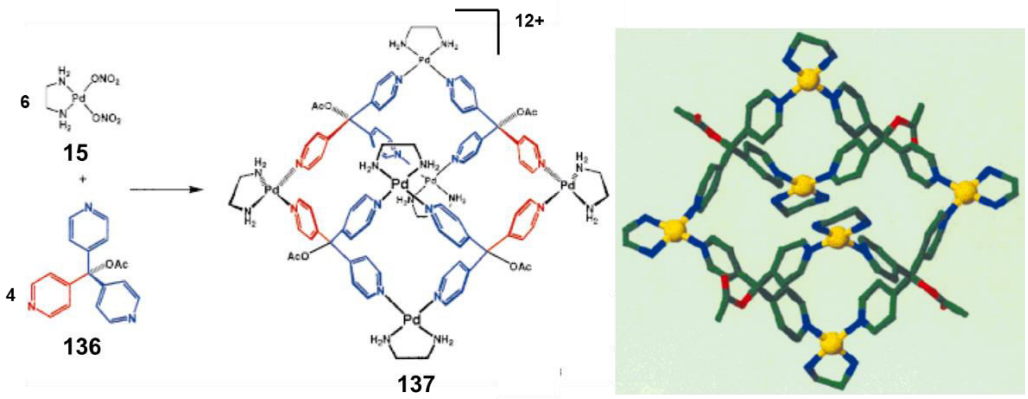

Scheme 1.28: Exclusive formation of double-square **137**, and its crystal structure. Reprinted with permission from *Organometallics*, **2007**, *26*, 3252. Copyright (2007) American Chemical Society.

The use of flexible tritopic linkers containing amide **134**[130] and ester[131] produces the trigonal-bipyramidal cage **135** (Scheme 1.27), exclusively. However, under same reaction condition, less flexible tritopic ligands, such as **136**, generated double-square **137**.[132,133] The formation of double-squares with less-flexible ligands can be attributed to

entropic factors. Since it is the smallest species that can be produced from this reaction, the system tends to produce these structures to compensate for the lack of enthalpy resulting from the bonding-strain of metal ions and less-flexible ligands.

1.2.2.6 Adamantoids

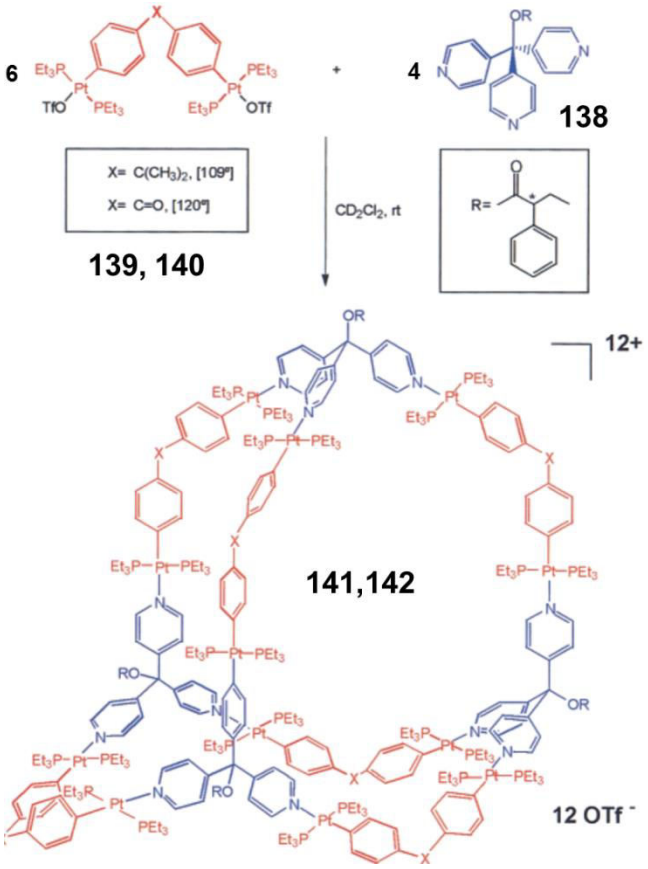

Scheme 1.29: Assembly of molecular adamantoids **141** and **142**. Reprinted with permission from *Org. Lett.*, **2000**, *2*, 1255. Copyright (2000) American Chemical Society.

Adamantoids have an extended tetrahedron-like configuration. It consists of four fused cyclohexane rings in their chair conformation with the bond angle of 109.5º. Design and synthesis of molecular adamantoids are based on the edge-directed strategy, where six 120º ditopic units and four 109.5º tritopic units are assembled to produce the desired

construct. Stang and co-workers have reacted different ditopic units (**139** or **140**) with tritopic unit (**138**) to obtain adamantine-like structures (**141** and **142**) in quantitative yield (Scheme 1.29).[134] The proposed architectures were confirmed by ^{1}H, ^{31}P NMR, and ESI-MS data.

Due to presence of a stereogenic center in the tritopic ligand **138**, all the complexes are chiral in nature. The same group has also reported Fréchet-type, dendron-decorated adamantoids (**143-145**) using a similar building-block approach.[135]

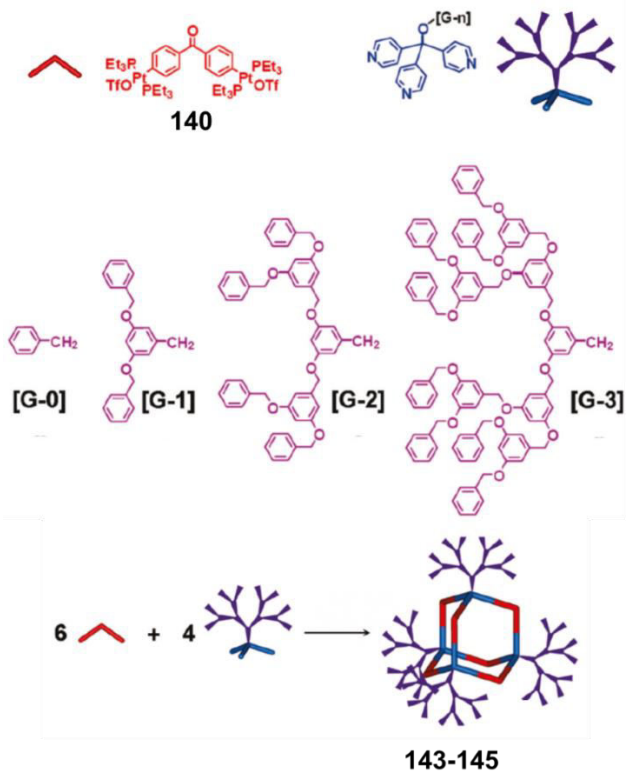

Scheme 1.30: Synthesis of Fréchet-type dendrimer modified adamantoids **143-145**. Reprinted with permission from *Inorg. Chem.*, **2010**, *49*, 4747. Copyright (2010) American Chemical Society.

1.2.2.7 Trigonal Prisms

A trigonal prism is a three-sided polyhedron with a triangular base. Although, M_3L_2 type prismatic cages are among the simplest 3D architectures, their synthesis has remained somewhat challenging because of the unavailability of suitable ligand systems. The early reports used either a template synthesis in solution or assembled only in solid state.[136-139] Structural examination revealed that a supramolecular trigonal prisms can, however, be synthesized by the combination of a tritopic donor, a linear connector and an end-capping acceptor.

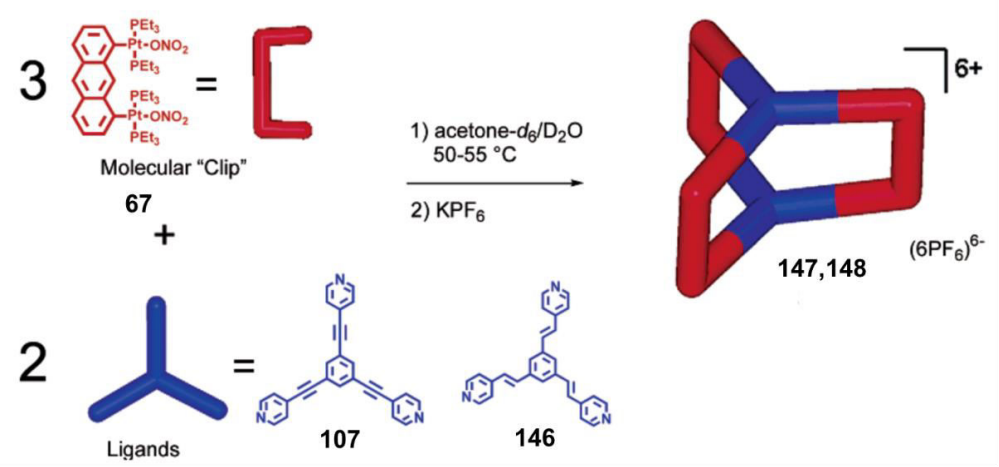

Scheme 1.31: Preparation of trigonal prisms **147** and **148**. Reprinted with permission from *Org. Lett.*, **2002**, *4*, 913. Copyright (2002) American Chemical Society.

Spontaneous-assembly of the trigonal prisms **147** and **148** was reported by Stang *et al.*,[140] by reacting a Pt-based molecular clip **67** with tripodal pyridyl linkers **107** and **146** in an exact 3:2 molar ratio (Scheme 1.31). These prisms were characterized by using a combination of multinuclear NMR and ESI-MS.

Fujita and co-workers have synthesized various trigonal prisms using a multicomponent assembly. Reaction of a tritopic triazine panel 2,4,6-tri(4-pyridyl)-1,3,5-

triazine (**99**), *cis*-blocked Pd-cap **15**, and different pyrazine derivatives (**150-152**) led to the formation of the desired trigonal prisms **153-155** (Scheme 1.32).[141] In this approach, there are possibilities of generating molecular-square and tetrahedron because of "*self-sorting*"; however, the use of large aromatic molecules, such as cornene (**149**), as guest, produces the trigonal prism in quantitative yield. The guest molecule can readily be removed by simple extraction with organic solvents; the cage is stable even after removal of the guest.

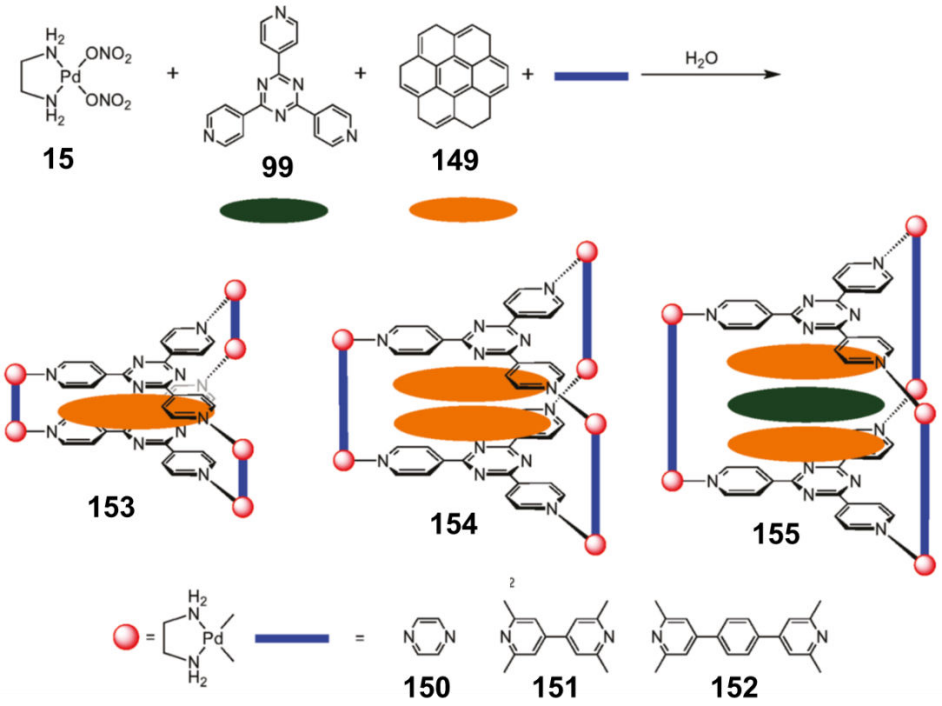

Scheme 1.32: Assembly of trigonal prisms **153-155**. Reprinted with permission from *Chem. Rev.*, **2011**, *111*, 6810. Copyright (2011) American Chemical Society.

Ko *et al*. have assembled supramolecular trigonal prisms using a larger molecular clip (Scheme 1.33).[142] A reaction of Pt_2 molecular clip **156**, with several tritopic pyridyl and isocyanide ligands (**107**, **157**) in again a precise 3:2 molar ratio produced the trigonal-prisms **158** and **159**. In a complementary work, Mukherjee *et al*. have used a tritopic Pt_3 acceptor and various organic clips to construct the prism **162** (Scheme 1.34).[143,144]

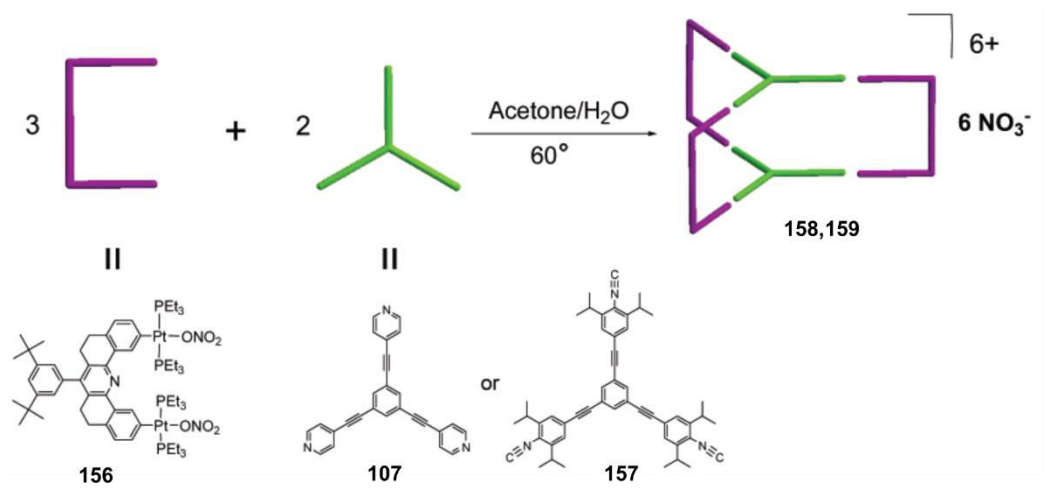

Scheme 1.33: Synthesis of trigonal prisms **158-159**. Reprinted with permission from *Inorg. Chem.*, **2005**, *44*, 7886. Copyright (2005) American Chemical Society.

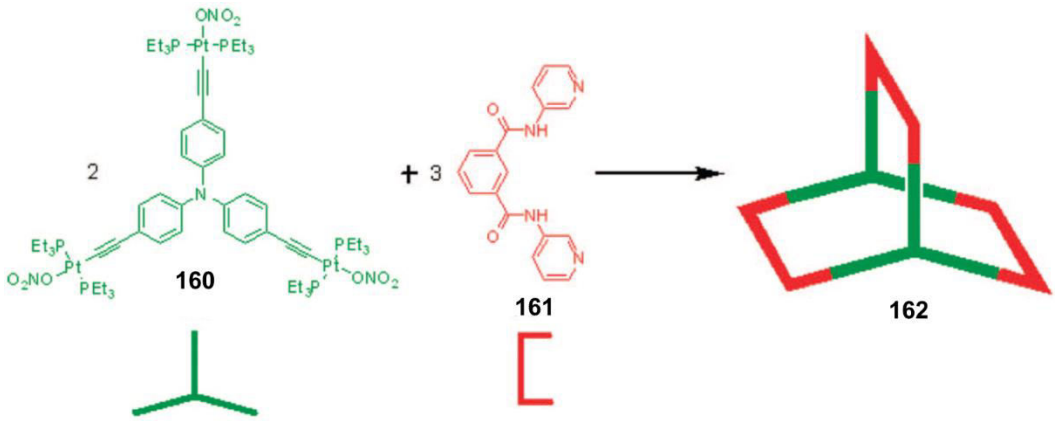

Scheme 1.34: Assembly of trigonal prism **162**. Reprinted with permission from *Organometallics*, **2008**, *27*, 316. Copyright (2008) American Chemical Society.

Bosnich and co-workers prepared trigonal prisms from the terpyridyl-Pd-based cleft **163** (Scheme 1.35). Assembly of planar *tris*pyridyl linkers with the Pd-based cleft in 1:1 molar ratio produced the molecular macrocycles **164** and **165** in near quantitative yields.[145] These prisms were shown to form 1:6 and 1:7 host-guest complexes with 9-methylanthracene and 1:2 complex with a tri-anthracene moiety.

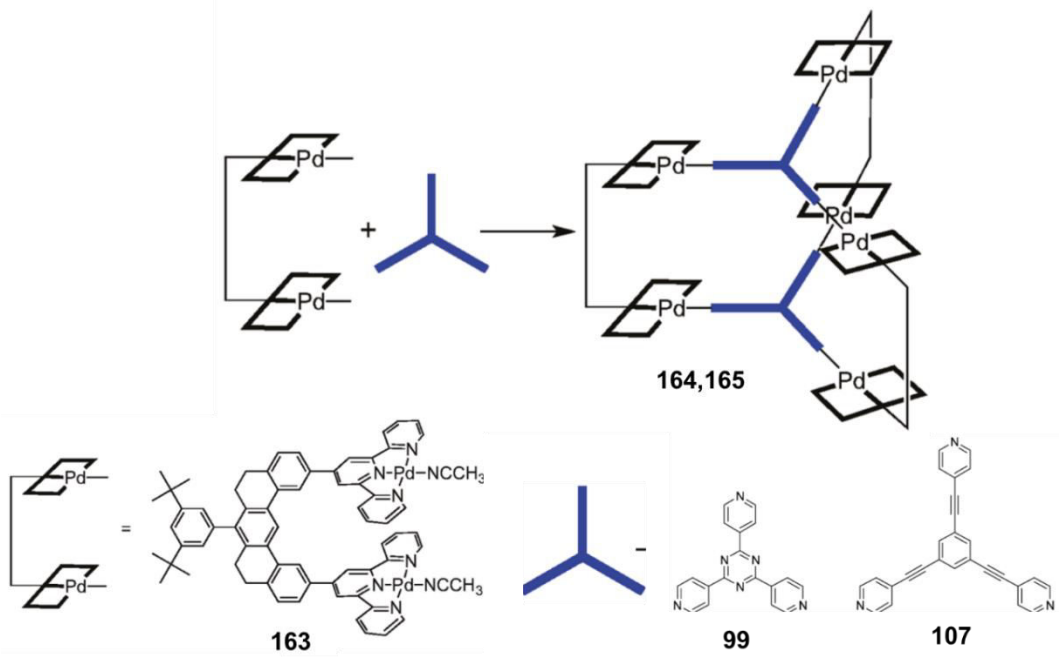

Scheme 1.35: Assembly of Pd-based trigonal prisms **164** and **165**. Reprinted with permission from *Chem. Commun.*, **2003**, 2824. Copyright (2003) American Chemical Society.

Porphyrin-based prisms bearing three, six or nine porphyrin panels have been assembled by Hupp *et al*. These complexes were formed by the reversible coordination of planar tritopic linkers with the Zn(II) sites of the porphyrinic dimers and trimer.[146,147] and were found to be dissociated either under high dilution conditions or in polar solvents; this is due to the weak bonding nature of Zn-pyridine bonds. Hence, the templated ring-closure metathesis (tRCM) was employed to permanently "set" the desired architecture, which resulted in formation of both metallated and metal-free porphyrin prisms.[148] Würthner *et al*. have described the preparation of a variety of trigonal prisms using a trimeric Zn-porphyrin complex and *bis*pyridyl-functionalized perylene *bis*imide.[149,150] Various triazine-based trigonal prisms were reported by Therrien *et al*., where six (η^6-arene)-

ruthenium(II) species, are held together by two trigonal 2,4,6-tri(4-pyridyl)-1,3,5-triazine panels.[151,152]

Stang and co-workers have reported synthesis of distorted trigonal prisms **168** and **169** by capping the trigonal-pyramidal acceptors **130**, **166**, and **167** with the Pt-based molecular clip **67**.[153] All the assemblies were confirmed by NMR, ESI-MS, and X-ray crystallography. In a complementary approach, reaction of organic donors with a 0º bite angle and tritopic tetrahedral carbon, silicon, and phosphorous moieties produced similar molecular prisms.[154]

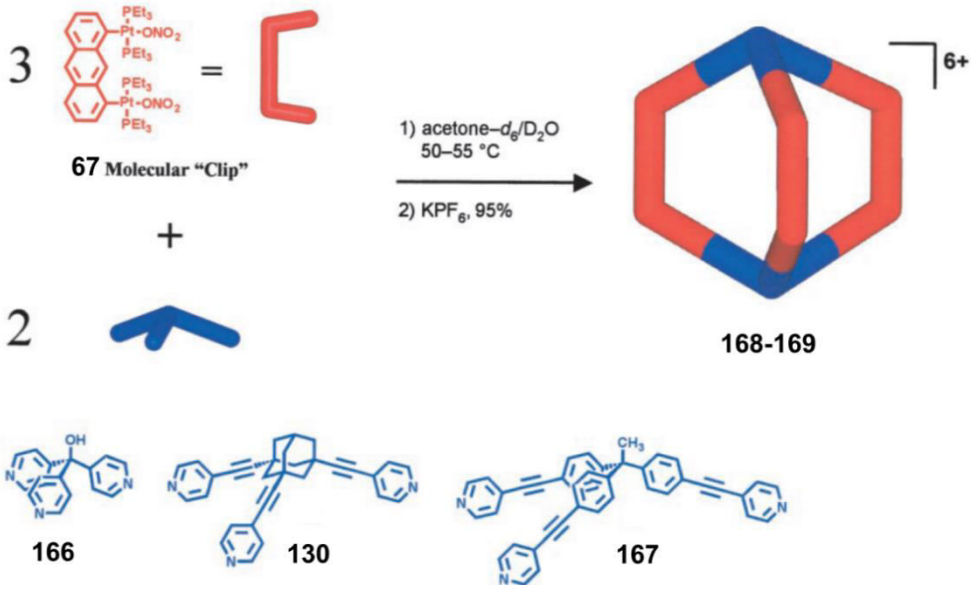

Scheme 1.36: Assembly of Pt-based trigonal prisms **168** and **169**. Reprinted with permission from *Proc. Natl. Acad. Sci.*, **2002**, *99*, 4932. Copyright (2002) National Academy of Science.

1.2.2.8 Tetragonal Prisms

Recently various supramolecular tetragonal prisms have been synthesized using different synthetic protocols. Atwood and co-workers have reported one of the earliest M_2L_4 cages with a tetragonal prismatic architecture.[155] Two octahedral Cu(II) ions were

linked by four *bis*pyridyl ligands **170** to form the desired **171** (Scheme 1.37). The equatorial positions of the octahedral Cu(II) were occupied by the *bis*pyridyl ligands and the axial positions were occupied by water molecules.

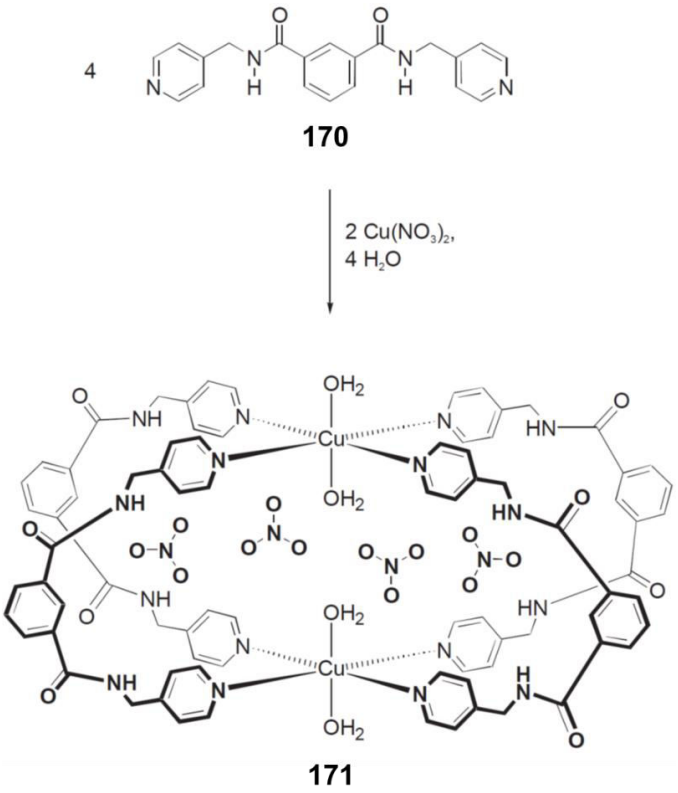

Scheme 1.37: Self-assembly of tetragonal prism **171**. Reprinted with permission from *Nature*, **1998**, *393*, 671. Copyright (1998) Nature Publishing Group.

A Pd(II)-based M_2L_4 tetragonal prism **173** was constructed by assembling a rigid organic tetratopic acceptor **172**, with $Pd(NO_3)_2$ in 1:2 molar ratio by Fujita *et al.*[156] The prism **173** was fully characterized by NMR, ESI-MS and X-ray crystallography (Scheme 1.38). One out of four nitrate counter ions was found to be encapsulated in the crystal structure of **173**. Steel[157] and co-workers and Puddephatt[158] *et al*. have prepared similar Pd(II) tetragonal cages **174** and **175** respectively, which can host anionic and cationic species (Figure 1.29).

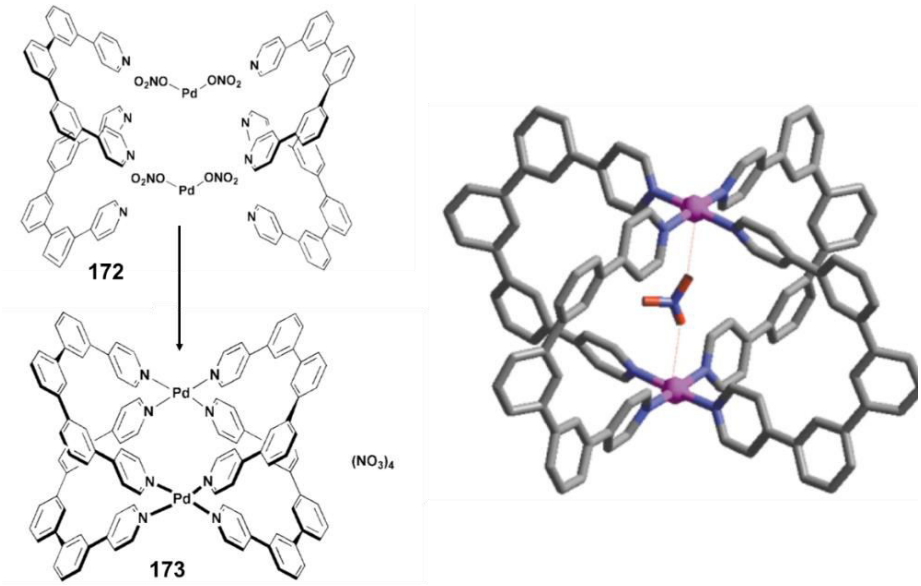

Scheme 1.38: Preparation of tetragonal prism **173** and its crystal structure. Reprinted with permission from *Chem. Commun.*, **2001**, 1652. Copyright (2001) Royal Society of Chemistry.

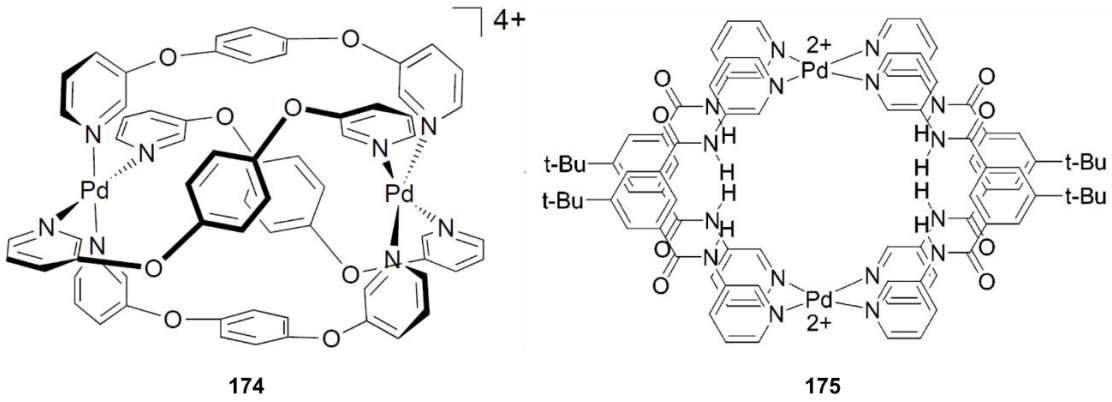

Figure 1.29: Structure of self-assembled tetragonal prism **174** and **175**. Reprinted with permission from *Angew. Chem. Int. Ed.*, **1998**, *37*, 3295. Copyright (1998) WILEY-VCH.

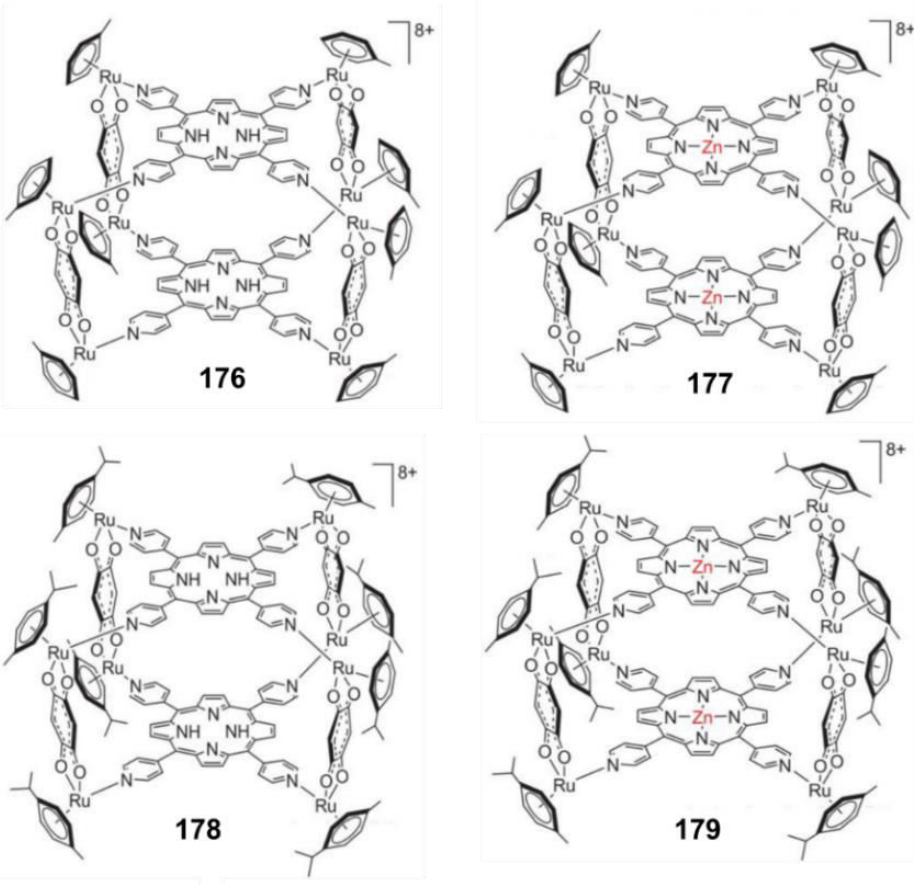

Figure 1.30: Structure of porphyrin-based tetragonal prisms **176-179**. Reprinted with permission from *Dalton Trans.*, **2009**, 10717. Copyright (2009) Royal Society of Chemistry.

Therrien *et al*. have reported a number of tetragonal prismatic architectures by using dhbq (2,5-dihydroxy-1,4-benzoquinonato) ligand.[159] This multi-component assembly of 5,10,15,20-tetra*kis*(4-pyridyl)porphyrin (tpp-H_2) panels with dinuclear arene ruthenium clips $[Ru_2(\eta^6\text{-arene})_2(dhbq)Cl_2]$ (arene = C_6H_5Me, *p*-cymene, C_6Me_6) produced the cationic prisms $[Ru_8(\mu^6\text{-}C_6H_5Me)_8(tpp\text{-}H_2)_2(dhbq)_4]^{8+}$ (**176**), $[Ru_8(\mu^6\text{-}p\text{-cymene})_8(tpp\text{-}H_2)_2(dhbq)_4]^{8+}$ (**178**), and $[Ru_8(\mu^6\text{-}C_6Me_6)_8(tpp\text{-}H_2)_2(dhbq)_4]^{8+}$. Analogous tetragonal prisms $[Ru_8(C_6H_5Me)_8(\mu\text{-tppZn})_2(dhbq)_4]^{8+}$ (**177**) and $[Ru_8(p\text{-}cymene)_8(\mu\text{-tppZn})_2(dhbq)_4]^{8+}$ (**179**) (Figure 1.30) were also prepared by reacting 5,10,15,20-tetra*kis*(4-

pyridyl)porphyrinzinc(II) (tpp-Zn) with toluene or *p*-cymene ruthenium building-blocks.[160] These molecular prisms strongly interact with the human telomeric quadruplex DNA. By following a similar design protocol, Jin *et al*. have synthesized tetragonal prisms by reacting a tetra-4-pyridylporphyrin, as a tetratopic donor, with an oxalate-bridged half-sandwich Ir(III), Rh(III) or Ru(II) connector.[161]

1.2.2.9 Molecular Boxes

Tetratopic ligands in combination with a 90º connector generate different supramolecular constructs for example trifacial molecular boxes or their higher analogues or even a molecular cube.

Stang *et al.* have synthesized several trifacial boxes by assembling tetrapyridyl connectors with 90º platinum linkers (Scheme 1.39).[162] The reaction of tetratopic planar donors **115**, **184-186** with *cis*-[$Pt(PMe_3)_2(OTf)_2$] in a precise 1:2 molar ratio produces specific molecular boxes **180-183**, which have been fully characterized by multinuclear (^1H and ^{31}P) and DOSY NMR and dual electrospray ionization-Fourier transform-ion cyclotron resonance-mass spectrometry (dual ESI-FT-ICR-MS).

Fujita and co-workers have synthesized trifacial molecular boxes by reacting Zn(II) tetra*kis*(3-pyridyl)porphyrin **187** with [$Pd(en)(NO_3)_2$] **15** (Scheme 1.40).[163] The proposed structure of **188** was confirmed by ^1H NMR, ESI-MS, and X-ray crystallography. It was observed that the encapsulation of pyrene into the cavity changes the conformation of the box from D_{3h} to C_2 symmetry. Following a similar synthetic strategy, they also reported the synthesis of other molecular boxes.[164]

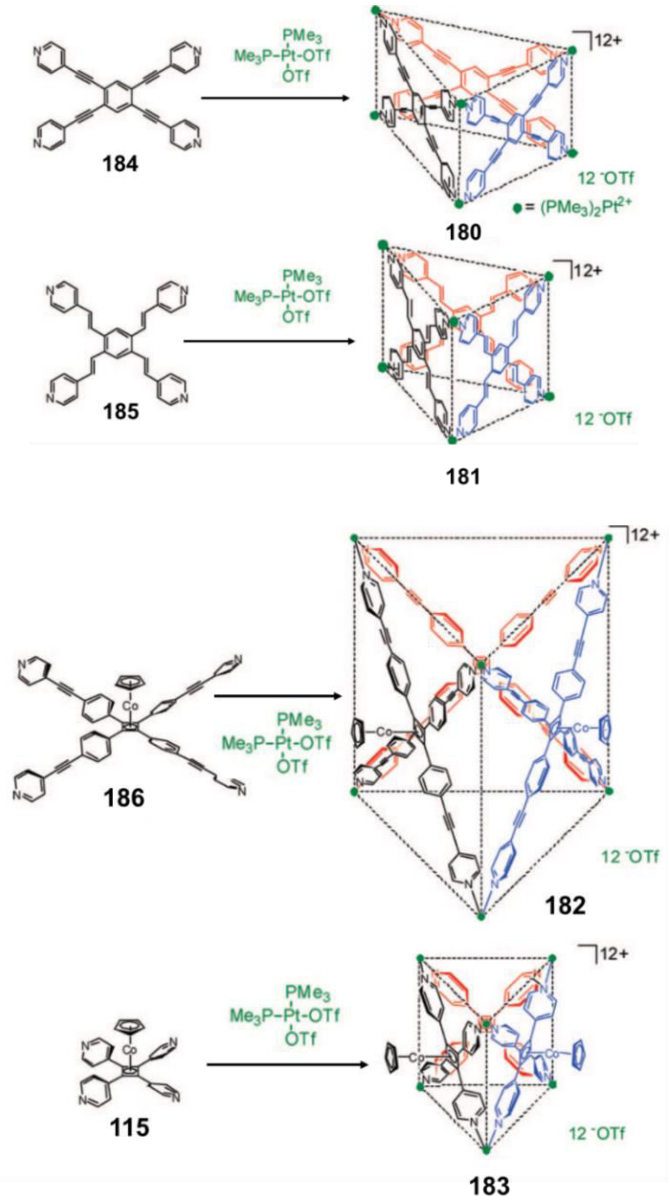

Scheme 1.39: Assembly of trifacial molecular boxes **180-183**. Reprinted with permission from *J. Am. Chem. Soc.*, **2008**, *130*, 7620. Copyright (2008) American Chemical Society.

Whereas, the tetrafacial molecular box was found to be in equilibrium with several other products, such as: trifacial and pentafacial boxes; however, this equilibrium can be tweaked to form tetrafacial box in overall quantitative yield by simply using biphenyl as a template, during the assembly process.

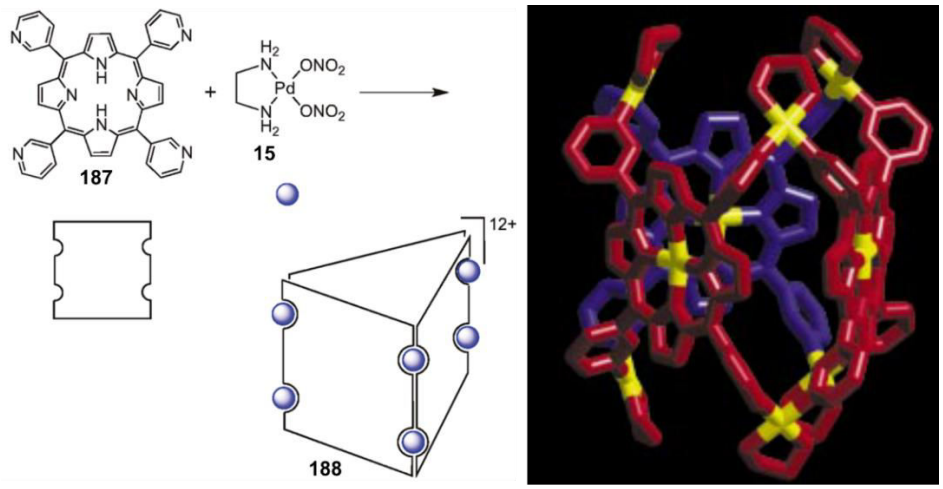

Scheme 1.40: Synthesis and crystal structure of molecular box **188**. Reprinted with permission from *Angew. Chem. Int. Ed.*, **2001**, *40*, 1718. Copyright (2001) WILEY-VCH.

Mukherjee and co-workers have reported a molecular barrel **189** by using 5,10,15,20-tetra*kis*-(4-pyridyl)porphyrin ($tppH_2$, **226**) and *cis*-[Pt(dppf)$(OTf)_2$] (**110**) (Scheme 1.41).[165] The structure was confirmed by NMR and single crystal diffraction, which revealed that the dimension of the hollow barrel is 2.7 nm × 2.7 nm × 1.9 nm with an internal volume of 13550 $Å^3$.

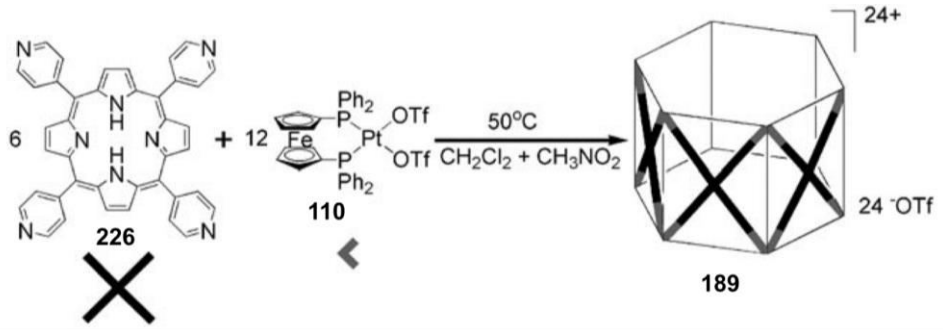

Scheme 1.41: Assembly of hexagonal open-box **189**. Reprinted with permission from *Angew. Chem. Int. Ed.*, **2008**, *47*, 8455-8459. Copyright (2008) WILEY-VCH.

1.3 Dynamic Assembly Approach

There are fewer examples on metal-coordination driven dynamic heteroleptic architectures that exist as the exclusive species in solution compared to step-wise directed constructs. The reason for this is that it is still challenging to control simultaneously the coordination of two or more ligands in solution, as in the absence of any structural "instruction"; thus the ligands prefer to self-assemble, "*self-sorting*" process.[166-171] However, a better understanding of the dynamic nature of the metal-ligand bonds and the availability of a large variety of designer building-blocks have started to pave the way for synthesis of intricate architectures *via* this dynamic assembly protocol.

1.3.1 Tetra-coordinated Systems

Schmittel *et al.* have described the synthesis of mononuclear phenanthroline-Cu(I) heteroleptic complexes by obstructing the formation of *bis*homoleptic complex by means of imbedded steric constrain.[172] This synthetic approach is based on using various bulky 2,9-diarylphenanthroline ligands along with its unhindered counterpart, which can lead to the quantitative formation of two component motifs. Using this design rationale, Schmittel and co-workers have constructed a large variety of heteroleptic architectures, such as nanoboxes,[173] nanobaskets,[174] nanogrids,[175] racks,[176] tweezers (**192** Scheme 1.42),[177] ring-in-ring structures (**195-197**, Figure 1.31),[178] rectangles[179] *etc*. The same research group has also reported a four component "porphyrin stack" (**193, 194**, Scheme 1.42) by applying a similar synthetic procedure.[177] All these supramolecular structures formed exclusively and quantitatively despite their dynamic nature.

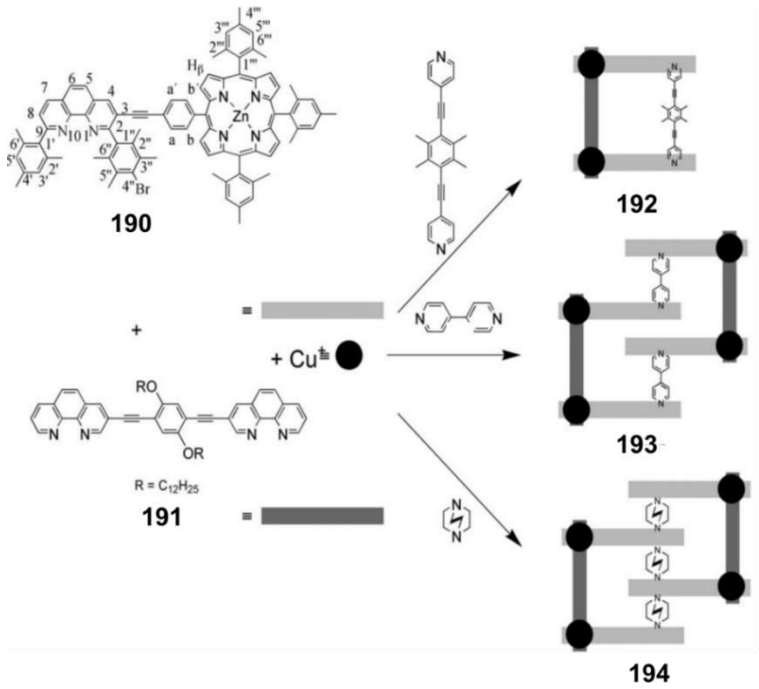

Scheme 1.42: Synthesis of molecular tweezer **192**, and molecular rack **193** and **194**. Reprinted with permission from *Chem. Eur. J.*, **2006**, *12*, 8136. Copyright (2006) WILEY-VCH.

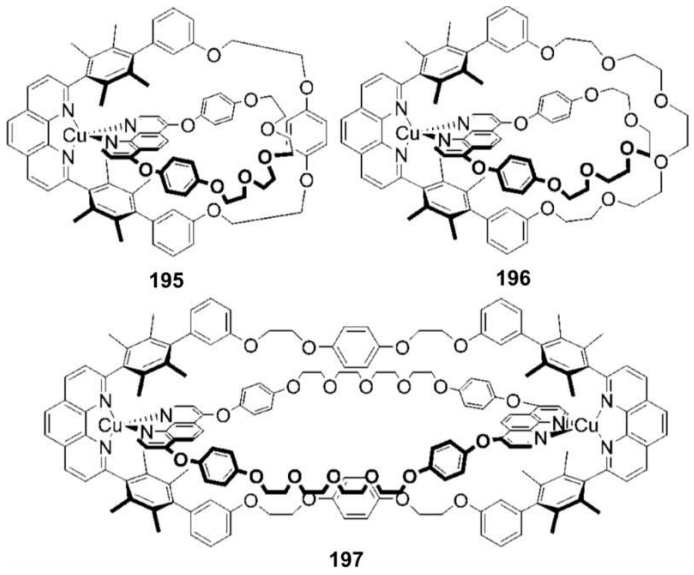

Figure 1.31: Cu-phenanthroline-based ring-in-ring structures. Reprinted *Org. Lett.*, **2002**, *4*, 2289. Copyright (2002) American Chemical Society.

Fujita *et al*. have reported the synthesis of a mononuclear, heteroleptic, square-planar palladium complex.[180] The proposed structure was obtained in quantitative yield by simply mixing equimolar amounts of pyridine and 2,6-dimethylpyridine in presence of *cis*-protected Pd(II) corner unit. Based on this synthetic strategy, assembly of diverse two- and three-dimensional, multi-component Pd(II) complexes has also been reported.[180] Utilizing similar steric hindrance methods, Stang *et al.* have prepared a molecular square by reacting a *cis*-protected corner unit with an unsymmetrical bipyridine units.[181] The squares were characterized by multinuclear NMR and ESI-MS.

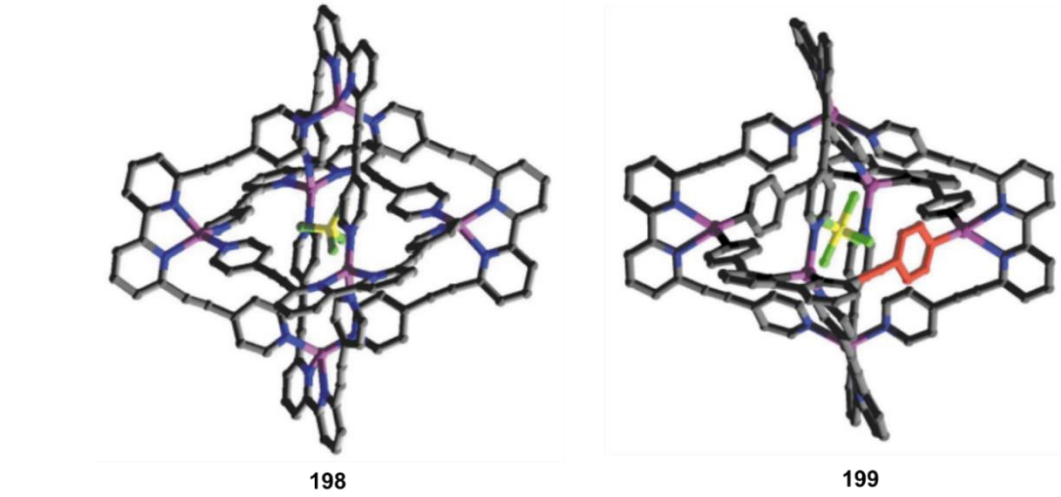

Figure 1.32: Crystal structures of Cu-Borromean cage (**198**) and Ag-Borromean cage (**199**). Reprinted with permission from *Chem. Commun.*, **2003**, 682. Copyright (2003) Royal Society of Chemistry.

Champness et *al*. have prepared a supramolecular Borromean cages without controlling the heteroleptic complex formation at the mononuclear stage.[182] The ligand 6,6'- *bis*(4-ethynylpyridine)-2,2'-bipyridine was reacted with Ag(I) and Cu(I) to obtain two hexanuclear cages **198** and **199** (Figure 1.32). These macrocycles were characterized by NMR and X-ray crystallography and were shown to encapsulate anions in the solid state.

1.3.2 Penta-coordinated Systems

Rizzarelli and co-workers have reported the controlled formation of a Cu(II)-(tpy)(bpy) complex.[183] The sole formation of this multicomponent complex is governed by thermodynamic parameter enthalpy. In the reaction, 50% of the Cu(II) can form the ideal octahedral complex with terpyridine, and the remaining other 50% can form an unfavored tetrahedral complex with bipyridine or, alternatively, all Cu(II) can form a pentacoordinated molecule. The reaction the production of the heteroleptic complex, infact, in quantitative yield as the formation of Cu(II)-(tpy)(bpy) is strongly exothermic (ΔG = -19.2 kcal mol^{-1}). This crafty design strategy was used by Lehn *et al*. to synthesize supramolecular helicates **200-202** (Figure 1.33).[184,185] These helicates were confirmed by FAB-MS and X-ray crystallography.

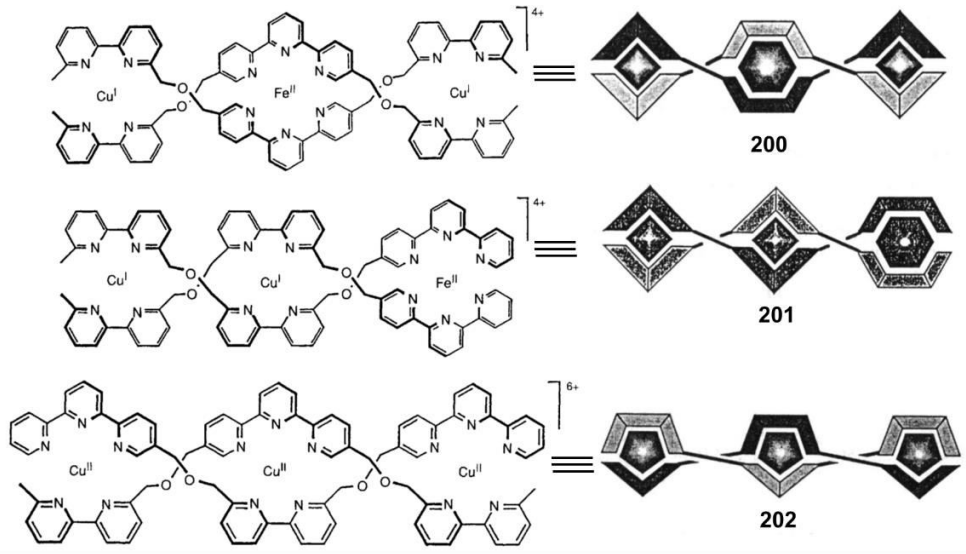

Figure 1.33: Structure of the heteroleptic helicates **200-202**. Reprinted with permission from *Proc. Natl. Acad. Sci.*, **1996**, *93*, 1397. Copyright (1996) National Academy of Science.

Sauvage and co-workers have used pentacoordinated Cu(I)-terpyridine-phenanthroline motifs to synthesize various rotaxanes[186-189] as well as "molecular muscles".[190,191] Macrocycles **203** and **204**[187] contain a thread involving 1,10-phenanthroline and 2,2'-bipyridine respectively, and a ring incorporating both a bidentate chelate (1,10-phenanthroline) and a tridentate fragment (terpyridine). They were shown to undergo an electrochemically driven pirouetting motion of the ring around the axis, which takes place on the millisecond timescale (Scheme 1.42). Rotaxane **205**[191] (Figure 1.34) is doubly threaded with 1,10-phenanthroline and terpyridine units. At the initial stage, two Cu(I) ions are coordinated by two phenanthrolines and was quantitatively demetallated by KCN. Addition of Zn(II) to the unmetallated rotaxane lead to the formation terpyridine complex, resulting in the contraction of the size of the molecule; on the other hand, addition of excess Cu(I) to the Zn(II)-complex formed the phenanthroline complex, causing expansion of the molecule, reminiscent of contraction and expansion of muscles.

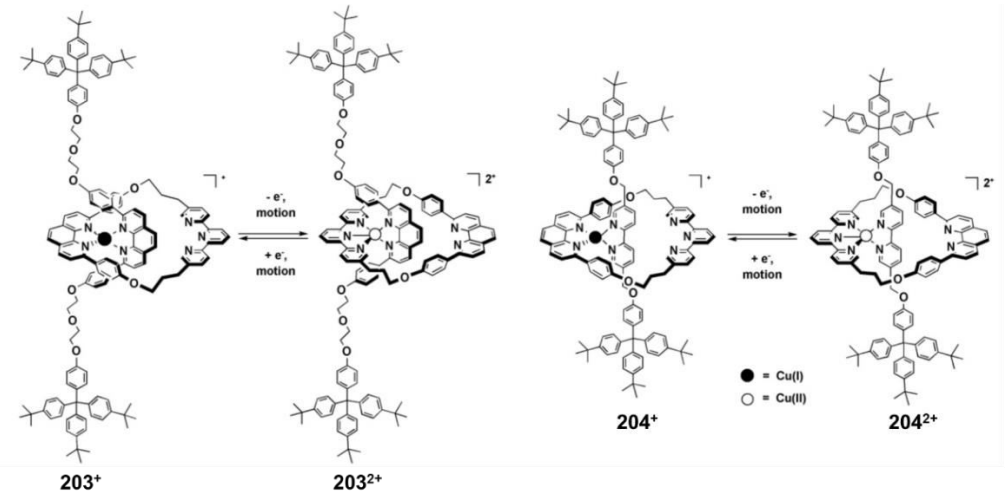

Scheme 1.43: Electrochemically driven pirouetting motion of **203** and **204**. Reprinted with permission from *Chem. Commun.*, **2004**, 474. Copyright (2004) Royal Society of Chemistry.

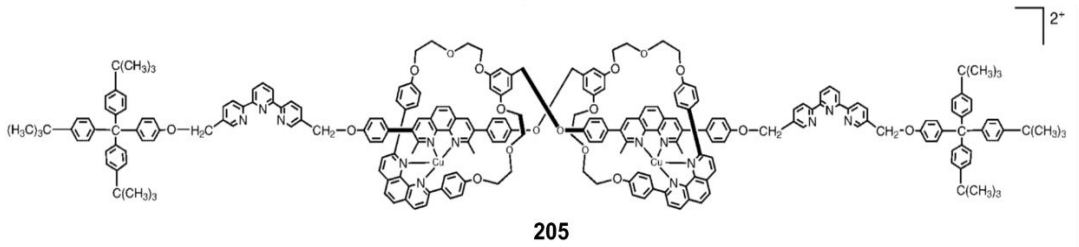

Figure 1.34: Terpyridine and phenanthroline-based molecular muscle **205**. Reprinted with permission from *Chem. Eur. J.*, **2002**, *8*, 1456. Copyright (2002) WILEY-VCH.

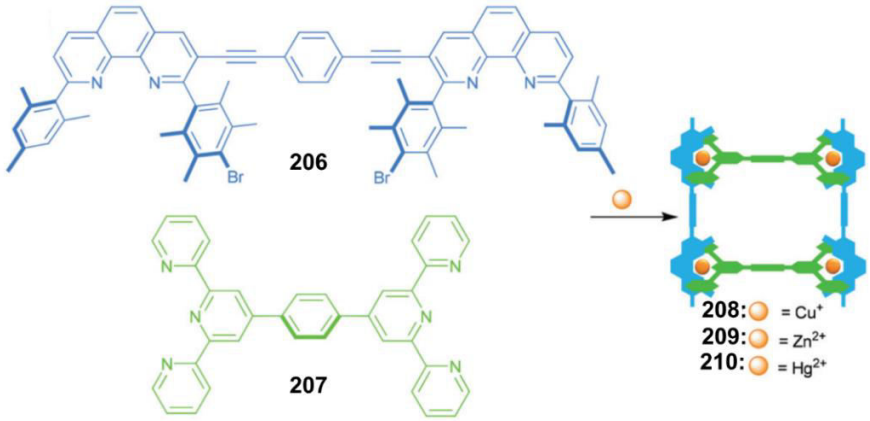

Scheme 1.44: Synthesis of nano-ladders **208-210**. Reprinted with permission from *J. Am. Chem. Soc.*, **2005**, *127*, 11544. Copyright (2005) American Chemical Society.

Schmittel *et al.* have used sterically hindered 2,9-diarylphenanthroline in combination with a terpyridine unit to form various heteroleptic architectures, including nano-ladder,[192] molecular dumbbell,[193] molecular wheel,[194] nano-prism,[195,196] and isosceles triangle.[197] The nano-ladders **208**-**210**,[192] assembled with Zn(II), Cu(II), and Hg(II) respectively; the proposed structures were confirmed by ^{1}H NMR, ESI-MS. The X-ray data of **209** showed that the pentacoordinated Zn(II) ions adopt a distorted trigonal-bipyramidal geometry. The nano-prisms[195] were constructed by reacting tritopic *tris*-phenanthroline and various *bis*terpyridine ligands with Cu(I). NMR and ESI-MS data revealed presence of a

small amount of oligomeric complexes in the solution; however, the use of *tris*pyridines as templates, produces the desired nano-prism as the exclusive product. The alternative approach, using a *tris*terpyridine as the tritopic panel and *bis*-phenanthroline, as the pillar, also produced the complimentary nano-prisms.[196]

1.3.3 Hexa-coordinated Systems

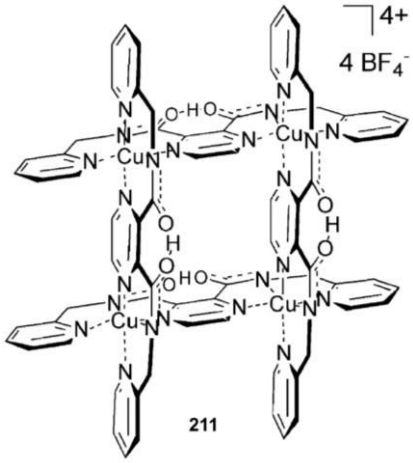

Figure 1.35: Tetranuclear nano-rack **211**. Reprinted with permission from *Inorg. Chem.*, **2009**, *48*, 2456. Copyright (2009) American Chemical Society.

Lehn and co-workers reported the formation of a triazine and terpyridine-based cylindrical architecture using Pb(II) metal ion.[198] The proposed structure was confirmed by spectral and crystallographic data. More recently, the same group has reported the synthesis of another molecular rack **211** (Figure 1.35) by assembling a terpyridine-based ligand with an imine-based ligand in presence of Cu(II).[199] X-ray crystallography data confirmed the structure; however, in solution the formation of some homoleptic complex was detected.

Stoddart *et al*. have reported the synthesis of molecular Borromean rings **213-215**.[200] These intertwined rings were generated *in situ* by reacting ligand **212** with Zn(II) and Cu(II) metal ions and their structures were characterized by NMR and ESI-MS.

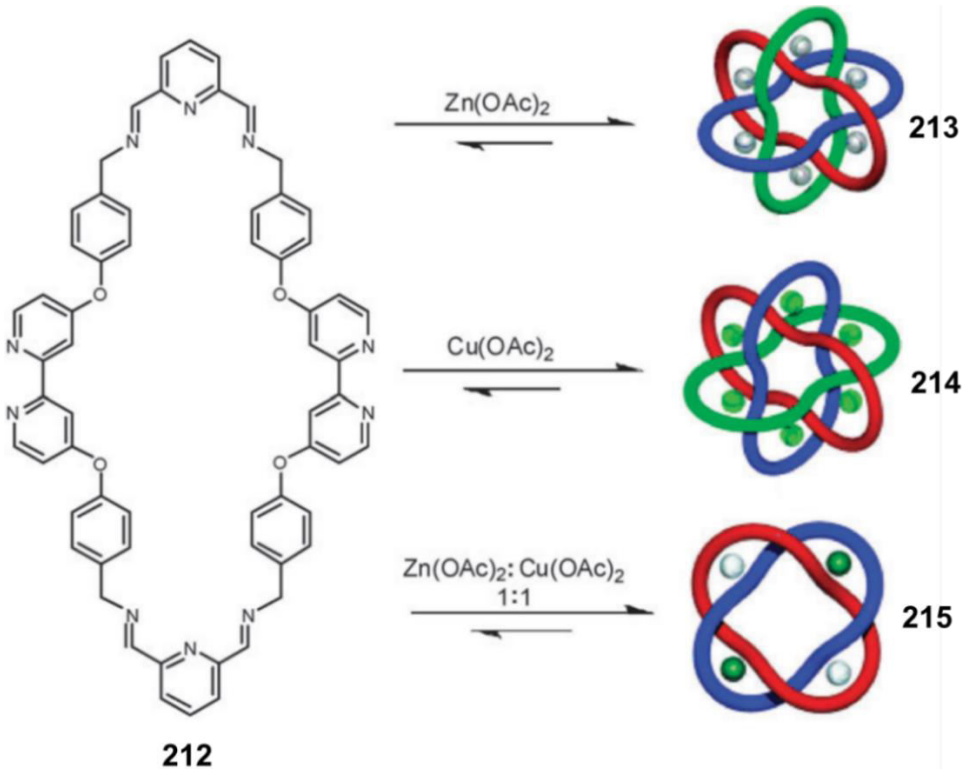

Scheme 1.45: Assembly of Borromean rings **213-215**. Reprinted with permission from *Science*, **2004**, *304*, 1308. Copyright (2004) The American Association for the Advancement of Science.

Newkome and co-workers have constructed various terpyridine-based heteroleptic architectures *via* the dynamic assembly approach, generating molecular spoked wheels,[201-204] molecular rhombus,[205] isomeric molecular bow-tie and butterfly,[26] and structural mimic of the G1 Sierpiński triangle.[27] The spoked wheel **219**[201] was quantitatively obtained by reacting a *tris*terpyridine **218** and a hexa*kis*(terpyridine) **217** in presence of Cd(II) (Scheme 1.46). The complex was characterized by NMR, ESI-MS, and TEM. On the other hand,

bicycle wheel **220**[202] was constructed by assembling two different *tris*terpyridine ligands **216** and **218** with Zn(II) in a near quantitative yield.

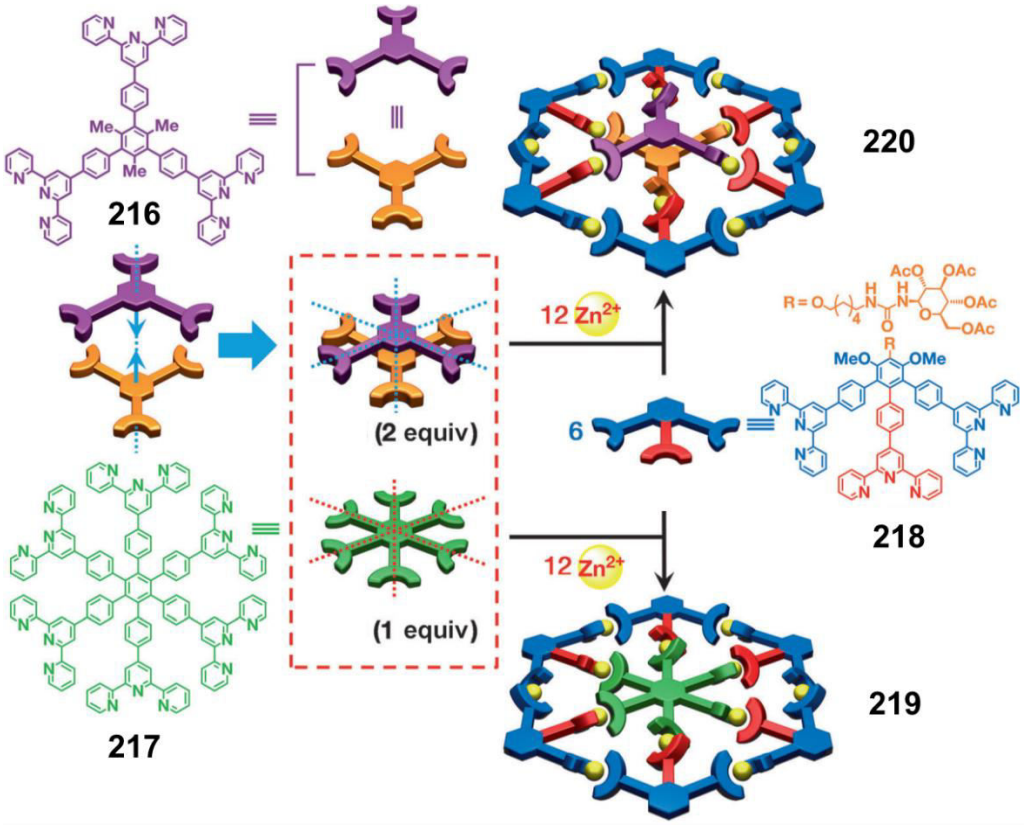

Scheme1.46: Synthesis of spoked-wheel **219** and bicycle wheel **220**. Reprinted with permission from *J. Am. Chem. Soc.*, **2014**, *136*, 18149. Copyright (2014) American Chemical Society.

The isomeric bow-tie **224** and **225** butterfly[26] were also obtained quantitatively by reacting Ru(II)-dimer **223** with two different tetra*kis*(terpyridine) ligands **221** and **222**, respectively, in presence of Cd(II) metal ion. These heteroleptic and heterometallic structures were confirmed by ^{1}H NMR and ESI- and TWIM MS data.

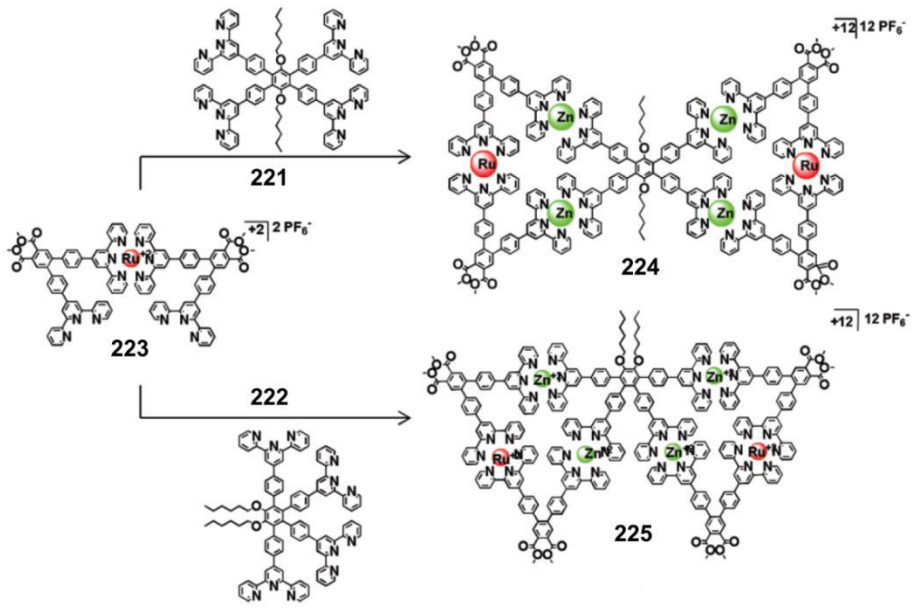

Scheme 1.47: Assembly of molecular bow-tie **224** and butterfly **225**. Reprinted with permission from *J. Am. Chem. Soc.*, **2012**, *134*, 7672. Copyright (2012) American Chemical Society.

1.4 Concluding Remarks

The design and synthesis of various heteroleptic and heterometallic constructs have been realized primarily by two different modes of assembly: step-wise and dynamic. The step-wise assembly has made considerable advancement in recent years due the to availability of a large variety of preprogramed monomers; however, the potential of dynamic assembly approach is yet to be fully appreciated since this procedure dictates that a single discrete assembly requires significant thermodynamic advantage over other possible combinations, in essence, one must plan the construction of unique directed building blocks.

CHAPTER II

MULTICOMPONENT REASSEMBLY OF TERPYRIDINE-BASED MATERIALS: QUANTITATIVE METALLOMACROCYCLIC REARRANGEMENTS

2.1 Introduction

Inspiration from supramolecular biological assemblies[201,202] has paved the way for many diverse and intricate structures. Pioneering works by Lehn[5] followed by that of Stoddart,[203] Fujita,[30] Stang,[18] Meijer,[204] Schmittel,[34] Newkome,[205] and others[49,206-210] have all successfully employed weak interactions to prepare well-defined, complex molecular architectures. Among all of the exploited non-covalent binding interactions, coordination-driven assembly has turned out to be one of the most prevalent methods due to the availability of a large assortment of ligands and metal ions.[19,35] More specifically, [2,2':6',2"]-terpyridine-based building blocks have drawn extensive attention due to their ability to form stable ML_2-type complexes with various transition metal ions and synthetic ease to instil predetermined structural features into the polytopic ligands.[45] The majority of metallosupramolecular constructs utilize a highly symmetric monomers involving homoleptic assemblies;[46] however, the scope of heteroleptic assemblies involving two or more components has not been entirely realized due to their inherent tendency to produce

competitive products resulting from "*self-sorting*".[16,47] Growing interest to incorporate greater structural complexity into molecular motifs via heteroleptic assemblies goes along with the challenge to produce a single, discrete architecture in a multi-component system.[211] Schmittel *et al*.[212] have reported eloquent catalytic "fusion", reminiscent of "gene shuffling," to obtain *tris*heterometallic scalene triangles by combining rectangular and equilateral motifs. As well, Stang and co-workers[213] have described the stoichiometric conversion of two homoleptic complexes into a heteroleptic structure. Recently, we reported the assembly of variety of novel architectures, such as a Sierpiński triangle,[27] molecular bow-tie and butterfly,[26] hexagonal spoked wheel,[214] and a molecular rhombus[215] using simple heteroleptic protocols.

Herein, we report synthesis of novel terpyridine-based, bimetallic triangles *via* metallomacrocyclic fusion transformations; ramifications include the utility of shape-specific, supramolecular species, as multicomponent building block donors, leading to more complex materials.

2.2 Results and Discussion

Initially, *bis*terpyridine **227** was prepared by a Suzuki cross-coupling from 4'-(4-boronatophenyl)-[2,2':6',2"]-terpyridine and 4,5-dibromo-1,2-dimethoxybenzene following a literature procedure.[27] Dimer **228** was synthesized from **227** by a slightly modified literature procedure.[216] Upon refluxing ligand **227** with $Ru(DMSO)_4Cl_2$ in $CHCl_3$/MeOH (1:1 v/v) for 12hr, followed by column chromatography (Al_2O_3, eluting with satd. KNO_3 (*aq*): H_2O:MeCN (1:1:60, v/v/v) afforded (50%) dimer **228**. Homoleptic triangles **229** and **230** (Scheme 2.1) were obtained in a quantitative yield by reacting ligand

227 with Zn(II) or Cd(II), respectively.[217] Dimer **228** was reacted with either Zn(II) or Cd(II) to obtain the heteroleptic tetrameric construct **231** and **232** (Scheme 2.1), respectively, in quantitative yield.[69] Metallo-triangles **229** and **230** and metallo-square **231** and **232** were completely characterized by NMR spectroscopy and ESI-MS spectrometry. To the Zn-triangle **229** in MeOH, the Ru-Zn-tetramer **231** in MeOH was added in a precise 1:1.5 ratio. The reaction mixture was stirred at 25 °C for 30 minutes, then a saturated solution of NH_4PF_6 in MeOH was added to exchange the counterions from NO_3^- to PF_6^-. The PF_6 complex was repeatedly washed with MeOH to remove any excess NH_4PF_6. The resulting bimetallic triangle **233** (Scheme 2.2) was collected without any further purification as an orange solid.

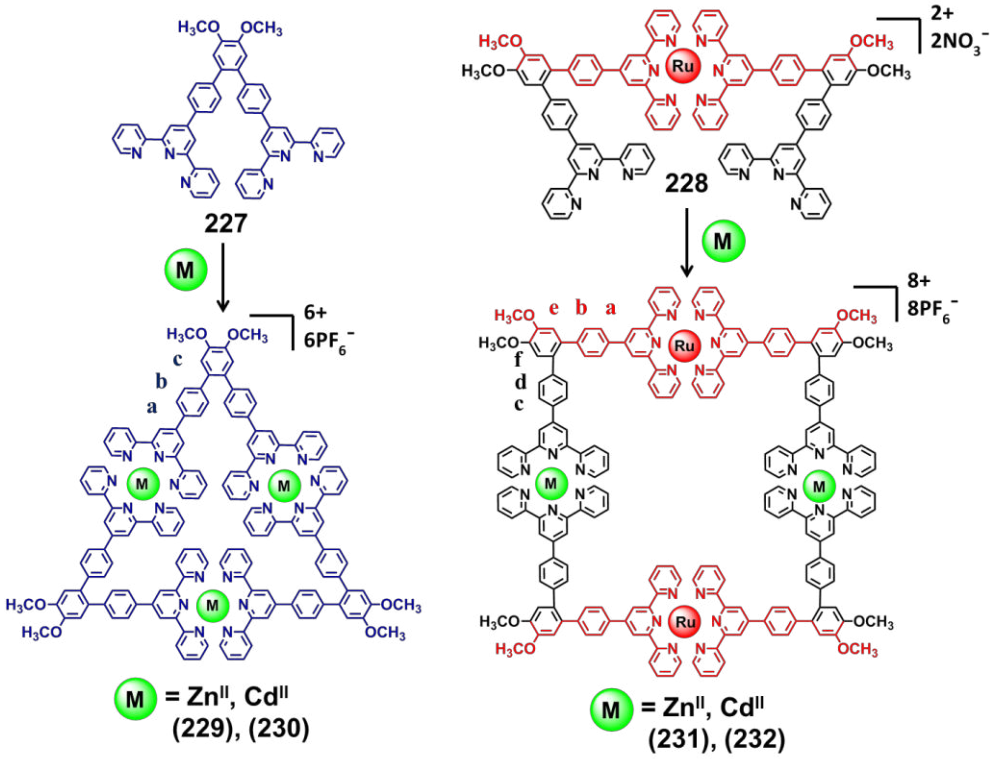

Scheme 2.1. Synthesis of triangle **229** and **230** and tetramer **231** and **232**.

The sharp, yet simple, ^{1}H NMR spectra (Figure 2.1) indicated the presence of a single discrete composition. Distinguished features of the ^{1}H NMR data include signals from three different 3',5'-tpy protons at 9.00, 8.97 and 8.96 ppm from arms **a**, **b** and **c**, (Scheme 2.2) respectively, with an ideal 1:1:1 integration ratio, which is in complete agreement with the proposed structure. The 3,3" and 6,6" protons showed the expected upfield and downfield shifts. The embedded methoxy markers appeared at 4.03, 4.02 and 4.01 ppm, respectively with an integration ratio of 1:1:1.

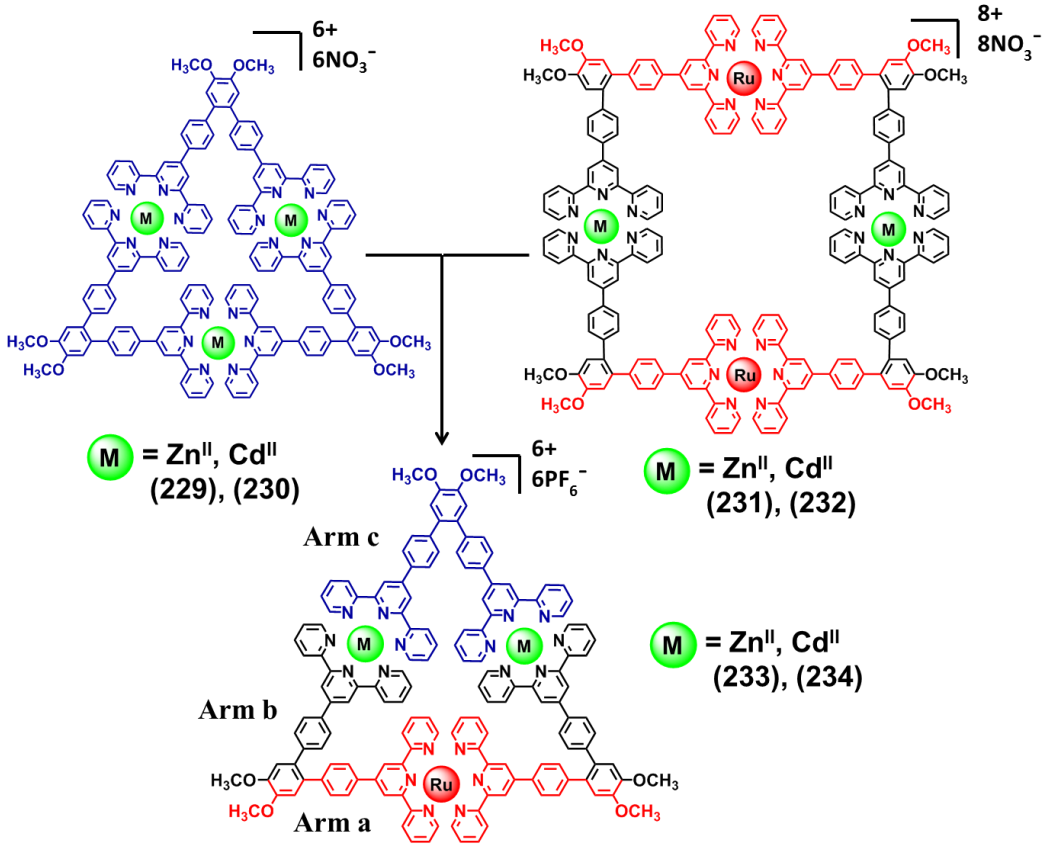

Scheme 2.2. Quantitative fusion of metallo-triangle **229** and **230** with metallo-square **231** and **232**, respectively, generated bimetallic triangles **233** and **234**. Arms **a**, **b**, and **c** are marked for ^{1}H NMR assignment.

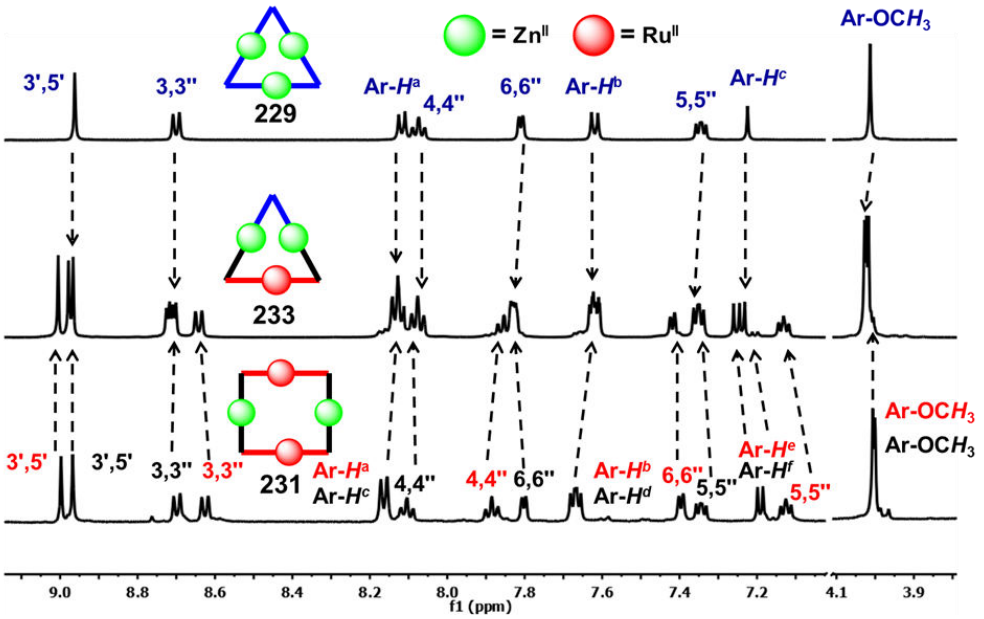

Figure 2.1: Stacked ^{1}H NMR spectra (500 MHz) of triangle **229** (top), tetramer **231** (bottom), and complex **233** (center) in CD_3CN.

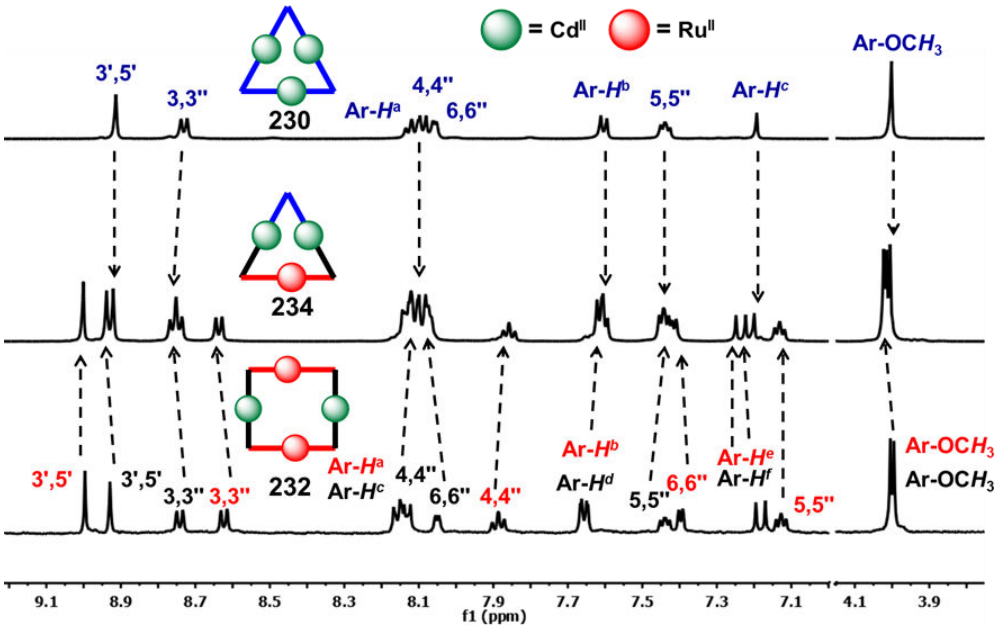

Figure 2.2: Stacked ^{1}H NMR spectra (500 MHz) of triangle **230** (top), tetramer **232** (bottom), and complex **234** (center) in CD_3CN.

All other terpyridine and aromatic protons were completely assigned with the aid of 2D-COSY and 2D-NOESY experiments. Triangle **233** was further characterized by ESI-MS coupled with TWIM-MS. In the ESI-MS (Figure 2.3), a series of dominant peaks was observed at m/z 415.1, 527.2, 695.2, 975.3, and 1534.9 corresponding to the states from +6 to +2 by the loss of PF_6^- anions. Additional support for **233** was obtained from ESI-TWIM MS. The TWIM-MS data (Figure 2.4) show a set of single, narrow bands for charge states 6+ to 3+, which is in complete agreement with the presence of a single discreet product. Triangle **233** could also be directly constructed from **227** and **228**. To an exact 1:1 mixture of ligand **227** and dimer **228** in $CHCl_3$, a methanolic solution of 2 equivalent $Zn(NO_3)_2 \cdot 6H_2O$ was added and was stirred for 30 minutes at 25 °C. The counterion was changed to PF_6^- and the bimetallic triangle **7** was recovered in quantitative yield. All the spectral data of **233** synthesized from either method were identical.

Bimetallic triangle **234** was constructed by following similar reaction conditions (Scheme 2.2). A methanolic solution of homoleptic Cd-triangle **230** and heteroleptic Ru-Cd-tetramer **232** in exact 1:1.5 ratio was stirred for 30 minutes at 25 °C. Counterion exchange generated (99%) triangle **234**, as an orange solid. Complex **234** was completely characterized by ^1H, COSY, NOESY, and ^{13}C NMR spectroscopy as well as ESI and TWIM-MS techniques. The ^1H NMR (Figure 2.2) exhibits three different 3',5' protons at 9.00, 8.94, and 8.92 ppm corresponding to arms **a**, **b**, and **c** (Scheme 2.2), respectively, with an expected 1:1:1 integration ratio, which is in excellent agreement with the suggested structure of **234**. Notable features of ^1H NMR data also include three sharp methoxy proton peaks at 4.02, 4.01, and 4.00 ppm, respectively, with the desired 1:1:1 integration ratio. All other

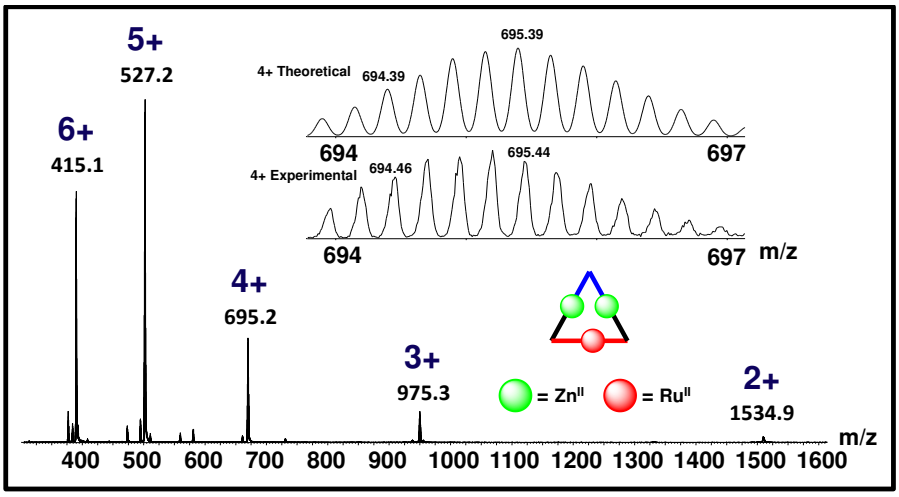

Figure 2.3: ESI-MS spectrum of **233** with calculated and experimental isotope patterns for the 4+ species.

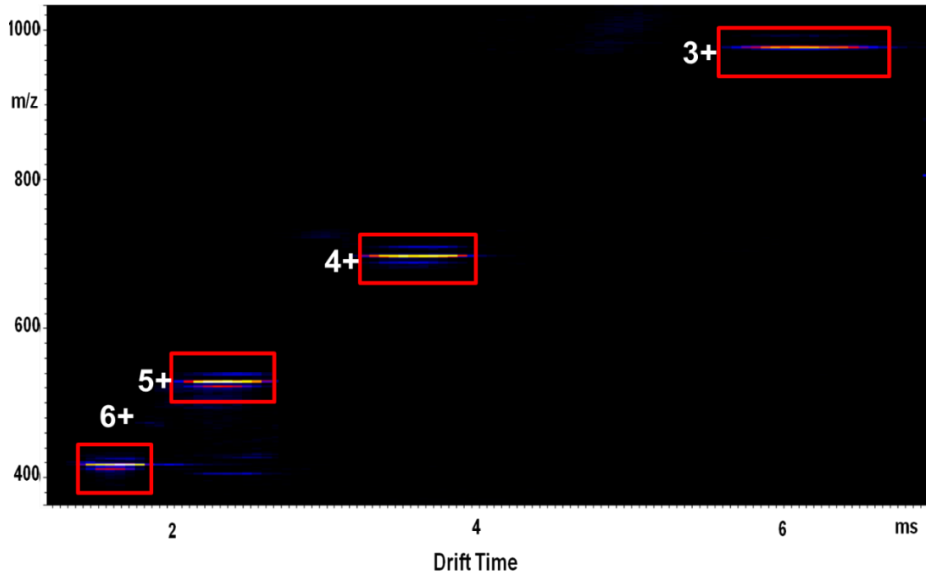

Figure 2.4: 2D ESI-TWIM-MS plot (mass-to-charge ratio *vs* drift time) of **233**. The charge states of intact assemblies are marked.

peaks for terpyridine and aromatic protons were easily assigned, based on the 2D-COSY and 2D-NOESY NMR data. Further evidence in support of **234** was obtained from ESI-MS coupled with TWIM-MS. In the ESI-MS (Figure 2.5), a series of peaks was observed

at m/z 430.1, 546.8, 718.2, 1006.9, and 1582.4 corresponding to the states from +6 to +2 by the loss of a varying number of PF_6^- anions; ESI-TWIM MS (Figure 2.6) showed a set of single narrow bands for charge states ranging from 6+ to 3+ indicative of a single component **234**. Alternatively, triangle **234** was also constructed from ligand **227** and dimer **228**. To an exact 1:1 mixture of ligand **227** and dimer **228** in $CHCl_3$, a methanolic solution of 2 equivalent $Cd(NO_3)_2 \cdot 4H_2O$ was added and then the reaction mixture was stirred for 30 minutes at 25 ºC. The counterion was changed to PF_6^- and the bimetallic triangle **234** was recovered in quantitative yield (99%). All of the spectroscopic data for **234** synthesized from either methods were identical.

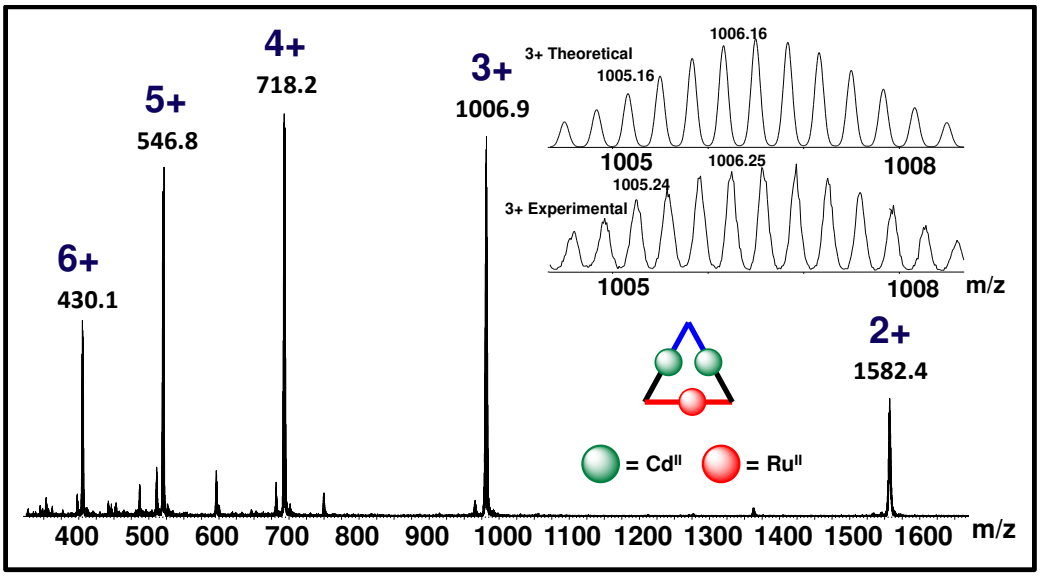

Figure 2.5: ESI-MS spectrum of **234** with calculated and experimental isotope patterns for the 4+ species.

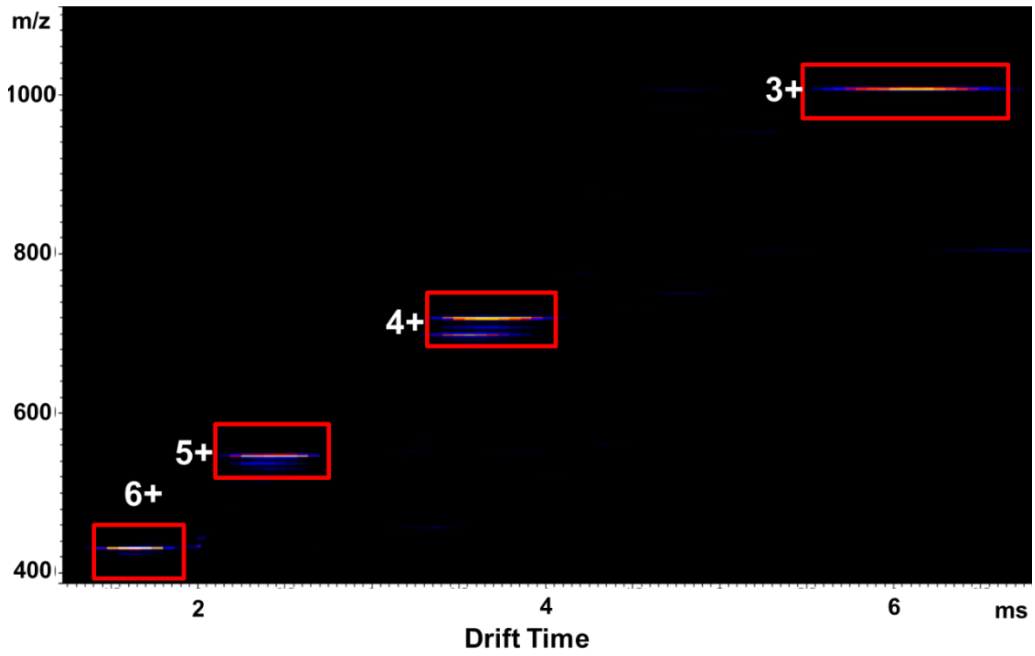

Figure 2.6: 2D ESI-TWIM-MS plot (mass-to-charge ratio *vs* drift time) of **234**. The charge states of intact assemblies are marked.

In addition, gradient MS (gMS^2) experiments for triangle **233** and **234** were performed to evaluate the stability of these heterometallic isosceles triangles and to give insight into their use as reagents in generating more complicated structures. The 5+ ion of **233** (Figure 2.7) at 527.2, which was exposed to collisionally activated dissociation at increasing energy, revealed stability up to 20 eV; at trap voltage of 35 eV, the 5+ charge almost dissipated, corresponding to a center-of-mass (COM) collision energy of 1.74 eV. Similarly, the gMS^2 spectra for triangle **234** were obtained (Figure 2.7) by exposing 5+ ion at 546.8 to collisionally activated dissociation at increasing collision energy. The experiment revealed that triangle **234** is less stable when compared to that of **233**. The 5+ charge of complex **234** showed good stability up to trap voltage 20 eV; it eventually disappeared at trap voltage of 33 eV, corresponding to a center-of-mass (COM) collision energy of 1.62 eV.

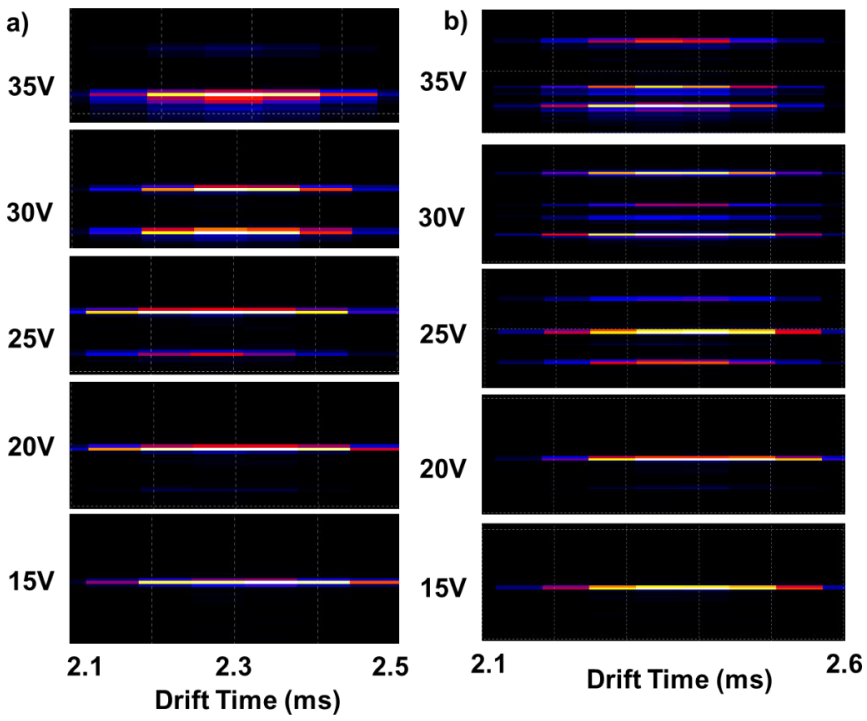

Figure 2.7: ESI TWIM-gMS^2 plot of the 5+ charge state of triangle a) **233** b) **234**.

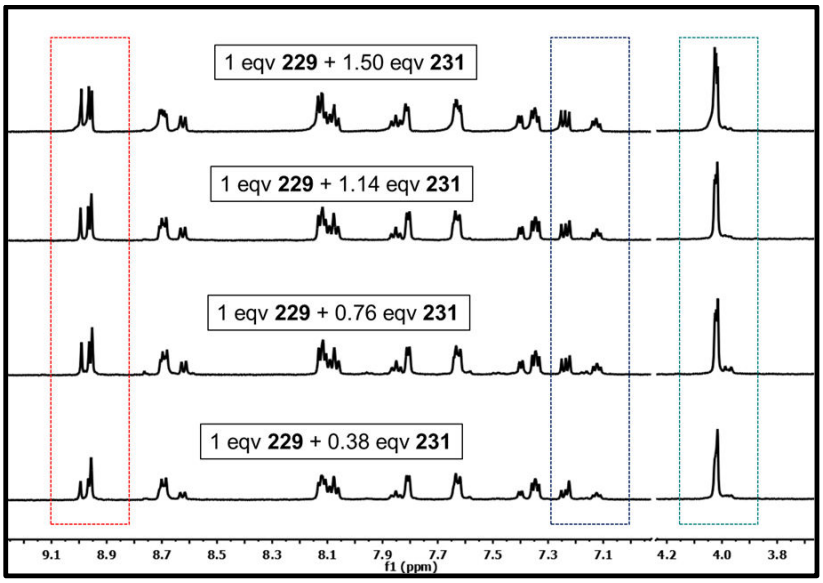

Figure 2.8: Stacked ^{1}H NMR spectra (500 MHz) of titration of triangle **229** with tetramer **231** to obtain bimetallic **233**.

The ^{1}H NMR titration experiments were performed to follow the progress of product formation. Thus, tetramers **231** and **232** were added in increasingly greater stoichiometric ratios to triangles **229** and **230**, respectively. The ^{1}H NMR spectra (Figures 2.8 and 2.9) exhibit the formation of the isosceles triangles **233** and **234** by the sequential appearance of product peaks; non-cyclic intermediates were not observed.

Photophysical properties of **227**, **229**-**234** have been studied using steady state absorption spectroscopy and fluorescence spectroscopy. Absorption spectra of **227**, **229**-

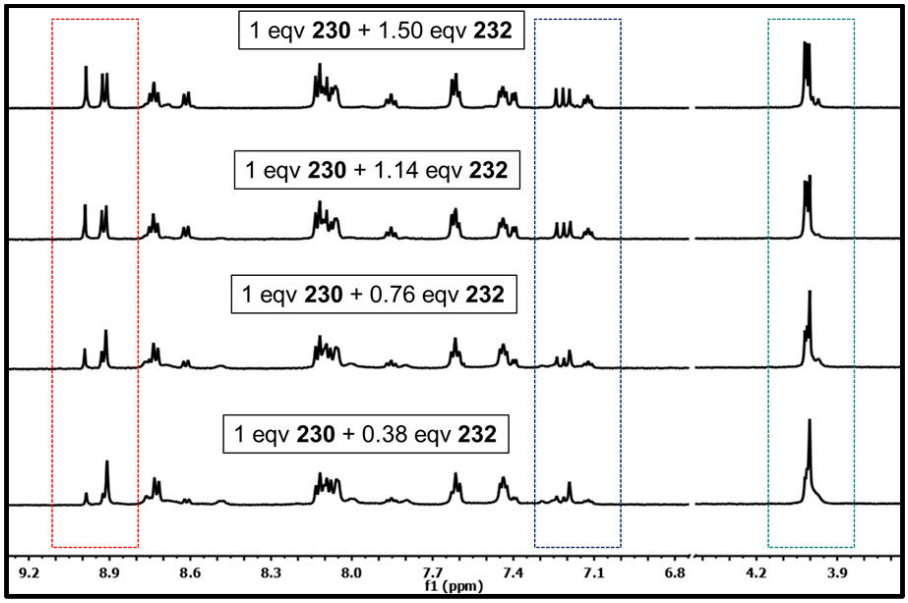

Figure 2.9: Stacked ^{1}H NMR spectra (500 MHz) of titration of triangle **230** with tetramer **232** to obtain bimetallic **234**.

234 are presented in (Figure 2.10). Ligand **227** exhibits typical ligand-to-ligand (LL) π-π* charge transfer (CT) bands at 285 and 330 nm are localized in the terpyridine-phenyl subunits. Complexation with Ru(II) results in a new metal-ligand charge transfer (MLCT) band at 483 nm due to the CT active Ru(II) center; however, MLCT band is not observed

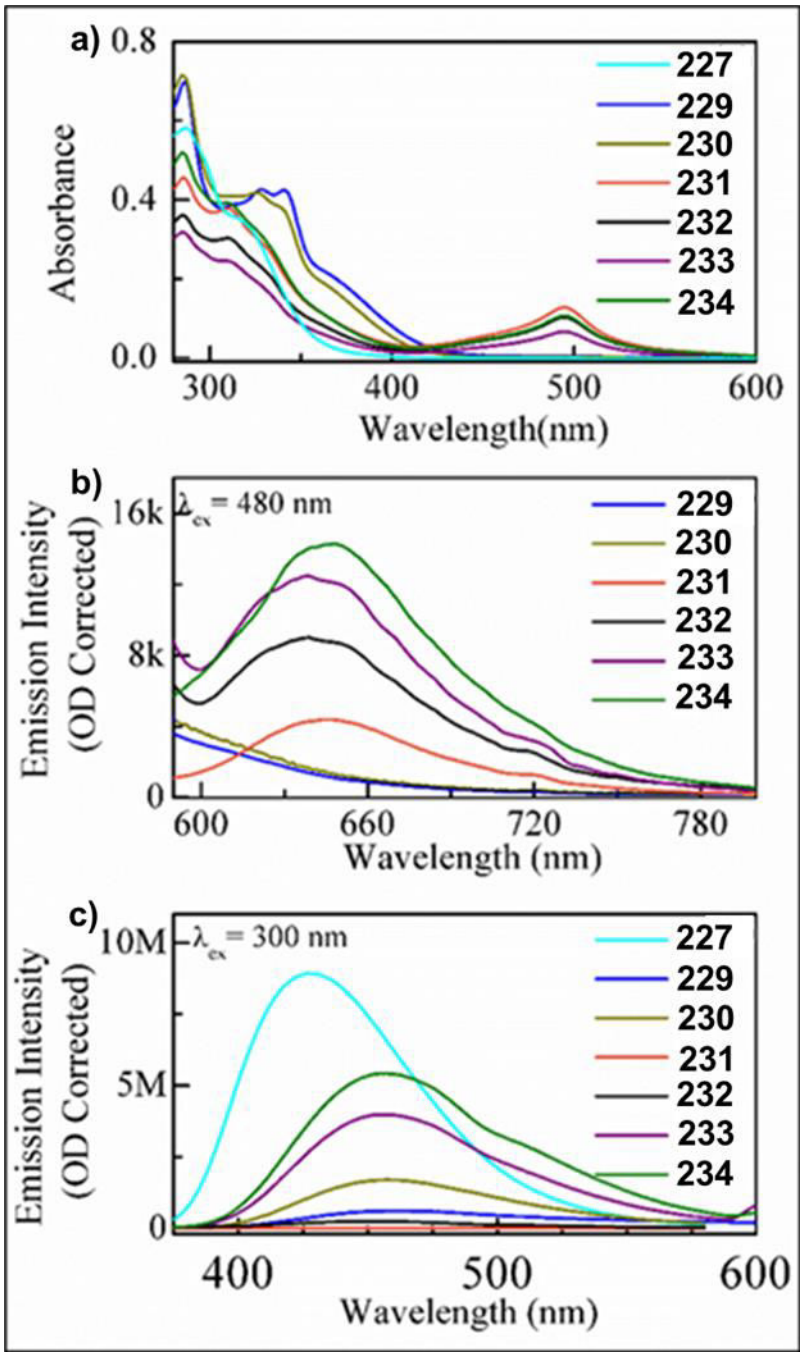

2.10 (a) Normalized UV-Visible spectra of **227**, **229**-**234**. (b) Corrected emission spectra of **229**-**234** by at the excitation wavelength λ_{ex}=480 nm. (c) Corrected emission spectra of **227**, **229**-**234** by at the excitation wavelength λ_{ex}=300 nm.

in case of tpy-Cd(II)-tpy and tpy-Zn(II)-tpy complexes. All photoluminescence spectra are corrected for fluctuation in absorbance at excitation wavelengths λ_{ex}= 480 nm and λ_{ex}= 300 nm. Emission intensities of the bimetallic triangles **233** and **234** are higher than those of bimetallic tetramers **231** and **232** at both the excitation wavelength 480 and 300 nm (Figure 2.7.1 b and c). All of the Cd(II) complexes show higher emission intensities when compared to their Zn(II) analogues, this is probably due to stronger quenching effect of Zn(II) than Cd(II).[218,219] Ligand centered π-π* charge transfer (CT) bands of **227** experienced red shift (Figure 2.7.1 c) upon complexation presumably because of change in electron distribution due to complexation.

2.3 Conclusion

In conclusion, two novel terpyridine-based heterometallic triangles were constructed by the reorganization of triangular and tetrameric metallomacrocyclic species, in quantitative yield. Both the resulting complexes **233** and **234** were unequivocally characterized using ^{1}H, COSY, NOESY, and ^{13}C NMR spectroscopy, as well as ESI and TWIM MS. The high yield preparation of these binuclear, precise molecular triangles, support their use as multicomponent sources, for example as 60° corner and capping reagents, in the preparation of higher generation supramolecular materials.

2.4 Experimental Section

General Procedures. Reagents and solvents were purchased from Sigma-Aldrich and used without purification. Thin layer chromatography (TLC) was performed on flexible sheets (Baker-flex) precoated with Al_2O_3 (IB-F) or SiO_2 (IB2-F) and visualized by UV light.

Column chromatography was conducted using basic Al_2O_3, Brockman Activity I (60-325 mesh) or SiO_2 (60-200 mesh) from Fisher Scientific. ^1H, ^{13}C, ^2D COSY, and NOESY NMR spectra were recorded on a Varian NMR 500. ESI mass spectrometry (MS) experiments were performed on a Waters Synapt HDMS quadrupole/time-of-flight (Q/ToF) tandem mass spectrometer. This instrument contains a triwave device between the Q and ToF analyzers, consisting of three collision cells in the order trap cell, ion mobility cell, and transfer cell. Trap and transfer cells are pressurized with Ar, and the ion mobility cell is pressurized with N_2 flowing in a direction opposite to that of the entering ions. In TWIM experiments, a pulsed field is applied to the ion mobility cell ("traveling wave" field) to separate the ions drifting inside it by their charge state and collision cross-section. MALDI-ToF-MS measurements were performed with a Bruker UltraFlex III ToF/ToF instrument, equipped with a Nd:YAG laser emitting at a wavelength of 355 nm. The proteins used to calibrate the drift time scale in TWIM-MS experiments in order to obtain collision cross-sections were acquired from Sigma-Aldrich. The ESI-TWIM-MS experiments were performed using the following parameters: ESI capillary voltage: 1.0 kV; sample cone voltage: 8 V; extraction cone voltage: 3.2 V; desolvation gas flow: 800 L h^{-1} (N_2); trap collision energy (CE): 1 eV; transfer CE: 1 eV; trap gas flow: 1.5 mL min^{-1} (Ar); ion-mobility cell gas flow: 22.7 mL min^{-1}(N_2); sample flow rate: 5μL min^{-1}; source temperature: 30 °C; desolvation temperature: 40 °C; TWIM traveling-wave height: 7.5 V; and TWIM traveling-wave velocity: 350 ms^{-1}. The sprayed solution was prepared by dissolving the sample (300 μg) in a mixture of MeCN/MeOH (1 mL; 1:1, v/v). Data analyses were conducted using the MassLynx 4.1 and DriftScope 2.1 programs provided by Waters. Photo luminescence spectra were collected by using a Horiba Jobin Yvon

FluoroMax-4 spectrofluorometer. The excitation and emission monochromators were set at 5 and 2 mm respectively, giving a spectral bandwidth of 4.25 nm. Quartz cell with 1 cm path length was used for all the experiments. The data interval was 0.5 nm and the integration time was 2.0 sec. Acetonitrile was used to prepare the solution for complexes and chloroform for ligand. Absorbance of the samples was kept less than 0.1 at the 480 nm excitation wavelength to avoid any inner-filter effect. The dark counts were subtracted and the spectra were corrected for wavelength-dependent instrument sensitivity. $Ru(DMSO)_4Cl_2$ was prepared according to a previously reported procedure.[251]

Synthesis of bimetallic triangle [(227)(228)(Zn^{2+})$_2$] (PF_6^-)$_6$ (233):

Method A: To a methanolic solution of triangle **229**[217] **[(227)$_3$$Zn_3^{2+}$] ($NO_3^-$)$_6$** (10 mg, 3.53×10^{-3} mmol), a methanolic solution of tetramer **231**[69] **[(2)$_2$(Zn^{2+})$_2$] (NO_3^-)$_8$** (20.35 mg, 5.30×10^{-3} mmol, 1.5 eq) was added. The solution was stirred for 30 minutes at 25 °C. Then excess NH_4PF_6 was added to obtain a light orange precipitate, which was filtered and washed repeatedly with MeOH to remove the excess NH_4PF_6. The product obtained (98%) as an orange solid: 35.02 mg.

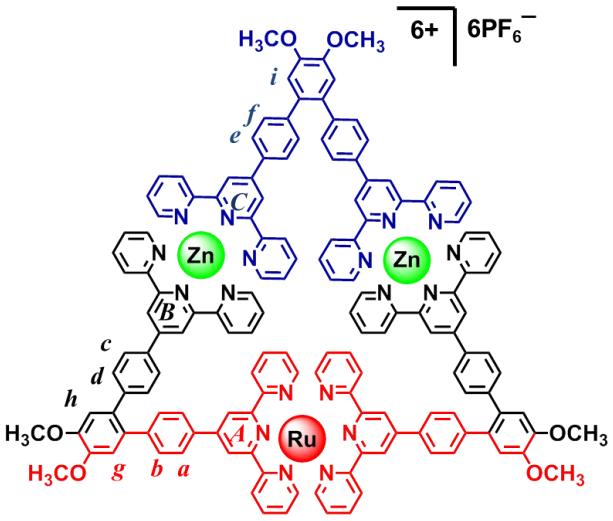

Method B: To a solution of ligand **227**[27] (5 mg, 6.64×10^{-3} mmol) and dimer **228**[216] (11.49 mg, 6.64×10^{-3} mmol) in $CHCl_3$ (10 mL), a methanolic solution (5 mL) of $Zn(NO_3)_2\cdot6H_2O$ (3.95 mg, 13.28×10^{-3} mmol) was added. The solution was stirred for 30 minutes at 25 °C then excess of NH_4PF_6 was added to generate a light orange precipitate, which was filtered and washed repeatedly with MeOH to remove excess NH_4PF_6. The product was obtained (98%) as an orange solid: 21.87 mg. ^{1}H NMR (CD_3CN, 500 MHz, ppm): δ 9.00 (s, 4H, tpy^A*H*$^{3',5'}$), 8.98 (s, 4H, tpy^B*H*$^{3',5'}$), 8.87 (s, 4H, tpy^C*H*$^{3',5'}$), 8.72 (d, *J* = 8.0 Hz, 4H, tpy^C*H*$^{3,3''}$), 8.70 (d, *J* = 8.0 Hz, 4H, tpy^B*H*$^{3,3''}$), 8.64 (d, *J* = 8.0 Hz, 4H, tpy^A*H*$^{3,3''}$), 8.14 (m, 12H, Ar-*H*^{a}, Ar-*H*^{c}, Ar-*H*^{e}), 8.08 (t, 8H, tpy^B*H*$^{4,4''}$, tpy^C*H*$^{4,4''}$), 7.83 (m, 12H, tpy^A*H*$^{4,4''}$, tpy^B*H*$^{6,6''}$, tpy^C*H*$^{6,6''}$), 7.62 (m, 12H, Ar-*H*^{b}, Ar-*H*^{d}, Ar-*H*^{f}), 7.42 (d, *J* = 5.0 Hz, 4H, tpy^A*H*$^{6,6''}$), 7.35 (m, 8H, tpy^B*H*$^{5,5''}$, tpy^C*H*$^{5,5''}$), 7.26 (s, 2H, Ar-*H*^{g}), 7.25 (s, 2H, Ar-*H*^{h}), 7.23 (s, 2H, Ar-*H*^{i}), 7.13 (dd, J_1 = 8.0 Hz, J_2 = 5.0 Hz, 4H, tpy^A*H*$^{5,5''}$) 4.03 (s, 6H, Ar-OC*H*$_3$), 4.02 (s, 6H, Ar-OC*H*$_3$), 4.01 (s, 6H, Ar-OC*H*$_3$); ^{13}C NMR (CD_3CN, 125 MHz, ppm): 157.28, 154.83, 154.49, 151.47, 148.86, 148.41, 148.35, 147.05, 146.96, 146.74, 143.54, 143.42, 142.59, 140.27, 137.06, 133.98, 133.33, 133.27, 131.13, 130.96, 130.90,

130.42, 126.85, 126.81, 126.60, 126.57, 126.50, 123.66, 122.33, 120.43, 113.24, 54.84. ESI-MS (*m/z*): 1534.9 $[M\text{-}2PF_6^-]^{2+}$ (calculated *m/z* = 1533.2) , 975.3 $[M\text{-}3PF_6^-]^{3+}$ (calcd. *m/z* =973.8), 695.2 $[M\text{-}4PF_6^-]^{4+}$ (calcd. *m/z* =694.2), 527.2 $[M\text{-}5PF_6^-]^{5+}$ (calcd. *m/z* = 526.3), 415.1 $[M\text{-}6PF_6^-]^{6+}$ (calcd. *m/z* = 414.4).

Synthesis of bimetallic triangle $[(227)(228)(Cd^{2+})_2]$ $(PF_6^-)_6$ (234):

Method A: To a methanolic solution of triangle **230**[217] $[(227)_3Cd_3^{2+}]$ $(NO_3^-)_6$ (10 mg, 3.36×10^{-3} mmol) a methanolic solution of tetramer **232**[69] $[(228)_2(Cd^{2+})_2]$ $(NO_3^-)_8$ (19.81 mg, 5.04×10^{-3} mmol, 1.5eqv) was added. The solution was stirred for 30 minutes at 25 °C. Then excess NH_4PF_6 was added to obtain a light orange precipitate, which was filtered and washed repeatedly with MeOH to remove excess NH_4PF_6. The product obtained (99%) as an orange solid: 34.67 mg.

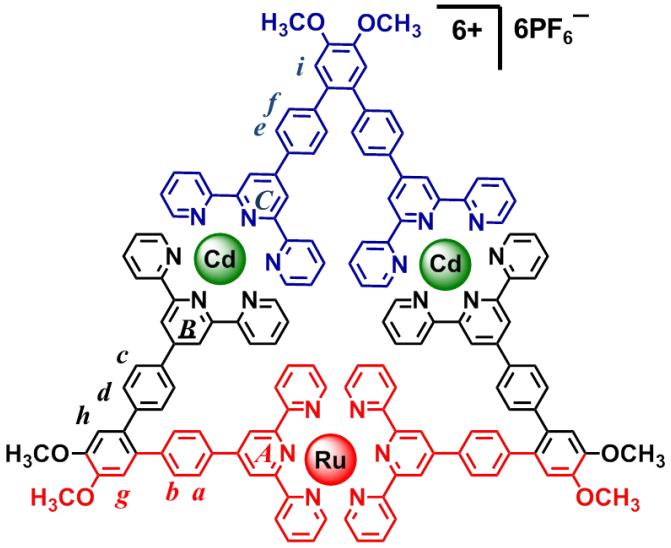

Method B: To a solution of ligand **227** (5 mg, 6.64×10^{-3} mmol) and dimer **228** (11.49 mg, 6.64×10^{-3} mmol) in $CHCl_3$ (10 mL), a methanolic solution (5 mL) of

$Cd(NO_3)_2 \cdot 4H_2O$ (4.10 mg, 13.28×10^{-3} mmol) was added. The solution was stirred for 30 minutes at 25 °C. Then excess NH_4PF_6 was added to give a light orange precipitate, which was filtered and washed repeatedly with MeOH to remove excess NH_4PF_6. The product obtained (99%) as an orange solid: 22.67 mg. ^{1}H NMR (CD_3CN, 500 MHz, ppm): δ 9.00 (s, 4H, tpy^A*H*$^{3',5'}$), 8.94 (s, 4H, tpy^B*H*$^{3',5'}$), 8.92 (s, 4H, tpy^C*H*$^{3',5'}$), 8.75 (t, 8H, tpy^B*H*$^{3,3''}$, tpy^C*H*$^{3,3''}$), 8.63 (d, J = 8.0 Hz, 4H, tpy^A*H*$^{3,3''}$), 8.10 (m, 28H, Ar-*H*^{a}, Ar-*H*^{c}, Ar-*H*^{e}, tpy^B*H*$^{4,4''}$, tpy^C*H*$^{4,4''}$, tpy^B*H*$^{6,6''}$ tpy^C*H*$^{6,6''}$), 7.86 (dd, J_1 = J_2 = 8.0 Hz, 4H, tpy^A*H*$^{4,4''}$) 7.64 (m, 12H, Ar-*H*^{b}, Ar-*H*^{d}, Ar-*H*^{f}), 7.47 (m, 8H, tpy^A*H*$^{6,6''}$, tpy^B*H*$^{5,5''}$, tpy^C*H*$^{5,5''}$), 7.28 (s, 2H, Ar-*H*^{g}), 7.26 (s, 2H, Ar-*H*^{h}), 7.24 (s, 2H, Ar-*H*^{i}), 7.17 (dd, J_1 =8.0 Hz, J_2 = 5.0 Hz, 4H, tpy^A*H*$^{5,5''}$) 4.06 (s, 6H, Ar-OC*H*$_3$), 4.05 (s, 6H, Ar-OC*H*$_3$), 4.04 (s, 6H, Ar-OC*H*$_3$); ^{13}C NMR (CD_3CN, 125 MHz, ppm): 157.34, 154.56, 153.88, 151.52, 149.40, 148.76, 148.47, 148.43, 147.96, 146.79, 143.47, 143.36, 142.72, 140.35, 137.11, 133.98, 133.38, 131.07, 130.45, 130.40, 130.42, 126.82, 126.77, 126.52, 126.43, 123.70, 122.84, 120.78, 120.52, 113.47, 113.40,113.36, 54.97, 54.95. ESI-MS (*m/z*): 1582.4 $[M\text{-}2PF_6^-]^{2+}$ (cald. *m/z* = 1583.2), 1006.9 $[M\text{-}3PF_6^-]^{3+}$ (calcd. *m/z* =1007.2), 718.2 $[M\text{-}4PF_6^-]^{4+}$ (calcd. *m/z* =719.1), 546.8 $[M\text{-}5PF_6^-]^{5+}$ (calcd. *m/z* = 546.3), 430.1 $[M\text{-}6PF_6^-]^{6+}$ (calcd. *m/z* = 431.1).

CHAPTER III

STEP-WISE CONSTRUCTION OF BIMETALLIC TRIANGLES BY SITE-SPECIFIC METALATION

3.1 Introduction

The assembly of supramolecular constructs *via* the spontaneous association of tailored organic modules has witnessed significant progress in past two decades.[46,220] Pioneering works of Lehn,[5,15,17] followed by contributions from Stang,[20,63,221] Fujita,[30,32,141] Newkome,[24,25,28] Schmittel,[33,34,222] and many others[35,38,40,49,223] have revealed the significance of metal-ligand coordinative interactions to build complex architectures. As proposed by Lehn, self-assembled supramolecules are generally an equilibrium distribution of all possible structure possessing comparable stabilities.[14,168] Thus, most supramolecular assemblies utilize symmetric building blocks in a homoleptic assembly to produce a single, discrete molecule.[46] Based on homoleptic methods numerous metallomacrocycles, such as: triangles,[56] squares and rectangles,[93] pentagons,[224] hexagons,[25] and other polygons[29,112,113,] have been synthesized. In contrast, mixtures of binary and multiple structures have been reported from heteroleptic assemblies.[18,23] Consequently, construction of intricate supramolecular architectures through a combination of two or more monomers still remains challenging. Various reaction conditions have been developed to isolate the most

thermodynamically stable species in a quantitative or near quantitative yield from a heteroleptic assembly.[26,34] These protocols have paved the way for the synthesis of higher ordered macrocycles *via* directed assemblies.[112,113,213,225] Terpyridine-based monomers have gained tremendous popularity due, in part, to the synthetic ease necessary to instil the pre-designed structural features and their ability to form complexes with different transition metals with varied stability.[45] We have assembled a molecular Sierpiński Gasket[24] and a molecular bow-tie and butterfly[26] *via* combination of step-wise and self-assembly protocol while modifying ligand structure as well as by taking advantage of the kinetic and thermodynamic nature of different <tpy-M^{II}-tpy> bonds. Recently, Wang *et al.* have reported step-wise synthesis of a terpyridine-based chair-like hexameric metallomacrocycle.[226] Herein, we report step-wise construction of three novel terpyridine-based bimetallic triangles *via* site-specific introduction of transition metal ions.

3.2 Results and Discussion

Initially, the 60º-based *bis*terpyridine **227** was readily prepared from 4,5-dibromoveratrole and 4'-(4-boronatophenyl)-[2,2':6',2'']-terpyridine using the Suzuki cross coupling reaction.[216] Ligand **227** was reacted with $Ru(DMSO)_4Cl_2$ to obtain oligomeric trimer **235** (Scheme 3.1). A 3:2 mixture of **227** and $Ru(DMSO)_4Cl_2$ in $CHCl_3$:MeOH (1:1 v/v) was refluxed for 24 hours. The reaction mixture was cooled to 25 ºC then dried *in vacuo* to generate a red residue, which was purified by column chromatography (Al_2O_3) eluting with satd. KNO_3:H_2O:MeCN (1:1:35 v/v/v) to obtain (48%) pure trimer **235**. Its ^1H NMR spectrum (Figure 3.1) displayed two very close yet distinctive 3',5'-terpyridine singlets at 9.00 (arm **A**) and 8.99 (arm **B**) ppm, respectively, corresponding to the two

complexed terpyridine and another singlet at 8.76 ppm (arm **C**) corresponding to uncomplexed terpyridine in an exact 1:1:1 ratio. The ^{1}H NMR spectrum also contains three singlets at 4.01, 3.99, and 3.97 ppm corresponding to three different –OCH_3 protons, which supports the proposed complex. All other aromatic protons were assigned with the help of 2D-COSY NMR data. Additional support for the proposed structure of **235** was provided by ESI-MS spectroscopy, *via* (Figure 3.6) a series of peaks at 1291.9, 840.9, and 615.7 corresponding to 2+, 3+, and 4+ charge states, respectively.

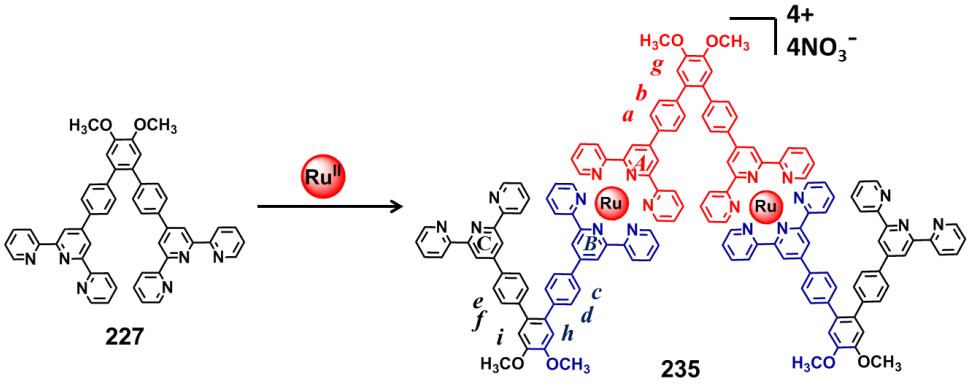

Scheme 3.1: Synthesis of oligomeric trimer **235** from *bis*terpyridine **227**.

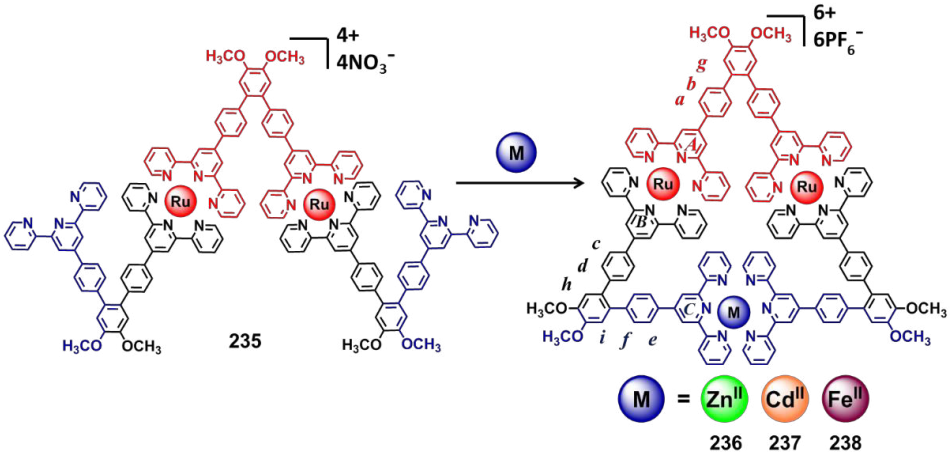

Scheme 3.2: Cyclization of trimer **235** to obtain bimetallic triangles **236**, **237**, **238**.

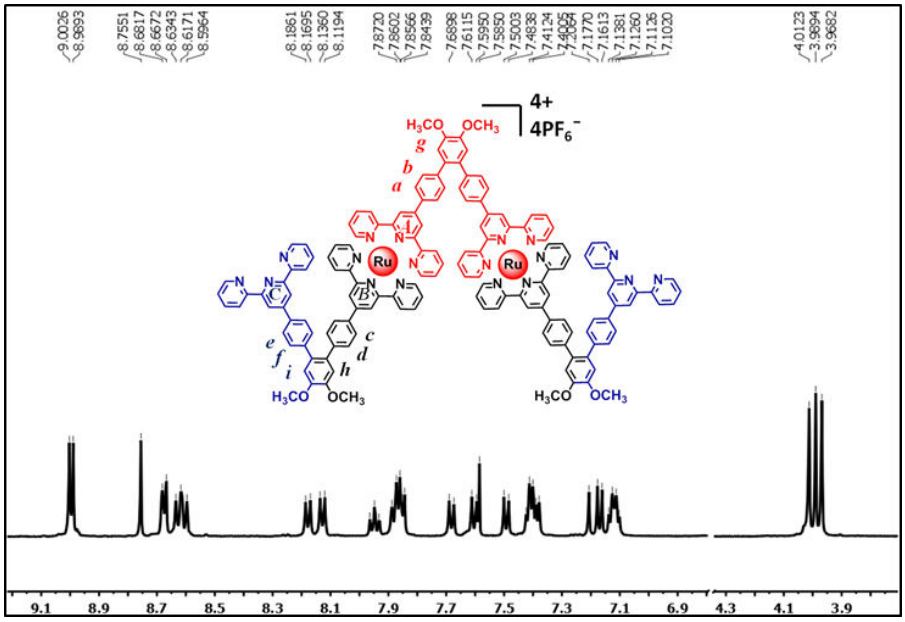

Figure 3.1: ^{1}H NMR spectrum of trimer **235**.

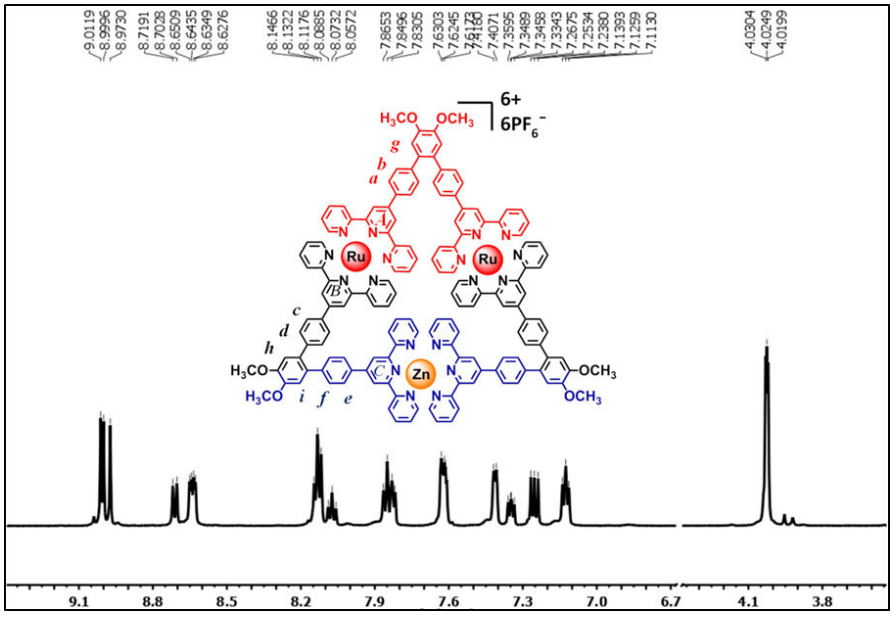

Figure 3.2: ^{1}H NMR spectrum of bimetallic triangle **236**.

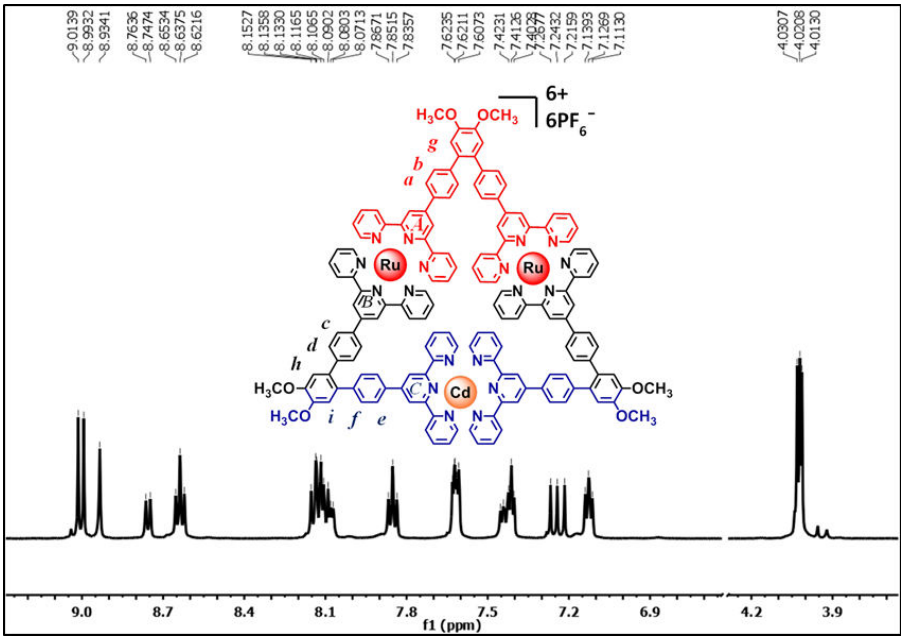

Figure 3.3: ^{1}H NMR spectrum of bimetallic triangle **237**.

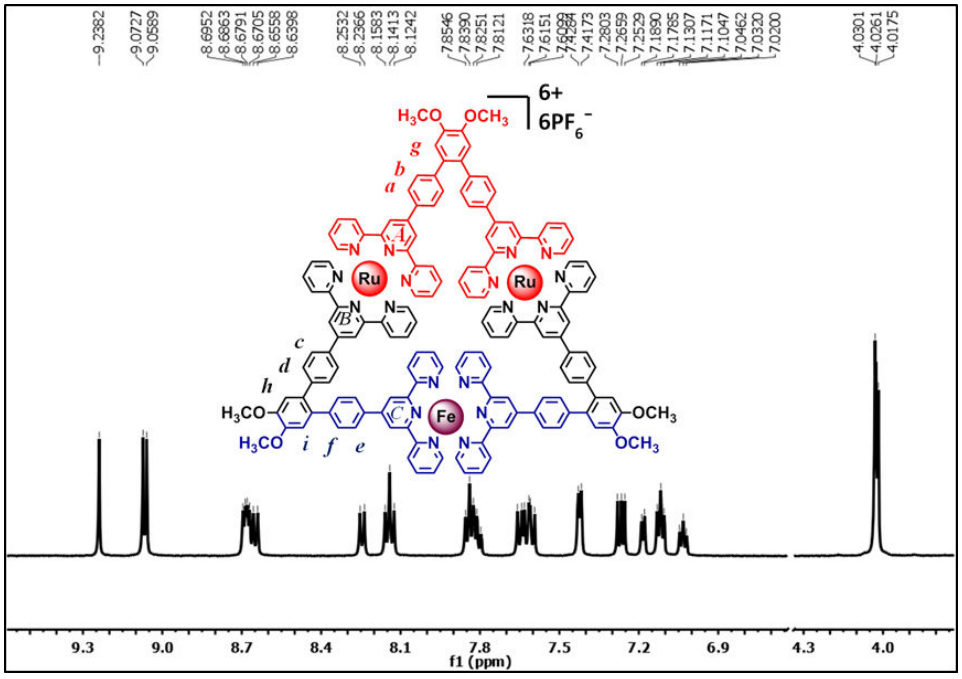

Figure 3.4: ^{1}H NMR spectrum of bimetallic triangle **238**.

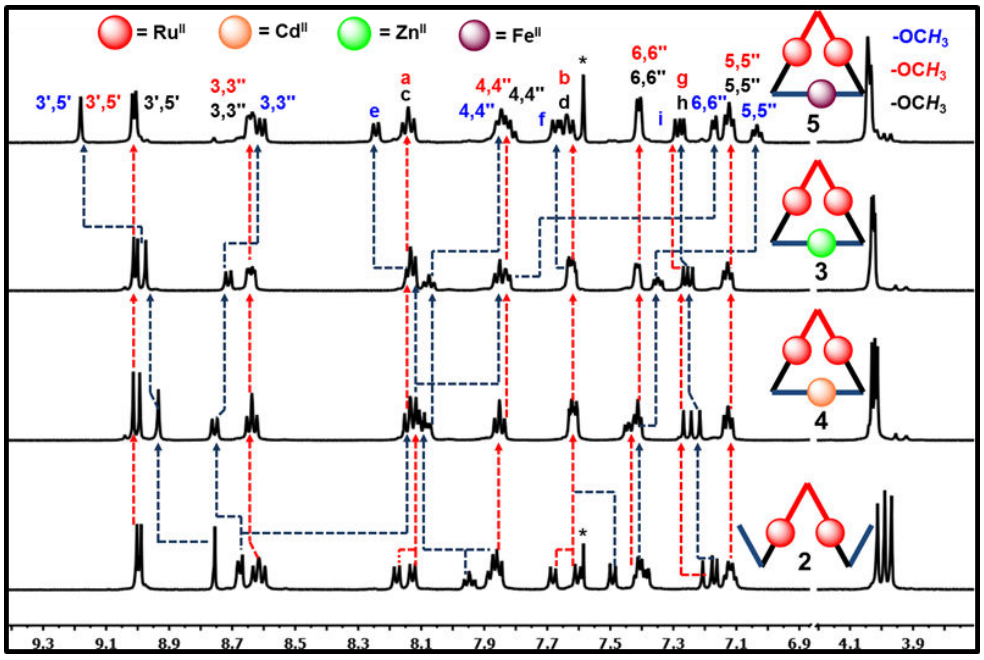

Figure 3.5: ^{1}H NMR overlay spectra (500 MHz) of trimer **235**, triangle **236**, **238**, and **237** (from bottom to the top) in CD_3CN.

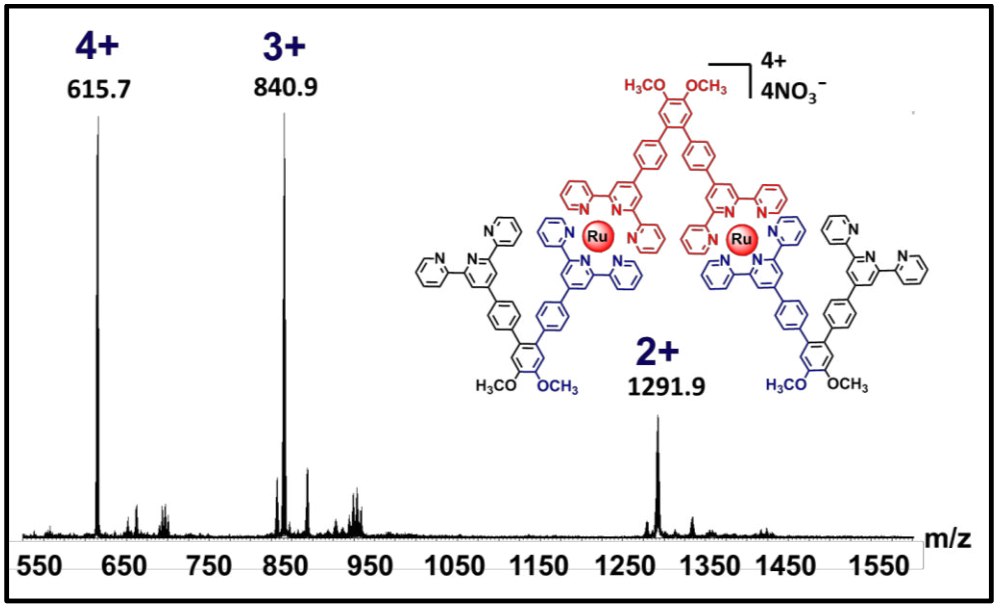

Figure 3.6: ESI-MS spectra of trimer **235**.

Upon obtaining trimer **235**, it was subjected to subsequent cyclization using Zn(II), Cd(II), and Fe(II) to obtain the desired bimetallic triangular macrocycles (Scheme 3.2). To a 1:1 MeOH/$CHCl_3$ (v/v) solution of trimer **235**, a methanolic solution of $Zn(NO_3)_2 \cdot 6H_2O$ was added in a precise 1:1 ratio. The reaction mixture was stirred at 25 ºC for 30 minutes, then a methanolic solution of NH_4PF_6 was added to effect a counter-ion exchange to PF_6^-. The light orange precipitate was filtered and washed repeatedly with MeOH to remove excess NH_4PF_6. Bimetallic macrocycle **236** was obtained (~99%) without any further purification as an orange solid. Triangle **236** was characterized by using NMR spectroscopy and ESI- and TWIM-MS spectrometry. The structural asymmetry is evident in ^{1}H NMR data in which (Figure 3.2) three distinct 3',5'-proton signals at 9.05, 9.04, and 9.00 ppm resulting from arms **A**, **B**, and **C** respectively, with an integration ratio of 1:1:1 was observed. The 6,6''-protons (at 7.87 ppm) corresponding to arm **C** of triangle 2**36** experience an upfield shift ($\Delta\delta$ = -0.8 ppm) and 3',5'-protons (at 9.00 ppm) from arm **C** experience a downfield

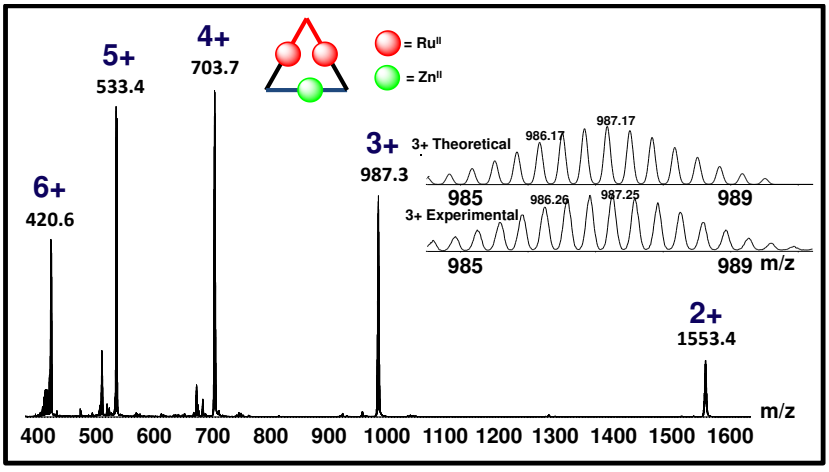

Figure 3.7: ESI-MS with simulated and experimental isotope pattern for 3+ species of **236**.

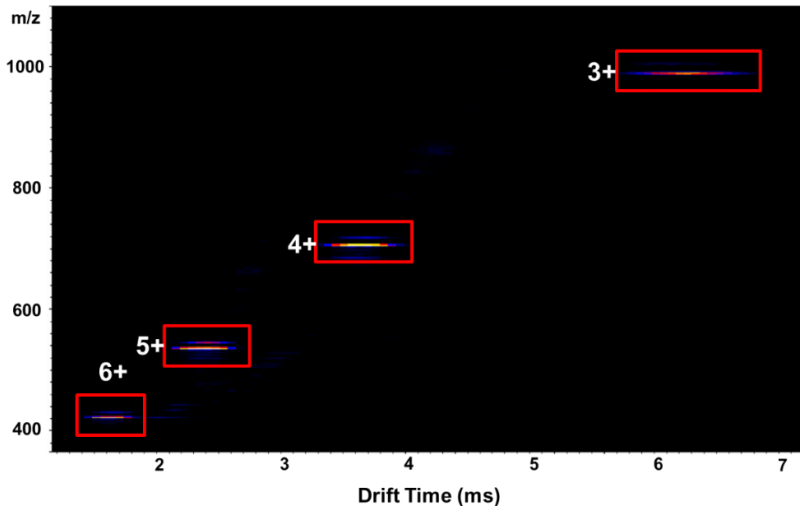

Figure 3.8: 2D ESI-TWIM-MS plot (mass-to-charge ratio *vs* drift time) of bimetallic triangle **236**.

shift ($\Delta\delta$ = 0.24 ppm) upon complexation (Figure 3.5) as anticipated. The NMR data also included signals from the three different –OC*H*$_3$ protons at 4.07, 4.06, and 4.05 ppm with an integration ratio of 1:1:1, again supporting the proposed structure. Another notable feature of the ^{1}H NMR data is the three sharp aromatic singlets at 7.30, 7.29, and 7.27 ppm with precise integration ratio of 1:1:1, which ascribes to aromatic protons ***g***, ***h*** and ***i***, respectively. All other aromatic protons were assigned by using 2D-COSY and 2D-NOESY NMR data. Further evidence for triangle **236** was obtained from the ESI-MS data (Figure 3.7), which showed a series of dominant peaks at m/z 420.6, 533.4, 703.7, 987.3, and 1553.4 corresponding to charge states from 6+ to 2+ *via* the loss of a varying number of PF_6^- anions. The isotope pattern for each peak fits with the simulated isotope pattern. Travelling-wave ion mobility (TWIM) MS data (Figure 3.8) provided additional support for triangle **236** by showing a set of single and narrow bands for charge states 6+ to 3+. This also supports the presence of a single discrete structure.

Trimer **235** was cyclized with $Cd(NO_3)_2 \cdot 4H_2O$ in a similar fashion to obtain the heterometallic triangle **237**. The light orange precipitate was filtered and washed repeatedly with MeOH to remove excess NH_4PF_6. Bimetallic triangle **237** was obtained without any further purification, as an orange color solid in 99% yield. Triangle **237** was also characterized by ^{1}H NMR data (Figure 3.3) showing three distinct singlets for 3',5'-protons (at 9.00, 8.99, and 8.93 ppm), -OC*H*$_3$ protons (at 4.03, 4.02, and 4.01 ppm) and aromatic protons ***g***, ***h***, and ***i*** (at 7.27, 7.24, and 7.22 ppm) as expected with an 1:1:1 integration ratio. The 3',5'-protons (at 8.93 ppm) and 6,6''-protons (at 8.10 ppm) from arm **C** showed the expected downfield ($\Delta\delta$ = 0.17 ppm) and upfield shift ($\Delta\delta$ = -0.57 ppm), respectively, upon complexation (Figure 3.5). All other aromatic protons were assigned with the aid of 2D-COSY and 2D-NOESY NMR data. The marked differences between the ^{1}H NMR data of triangles **236** and **237** are signals from 3',5'-protons and 6,6''-protons from arm **C**. The 3',5'-proton signal from arm **C** of triangle **236** appears more downfield ($\Delta\delta$ = 0.07 ppm) and the 6,6''- protons appear more upfield ($\Delta\delta$ = - 0.23 ppm) when compared to triangle **237** (Figure 3.5). In the ESI-MS (Figure 3.9) a series of dominant peaks were generated at m/z 428.6, 543.7, 716.2, 1002.9, and 1577.7 corresponding to charge states from 6+ to 2+ resulting from loss of varied number of PF_6^- anions. Experimental isotope distribution pattern for each peak fits well with the theoretical isotope distribution pattern. TWIM-MS data (Figure 3.10) of **237** show a set of narrow bands for charge states 6+ to 3+ supporting the desired assignment.

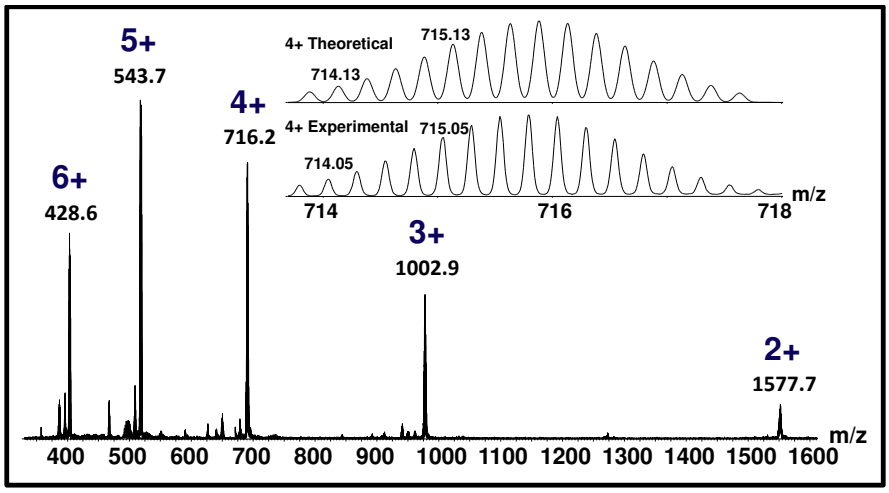

Figure 3.9: ESI-MS with simulated and experimental isotope pattern for 4+ species of **237**.

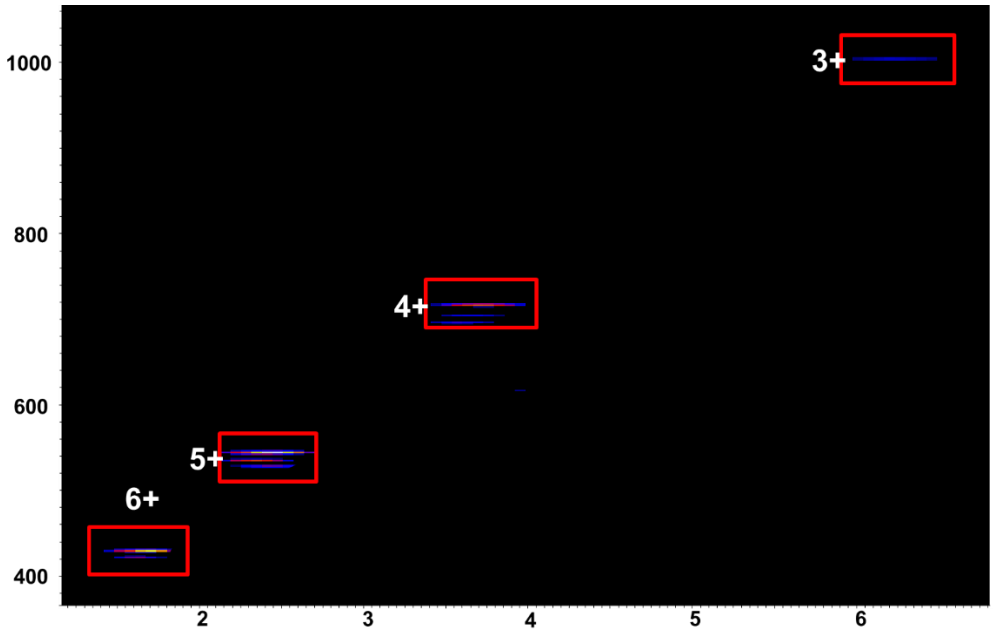

Figure 3.10: 2D ESI-TWIM-MS plot (mass-to-charge ratio *vs* drift time) of bimetallic triangle **237**.

Triangle **238** was obtained by reacting oligomeric trimer **235** with Fe(II) (Scheme 3.2). A methanolic solution of $FeCl_2 \cdot 4H_2O$ was added to a 1:1 MeOH/$CHCl_3$ (v/v) solution of trimer **235** in a precise 1:1 ratio and was subsequently stirred for 4 hour at 25 ºC. The reaction mixture was then dried *in vacuo* and was column chromatographed (SiO_2) using a

mixed solvent system of satd. KNO_3:H_2O:MeCN 1:1:30 (v/v/v), as eluent. The pure fraction was dried and washed repeatedly with water to wash away excess KNO_3. Then the product was dissolved in MeOH and excess NH_4PF_6 was added to exchange the counterions from NO_3^- to PF_6^-. The PF_6 salt was filtered and washed repeatedly to remove excess NH_4PF_6. The bimetallic triangle **238** was obtained (72%) as a magenta colored solid. The ^{1}H NMR spectrum of **238** (Figure 3.4) shows a similar characteristic pattern with certain difference compared to 2**36** and **237**. The spectrum for **238** contains signals from three 3',5'-protons (at 9.24, 9.07, and 9.06 ppm for arm **B**, **A**, and **C**, respectively), three -OC*H*$_3$ protons (at 4.03, 4.02, and 4.01 ppm) and three phenyl protons ***g***, ***h***, and ***i*** (at 7.28, 7.27, and 7.25 ppm) as expected with an anticipated 1:1:1 integration ratio. Both the 3',5'-protons (at 9.24 ppm) and 6,6'' protons (at 7.18 ppm) from Arm **C** experience a larger upfield shift ($\Delta\delta$ = 0.48) and downfield shift ($\Delta\delta$ = -1.49 ppm), respectively, upon complexation (Figure 3.5). All other aromatic protons were assigned based on the 2D-COSY and 2D-NOESY NMR data.

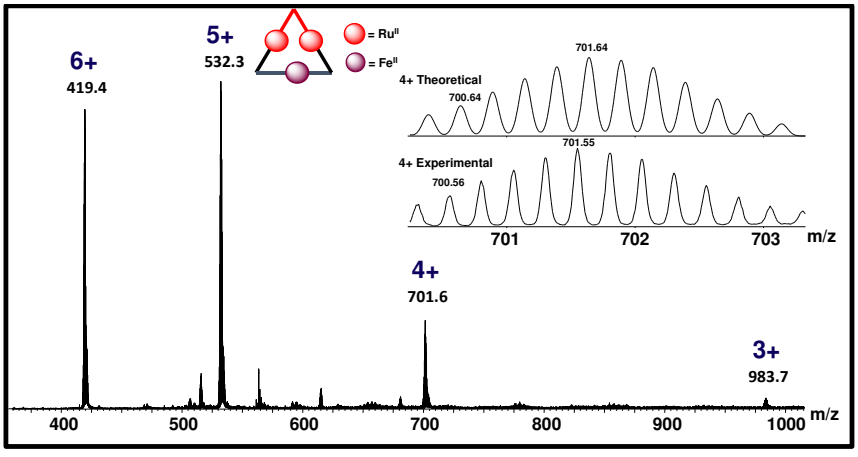

Figure 3.11: ESI-MS with simulated and experimental isotope pattern for 4+ species of **238**.

The ESI-MS spectrum (Figure 3.11) showed a series of peaks at m/z 419.4, 532.3, 701.6, and 983.7 corresponding to the charge states from 6+ to 2+ generated by the loss of different number of PF_6^- ions.

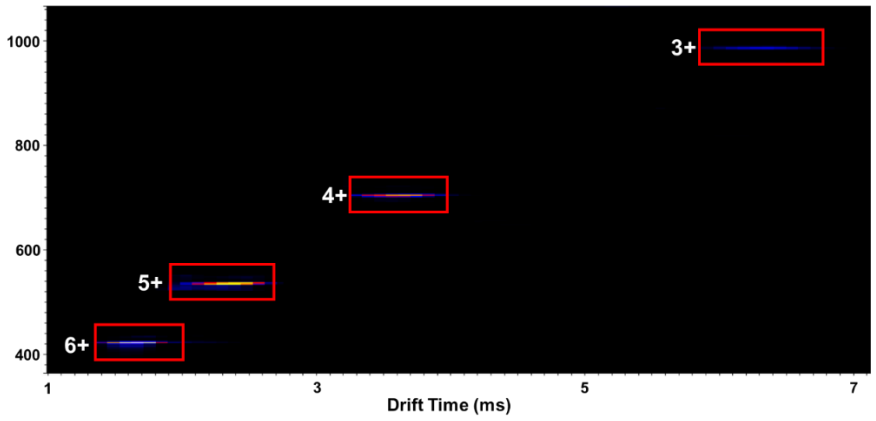

Figure 3.12: 2D ESI-TWIM-MS plot (mass-to-charge ratio *vs* drift time) of bimetallic triangle **238**.

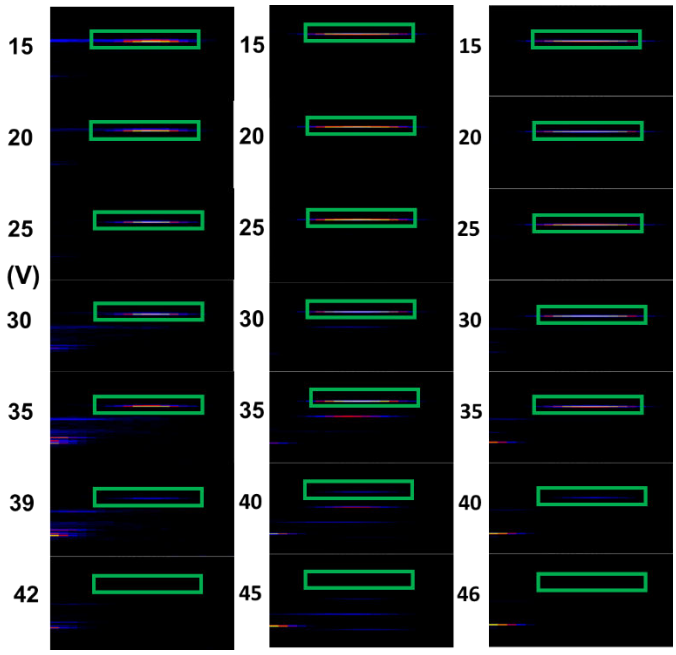

Figure 3.13: ESI TWIM-gMS^2 plot of the 5+ charge state of triangle a) **236**, b) **237**, and c) **238**.

The experimental isotope pattern for each peak is in complete agreement with the calculated isotope pattern. The TWIM-MS data (Figure 3.12) showed a series of single and discrete bands for charge states 6+ to 3+ providing further evidence for the assignment. Gradient MS (gMS^2) for triangle **236**, **237**, and **238** was performed to add a perspective on understanding their stabilities. The 3+ ion of all the triangles (Figure 3.13) was exposed to collisionally activated dissociation at increasing collision energy. Gradient MS data revealed that complex **236**, **237**, and **238** have very comparable stabilities. All of them are stable up to collision energy of 30 eV. Macrocycle **236** and **237** start dissociating at ca. 35 eV and completely dissociates at 42 and 45 V. While compound **238** remains intact up to 35 V and completely disintegrates at 46 V. The center-of-mass (COM) collision energy calculated from the dissociation energy for **236**, **237**, and **238** are 1.68 eV, 1.77 eV and 1.85 eV respectively.

Photophysical properties of **236**-**238** have been studied using steady state absorption spectroscopy and fluorescence spectroscopy. Their absorption spectra are presented in Figure 3.14a. Ligand **227** exhibits a typical ligand-to-ligand (LL) π-π* charge transfer (CT) bands at 285 and 330 nm, which are localized on terpyridine-phenyl subunits. Complexation with Ru(II) results in a new metal-ligand charge transfer (MLCT) band at 483 nm due to CT active Ru(II) center; whereas, **238** possesses a second MLCT band at 575 nm, arising from the characteristic Fe(II)-tpy absorption band. The emission intensities of bimetallic triangles 2**36, 237**, and **238** are lower than the intensities of trimer **235** at the excitation wavelength 480 nm (Figure 3.14b), which is probably due to quenching effect of Zn(II),Cd(II), and Fe(II).[218]

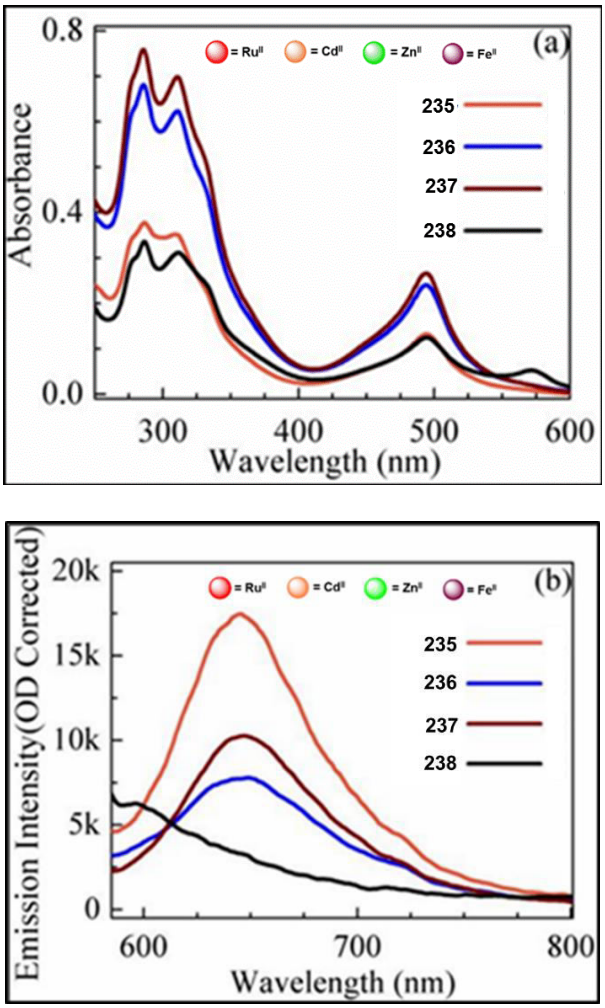

Figure 3.14: (a) Normalized UV-Visible spectra of **235-238**. (b) Corrected emission spectra of **235-238** by at the excitation wavelength λ_{ex}=480 nm. All photoluminescence spectra are corrected for fluctuation in absorbance at excitation wavelengths λ_{ex} = 480 nm.

3.3. Conclusion

The step-wise synthesis of three bimetallic triangles utilizing site-specific metalation has been accomplished. Oligomeric trimer **235** was readily synthesized from ligand **227**. Subsequent cyclization of trimer **235** with Zn(II) and Cd(II) gave triangle **236** and **237** in quantitative yields. On the other hand, cyclization of **235** with Fe(II) followed by purification by column chromatography afforded triangle **238** in high yield. All the triangles were completely characterized by ^{1}H, COSY, NOESY, and ^{13}C NMR

spectroscopy as well as ESI and TWIM mass spectrometry. Gradient MS (gMS^2) experiment provided considerable insight into their stability. Utilization of site-specific metalation to construct structures with a combination of different metal connectivity is currently underway.

3.4 Experimental section:

General Procedures: See page 88-89 for general synthetic procedures. Photoluminescence spectra were collected by using a Horiba Jobin Yvon FluoroMax-4 spectrofluorometer. The excitation and emission monochromators were set at 5 and 2 mm respectively, giving a spectral bandwidth of 4.25 nm. Quartz cell with 1 cm path length was used for all the experiments. The data interval was 0.5 nm and the integration time was 2.0 sec. The MeCN was used to prepare the solution for complexes and $CHCl_3$ for ligand. Absorbance of the samples was kept less than 0.1 at the 480 nm excitation wavelength to avoid any inner-filter effect. The dark counts were subtracted and the spectra were corrected for wavelength-dependent instrument sensitivity.

Synthesis of trimer [$(227)_3$ $(Ru^{2+})_2$] $(NO_3^-)_4$ (235):

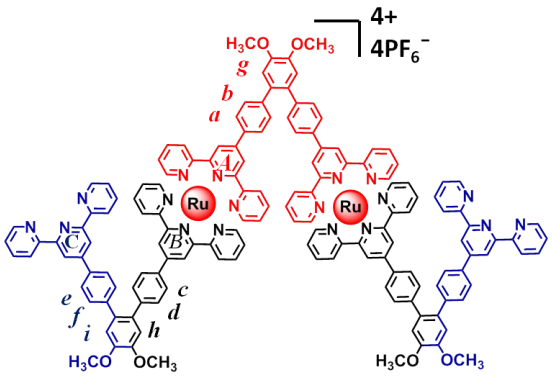

To a 1L round bottom flask ligand **227** (542 mg, 0.72 mmol), $RuCl_2(DMSO)_4$[251] (236 mg, 0.48 mmol), and 1:1 $CHCl_3$:MeOH (700 mL) were added. After refluxing for 24 hour, the reaction mixture was dried *in vacuo* to produce a red powder which was column chromatographed (Al_2O_3) eluting with $CHCl_3$ to remove unreacted ligand **227** then elution with a solvent mixture of H_2O:saturated KNO_3:MeCN (1:1:35) gave pure **235** (48%), as red powder: 312 mg; m.p. > 300 ºC.

^{1}H NMR (CD_3CN, 500 MHz, ppm): δ 9.00 (s, 4H, tpy^A*H*$^{3',5'}$), 8.99 (s, 4H, tpy^B*H*$^{3',5'}$), 8.76 (s, 4H, tpy^C*H*$^{3',5'}$), 8.67 (m, 8H, tpy^C*H*$^{6,6''}$, tpy^C*H*$^{3,3''}$), 8.62 (m, 8H, tpy^A*H*$^{3,3''}$, tpy^B*H*$^{3,3''}$), 8.17 (d, 4H, *J* = 8.0 Hz, Ar-*H*^{a}), 8.12 (d, 4H, *J* = 8.0 Hz, Ar-*H*^{c}), 7.95 (dd, $J_1 = J_2 = 8.0$ Hz, tpy^C*H*$^{4,4''}$), 7.86 (m, 12H, tpy^A*H*$^{4,4''}$, tpy^B*H*$^{4,4''}$, Ar-*H*^{e}) 7.68 (d, *J* = 8.0 Hz, 4H, Ar-*H*^{b}), 7.60 (d, *J* = 8.0 Hz, 4H, Ar-*H*^{d}), 7.49 (d, *J* = 8.0 Hz, 4H, Ar-*H*^{f}), 7.41 (m, 12H, tpy^A*H*$^{6,6''}$, tpy^B*H*$^{6,6''}$, tpy^C*H*$^{5,5''}$), 7.21 (s, 2H, Ar-*H*^{g}), 7.18 (s, 2H, Ar-*H*^{h}), 7.16 (s, 2H, Ar-*H*^{i}), 7.12 (m, 8H, tpy^A*H*$^{5,5''}$, tpy^B*H*$^{5,5''}$) 4.01 (s, 6H, Ar-OC*H*$_3$), 3.99 (s, 6H, Ar-OC*H*$_3$), 3.97 (s, 6H, Ar-OC*H*$_3$). ESI-MS (*m/z*): 1291.9 $[M\text{-}2NO_3^-]^{2+}$ (calcd. *m/z* = 1292.3) , 840.9 $[M\text{-}3NO_3^-]^{3+}$ (calcd. *m/z* =840.8), 615.7 $[M\text{-}4NO_3^-]^{4+}$ (calcd. *m/z* =615.2).

Synthesis of bimetallic triangle [(235) (Zn^{2+})] (PF_6^-)$_6$ (236):

To a 10 mL (1:1 $CHCl_3$:MeOH) solution of trimer **235** (20 mg, 7.38×10^{-3} mmol), a methanolic solution (5 mL) of $Zn(NO_3)_2\cdot6H_2O$ (2.20 mg, 7.38×10^{-3} mmol) was added. The solution was stirred for 30 minutes at 25 °C. Then excess NH_4PF_6 was added to generate a light yellow precipitate, which was filtered and washed repeatedly with MeOH to remove excess NH_4PF_6. The product obtained (99%) as an orange solid: 24.80 mg.

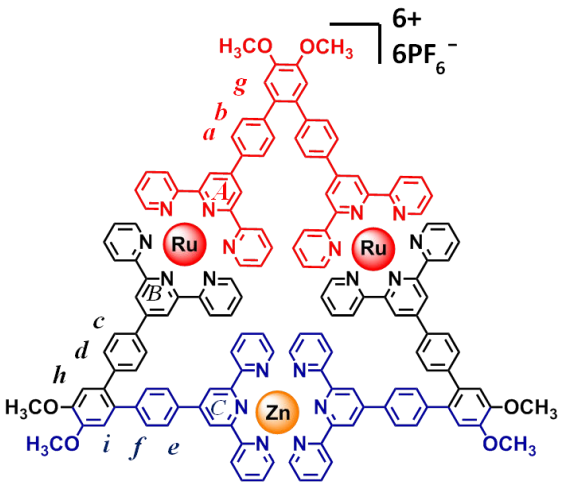

^{1}H NMR (CD_3CN, 500 MHz, ppm): δ 9.05 (s, 4H, tpy$^{A}H^{3',5'}$), 9.04 (s, 4H, tpy$^{B}H^{3',5'}$), 9.00 (s, 4H, tpy$^{C}H^{3',5'}$), 8.74 (d, J = 8.0 Hz, 4H, tpy$^{C}H^{3,3''}$), 8.68 (m, 8H, tpy$^{A}H^{3,3''}$, tpy$^{B}H^{3,3''}$), 8.17 (m, 12H, Ar-H^{a}, Ar-H^{c}, Ar-H^{e}), 8.11(dd, J_1 = J_2 = 8.0 Hz, 4H, tpy$^{C}H^{4,4''}$), 7.87 (m, 12H, tpy$^{A}H^{4,4''}$, tpy$^{B}H^{4,4''}$, tpy$^{C}H^{6,6''}$), 7.65 (m, 12H, Ar-H^{b}, Ar-H^{d}, Ar-H^{f}), 7.44 (m, 8H, tpy$^{A}H^{6,6''}$, tpy$^{B}H^{6,6''}$), 7.38 (dd, J_1 =8.0 Hz, J_2 = 5.0 Hz, 4H, tpy$^{C}H^{5,5''}$), 7.30 (s, 2H, Ar-H^{g}), 7.29 (s, 2H, Ar-H^{h}), 7.27 (s, 2H, Ar-H^{i}), 7.16 (m, 8H, tpy$^{A}H^{5,5''}$, tpy$^{B}H^{5,5''}$) 4.07 (s, 6H, Ar-OCH_3), 4.06 (s, 6H, Ar-OCH_3), 4.05 (s, 6H, Ar-OCH_3); ^{13}C NMR (CD_3CN, 125 MHz, ppm): 157.28, 154.84, 154.48, 151.46, 148.85, 148.35, 147.05, 146.96, 146.75, 143.53, 142.69, 140.27, 137.06, 133.94, 133.32, 130.97, 130.82, 130.44, 126.82, 126.56, 126.50, 123.66, 122.32, 120.53, 120.44, 113.25, 54.88. ESI-MS (m/z): 1553.4 [M-2PF_6^-]$^{2+}$ (calcd. m/z = 1552.2) , 987.3 [M-3PF_6^-]$^{3+}$ (calcd. m/z =986.5), 703.7 [M-4PF_6^-]$^{4+}$ (calcd. m/z =703.6), 533.4 [M-5PF_6^-]$^{5+}$ (calcd. m/z = 533.9), 420.6 [M-6PF_6^-]$^{6+}$ (calcd. m/z = 420.7).

Synthesis of bimetallic triangle [(235) (Cd^{2+})] ($(PF_6^-)_6$ (237):

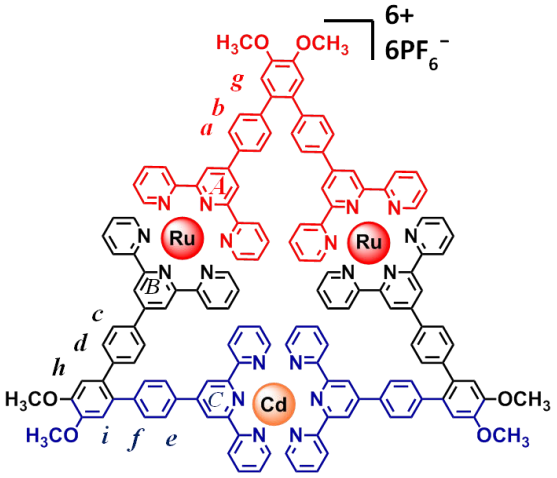

To a 10 mL (1:1 $CHCl_3$:MeOH) solution of trimer **235** (20 mg, 7.38×10^{-3} mmol), a methanolic solution (5 mL) of $Cd(NO_3)_2\cdot4H_2O$ (2.28 mg, 7.38×10^{-3} mmol) was added. The solution was stirred for 30 minutes at 25 °C. Then excess NH_4PF_6 was added to obtain a light yellow precipitate, which was filtered and washed repeatedly with MeOH to remove excess NH_4PF_6. The product obtained (99%) as an orange solid: 25.08 mg. m.p. > 300 ºC; ^{1}H NMR (CD_3CN, 500 MHz, ppm): δ 9.00 (s, 4H, tpy^A*H*$^{3',5'}$), 8.99 (s, 4H, tpy^B*H*$^{3',5'}$), 8.93 (s, 4H, tpy^C*H*$^{3',5'}$), 8.75 (d, *J* = 8.0 Hz, 4H, tpy^C*H*$^{3,3''}$), 8.64 (m, 8H, tpy^A*H*$^{3,3''}$, tpy^B*H*$^{3,3''}$), 8.10 (m, 16H, Ar-*H*^{a}, Ar-*H*^{c}, Ar-*H*^{e}, tpy^C*H*$^{4,4''}$, tpy^C*H*$^{6,6''}$), 7.85 (m, 8H, tpy^A*H*$^{4,4''}$, tpy^B*H*$^{4,4''}$), 7.62 (m, 12H, , Ar-*H*^{b}, Ar-*H*^{d}, Ar-*H*^{f}), 7.43 (m, 12H, tpy^A*H*$^{6,6''}$, tpy^B*H*$^{6,6''}$, tpy^C*H*$^{5,5''}$), 7.27 (s, 2H, Ar-*H*^{g}), 7.24 (s, 2H, Ar-*H*^{h}), 7.22 (s, 2H, Ar-*H*^{i}), 7.13 (m, 8H, tpy^A*H*$^{5,5''}$, tpy^B*H*$^{5,5''}$), 4.03 (s, 6H, Ar-OC*H*$_3$), 4.02 (s, 6H, Ar-OC*H*$_3$), 4.01 (s, 6H, Ar-OC*H*$_3$); ^{13}C NMR (CD_3CN, 125 MHz, ppm): 157.30, 154.50, 153.83, 151.48, 151.46, 149.33, 148.72, 148.39, 148.35, 147.88, 146.74, 146.75, 143.36, 142.72, 140.31, 137.07, 133.98, 133.89, 133.42, 131.16, 131.01, 130.45, 130.42, 126.50, 126.44, 126.40, 123.67, 122.81, 120.77, 120.44, 113.30, 113.29, 54.90, 54.88; ESI-MS (*m/z*): 1577.7 [M-2PF_6^-]$^{2+}$ (calcd. *m/z* = 1577.2) , 1002.9

$[M-3PF_6^-]^{3+}$ (calcd. *m/z* =1003.2), 716.2 $[M-4PF_6^-]^{4+}$ (calcd. *m/z* =716.1), 543.7 $[M-5PF_6^-]^{5+}$ (calcd. *m/z* = 543.9), 428.6 $[M-6PF_6^-]^{6+}$ (calcd. *m/z* = 429.1).

Synthesis of bimetallic triangle [(235) (Fe^{2+})] ($(PF_6^-)_6$ (238):

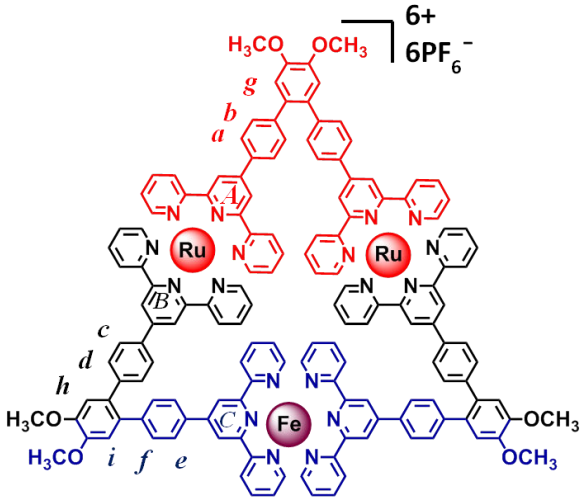

To a 10 mL (1:1 $CHCl_3$:MeOH) solution of trimer **235** (40 mg, 14.76×10^{-3} mmol), a methanolic solution (5 mL) of $FeCl_2\cdot4H_2O$ (2.93 mg, 14.76×10^{-3} mmol) was added. The solution was stirred for 4 hour at 25 °C. Then the reaction mixture was concentrated *in vacuo* and was subjected SiO_2 column chromatography using a mixed solvent of water:saturated KNO_3 solution:MeCN (1:1:30), as eluent. The purified fraction was dried and washed repeatedly with water to remove excess KNO_3. The dried sample was dissolved in MeOH and excess NH_4PF_6 was added to exchange the counter ion from NO_3^- to PF_6^-. The PF_6 salt precipitated as a dark purple solid which was filtered and washed repeatedly with MeOH to remove excess NH_4PF_6. The product obtained (72%) as a magenta color solid: 42.77 mg. m.p. > 300 ºC;

^{1}H NMR (CD_3CN, 500 MHz, ppm): δ 9.24 (s, 4H, tpy$^{C}H^{3',5'}$), 9.07 (s, 4H, tpy$^{A}H^{3',5'}$), 9.06(s, 4H, tpy$^{B}H^{3',5'}$), 8.69 (m, 8H, tpy$^{A}H^{3,3''}$, tpy$^{B}H^{3,3''}$), 8.64 (d, J = 8.0 Hz, 4H, tpy$^{C}H^{3,3''}$), 8.24 (d, J = 8.0 Hz, 4H, Ar-H^{e}), 8.14 (m, 8H, Ar-H^{a}, Ar-H^{c}), 7.83 (m , 12H, tpy$^{A}H^{4,4''}$, tpy$^{B}H^{4,4''}$, tpy$^{C}H^{4,4''}$), 7.65 (d, J = 8.0 Hz, 4H, Ar-H^{f}), 7.62 (d, J = 8.0 Hz, 4H, Ar-H^{b}), 7.60 (d, J = 8.0 Hz, 4H, Ar-H^{d}), 7.42 (m, 8H, tpy$^{A}H^{6,6''}$, tpy$^{B}H^{6,6''}$), 7.28 (s, 2H, Ar-H^{i}), 7.27 (s, 2H, Ar-H^{g}), 7.25 (s, 2H, Ar-H^{h}), 7.18 (d, J = 5.0 Hz, 4H, tpy$^{C}H^{6,6''}$), 7.12 (m, 8H, tpy$^{A}H^{5,5''}$, tpy$^{B}H^{5,5''}$), 7.03 (dd, J_1 =8.0 Hz, J_2 = 5.0 Hz, 4H, tpy$^{C}H^{5,5''}$), 4.03 (s, 6H, Ar-OCH_3), 4.02 (s, 6H, Ar-OCH_3), 4.01 (s, 6H, Ar-OCH_3); ^{13}C NMR (CD_3CN, 125 MHz, ppm): 159.30, 157.25, 157.10, 154.45, 151.96, 151.33, 148.94, 148.28, 146.81, 142.91, 142.57, 137.70, 137.00, 133.95, 133.75, 131.10, 130.45, 130.37, 126.57, 126.46, 126.29, 123.63, 122.92, 120.47, 116.43, 113.12, 54.80, 54.79; ESI-MS (m/z): 983.7 [M-3PF_6^-]$^{3+}$ (calcd. m/z =983.8), 701.6 [M-4 PF_6^-]$^{4+}$ (calcd. m/z =701.6), 532.3 [M-5PF_6^-]$^{5+}$ (calcd. m/z = 532.3), 419.4 [M- PF_6^-]$^{6+}$ (calcd. m/z = 419.4).

CHAPTER IV

ONE-STEP, MULTICOMPONENT, SELF-ASSEMBLY OF A FIRST-GENERATION SIERPIŃSKI TRIANGLE: FROM A FRACTAL DESIGN TO CHEMICAL REALITY

4.1 Introduction

Naturally occurring species often self-assemble into fractal shapes and forms.[227] Fractal moieties are generated by repeating a smaller identical motif into a larger structure.[228] In 1915, Polish mathematician Waclaw Sierpiński formulated an equilateral triangular fractal, which was constructed by connecting smaller equilateral triangles[229] (Figure 4.1). Later, Benoit Mandlebrot described these triangular fractals as Sierpiński gaskets (triangles or sieves).[227,230] The number of triangles in a Sierpiński triangle can be found by using the formula $\boldsymbol{N_n = 3^n}$, where N = no. of triangles and n = no. of iterations.[231]

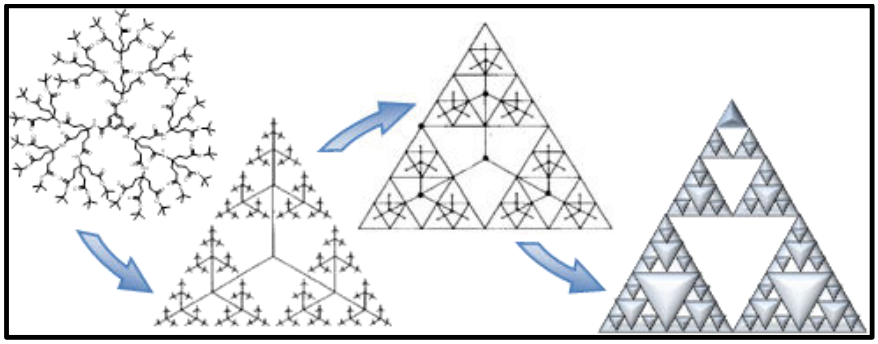

Figure 4.1: Conceptual progression and geometric relationship of a 1→3 dendritic branching pattern.to the classical Sierpiński triangle.

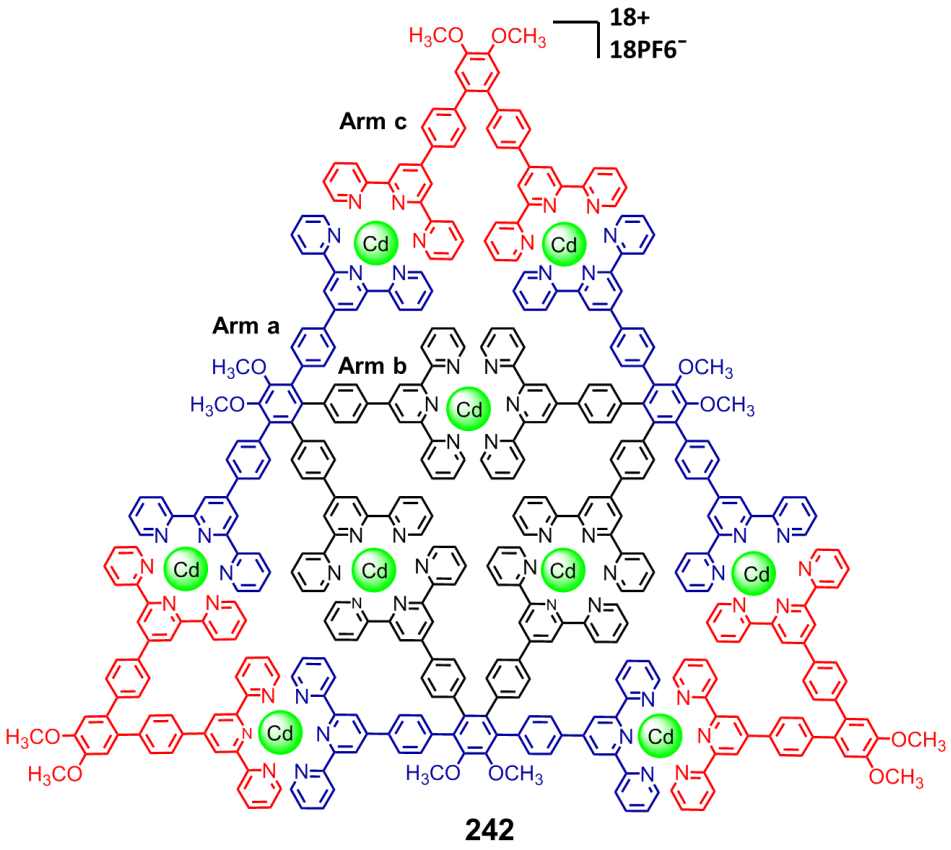

Figure 4.2: Terpyridine-based, G1 Sierpiński triangle **242**.

Simple fractal motifs have been successfully integrated into synthetic organic entities over the past thirty years in the form of dendrimers.[24,232-235] There is a unique relationship between the 1→3 branched dendrimers[232,233] and the Sierpiński triangle, which is presented in Figure 4.1.[236,237] Recent advances in supramolecular chemistry[220] have paved the way to a better understanding of how to quantitatively assemble various simple architectures in one step,[25,34,56,93,112,224,238-241] including the desired triangular predecessor constructs.[34,56]

Coordination driven self-assembly, using tailored [2,2':6',2"]-terpyridine (tpy) building blocks, has highlighted their ability to form stable, linear, <tpy-M^{II}-tpy>

complexes as the structural walls of the polygons possessing rigid organic vertices. Therefore, programmed structural features are easily incorporated into the poly(terpyridine) building blocks generating avenues to novel supramolecular constructs[242] in quantitative or near-quantitative yields.[243] Both homoleptic and heteroleptic connectivity has been used extensively in these assemblies, but heteroleptic assembly with a need for multicomponent building blocks still remains challenging owing to a tendency to produce competitive products.[244-246] Recently, we have reported various heteroleptic architectures, such as a hexagonal spoked wheel,[214] molecular bowtie and butterfly,[26] and a molecular rhombus,[215] which were obtained by either multi-component or one step assembly. Herein, we report the design and synthesis of a first-generation (G1), molecular Sierpiński triangle using two unique ligands with <tpy-Cd^{II}-tpy> connectivity (Figure 4.2)

Retro-synthetic analysis of the first-generation Sierpiński triangle revealed that it would require two easily accessible components for the assembly: a tetra*kis*(terpyridine) "K" unit, for the walls and the core region and a ditopic 60º-directed "V" for the vertices. Cadmium was chosen owing to a unique combination of thermodynamic stability and kinetic lability for its complexes. A 1:1 ratio of these "K" and "V" ligands was coupled with precisely three equivalents Cd^{II}; the overall stability of the highly symmetric poly-triangular architecture was projected to be favored over any oligomeric possibilities. In essence, there would be no loose ends or uncoordinated ligands.

4.2 Results and Discussion

Initially, a THF solution of 3,4,5,6-tetrabromocatechol and iodomethane (Scheme 4.1) was heated at reflux in an inert atmosphere (N_2, K_2CO_3, 12 h) generating **240**. Boronic acid **239** was prepared using commercially available 4-formylphenylboronic acid.[247]

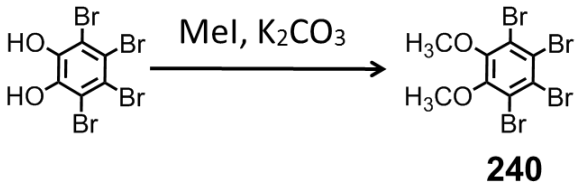

Scheme 4.1: Synthesis of 3,4,5,6-tetrabromoveratrole **240**.

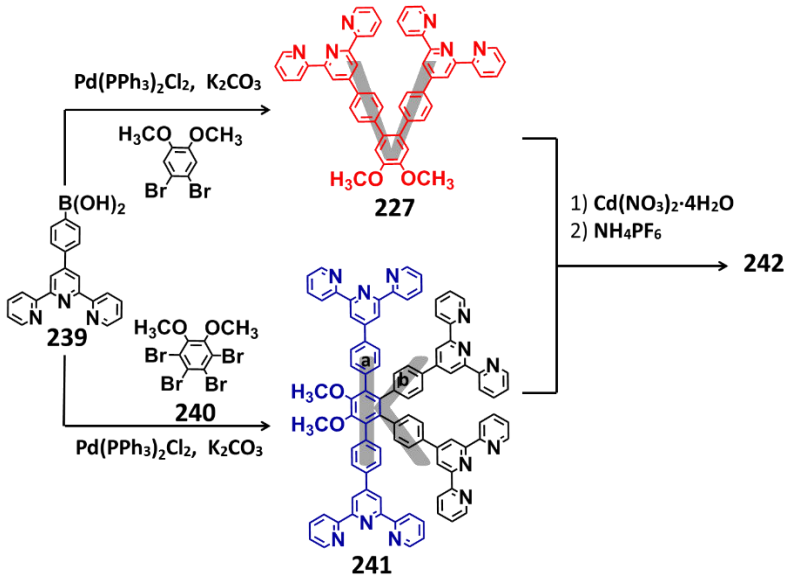

Scheme 4.2: Synthesis of the key terpyridine building blocks **227** ("V") and **241** ("K") and assembly of Sierpiński triangle **242**.

The desired "K" ligand **241** was easily synthesized (72%) from **240** by treatment with **239** using the standard Suzuki cross-coupling reaction, [K_2CO_3, $Pd(PPh_3)_2Cl_2$] under an atmosphere of Argon. (Scheme 4.2)[26] Its ^1H NMR spectrum (Figure 4.3) showed the characteristic peak at 3.76 ppm for the instilled -OC*H*$_3$ marker and the presence of two completely different arms ***a*** and ***b*** (Figure 4.3). ^{13}C NMR (Figure 4.4) spectrum of **241** showed a peak at 60.76 ppm for the O*C*H$_3$ substituents.

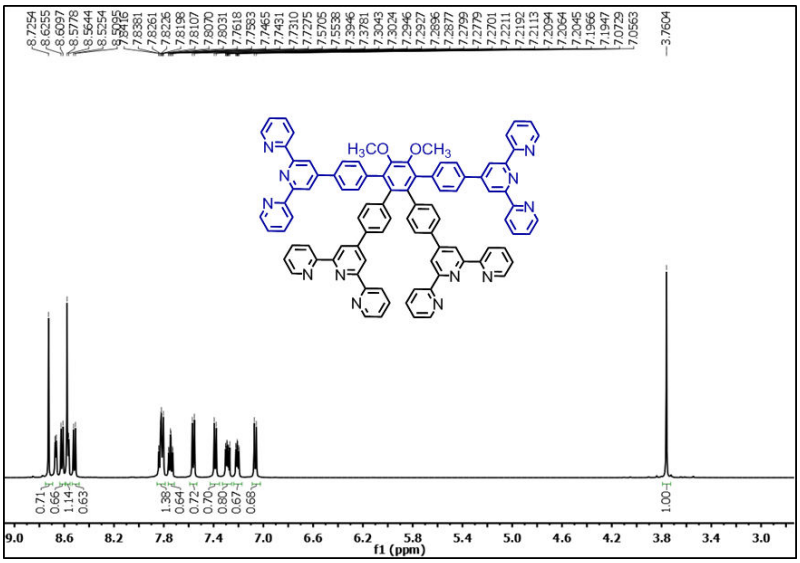

Figure 4.3: ^{1}H NMR spectrum of ligand **241**.

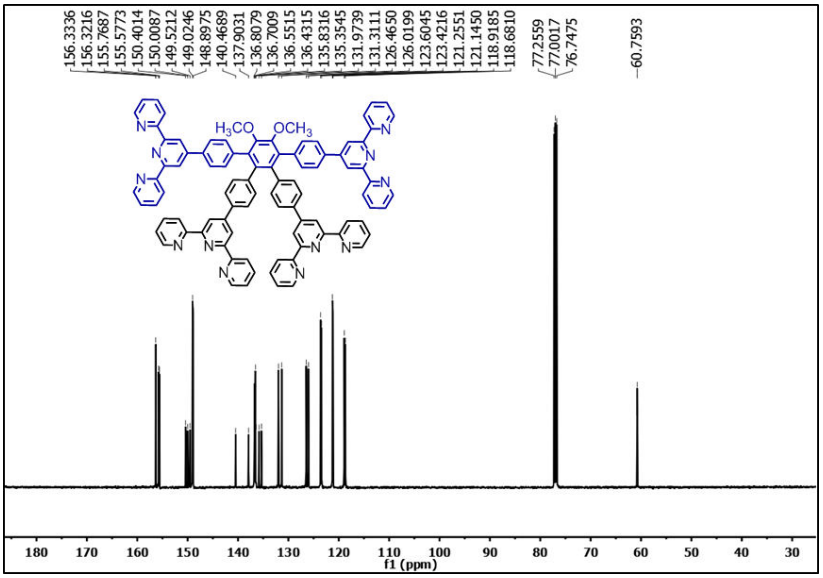

Figure 4.4: ^{13}C NMR spectrum of ligand **241**.

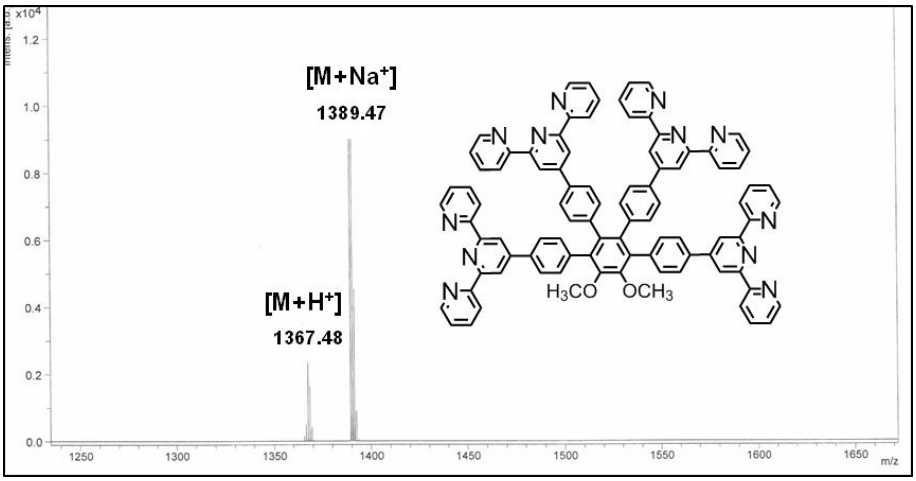

Figure 4.5: MALDI-ToF spectrum of ligand **241**.

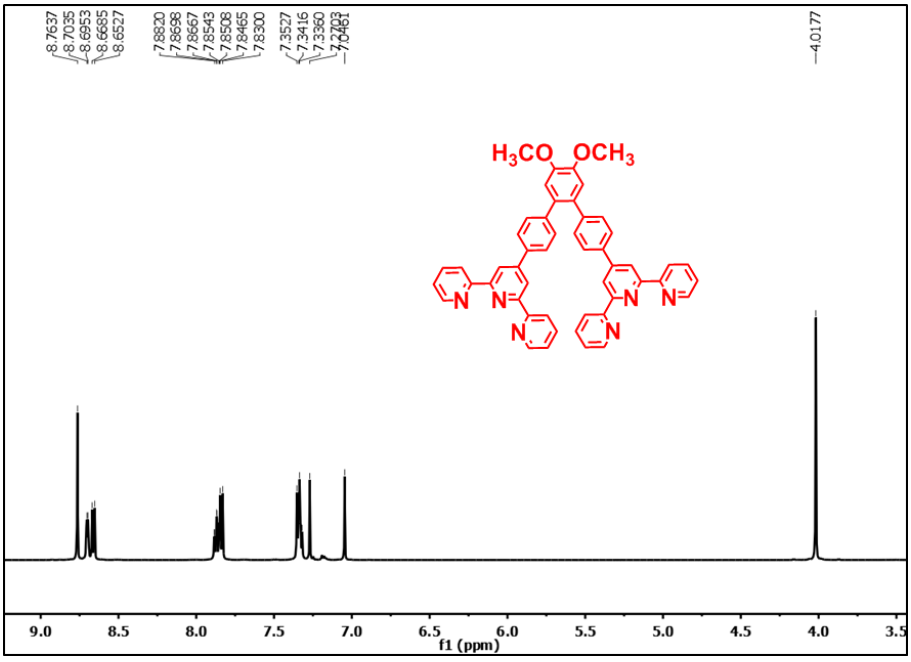

Figure 4.6: ^{1}H NMR spectrum of ligand **227**.

All proton peaks were assigned using COSY NMR spectroscopy. The ^{13}C NMR assignments and MALDI-ToF MS data (Figure 4.5) are in full agreement with the ligand structure. The colorless "V" ligand **227** was also synthesized (80%) by a slightly modified literature procedure[217] from commercially available 4,5-dibromo-1,2-dimethoxybenzene

under Suzuki cross-coupling reaction conditions. It was fully characterized by ^{1}H NMR spectroscopy and mass spectrometry. The aromatic region of ligand **227** (Figure 4.6) showed one set of characteristic terpyridine peaks, one set of aromatic phenyl-spacer peaks and sharp singlet at 4.02 ppm for the -OC*H*$_3$ vertex tag. The ^{13}C NMR (Figure 4.7) displayed a single peak at 56.40 ppm for the -O*C*H$_3$ group.

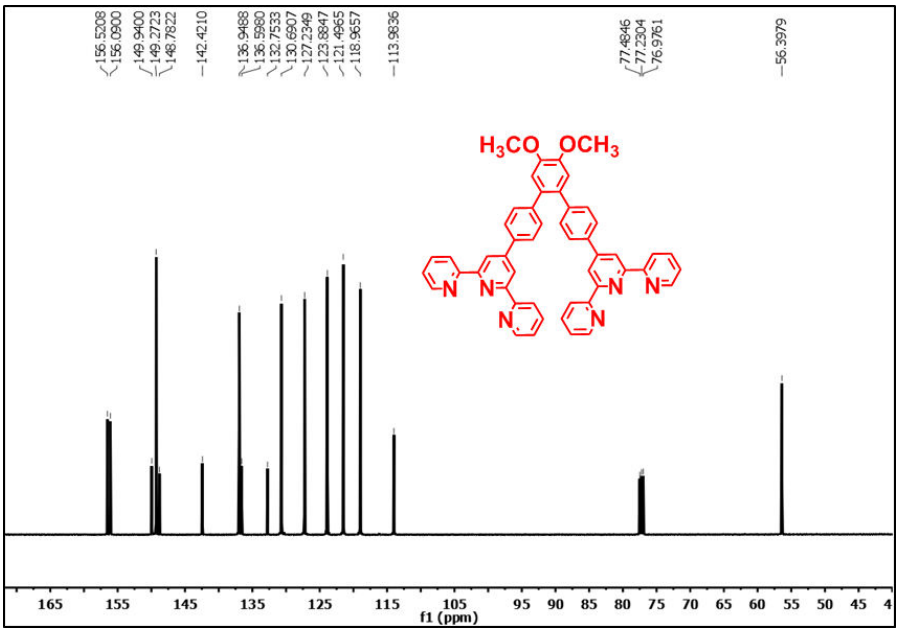

Figure 4.7: ^{13}C NMR spectrum of ligand **227**

The facile one-step assembly of Sierpiński triangle **242** (Scheme 4.2) utilized a precise 1:1 solution of **227** and **241** in $CHCl_3$, to which a methanolic solution of $Cd(NO_3)_2 \cdot 4H_2O$ (3 equivalent) was added. The solution was stirred for 30 minutes at 25 °C, and then excess NH_4PF_6 was added to exchange the counterion to PF_6^-. The desired PF_6 complex precipitated as a light yellow solid, which was filtered and repeatedly washed with MeOH to remove excess NH_4PF_6. Complex **242** was obtained without any further purification as a light yellow solid in > 95% yield.

The ^{1}H NMR spectrum of **242** (Figure 4.8) showed the characteristics of <tpy-Cd^{II}-tpy> complex with a sharp and simple pattern indicating the formation of a discrete moiety with high degree of inherent structural symmetry. The structural simplicity and high symmetry were reflected in the ^{1}H NMR spectra. The imbedded methoxy markers within each ligand appear in the product only as two distinct singlets at 3.98 (from "V") and 3.87 (from "K") ppm with a precise 1:1 ratio initially supporting the product that possesses a highly D_{3h} symmetry. Notably, peaks that would be expected for polymeric structures and impurities were not observed. The aromatic region of the ^{1}H NMR exhibited the expected ratio of three different sets of

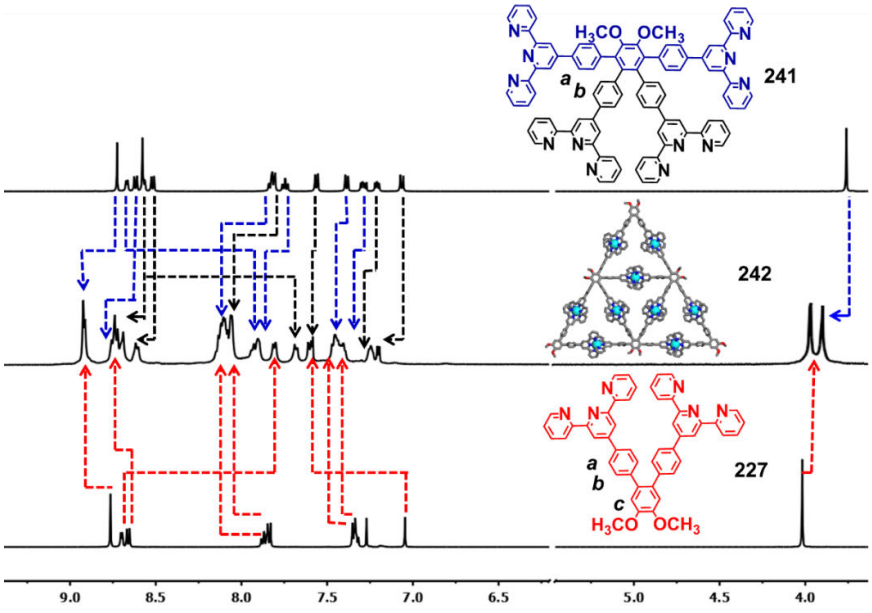

Figure 4.8: ^{1}H NMR stacked spectra (500 MHz) of ligands **227** (bottom) and **241** (top) in $CDCl_3$ and complex **242** in CD_3CN (center). Arrows indicate assigned resonance shifts that occur upon complex formation.

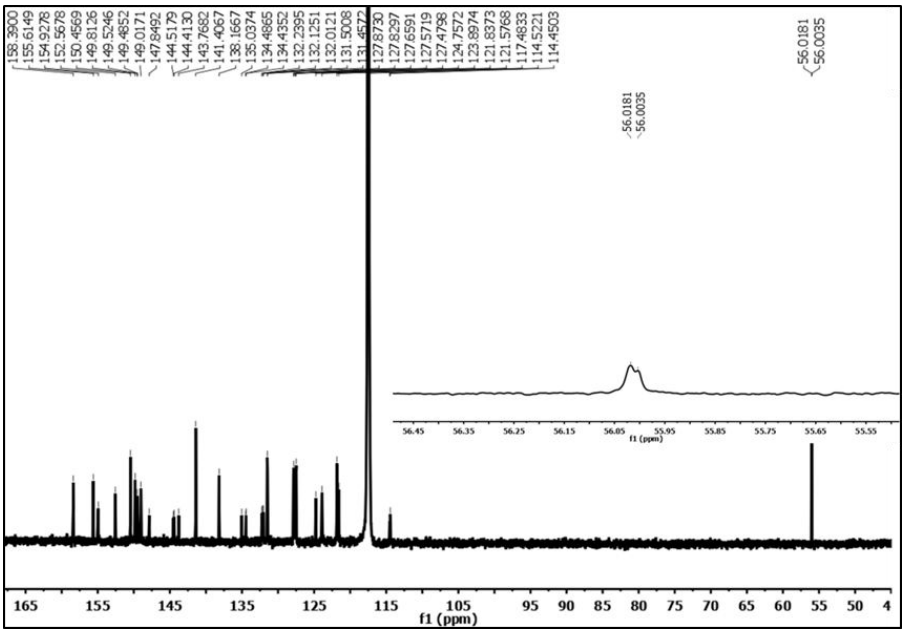

Figure 4.9: ^{13}C NMR spectrum of Sierpiński triangle **242**.

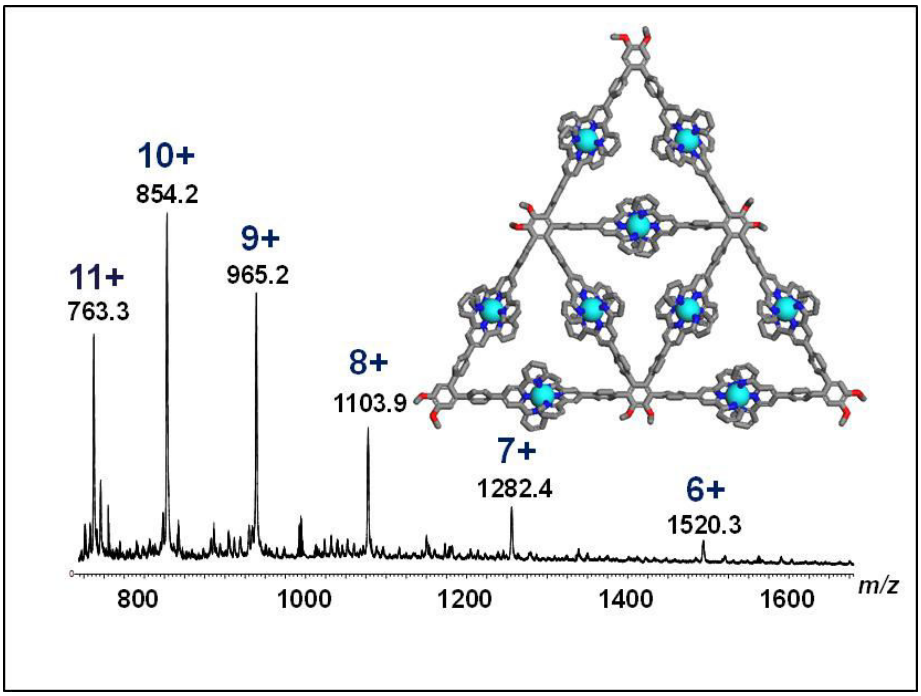

Figure 4.10: ESI-MS spectrum of Sierpiński triangle **242**. The charge states of intact assemblies are marked.

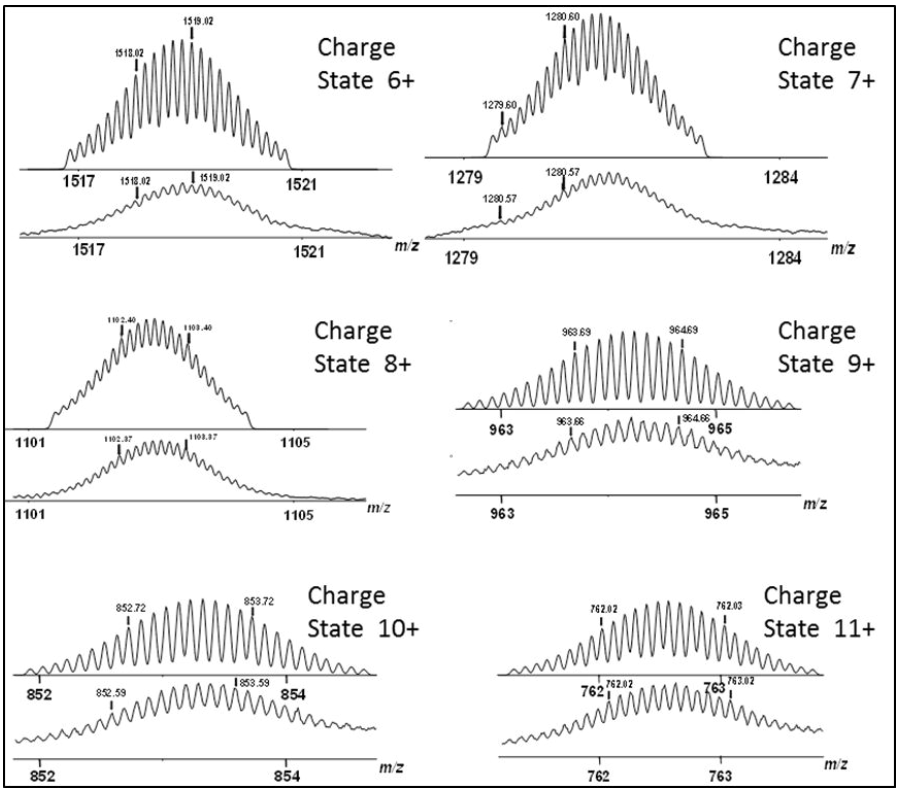

Figure 4.11: Theoretical and experimental isotope distribution patterns of charge states 6+ to 11+ observed for the Sierpiński triangle **242**.

3',5'-tpy*H* for arms **a**, **b**, and **c** (8.92, 8.91, and 8.74 ppm respectively; the downfield shifts resulted from the deshielding upon complexation. The 6,6''-tpy*H* were noticeably shifted upfield (7.92, 7.68, 7.80 ppm, respectively for **a**, **b**, and **c**) when compared with the ligands, as expected. All the peaks in the ^{1}H NMR spectrum were assigned with the help of 2D-COSY and 2D-NOESY experiments and are in complete agreement with the proposed structure. The ^{13}C NMR of the complex **242** (Figure 4.9) exhibits three signals for the different and readily identifiable 3',5'-tpy carbon atoms at 158.39, 155.32, and 154.93 ppm, respectively, along with two very close yet distinct peaks for –O*C*H$_3$ substituents at 56.02 and 56.00 ppm, which further supports the proposed structure.

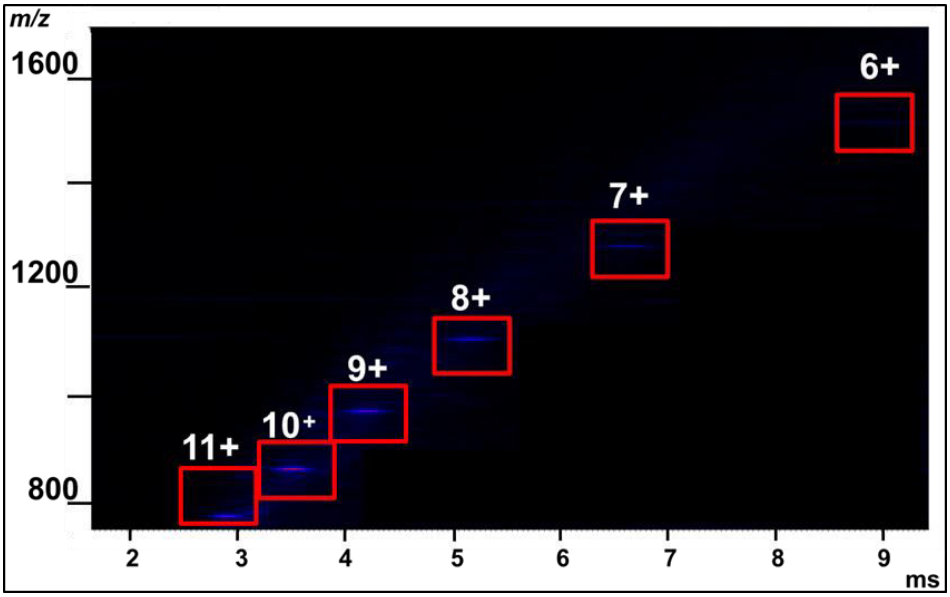

Figure 4.12: 2D ESI-TWIM-MS plot (mass-to-charge ratio *vs* drift time) of **242**. The charge states of intact assemblies are marked.

Sierpiński triangle **242** was further characterized by ESI-MS coupled with travelling-wave ion mobility (TWIM) mass spectrometry. In ESI-MS (Figure 4.10), a series of dominant peaks were generated at m/z 763.4, 854.2, 965.2, 1103.9, 1282.4, and 1520.3, which corresponds to charge states from 11+ to 6+ from the loss of varying number of PF_6^- anions. The isotope pattern of each peak is in agreement with the corresponding simulated isotope pattern (Figure 4.11). Additional evidence of the Sierpiński triangle **242** was provided by ESI-TWIM MS (Figure 4.12); the corresponding spectrum showed a set of single and narrow bands for charges states 11+ to 6+, which in agreement with the presence of one single structure **242**.

The structure of complex **242** was further confirmed by comparison of the experimental CCSs (collision cross-sections) of charge states 11+ to 6+, deduced from their drift times measured by ESI-TWIM MS, with the theoretical CCS of the complex without

any counterions (100 energy-minimized structures obtained by molecular modeling). Experimental and theoretical CCSs of triangle **242** are shown in Table 4.1.

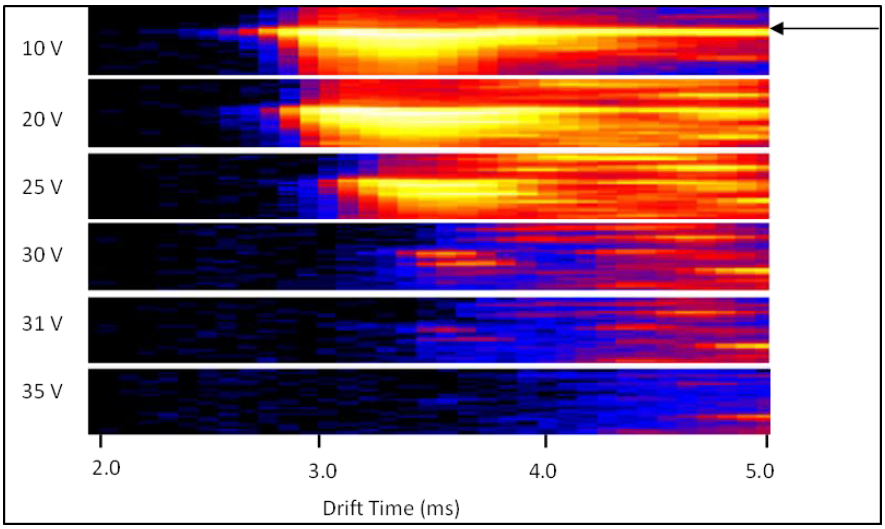

Figure 4.13. ESI TWIM-gMS^2 plots of *m/z* 854.2 (10+) for the Sierpiński triangle **242** acquired by CAD (Ar) in the trap cell at collision energies in 10 - 35 eV range followed by TWIM separation, at a traveling wave velocity of 350 m/s and a traveling wave height of 7.5 V, and ToF mass analysis.

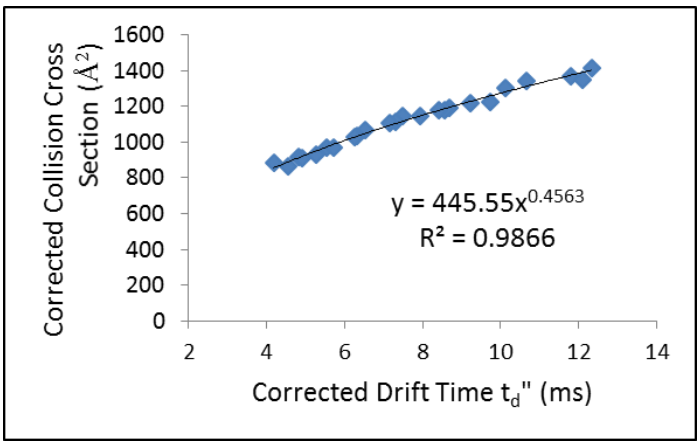

Figure 4.14: Calibration curve constructed from corrected drift times plotted against corrected published cross sections for the multiple charged ions arising from insulin (bovine pancreas), ubiquitin (bovine red blood cells) and cytochrome C (horse heart). Drift times were measured at a traveling wave velocity of 350 m/s and a traveling wave height of 7.5 V.

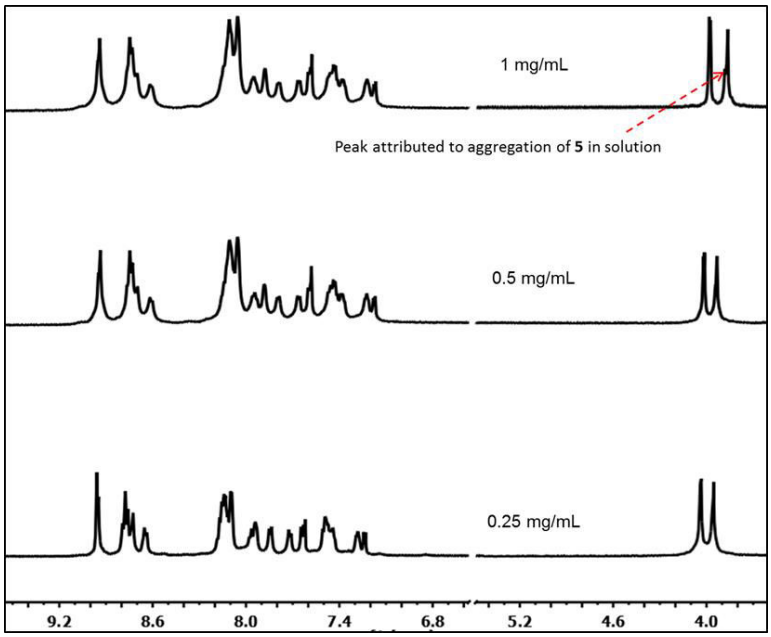

Figure 4.15: Stacked ^{1}H NMR spectra of triangle **242** recorded at concentrations of 1, 0.5, and 0.25 mg/mL. Notable changes in the spectra progressing to lower concentration include the disappearance of the shoulder attributed to stacking or aggregation that results in a slightly different environment for the "K"–OCH_3 markers, as well as overall sharpening of all the peaks in the aromatic region.

Transmission electron microscopy (TEM) provided the visualization (Figure 4.16) of the triangle **242**, which revealed direct correlation of both size and shape of single molecules upon deposition of a dilute (*ca*. 10^{-5} M) MeCN solution of complex **242** with PF_6^- counterions on carbon-coated copper grids (300 mesh). The molecular framework is observed as a pure dispersion of individual molecules with triangular shape, clear edges and discernable vertices. The average distance (5.6 nm) between the vertices perfectly fits the size obtained from the optimized molecular model. The TEM image (Figure 4.16) also indicates aggregation at higher concentration, where two Sierpiński triangles can lie one top another to generate "Star of David" like structures. This phenomenon is also supported by ^{1}H NMR dilution experiment of complex **242**. At higher concentration the –OCH_3 marker on the central "K" ligand shows a distinctive shoulder, presumably due to stacking,

but exhibits smooth pattern at lower concentrations but the –OCH_3 marker on the ligand "V" remains unaffected by the concentration (Figure 4.15), since there is no adjacent ring current.

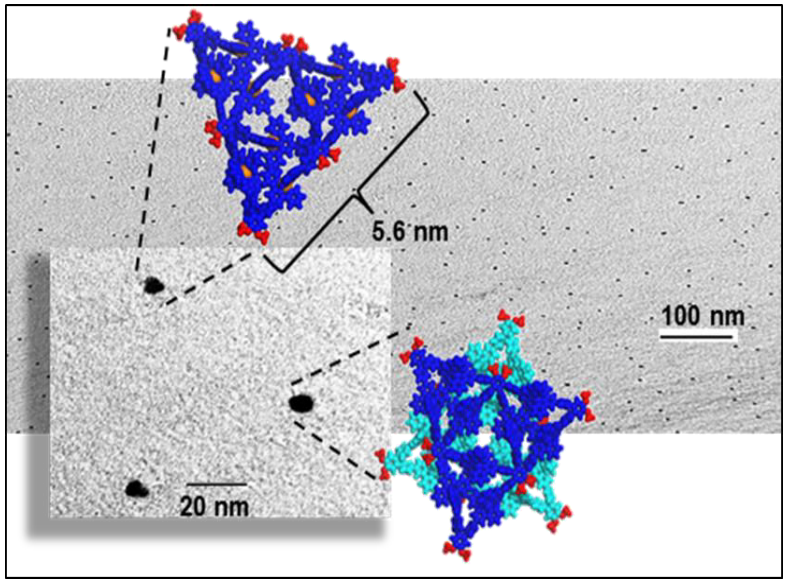

Figure 4.16: Low magnification, TEM image of the Sierpiński triangle **242** showing a uniform field of particles. The high magnification TEM image clearly exhibits triangular motifs and a slightly larger and rounded picture of a proposed aggregate. Computer-generated models illustrate the different CH_3O (red markers) environments observed in ^{1}H NMR dilution experiments to ascertain individual *vs.* stacked species.

Table 4.1: Drift times and collision cross-sections for the Sierpiński triangle **242**.

Charges	Drift time (ms)	CCS_{exp}(Å^2)	CCS_{theory} (Å^2)
6+	8.93	1309.2	1388.3 (averaged)
7+	6.49	1295.5	
8+	5.01	1288.7	
9+	4.11	1297.2	
10+	3.40	1288.5	
11+	2.76	1242.3	

4.3 Conclusion

In conclusion, we have achieved the self-assembly of a first first-generation Sierpiński triangle possessing D_{3h} symmetry using <tpy-Cd^{II}-tpy> connectivity in near quantitative yield through the use of structurally directed multi-topic [2,2':6',2'']-terpyridine ligands possessing programmed structural features. NMR spectroscopy, ESI-MS, TWIM mass spectrometry, and TEM provided insight into the size, shape, symmetry, and the molecular structure of the assembled product. The application of this ligand directivity to the assembly of the higher generation structures is currently underway.

4.4 Experimental Section

General Procedures: See page 88-89 for general synthetic procedures. For the TEM investigation, the sample was dissolved in MeCN at a concentration within the range 10^{-6} to 10^{-7} M. The solutions were drop cast onto a carbon-coated copper grid and extra solution was absorbed by filter paper to avoid aggregation. The TEM images of the drop cast samples were taken with a Jeol JEM-1230 transmission electron microscope.

Collision Cross-section Calibration. The drift time scale of the TWIM-MS experiments was converted to a collision cross-section scale. Briefly, the corrected collision cross sections of the molecular ions of insulin (bovine pancreas), ubiquitin (bovine red blood cells), and cytochrome C (horse heart), obtained from published work, were plotted against the corrected drift times (arrival times) of the corresponding molecular ions measured in TWIM-MS experiments at the same traveling-wave velocity, traveling-wave height and ion-mobility gas flow settings, *viz.* 350 ms^{-1}, 7.5 V and 22.7 mL min^{-1}. All charge states observed for the calibrants were used in the construction of the curve.

Molecular Modeling. Energy minimization of the macrocycles was conducted with the Materials Studio version 6.0 program using the Anneal and Geometry Optimization tasks in the Forcite module (Accelrys Software, Inc.). The counterions were omitted. An initially energy-minimized structure was subjected to 100 anneal cycles with initial and mid-cycle temperatures of 300 and 1500 K, respectively, twenty heating ramps per cycle, one thousand dynamics steps per ramp, and one dynamics step per femtosecond. Constant volume/constant energy (NVE) ensemble was used; the geometry was optimized after each cycle. All geometry optimizations used a universal force field with atom-based summation and cubic spline truncation for both the electrostatic and van der Waals parameters. For each macrocycle, 100 candidate structures were generated for the calculation of collision cross sections.

^{1}H NMR spectra of Triangle 242 obtained at successively dilute concentrations. ^{1}H NMR spectra of **242** were recorded at 1, 0.5, and 0.25 mg per 1 mL (25 °C, CD_3CN) using a Varian 500 MHz NMR spectrometer. Dilution of 0.5 mL of a stock solution of **242** (1.0 mg/mL, CD_3CN) to 1.0 mL afforded a 0.5 mg/mL solution. Repetition of the procedure gave the lower concentration sample.

Synthesis of 3,4,5,6-Tetrabromoveratrole (240):

To a deaerated solution of 2,3,5,6-tetrabromocatechol (1g, 2.35 mmol) and MeI (730 mg, 5.17 mmol) in THF (100 mL), K_2CO_3 (970 mg, 7.05 mmol) was added, then the reaction mixture was refluxed under N_2 for 12 hour. After cooling to the 25 °C, the reaction mixture was dried *in vacuo* to give a residue, which was dissolved in CH_2Cl_2 (100 mL) then washed with (3×100 mL) water. The organic phase was collected and dried *in vacuo* to give a light brown solid, which was purified using SiO_2 column chromatography eluting with 5% EtOAc in hexane. The pure product **240** was obtained (85 %) as light yellow solid: m.p. 107 ºC; 910 mg; ^{1}H NMR ($CDCl_3$, 500 MHz, ppm): δ 3.91 (s, 6H, Ar-OC*H*$_3$); ^{13}C NMR (125 MHz, ppm): δ 151.25, 123.54, 121.61, 60.92. ESI- MS (m/z) 471.10 amu [M+Na].

Synthesis of Ligand 241:

To a solution of 3,4,5,6-tetrabromoveratrole (**240**, 450 mg, 1 mmol) in mixed solvent of toluene:H_2O:EtOH (150:150:50), 4'-(4-boronatophenyl)[2,2':6',2'']terpyridine (**239**; 2.12g, 6 mmol) and K_2CO_3 (4.14 g, 30 mmol) were added. This reaction mixture was freeze-pump-thawed (3X), then back filled with argon. The reaction mixture was then heated and when refluxing began $Pd(PPh_3)_2Cl_2$ (140 mg, 200 μmol, 5 mol%) was added under argon. After 4 days, the reaction mixture was cooled to 25 °C, the organic phase was separated and washed with water, then dried over $MgSO_4$. After concentrating *in vacuo*, the residue was column chromatographed (Al_2O_3) eluting with $CHCl_3$. The product was a white amorphous solid: 980 mg (72%); m.p. 298 °C.

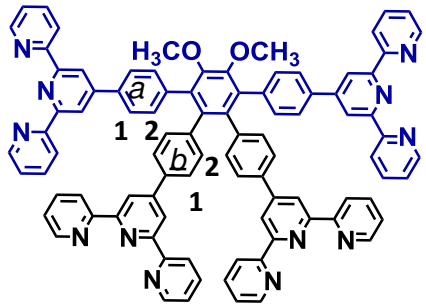

^{1}H NMR ($CDCl_3$, 500 MHz, ppm): δ 8.73 (s, 4H, tpy^a*H*$^{3',5'}$), 8.67 (d, *J* = 5.0 Hz , 4H, tpy^a*H*$^{6,6''}$), 8.62 (d, *J* = 8.0 Hz, 4H, tpy^a*H*$^{3,3''}$), 8.57 (m, 8H, tpy^b*H*$^{3',5'}$, tpy^b*H*$^{6,6''}$), 8.52 (d, *J* = 8.0 Hz, 4H, tpy^b*H*$^{3,3''}$), 7.82 (m, 8H, tpy^a*H*$^{4,4''}$, Ph^{a1}*H*), 7.74 (dd,4H, J_1 = 8.0, , J_2 = 8.0 Hz, J_3 = 2.0 Hz, tpy^b*H*$^{4,4''}$), 7.56 (d, 4H, *J* = 8.0 Hz, Ph^{b1}*H*), 7.39 (d, 4H, *J* = 8.0 Hz, Ph^{a2}*H*), 7.29 (dd, 4H, , J_1 = 8.0 Hz , J_2 = 5.0 Hz, tpy^a*H*$^{5,5''}$), 7.21 (dd, 4H, , J_1 = 8.0 Hz, J_2 = 5.0 Hz, tpy^b*H*$^{5,5''}$), 7.06 (d, 4H, *J* = 8.0 Hz, Ph^{b2}*H*), 3.76 (s, 6H, PhOC*H*$_3$); ^{13}C NMR (125 MHz, ppm): δ 156.56, 156.55, 155.99, 155.80, 150.63, 150.24, 149.75, 149.25, 149.12, 140.69, 138.13, 137.04, 136.93, 136.78, 136.66, 136.06, 135.58, 132.20, 131.54, 126.69, 126.25, 123.83, 123.65, 121.48, 121.37, 119.15, 118.90, 60.99; MALDI-MS (*m/z*) 1389.47 amu [M+Na].

Synthesis of ligand 227:

To a solution of 4,5-dibromoveratrole (296 mg, 1 mmol) in mixed solvent of toluene:H_2O:EtOH (150:150:50), 4'-(4-boronatophenyl)[2,2':6',2"]terpyridine (1.06 g, 3 mmol) and K_2CO_3 (2.07 g, 15 mmol) were added. The whole mixture was freeze-pump-thawed (3X) to remove any oxygen from the system and then back filled with argon. The reaction mixture was brought to reflux and when the refluxing starts $Pd(PPh_3)_2Cl_2$ (70 mg, 0.1 mmol, 5 mol%) was added under argon. The reaction mixture was refluxed for 2 days, then cooled to 25 ºC, and the organic phase was separated, washed with water, and dried

over $MgSO_4$. After concentrating *in vacuo*, the residue was purified using Al_2O_3 column chromatography with $CHCl_3$, as eluent. The product was obtained as white amorphous solid. 600 mg (80%); m.p. 269 ºC;

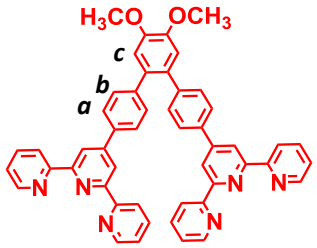

^{1}H NMR ($CDCl_3$, 500 MHz, ppm): δ 8.76 (s, 4H, tpy$H^{3',5'}$), 8.70 (d, J = 5.0 Hz, 4H, tpy$H^{6,6''}$), 8.66 (d, J = 8.0 Hz, 4H, tpy$H^{3,3''}$), 7.86 (m, 8H, tpy$H^{4,4''}$, Ph^{a}H), 7.34 (m, 8H, tpy$H^{5,5''}$, Ph^{b}H), 7.04 (s, 2H, Ph^{c}H), 4.02 (s, 6H, Ph^{c}OCH_3); ^{13}C NMR (125 MHz, ppm): 156.52, 156.09, 149.94, 149.27, 148.78, 142.42, 136.95, 136.59, 132.75, 130.69, 127.23, 121.88, 121.50, 118.96, 113.98, 56.40; ESI-MS (*m/z*) 753.3 amu [M+H].

Synthesis of Sierpiński Triangle 242:

To a solution of ligand **227** (5 mg, 6.64×10^{-3} mmol) and **242** (9.08 mg, 6.64×10^{-3} mmol) in $CHCl_3$ (50 mL), a MeOH solution (25 mL) of $Cd(NO_3)_2\cdot4H_2O$ (6.15 mg, 19.92×10^{-3} mmol) was added. The solution was stirred for 30 minutes at 25 °C. Then excess NH_4PF_6 was added to obtain a light yellow precipitate, which was filtered and washed repeatedly with MeOH to remove any leftover NH_4PF_6. The product obtained (95%) as a light yellow solid: 19.22 mg; m.p .> 300 ºC;

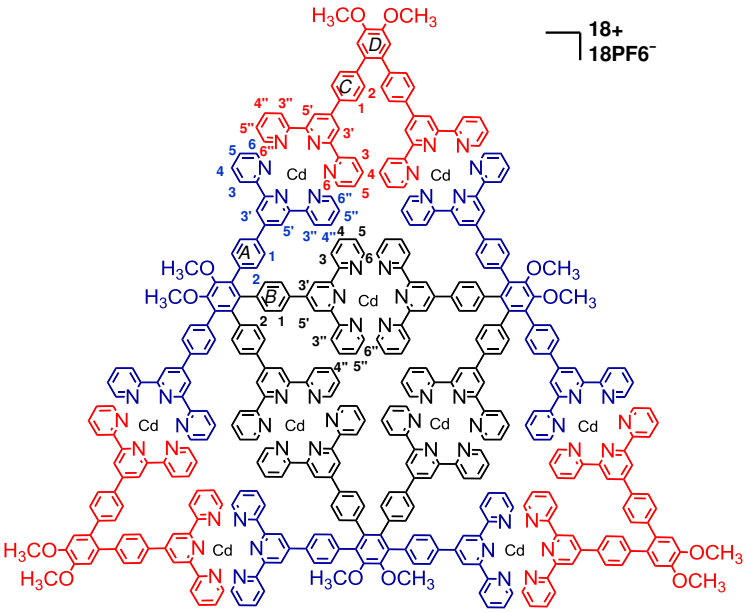

^{1}H NMR (CD_3CN, 500 MHz, ppm): δ 8.92 (s, 12H, tpy$^{A}H^{3',5'}$), 8.91 (s, 12H, tpy$^{C}H^{3',5'}$), 8.72 (m, 36H, tpy$^{A}H^{3,3''}$, tpy$^{B}H^{3',5'}$, tpy$^{C}H^{3,3''}$), 8.60 (d, J = 8.0 Hz, 12H, tpy$^{B}H^{3,3''}$), 8.10 (m, 48H, tpy$^{A}H^{4,4''}$, tpy$^{C}H^{4,4''}$, Ph$^{A}H^{1}$, Ph$^{C}H^{1}$), 7.92 (m, 24H, tpy$^{B}H^{4,4''}$, tpy$^{A}H^{6,6''}$), 7.80 (d, J = 5.0 Hz, 12H, tpy$^{C}H^{6,6''}$), 7.68 (d, J = 5.0 Hz, 12H, tpy$^{B}H^{6,6''}$) 7.59 (d, J = 8.0 Hz 12H, Ph$^{B}H^{1}$) 7.58 (s, 6H, Ph^{D}H) 7.43 (m, 48H, tpy$^{A}H^{5,5''}$, tpy$^{C}H^{5,5''}$, Ph$^{A}H^{2}$, Ph$^{C}H^{2}$) 7.25 (dd, J_1 = 8.0 Hz, J_2 = 5.0 Hz, 12H, tpy$^{B}H^{5,5''}$), 7.20 (d, J = 8.0 Hz, 12H, Ph$^{B}H^{2}$), 3.98 (s, 18H, Ph-OCH_3), 3.87 (s, 18H, Ph-OCH_3); ^{13}C NMR (CD_3CN, 125 MHz, ppm): 158.39, 155.62, 154.93, 152.57, 150.46, 149.81, 149.52, 149.01, 144.52, 144.41, 143.77, 141.67, 139.07, 135.03, 134.48, 134.43, 132.24, 132.13, 132.01, 131.50, 131.45, 127.87, 127.83, 127.60, 127.57, 127.48, 124.57, 123.89, 121.84, 121.58, 114.52, 114.45, 56.02, 56.00; ESI-MS (*m/z*) 1520.3 $[M\text{-}6PF_6^-]^{6+}$ (calcd. *m/z* = 1520.2) , 1282.4 $[M\text{-}7PF_6^-]^{7+}$ (calcd. *m/z* =1282.3), 1103.9 $[M\text{-}8PF_6^-]^{8+}$ (calcd. *m/z* =1103.9), 965.2 $[M\text{-}9PF_6^-]^{9+}$ (calcd. *m/z* = 965.1), 854.2 $[M\text{-}10PF_6^-]^{10+}$ (calcd. *m/z* = 854.1), 763. 3 $[M\text{-}11PF_6^-]^{11+}$ (calcd. *m/z* = 763.3).

CHAPTER V

SUMMARY

Two heterobimetallic triangles were synthesized by catalytic fusion of a triangular and a tetrameric architecture in quantitative yield. Initially, two cyclic metallo-trimers were obtained quantitatively by reacting 60º-directed *bis*terpyridine ligand either with Zn(II) or Cd(II) and the metallo-squares were prepared, also in quantitative yield, by mixing Ru(II)-dimer of the same 60º-directed building-block either with Zn(II) or Cd(II). The triangular and tetrameric constructs were reacted in precise 1:1.5 ratio to forge the bimetallic triangles. All the proposed complexes were characterized by ^{1}H, ^{13}C, 2D-COSY, 2D-NOESY NMR, ESI- and TWIM MS data. The gradient tandem (gMS^{2}) mass spectrometric data provided the stability of the triangles.

Three bimetallic triangles were synthesized *via* a step-wise directed assembly method. The 60º-directed ligand was reacted with Ru(II) to produce an oligomeric trimer, which was subsequently reacted with Zn(II) and Cd(II) to obtain two bimetallic triangles in quantitative yield and on the other hand reaction of the trimer with Fe(II) produces another bimetallic triangle in a very high yield. All the triangles were characterized by ^{1}H, ^{13}C, 2D-COSY, 2D-NOESY NMR, ESI- and TWIM MS data. The gradient tandem mass

spectrometric data revealed the order of stability for the triangle is Fe(II)-triangle > Zn(II)-triangle > Cd(II)-triangle.

A structural mimic of the first-generation, Sierpiński triangle was conceived and prepared using a heteroleptic assembly technique, based on retro-synthetic analysis that suggested requirement of two different building-blocks; a 60º-directed *bis*terpyridine ligand - "V", and a tetra*kis*(terpyridine) ligand - "K". The ligands were readily prepared by Suzuki-cross coupling reactions and then reacted with Cd(II) in precise 1:1:3 ratio to produce the desired architecture in near quantitative yield. The ^{1}H, 2D-COSY, 2D-NOESY NMR data, ESI- and TWIM-MS, and collision cross-section data confirmed the presence of a single discrete entity and TEM images provided the visualization of the Sierpiński triangle.

REFERENCES

1. Watson, J. D.; Crick, F. H. C., *Nature* **1953**, *171*, 737-738.

2. Fisher, O. Z.; Khademhosseini, A.; Langer, R.; Peppas, N. A., *Acc. Chem. Res.* **2010**, *43*, 419-428.

3. McConney, M. E.; Anderson, K. D.; Brott, L. L.; Naik, R. R.; Tsukruk, V. V., *Adv. Funct. Mater.* **2009**, *19*, 2527-2544.

4. Mohammed, J. S.; Murphy, W. L., *Adv. Mater.* **2009**, *21*, 2361-2374.

5. Lehn, J.-M., *Angew. Chem. Int. Ed.* **1988**, *27*, 89-112.

6. Cram, D. J., *Angew. Chem. Int. Ed.* **1988**, *27*, 1009-1020.

7. Pedersen, C. J., *Angew. Chem. Int. Ed.* **1988**, *27*, 1021-1027.

8. Morris, R. E.; Wheatley, P. S., *Angew. Chem. Int. Ed.* **2008**, *47*, 4966-4981.

9. Murray, L. J.; Dinca, M.; Long, J. R., *Chem. Soc. Rev.* **2009**, *38*, 1294-1314.

10. Fiedler, D.; Leung, D. H.; Bergman, R. G.; Raymond, K. N., *Acc. Chem. Res.* **2005**, *38*, 349-358.

11. Joachim, C.; Gimzewski, J. K.; Aviram, A., *Nature* **2000**, *408*, 541-548.

12. Vallet-Regi, M.; Balas, F.; Arcos, D., *Angew. Chem. Int. Ed.* **2007**, *46*, 7548-7558.

13. Lehn, J.-M., *Chem. Soc. Rev.* **2007**, *36*, 151.

14. Ruben, M.; Rojo, J.; Romero-Salguero, F. J.; Uppadine, L. H.; Lehn, J.-M., *Angew. Chem. Int. Ed.* **2004**, *43*, 3644-3662.

15. Lehn, J.-M., *Science* **1985**, *227*, 849-856.

16. Lehn, J.-M.; Eliseev, A. V., *Science* **2001**, *291*, 2331-2332.

17. Koert, U.; Harding, M. M.; Lehn, J.-M., *Nature* **1990**, *346*, 339-342.

18. Northrop, B. H.; Zheng, Y.-R.; Chi, K.-W.; Stang, P. J., *Acc. Chem. Res.* **2009**, *42*, 1554-1563.

19. Seidel, S. R.; Stang, P. J., *Acc. Chem. Res.* **2002**, *35*, 972-983.

20. Chakrabarty, R.; Mukherjee, P. S.; Stang, P. J., *Chem. Rev.* **2011**, *111*, 6810-6918.

21. Maran, U.; Britt, D.; Fox, C. B.; Harris, J. M.; Orendt, A. M.; Conley, H.; Davis, R.; Hlady, V.; Stang, P. J., *Chem. Eur. J.* **2009**, *15*, 8566-8577.

22. Zhao, Z.; Zheng, Y.-R.; Wang, M.; Pollock, J. B.; Stang, P. J., *Inorg. Chem.* **2010**, *49*, 8653-8655.

23. Zheng, Y.-R.; Stang, P. J., *J. Am. Chem. Soc.* **2009**, *131*, 3487-3489.

24. Newkome, G. R.; Wang, P.; Moorefield, C. N.; Cho, T. J.; Mohapatra, P. P.; Li, S.; Hwang, S.-H.; Lukoyanova, O.; Echegoyen, L.; Palagallo, J. A.; Iancu, V.; Hla, S.-W., *Science* **2006**, *312*, 1782-1785.

25. Newkome, G. R.; Cho, T. J.; Moorefield, C. N.; Baker, G. R.; Cush, R.; Russo, P. S., *Angew. Chem. Int. Ed.* **1999**, *38*, 3717-3721.

26. Schultz, A.; Li, X.; Barkakaty, B.; Moorefield, C. N.; Wesdemiotis, C.; Newkome, G. R., *J. Am. Chem. Soc.* **2012**, *134*, 7672-7675.

27. Sarkar, R.; Guo, K.; Moorefield, C. N.; Saunders, M. J.; Wesdemiotis, C.; Newkome, G. R., *Angew. Chem. Int. Ed.* **2014**, *53*, 12182-12185.

28. Newkome, G. R.; Moorefield, C. N., *Chem. Soc. Rev.* **2015**, *44*, 3954-3967.

29. Ludlow III, J. M.; Xie, T.; Guo, Z.; Guo, K.; Saunders, M. J.; Moorefield, C. N.; Wesdemiotis, C.; Newkome, G. R., *Chem. Commun.* **2015**, *51*, 3820-3823.

30. Sun, Q.-F.; Iwasa, J.; Ogawa, D.; Ishido, Y.; Sato, S.; Ozeki, T.; Sei, Y.; Yamaguchi, K.; Fujita, M., *Science* **2010**, *328*, 1144-1147.

31. Sun, Q.-F.; Murase, T.; Sato, S.; Fujita, M., *Angew. Chem. Int. Ed.* **2011**, *50*, 10318-10321.

32. Tominaga, M.; Suzuki, K.; Kawano, M.; Kusukawa, T.; Ozeki, T.; Sakamoto, S.; Yamaguchi, K.; Fujita, M., *Angew. Chem. Int. Ed.* **2004**, *43*, 5621-5625.

33. De, S.; Mahata, K.; Schmittel, M., *Chem. Soc. Rev.* **2010**, *39*, 1555.

34. Saha, M. L.; Neogi, S.; Schmittel, M., *Dalton Trans.* **2014**, *43*, 3815-3834.

35. Gianneschi, N. C.; Masar, M. S.; Mirkin, C. A., *Acc. Chem. Res.* **2005**, *38*, 825-837.

36. Balzani, V.; Credi, A.; Marchioni, F.; Stoddart, J. F., *Chem. Commun.* **2001**, 1860-1861.

37. Flamigni, L.; Dixon, I. M.; Collin, J.-P.; Sauvage, J.-P., *Chem. Commun.* **2000**, 2479-2480.

38. Rebek, J. Jr., *Angew. Chem. Int. Ed.* **2005**, *44*, 2068-2078.

39. Goze, C.; Kozlov, D. V.; Castellano, F. N.; Suffert, J.; Ziessel, R., *Tetrahedron Lett.* **2003**, *44*, 8713-8716.

40. Constable, E. C., *Chem. Soc. Rev.* **2007**, *36*, 246.

41. Schubert, U. S.; Hummel, J.; Winter, A.; Baumgaertel, A.; Risch, N., *Synlett* **2009**, *2010*, 61-66.

42. Bolisetty, S.; Schneider, C.; Polzer, F.; Ballauff, M.; Li, W.; Zhang, A.; Schluter, A. D., *Macromolecules* **2009**, *42*, 7122-7128.

43. Cook, T. R.; Zheng, Y.-R.; Stang, P. J., *Chem. Rev.* **2013**, *113*, 734-777.

44. Oliveri, C. G.; Ulmann, P. A.; Wiester, M. J.; Mirkin, C. A., *Acc. Chem. Res.* **2008**, *41*, 1618-1629.

45. Schubert, U. S.; Hofmeier, H.; Newkome, G. R., *Modern Terpyridine Chemistry*. Wiley:VCH, **2006**.

46. Atwood, J. L.; Steed, J. W., *Encyclopedia of Supramolecular Chemistry*. M. Dekker: **2004**.

47. Zheng, Y.-R.; Yang, H.-B.; Ghosh, K.; Zhao, L.; Stang, P. J., *Chem. Eur. J.* **2009**, *15*, 7203-7214.

48. De, S.; Mahata, K.; Schmittel, M., *Chem. Soc. Rev.* **2010**, *39*, 1555-1575.

49. Baranoff, E.; Collin, J.-P.; Flamigni, L.; Sauvage, J.-P., *Chem. Soc. Rev.* **2004**, *33*, 144-147.

50. Stang, P. J.; Cao, D. H., *J. Am. Chem. Soc.* **1994**, *116*, 4981-4982.

51. Fujita, M.; Yazaki, J.; Ogura, K., *J. Am. Chem. Soc.* **1990**, *112*, 5645-5647.

52. Zangrando, E.; Casanova, M.; Alessio, E., *Chem. Rev.* **2008**, *108*, 4979-5013.

53. Hall, J. R.; Loeb, S. J.; Shimizu, G. K. H.; Yap, G. P. A., *Angew. Chem. Int. Ed.* **1998**, *37*, 121-123.

54. Kryschenko, Y. K.; Seidel, S. R.; Arif, A. M.; Stang, P. J., *J. Am. Chem. Soc.* **2003**, *125*, 5193-5198.

55. Jude, H.; Disteldorf, H.; Fischer, S.; Wedge, T.; Hawkridge, A. M.; Arif, A. M.; Hawthorne, M. F.; Muddiman, D. C.; Stang, P. J., *J. Am. Chem. Soc.* **2005**, *127*, 12131-12139.

56. Hwang, S.-H.; Moorefield, C. N.; Fronczek, F. R.; Lukoyanova, O.; Echegoyen, L.; Newkome, G. R., *Chem. Commun.* **2005**, 713-715.

57. Qin, Z.; Jennings, M. C.; Puddephatt, R. J., *Chem. Commun.* **2001**, 2676-2677.

58. Qin, Z.; Jennings, M. C.; Puddephatt, R. J., *Inorg. Chem.* **2003**, *42*, 1956-1965.

59. Mukherjee, P. S.; Das, N.; Kryschenko, Y. K.; Arif, A. M.; Stang, P. J., *J. Am. Chem. Soc.* **2004**, *126*, 2464-2473.

60. Wurthner, F.; You, C.-C.; Saha-Moller, C. R., *Chem. Soc. Rev.* **2004**, *33*, 133-146.

61. Fujita, M.; Yazaki, J.; Ogura, K., *Chem. Lett.* **1991**, *20*, 1031-1032.

62. Stang, P. J., *J. Org. Chem.* **2009**, *74*, 2-20.

63. Northrop, B. H.; Chercka, D.; Stang, P. J., *Tetrahedron* **2008**, *64*, 11495-11503.

64. Stang, P. J.; Olenyuk, B.; Fan, J.; Arif, A. M., *Organometallics* **1996**, *15*, 904-908.

65. Whiteford, J. A.; Lu, C. V.; Stang, P. J., *J. Am. Chem. Soc.* **1997**, *119*, 2524-2533.

66. Stang, P. J.; Cao, D. H.; Chen, K.; Gray, G. M.; Muddiman, D. C.; Smith, R. D., *J. Am. Chem. Soc.* **1997**, *119*, 5163-5168.

67. Stang, P. J.; Fan, J.; Olenyuk, B., *Chem. Commun.* **1997**, 1453-1454.

68. Sun, S.-S.; Lees, A. J., *Inorg. Chem.* **2001**, *40*, 3154-3160.

69. Schultz, A.; Li, X.; McCusker, C. E.; Moorefield, C. N.; Castellano, F. N.; Wesdemiotis, C.; Newkome, G. R., *Chem. Eur. J.* **2012**, *18*, 11569-11572.

70. Shanmugaraju, S.; Bar, A. K.; Chi, K.-W.; Mukherjee, P. S., *Organometallics* **2010**, *29,* 2971-2980.

71. Gianneschi, N. C.; Mirkin, C. A.; Zakharov, L. N.; Rheingold, A. L., *Inorg. Chem.* **2002**, *41*, 5326-5328.

72. Brasey, T.; Scopelliti, R.; Severin, K., *Inorg. Chem.* **2005**, *44*, 160-162.

73. Fujita, M.; Sasaki, O.; Mitsuhashi, T.; Fujita, T.; Yazaki, J.; Yamaguchi, K.; Ogura, K., *Chem. Commun.* **1996**, 1535-1536.

74. Lee, S. B.; Hwang, S.; Chung, D. S.; Yun, H.; Hong, J.-I., *Tetrahedron Lett.* **1998**, *39,* 873-876.

75. Weilandt, T.; Troff, R. W.; Saxell, H.; Rissanen, K.; Schalley, C. A., *Inorg. Chem.* **2008**, *47*, 7588-7598.

76. Sautter, A.; Schmid, D. G.; Jung, G.; Würthner, F., *J. Am. Chem. Soc.* **2001**, *123*, 5424-5430.

77. Schweiger, M.; Seidel, S. R.; Arif, A. M.; Stang, P. J., *Inorg. Chem.* **2002**, *41*, 2556-2559.

78. Uehara, K.; Kasai, K.; Mizuno, N., *Inorg. Chem.* **2007**, *46*, 2563-2570.

79. Ferrer, M.; Mounir, M.; Rossell, O.; Ruiz, E.; Maestro, M. A., *Inorg. Chem.* **2003**, *42*, 5890-5899.

80. Ferrer, M.; Gutierrez, A.; Mounir, M.; Rossell, O.; Ruiz, E.; Rang, A.; Engeser, M., *Inorg. Chem.* **2007**, *46*, 3395-3406.

81. Hollo-Sitkei, E.; Tarkanyi, G.; Parkanyi, L.; Megyes, T.; Besenyei, G., *Eur. J. Inorg. Chem.* **2008**, 1573-1583.

82. Rubin, Y.; Knobler, C. B.; Diederich, F., *J. Am. Chem. Soc.* **1990**, *112*, 4966-4968.

83. McQuillan, F. S.; Berridge, T. E.; Chen, H.; Hamor, T. A.; Jones, C. J., *Inorg. Chem.* **1998**, *37*, 4959-4970.

84. Yu, S.-Y.; Huang, H.-P.; Li, S.-H.; Jiao, Q.; Li, Y.-Z.; Wu, B.; Sei, Y.; Yamaguchi, K.; Pan, Y.-J.; Ma, H.-W., *Inorg. Chem.* **2005**, *44*, 9471-9488.

85. Cotton, F. A.; Daniels, L. M.; Lin, C.; Murillo, C. A., *J. Am. Chem. Soc.* **1999**, *121*, 4538-4539.

86. Bera, J. K.; Angaridis, P.; Cotton, F. A.; Petrukhina, M. A.; Fanwick, P. E.; Walton, R.A., *J. Am. Chem. Soc.* **2001**, *123*, 1515-1516.

87. Berben, L. A.; Faia, M. C.; Crawford, N. R. M.; Long, J. R., *Inorg. Chem.* **2006**, *45*, 6378-6386.

88. Lau, V. C.; Berben, L. A.; Long, J. R., *J. Am. Chem. Soc.* **2002**, *124*, 9042-9043.

89. Kuehl, C. J.; Huang, S. D.; Stang, P. J., *J. Am. Chem. Soc.* **2001**, *123*, 9634-9641.

90. Resendiz, M. J. E.; Noveron, J. C.; Disteldorf, H.; Fischer, S.; Stang, P. J., *Org. Lett.* **2004**, *6*, 651-653.

91. Kaim, W.; Schwederski, B.; Dogan, A.; Fiedler, J.; Kuehl, C. J.; Stang, P. J., *Inorg. Chem.* **2002**, *41*, 4025-4028.

92. Ghosh, S.; Chakrabarty, R.; Mukherjee, P. S., *Inorg. Chem.* **2009**, *48*, 549-556.

93. Sommer, R. D.; Rheingold, A. L.; Goshe, A. J.; Bosnich, B., *J. Am. Chem. Soc.* **2001**, *123*, 3940-3952.

94. Yan, H.; Suss-Fink, G.; Neels, A.; Stoeckli-Evans, H., *J. Chem. Soc., Dalton Trans.* **1997**, 4345-4350.

95. Mattsson, J.; Govindaswamy, P.; Renfrew, A. K.; Dyson, P. J.; Štěpnička, P.; Suss-Fink, G.; Therrien, B., *Organometallics* **2009**, *28*, 4350-4357.

96. Barry, N. P. E.; Edafe, F.; Therrien, B., *Dalton Trans.* **2011**, *40*, 7172-7180.

97. Barry, N. P. E.; Furrer, J.; Freudenreich, J.; Suss-Fink, G.; Therrien, B., *Eur. J. Inorg. Chem.* **2010**, 725-728.

98. Barry, N. P. E.; Furrer, J.; Therrien, B., *Helv. Chim. Acta* **2010**, *93*, 1313-1328.

99. Han, Y.-F.; Jia, W.-G.; Lin, Y.-J.; Jin, G.-X., *Organometallics* **2008**, *27*, 5002-5008.

100. Han, Y.-F.; Fei, Y.; Jin, G.-X., *Dalton Trans.* **2010**, *39*, 3976-3984.

101. Lindner, E.; Zong, R.; Eichele, K.; Weisser, U.; Strobele, M., *Eur. J. Inorg. Chem.* **2003**, 705-712.

102. Fujita, M.; Ibukuro, F.; Hagihara, H.; Ogura, K., *Nature* **1994**, *367*, 720-723.

103. Fujita, M.; Aoyagi, M.; Ogura, K., *Inorg. Chim. Acta* **1996**, *246*, 53-57.

104. Fujita, M.; Ibukuro, F.; Seki, H.; Kamo, O.; Imanari, M.; Ogura, K., *J. Am. Chem. Soc.* **1996**, *118*, 899-900.

105. Fujita, M.; Ibukuro, F.; Yamaguchi, K.; Ogura, K., *J. Am. Chem. Soc.* **1995**, *117*, 4175-4176.

106. Schmitz, M.; Leininger, S.; Fan, J.; Arif, A. M.; Stang, P. J., *Organometallics* **1999**, *18*, 4817-4824.

107. Yang, H.-B.; Das, N.; Huang, F.; Hawkridge, A. M.; Diaz, D. D.; Arif, A. M.; Finn, M. G.; Muddiman, D. C.; Stang, P. J., *J. Org. Chem.* **2006**, *71*, 6644-6647.

108. Stang, P. J.; Persky, N. E.; Manna, J., *J. Am. Chem. Soc.* **1997**, *119*, 4777-4778.

109. Hasenknopf, B.; Lehn, J.-M.; Kneisel, B. O.; Baum, G.; Fenske, D., *Angew. Chem. Int. Ed.* **1996**, *35*, 1838-1840.

110. Mamula, O.; von Zelewsky, A.; Bernardinelli, G., *Angew. Chem. Int. Ed.* **1998**, *37*, 289-293.

111. Newkome, G. R.; Cho, T. J.; Moorefield, C. N.; Mohapatra, P. P.; Godinez, L. A., *Chem. Eur. J.* **2004**, *10*, 1493-1500.

112. Chan, Y.-T.; Li, X.; Yu, J.; Carri, G. A.; Moorefield, C. N.; Newkome, G. R.; Wesdemiotis, C., *J. Am. Chem. Soc.* **2011**, *133*, 11967-11976.

113. Chan, Y.-T.; Li, X.; Moorefield, C. N.; Wesdemiotis, C.; Newkome, G. R., *Chem. Eur. J.* **2011**, *17*, 7750-7754.

114. Saalfrank, R. W.; Stark, A.; Peters, K.; von Schnering, H. G., *Angew. Chem. Int. Ed.* **1988**, *27*, 851-853.

115. Fujita, M.; Oguro, D.; Miyazawa, M.; Oka, H.; Yamaguchi, K.; Ogura, K., *Nature* **1995**, *378*, 469-471.

116. Kusukawa, T.; Fujita, M., *J. Am. Chem. Soc.* **2002**, *124*, 13576-13582.

117. Yamashita, K.-i.; Kawano, M.; Fujita, M., *Chem. Commun.* **2007**, 4102-4103.

118. Leininger, S.; Fan, J.; Schmitz, M.; Stang, P. J., *Proc. Natl. Acad. Sci.* **2000**, *97*, 1380-1384.

119. Stang, P. J.; Olenyuk, B.; Muddiman, D. C.; Smith, R. D., *Organometallics* **1997**, *16*, 3094-3096.

120. Schweiger, M.; Yamamoto, T.; Stang, P. J.; Blaser, D.; Boese, R., *J. Org. Chem.* **2005**, *70*, 4861-4864.

121. Roche, S.; Haslam, C.; L. Heath, S.; A. Thomas, J., *Chem. Commun.* **1998**, 1681-1682.

122. Johannessen, S. C.; Brisbois, R. G.; Fischer, J. P.; Grieco, P. A.; Counterman, A. E.; Clemmer, D. E., *J. Am. Chem. Soc.* **2001**, *123*, 3818-3819.

123. Heinrich, J. L.; Berseth, P. A.; Long, J. R., *Chem. Commun.* **1998**, 1231-1232.

124. Prakash, M. J.; Zou, Y.; Hong, S.; Park, M.; Bui, M.-P. N.; Seong, G. H.; Lah, M. S., *Inorg. Chem.* **2009**, *48*, 1281-1283.

125. Olenyuk, B.; Whiteford, J. A.; Fechtenkotter, A.; Stang, P. J., *Nature* **1999**, *398*, 796-799.

126. Argent, S. P.; Adams, H.; Riis-Johannessen, T.; Jeffery, J. C.; Harding, L. P.; Ward, M. D., *J. Am. Chem. Soc.* **2006**, *128*, 72-73.

127. Al-Rasbi, N. K.; Tidmarsh, I. S.; Argent, S. P.; Adams, H.; Harding, L. P.; Ward, M. D., *J. Am. Chem. Soc.* **2008**, *130*, 11641-11649.

128. Fujita, M.; Nagao, S.; Ogura, K., *J. Am. Chem. Soc.* **1995**, *117*, 1649-1650.

129. Radhakrishnan, U.; Schweiger, M.; Stang, P. J., *Org. Lett.* **2001**, *3*, 3141-3143.

130. Mukherjee, P. S.; Das, N.; Stang, P. J., *J. Org. Chem.* **2004**, *69*, 3526-3529.

131. Ghosh, S.; Mukherjee, P. S., *Tetrahedron Lett.* **2006**, *47*, 9297-9300.

132. Fujita, M.; Yu, S.-Y.; Kusukawa, T.; Funaki, H.; Ogura, K.; Yamaguchi, K., *Angew. Chem. Int. Ed.* **1998**, *37*, 2082-2085.

133. Ghosh, S.; Batten, S. R.; Turner, D. R.; Mukherjee, P. S., *Organometallics* **2007**, *26*, 3252-3255.

134. Schweiger, M.; Seidel, S. R.; Schmitz, M.; Stang, P. J., *Org. Lett.* **2000**, *2*, 1255-1257.

135. Zheng, Y.-R.; Ghosh, K.; Yang, H.-B.; Stang, P. J., *Inorg. Chem.* **2010**, *49*, 4747-4749.

136. Hiraoka, S.; Kubota, Y.; Fujita, M., *Chem. Commun.* **2000**, 1509-1510.

137. Ikeda, A.; Udzu, H.; Zhong, Z.; Shinkai, S.; Sakamoto, S.; Yamaguchi, K., *J. Am. Chem. Soc.* **2001**, *123*, 3872-3877.

138. Ikeda, A.; Yoshimura, M.; Udzu, H.; Fukuhara, C.; Shinkai, S., *J. Am. Chem. Soc.* **1999**, *121*, 4296-4297.

139. Liu, H.-K.; Sun, W.-Y.; Ma, D.-J.; Yu, K.-B.; Tang, W.-X., *Chem. Commun.* **2000**, 591-592.

140. Kuehl, C. J.; Yamamoto, T.; Seidel, S. R.; Stang, P. J., *Org. Lett.* **2002**, *4*, 913-915.

141. Kumazawa, K.; Biradha, K.; Kusukawa, T.; Okano, T.; Fujita, M., *Angew. Chem. Int. Ed.* **2003**, *42*, 3909-3913.

142. Kim, D.; Paek, J. H.; Jun, M.-J.; Lee, J. Y.; Kang, S. O.; Ko, J., *Inorg. Chem.* **2005**, *44*, 7886-7894.

143. Ghosh, S.; Gole, B.; Bar, A. K.; Mukherjee, P. S., *Organometallics* **2009**, *28*, 4288-4296.

144. Ghosh, S.; Mukherjee, P. S., *Organometallics* **2008**, *27* (3), 316-319.

145. Crowley, J. D.; Goshe, A. J.; Bosnich, B., *Chem. Commun.* **2003**, 2824-2825.

146. Lee, S. J.; Mulfort, K. L.; O'Donnell, J. L.; Zuo, X.; Goshe, A. J.; Wesson, P. J.; Nguyen, S. T.; Hupp, J. T.; Tiede, D. M., *Chem. Commun.* **2006**, 4581-4583.

147. Kelley, R. F.; Lee, S. J.; Wilson, T. M.; Nakamura, Y.; Tiede, D. M.; Osuka, A.; Hupp, J. T.; Wasielewski, M. R., *J. Am. Chem. Soc.* **2008**, *130*, 4277-4284.

148. Youm, K.-T.; Nguyen, S. T.; Hupp, J. T., *Chem. Commun.* **2008**, 3375-3377.

149. Oliva, A. I.; Ventura, B.; Wurthner, F.; Camara-Campos, A.; Hunter, C. A.; Ballester, P.; Flamigni, L., *Dalton Trans.* **2009**, 4023-4037.

150. Indelli, M. T.; Chiorboli, C.; Scandola, F.; Iengo, E.; Osswald, P.; Wurthner, F., *J. Phys. Chem. B* **2010**, *114*, 14495-14504.

151. Govindaswamy, P.; Suss-Fink, G.; Therrien, B., *Organometallics* **2007**, *26*, 915-924.

152. Govindaswamy, P.; Linder, D.; Lacour, J.; Suss-Fink, G.; Therrien, B., *Chem. Commun.* **2006**, 4691-4693.

153. Kuehl, C. J.; Kryschenko, Y. K.; Radhakrishnan, U.; Seidel, S. R.; Huang, S. D.; Stang, P. J., *Proc. Natl. Acad. Sci.* **2002**, *99*, 4932-4936.

154. Kryschenko, Y. K.; Seidel, S. R.; Muddiman, D. C.; Nepomuceno, A. I.; Stang, P. J., *J. Am. Chem. Soc.* **2003**, *125*, 9647-9652.

155. Barbour, L. J.; Orr, G. W.; Atwood, J. L., *Nature* **1998**, *393*, 671-673.

156. Chand, D. K.; Biradha, K.; Fujita, M., *Chem. Commun.* **2001**, 1652-1653.

157. McMorran, D. A.; Steel, P. J., *Angew. Chem. Int. Ed.* **1998**, *37*, 3295-3297.

158. Yue, N. L. S.; Eisler, D. J.; Jennings, M. C.; Puddephatt, R. J., *Inorg. Chem.* **2004**, *43*, 7671-7681.

159. Barry, N. P. E.; Govindaswamy, P.; Furrer, J.; Suss-Fink, G.; Therrien, B., *Inorg. Chem. Commun.* **2008**, *11*, 1300-1303.

160. Barry, N. P. E.; Abd Karim, N. H.; Vilar, R.; Therrien, B., *Dalton Trans.* **2009**, 10717-10719.

161. Han, Y.-F.; Lin, Y.-J.; Weng, L.-H.; Berke, H.; Jin, G.-X., *Chem. Commun.* **2008**, 350-352.

162. Caskey, D. C.; Yamamoto, T.; Addicott, C.; Shoemaker, R. K.; Vacek, J.; Hawkridge, A. M.; Muddiman, D. C.; Kottas, G. S.; Michl, J.; Stang, P. J., *J. Am. Chem. Soc.* **2008**, *130*, 7620-7628.

163. Fujita, N.; Biradha, K.; Fujita, M.; Sakamoto, S.; Yamaguchi, K., *Angew. Chem. Int. Ed.* **2001**, *40*, 1718-1721.

164. Yamanoi, Y.; Sakamoto, Y.; Kusukawa, T.; Fujita, M.; Sakamoto, S.; Yamaguchi, K., *J. Am. Chem. Soc.* **2001**, *123*, 980-981.

165. Bar, A. K.; Chakrabarty, R.; Mostafa, G.; Mukherjee, P. S., *Angew. Chem. Int. Ed.* **2008**, *47*, 8455-8459.

166. Nitschke, J. R., *Acc. Chem. Res.* **2007**, *40*, 103-112.

167. Safont-Sempere, M. M.; Fernandez, G.; Wurthner, F., *Chem. Rev.* **2011**, *111*, 5784-5814.

168. Lehn, J.-M., *Chem. Soc. Rev.* **2007**, *36*, 151-160.

169. Ziegler, M.; Miranda, J. J.; Andersen, U. N.; Johnson, D. W.; Leary, J. A.; Raymond, K. N., *Angew. Chem. Int. Ed.* **2001**, *40*, 733-736.

170. Albrecht, M.; Janser, I.; Frohlich, R., *Chem. Commun.* **2005**, 157-165.

171. Severin, K., *Chem. Commun.* **2006**, 3859-3867.

172. Schmittel, M.; Ganz, A., *Chem. Commun.* **1997**, 999-1000.

173. Schmittel, M.; Ammon, H.; Kalsani, V.; Wiegrefe, A.; Michel, C., *Chem. Commun.* **2002**, 2566-2567.

174. Kalsani, V.; Ammon, H.; Jackel, F.; Rabe, J. P.; Schmittel, M., *Chem. Eur. J.* **2004**, *10*, 5481-5492.

175. Schmittel, M.; Kalsani, V.; Fenske, D.; Wiegrefe, A., *Chem. Commun.* **2004**, 490-491.

176. Kalsani, V.; Bodenstedt, H.; Fenske, D.; Schmittel, M., *Eur. J. Inorg. Chem.* **2005**, 1841-1849.

177. Kishore, R. S. K.; Paululat, T.; Schmittel, M., *Chem. Eur. J.* **2006**, *12*, 8136-8149.

178. Schmittel, M.; Ganz, A.; Fenske, D., *Org. Lett.* **2002**, *4*, 2289-2292.

179. Kishore, R. S. K.; Kalsani, V.; Schmittel, M., *Chem. Commun.* **2006**, 3690-3692.

180. Yoshizawa, M.; Nagao, M.; Kumazawa, K.; Fujita, M., *J. Organomet. Chem.* **2005**, *690*, 5383-5388.

181. Zhao, L.; Northrop, B. H.; Zheng, Y.-R.; Yang, H.-B.; Lee, H. J.; Lee, Y. M.; Park, J. Y.; Chi, K.-W.; Stang, P. J., *J. Org. Chem.* **2008**, *73*, 6580-6586.

182. Dolomanov, O. V.; Blake, A. J.; Champness, N. R.; Schroder, M.; Wilson, C., *Chem. Commun.* **2003**, 682-683.

183. Arena, G.; Bonomo, R. P.; Musumeci, S.; Purrello, R.; Rizzarelli, E.; Sammartano, S., *J. Chem. Soc., Dalton Trans.* **1983**, 1279-1283.

184. Hasenknopf, B.; Lehn, J. M.; Baum, G.; Fenske, D., *Proc. Natl. Acad. Sci.* **1996**, *93*, 1397-1400.

185. Smith, V. C. M.; Lehn, J.-M., *Chem. Commun.* **1996**, 2733-2734.

186. Collin, J.-P.; Dietrich-Buchecker, C.; Gavina, P.; Jimenez-Molero, M. C.; Sauvage, J.-P., *Acc. Chem. Res.* **2001**, *34*, 477-487.

187. Poleschak, I.; Kern, J.-M.; Sauvage, J.-P., *Chem. Commun.* **2004**, 474-476.

188. Periyasamy, G.; Collin, J.-P.; Sauvage, J.-P.; Levine, R. D.; Remacle, F., *Chem. Eur. J.* **2009**, *15*, 1310-1313.

189. Letinois-Halbes, U.; Hanss, D.; Beierle, J. M.; Collin, J.-P.; Sauvage, J.-P., *Org. Lett.* **2005**, *7*, 5753-5756.

190. Jimenez-Molero, M. C.; Dietrich-Buchecker, C.; Sauvage, J.-P., *Chem. Commun.* **2003**, 1613-1616.

191. Jimenez-Molero, M. C.; Dietrich-Buchecker, C.; Sauvage, J.-P., *Chem. Eur. J.* **2002**, *8*, 1456-1466.

192. Schmittel, M.; Kalsani, V.; Kishore, R. S. K.; Colfen, H.; Bats, J. W., *J. Am. Chem. Soc.* **2005**, *127*, 11544-11545.

193. Schmittel, M.; Kalsani, V.; Mal, P.; Bats, J. W., *Inorg. Chem.* **2006**, *45*, 6370-6377.

194. Schmittel, M.; Mal, P., *Chem. Commun.* **2008**, 960-962.

195. Schmittel, M.; He, B.; Mal, P., *Org. Lett.* **2008**, *10*, 2513-2516.

196. Schmittel, M.; He, B., *Chem. Commun.* **2008**, 4723-4725.

197. Schmittel, M.; Mahata, K., *Inorg. Chem.* **2009**, *48*, 822-824.

198. Garcia, A. M.; Bassani, D. M.; Lehn, J.-M.; Baum, G.; Fenske, D., *Chem. Eur. J.* **1999**, *5*, 1234-1238.

199. Ramirez, J.; Stadler, A.-M.; Rogez, G.; Drillon, M.; Lehn, J.-M., *Inorg. Chem.* **2009**, *48*, 2456-2463.

200. Chichak, K. S.; Cantrill, S. J.; Pease, A. R.; Chiu, S.-H.; Cave, G. W. V.; Atwood, J. L.; Stoddart, J. F., *Science* **2004**, *304*, 1308-1312.

201. Wang, J.-L.; Li, X.; Lu, X.; Hsieh, I. F.; Cao, Y.; Moorefield, C. N.; Wesdemiotis, C.; Cheng, S. Z. D.; Newkome, G. R., *J. Am. Chem. Soc.* **2011**, *133*, 11450-11453.

202. Lu, X.; Li, X.; Guo, K.; Xie, T.-Z.; Moorefield, C. N.; Wesdemiotis, C.; Newkome, G. R., *J. Am. Chem. Soc.* **2014**, *136*, 18149-18155.

203. Lu , X.; Li , X.; Guo, K.; Wang, J.; Huang, M.; Wang, J.-L.; Xie, T.-Z.; Moorefield, C. N.; Cheng, S. Z. D.; Wesdemiotis, C.; Newkome, G. R., *Chem. Eur. J.* **2014**, *20*, 13094-13098.

204. Lu, X.; Li, X.; Cao, Y.; Schultz, A.; Wang, J.-L.; Moorefield, C. N.; Wesdemiotis, C.; Cheng, S. Z. D.; Newkome, G. R., *Angew. Chem. Int. Ed.* **2013**, *52*, 7728-7731.

205. Lu, X.; Li, X.; Wang, J.-L.; Moorefield, C. N.; Wesdemiotis, C.; Newkome, G. R., *Chem. Commun.* **2012**, *48*, 9873-9875.

206. Yusupov, M. M.; Yusupova, G. Z.; Baucom, A.; Lieberman, K.; Earnest, T. N.; Cate, J. H. D.; Noller, H. F., *Science* **2001**, *292*, 883-896.

207. Korostelev, A.; Trakhanov, S.; Laurberg, M.; Noller, H. F., *Cell* **2006**, *126*, 1065-1077.

208. Zhao, Y.-L.; Stoddart, J. F., *Acc. Chem. Res.* **2009**, *42*, 1161-1171.

209. Schenning, A. P. H. J.; Meijer, E. W., *Chem. Commun.* **2005**, 3245-3258.

210. Newkome, G. R.; Moorefield, C. N., *Chem. Soc. Rev.* **2015**, *44*, 3954-3967.

211. Lledo, A.; Kamioka, S.; Sather, A. C.; Rebek, J. Jr., *Angew. Chem. Int. Ed.* **2011**, *50*, 1299-1301.

212. Camerel, F.; Donnio, B.; Bourgogne, C.; Schmutz, M.; Guillon, D.; Davidson, P.; Ziessel, R., *Chem. Eur. J.* **2006**, *12*, 4261-4274.

213. Constable, E. C.; Housecroft, C. E.; Neuburger, M.; Schaffner, S.; Scherer, L. J., *Dalton Trans.* **2004**, 2635.

214. Winter, A.; Hoeppener, S.; Newkome, G. R.; Schubert, U. S., *Adv. Mater.* **2011**, *23*, 3484-3498.

215. Schneider, H.-J., *Angew. Chem. Int. Ed.* **2009**, *48*, 3924-3977.

216. Angurell, I.; Ferrer, M.; Gutierrez, A.; Martinez, M.; Rodriguez, L.; Rossell, O.; Engeser, M., *Chem. Eur. J.* **2010**, *16*, 13960-13964.

217. Saha, M. L.; Pramanik, S.; Schmittel, M., *Chem. Commun.* **2012**, *48*, 9459-9461.

218. Zheng, Y.-R.; Zhao, Z.; Wang, M.; Ghosh, K.; Pollock, J. B.; Cook, T. R.; Stang, P. J., *J. Am. Chem. Soc.* **2010,** *132*, 16873-16882.

219. Schultz, A.; Li, X.; Moorefield, C. N.; Wesdemiotis, C.; Newkome, G. R., *Eur. J. Inorg. Chem.* **2013**, 2492-2497.

220. Schultz, A.; Cao, Y.; Huang, M.; Cheng, S. Z. D.; Li, X.; Moorefield, C. N.; Wesdemiotis, C.; Newkome, G. R., *Dalton Trans.* **2012**, *41*, 11573-11575.

221. Steiner, R. F.; Kirby, E. P., *J. Phys. Chem.* **1969**, *73*, 4130-4135.

222. Siebert, R.; Tian, Y.; Camacho, R.; Winter, A.; Wild, A.; Krieg, A.; Schubert, U. S.; Popp, J.; Scheblykin, I. G.; Dietzek, B., *J. Mater. Chem.* **2012**, *22*, 16041-16050.

223. Lehn, J.-M., *Supramolecular Chemistry*. Wiley: **1995**.

224. Yang, H.-B.; Northrop, B. H.; Zheng, Y.-R.; Ghosh, K.; Stang, P. J., *J. Org. Chem.* **2009**, *74*, 7067-7074.

225. Mahata, K.; Saha, M. L.; Schmittel, M., *J. Am. Chem. Soc.* **2010**, *132*, 15933-15935.

226. Hoogenboom, R.; Fournier, D.; Schubert, U. S., *Chem. Commun.* **2008**, 155-162.

227. Hwang, S.-H.; Wang, P.; Moorefield, C. N.; Godinez, L. A.; Manriquez, J.; Bustos, E.; Newkome, G. R., *Chem. Commun.* **2005**, 4672-4674.

228. Zhao, L.; Ghosh, K.; Zheng, Y.-R.; Stang, P. J., *J. Org. Chem.* **2009**, *74*, 8516-8521.

229. Li, Y.; Jiang, Z.; Yuan, J.; Liu, D.; Wu, T.; Moorefield, C. N.; Newkome, G. R.; Wang, P., *Chem. Commun.* **2015**, *51*, 5766-5769.

230. Mandelbrot, B. B., *The Fractal Geometry of Nature*, Freeman, San Franscisco, CA, **1982**.

231. Richardson, L. F., *Proc. R. Soc. London. Ser. A*, **1926**, *110*, 709-737.

232. Sierpiński, W., *C. R. Hebd. Seances Acad. Sci.* **1915**, *160*, 302-305.

233. Fraenkel, A.; Kontorovich, A.; *Proc. Integers Conference* **2007**, 209-227.

234. Browein, J. M.; Bailey, J. H.; *Mathematics by Experiment: Plausible Reasoning in the 21st Century*, A. K. Peters, Ltd, Welsley, MA, **2003**.

235. Newkome, G. R.; Yao, Z.; Baker, G. R.; Gupta, V. K., *J. Org. Chem.* **1985**, *50*, 2003-2004.

236. Newkome, G. R.; Shreiner, C., *Chem. Rev.* **2010**, *110*, 6338-6442.

237. Astruc, D.; Boisselier, E.; Ornelas, C., *Chem. Rev.* **2010**, *110*, 1857-1959.

238. Matsumoto, K.; Kannami, M.; Inokuchi, D.; Kurata, H.; Kawase, T.; Oda, M., *Org. Lett.* **2007**, *9*, 2903-2906.

239. Figure 4.1 derived from: Peitgen, H.-O.; Jurgens, H.; Saupe, D.; *Chaos and Fractals, New Frontiers of Science*, Springer, New York, **1992**.

240. Peitgen, H.-O.; personal assistance, **2011**.

241. Constable, E. C.; Hermann, B. A.; Housecroft, C. E.; Neuburger, M.; Schaffner, S.; Scherer, L. J., *New J. Chem.* **2005**, *29*, 1475-1481.

242. Stepanenko, V.; Würthner, F., *Small* **2008**, *4*, 2158-2161.

243. Perera, S.; Li, X.; Soler, M.; Schultz, A.; Wesdemiotis, C.; Moorefield, C. N.; Newkome, G. R., *Angew. Chem. Int. Ed.* **2010**, *49*, 6539-6544.

244. Chan, Y.-T.; Li, S.; Moorefield, C. N.; Wang, P.; Shreiner, C. D.; Newkome, G. R., *Chem. Eur. J.* **2010**, *16*, 4164-4168.

245. Schubert, U. S.; Winter, A.; Newkome, G. R., *Terpyridine-based Materials: For Catalytic, Optoelectronic and Life Science Applications*. Wiley-VCH, Weinheim, **2011**.

246. Chan, Y.-T.; Li, X.; Soler, M.; Wang, J.-L.; Wesdemiotis, C.; Newkome, G. R., *J. Am. Chem. Soc.* **2009**, *131*, 16395-16397.

247. Andres, P. R.; Schubert, U. S., *Macromol. Rapid Commun.* **2004**, *25*, 1371-1375.

248. Constable, E. C.; Harris, K.; Housecroft, C. E.; Neuburger, M., *Dalton Trans.* **2011**, *40*, 1524.

249. Cardenas, D. J.; Sauvage, J.-P., *Inorg. Chem.* **1997**, *36*, 2777-2783.

250. Jarosz, P.; Lotito, K.; Schneider, J.; Kumaresan, D.; Schmehl, R.; Eisenberg, R., *Inorg. Chem.* **2009**, *48*, 2420-2428.

251. Alessio, E., *Chem. Rev.* **2004,** *104*, 4203-4242.

APPENDICES

APPENDIX A

PUBLICATIONS

1. "***Preparation of Different Dendritic-layered Silicate Nanocomposites***." – Amin, A.; Sarkar, R.; Moorefield, C. N.; Newkome, G. R. *Polym. Eng. Science* **2013**, *53*, 2166-2174.

2. "***Synthesis of Polymer-Clay Nanocomposites of some Vinyl Monomers by Surface-initiated Atom Transfer Radical Polymerization***."- Amin, A., Sarkar, R.; Moorefield, C. N.; Newkome, G. R. *Designed Monomers and Polymers* **2013**, *16*, 528-536.

3. "***One-Step Multicomponent Self-Assembly of a First-Generation Sierpiński Triangle: From Fractal Design to Chemical Reality***." – Sarkar, R.; Guo, K.; Moorefield, C. N.; Wesdemiotis, C.; Newkome, G. R. *Angew. Chem. Int. Ed.* **2014**, *53*, 12182-12185.

4. "***Multicomponent Reassembly of Terpyridine-based Materials: Quantitative Metallomacrocyclic Rearrangement***." – Sarkar, R.; Guo, Z.; Burai, T.N.; Moorefield, C. N.; Wesdemiotis, C.; Newkome, G. R. *Chem. Commun.* **2015**, *51*, 12851-12854.

5. "***Step-Wise Construction of Bimetallic Triangles: Site-specific Metallation of Terpyridine Building-blocks***." – Sarkar, R.; Guo, Z.; Moorefield, C. N.; Wesdemiotis, C.; Newkome, G.R. (manuscript in preparation).

6. "***Towards Molecular Construction Platforms: Synthesis of a Metallotricyclic Spirane Based on Bis(2,2':6',2''-Terpyridine)Ru^{II} Connectivity***."- Xie, T.-Z.; Guo, K.; Huang, M.; Lu, X.; Sarkar, R.; Moorefield, C. N.; Cheng, S.Z.D.; Newkome, G. R. *Chem. Eur. J.* **2014**, *36*, 11291-11294.

7. "***A Rigid Metallohexameric Macrocycle Composed of Endo-a nd Exo-cyclic Bis-terpyridine Metal Complex***."- Li, S.; Moorefield, C. N.; Shreiner, C. D.; Wang, P.-S.; Sarkar, R.; Newkome, G. R. *New J. Chem.* **2011**, *35*, 2130-2135.

APPENDIX B

SUPPORTING NMR SPECTRA

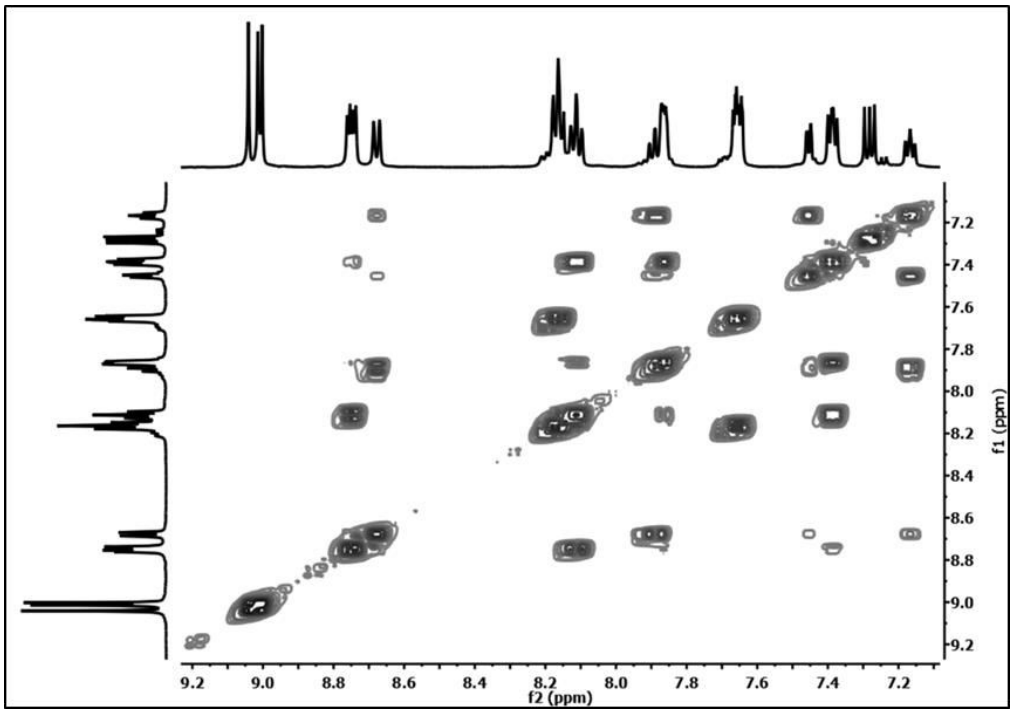

Figure A1: 2D-COSY spectrum of bimetallic triangle **233**.

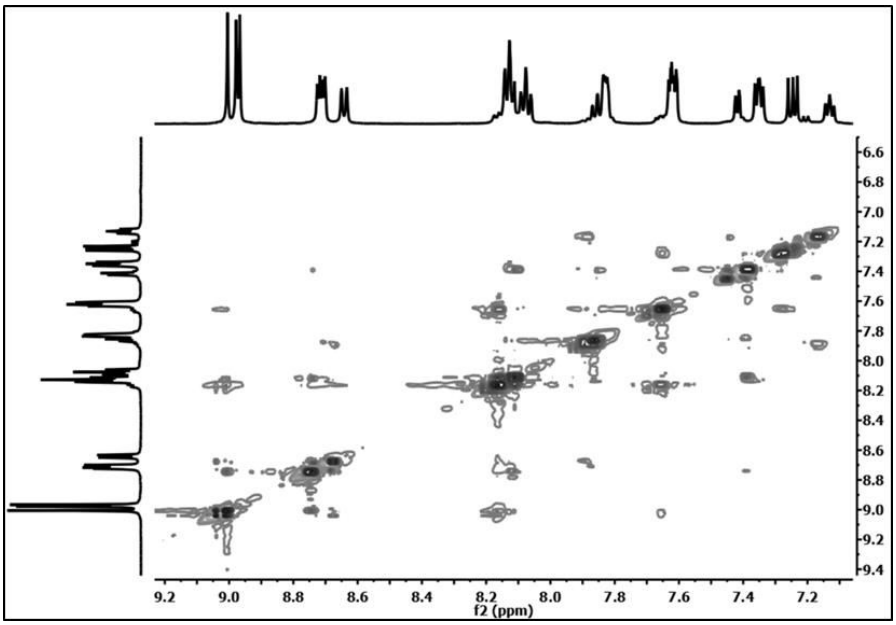

Figure A2: 2D-NOESY spectrum of bimetallic triangle **233**.

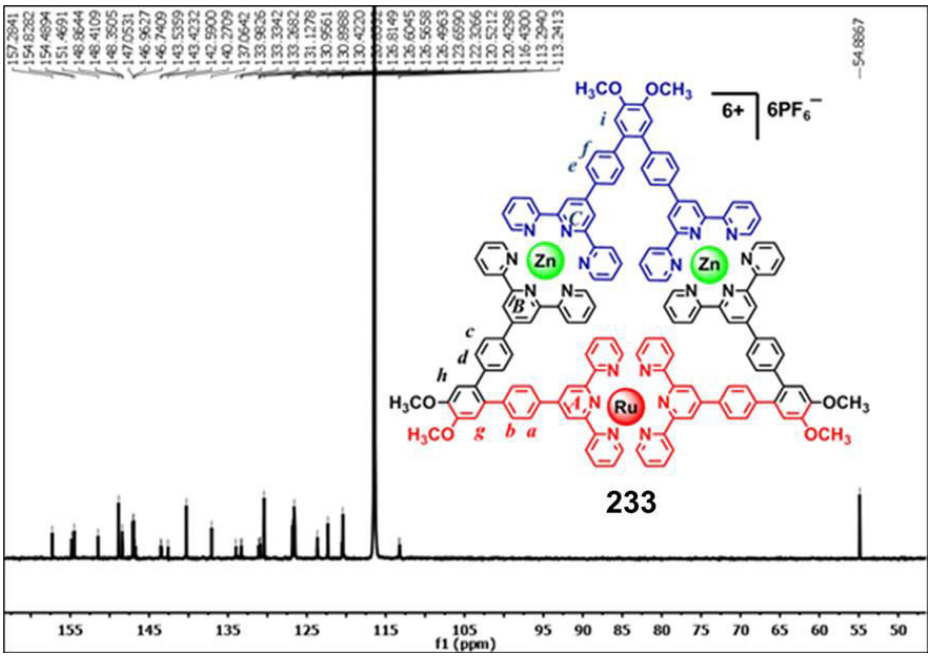

Figure A3: ^{13}C NMR spectrum of isosceles triangle **233**.

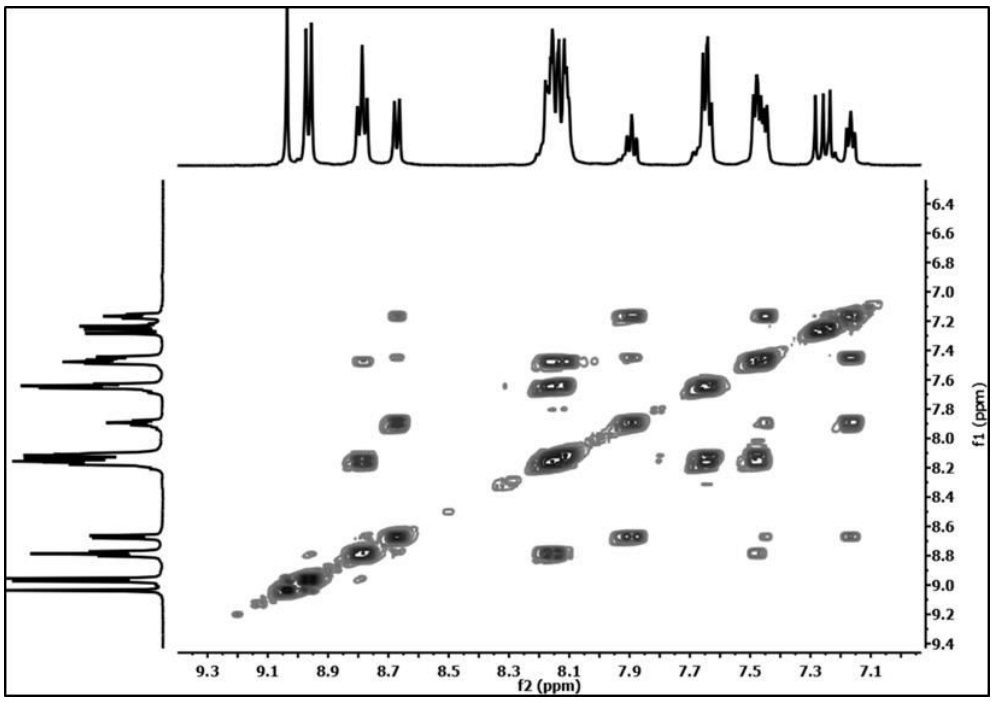

Figure A4: 2D-COSY spectrum of bimetallic triangle **234**.

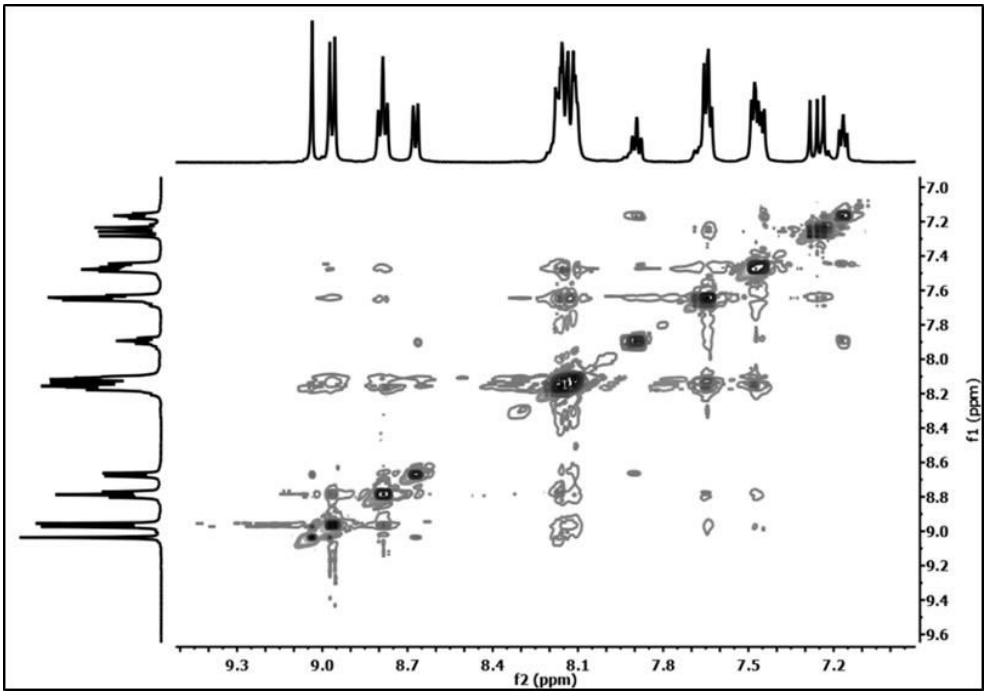

Figure A5: 2D-NOESY spectrum of bimetallic triangle **234**.

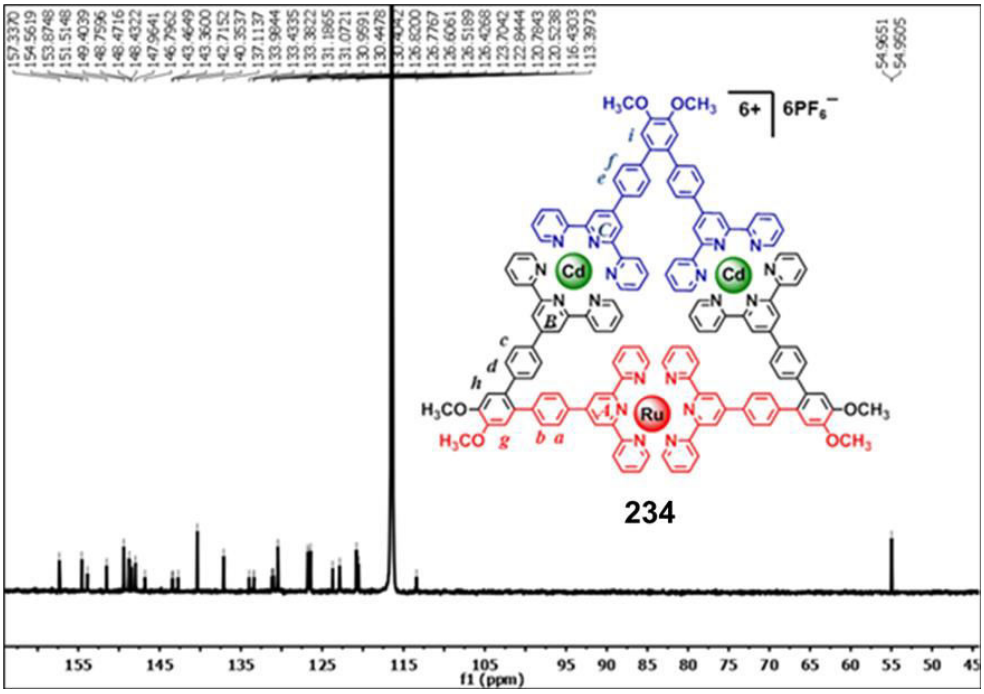

Figure A6: ^{13}C NMR spectrum of isosceles triangle **234**.

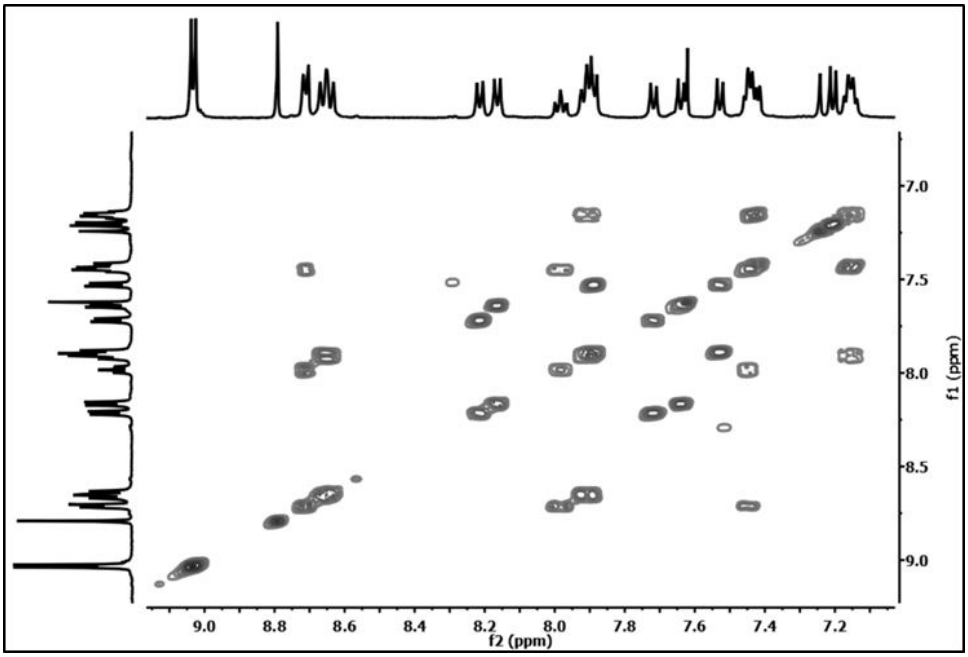

Figure A7: 2D-COSY spectrum of trimer **235**.

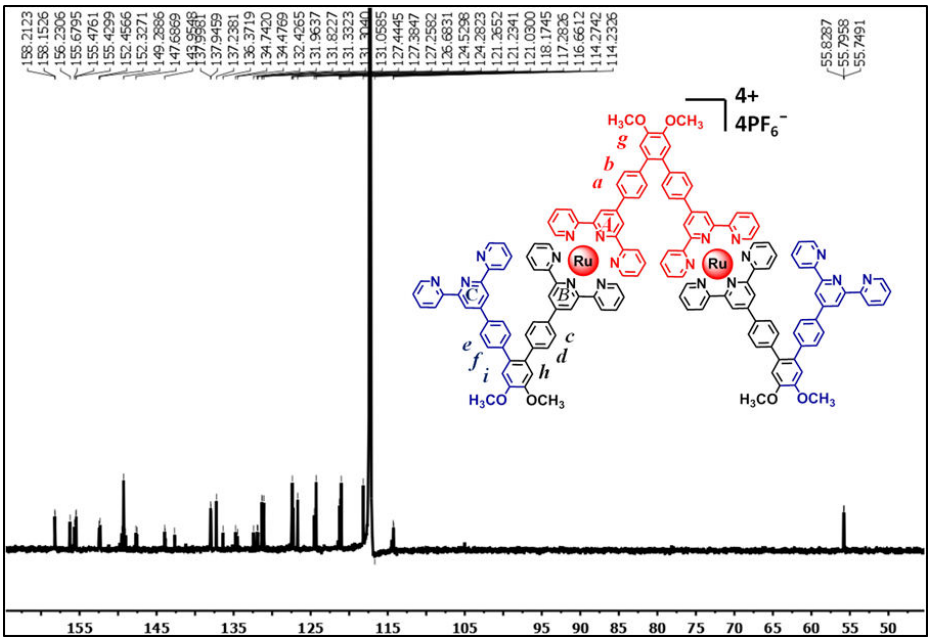

Figure A8: ^{13}C NMR spectrum of trimer **235**.

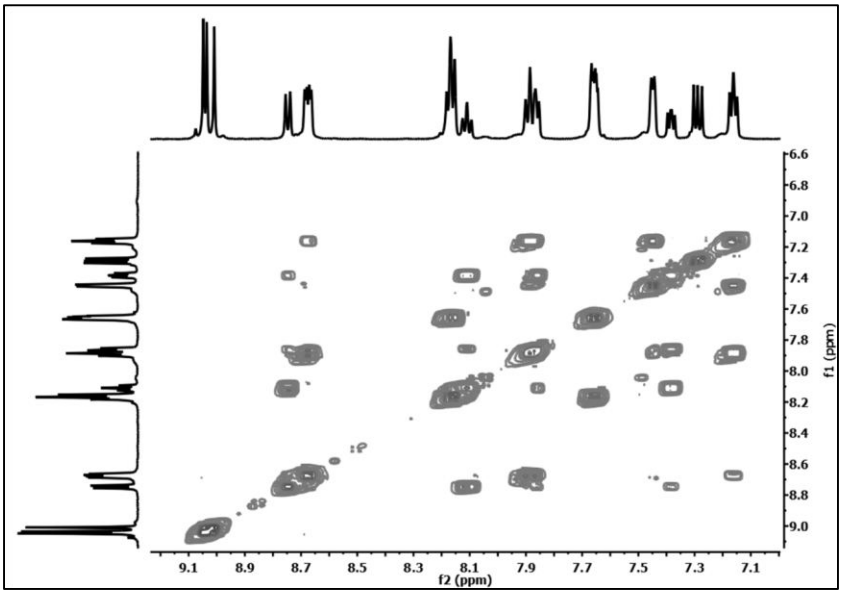

Figure A9: 2D-COSY spectrum of bimetallic triangle **236**.

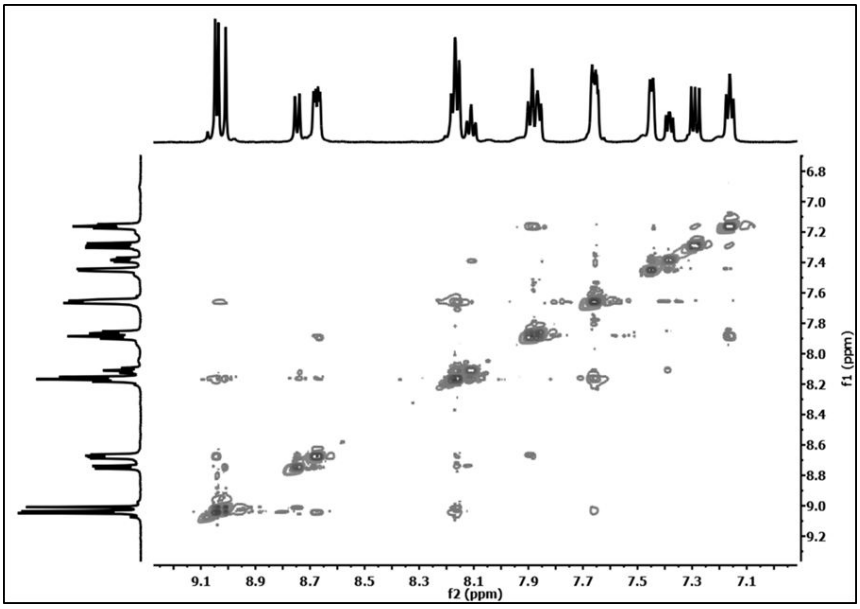

Figure A10: 2D-NOESY spectrum of bimetallic triangle **236**.

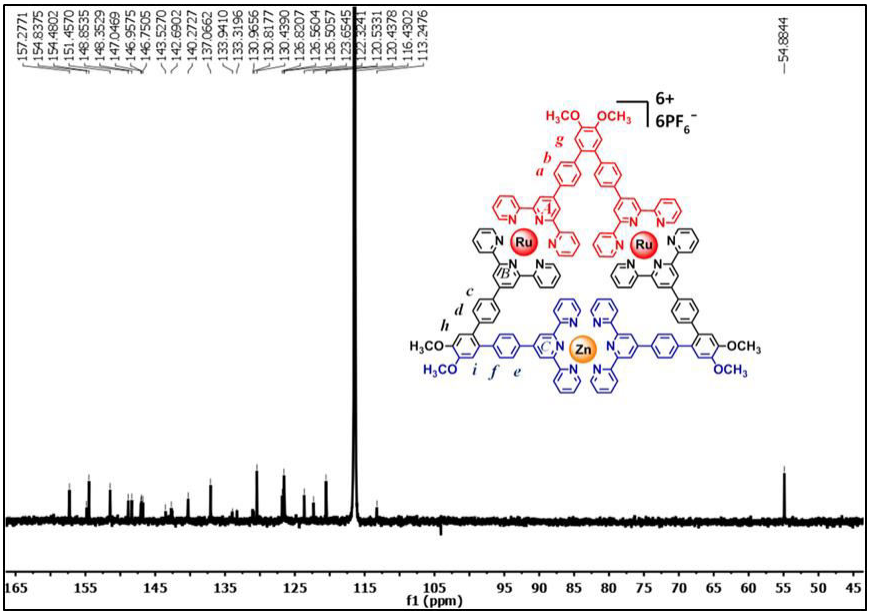

Figure A11: ^{13}C NMR spectrum of bimetallic triangle **236**.

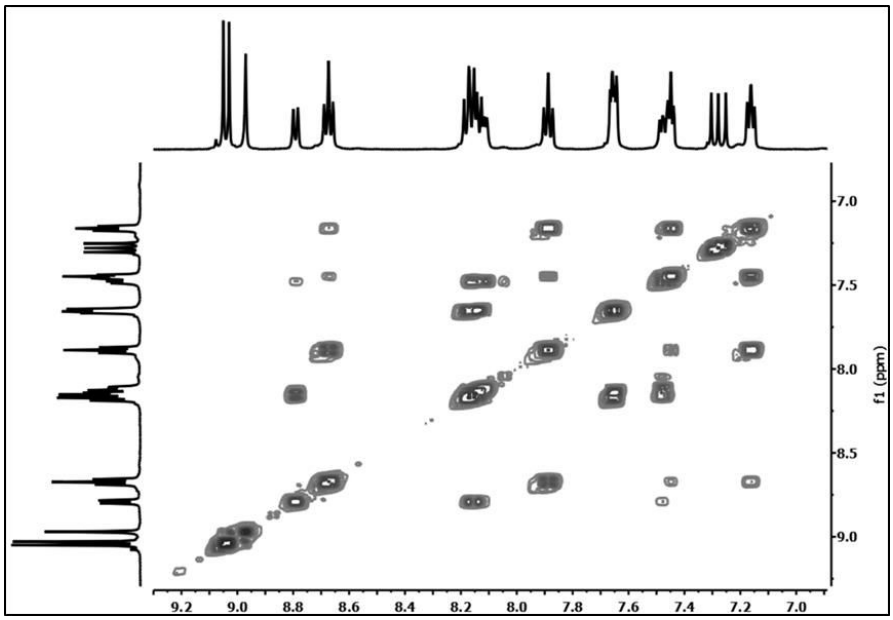

Figure A12: 2D-COSY spectrum of bimetallic triangle **237**.

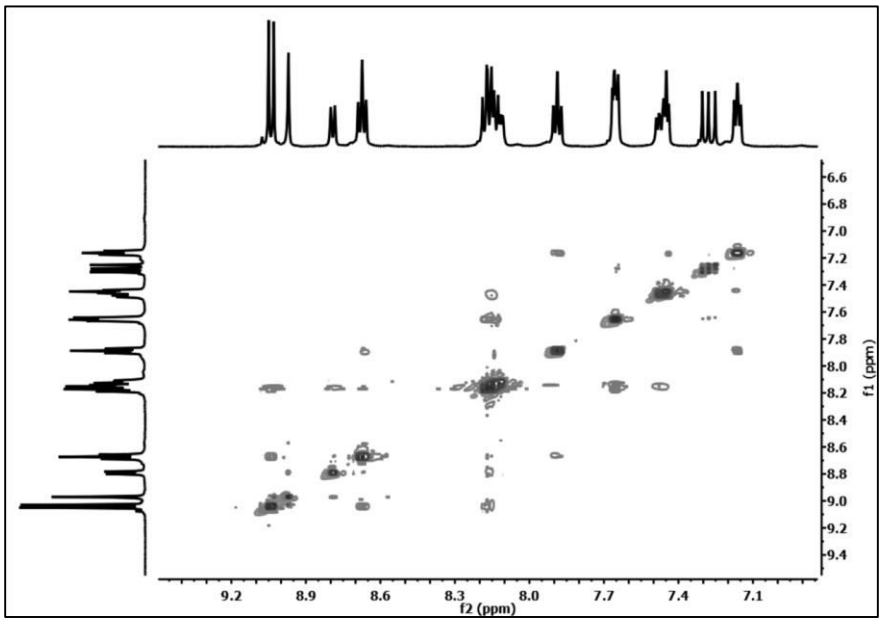

Figure A13: 2D-NOESY spectrum of bimetallic triangle **237**.

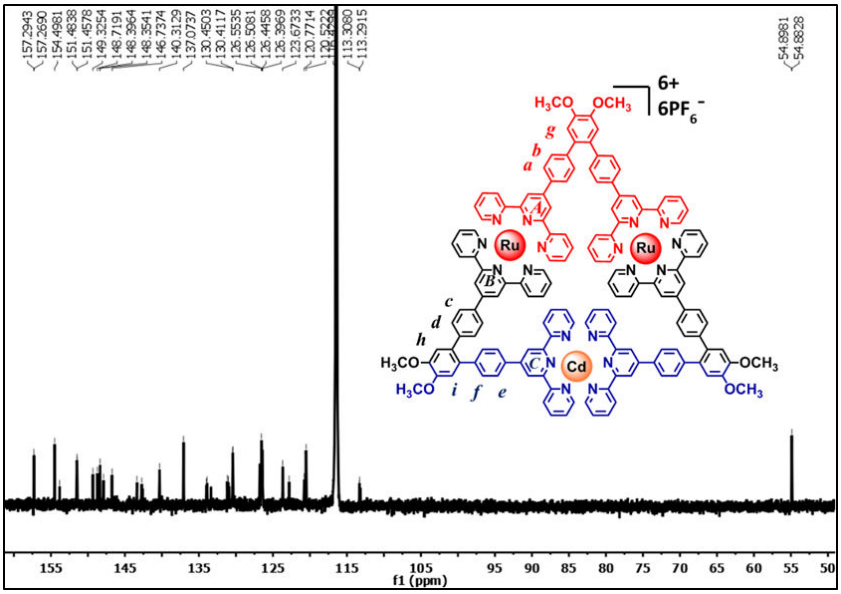

Figure A14: ^{13}C NMR spectrum of bimetallic triangle **238**.

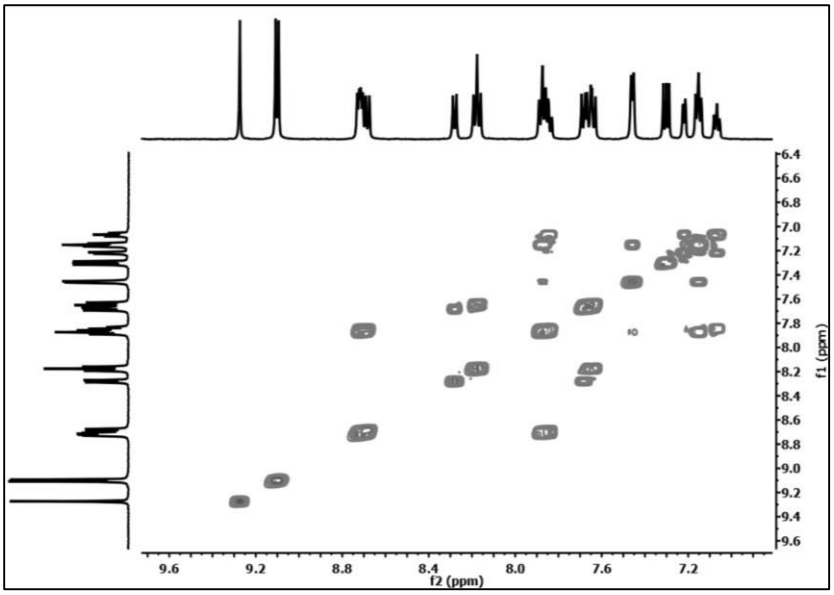

Figure A15: 2D-COSY spectrum of bimetallic triangle **238**.

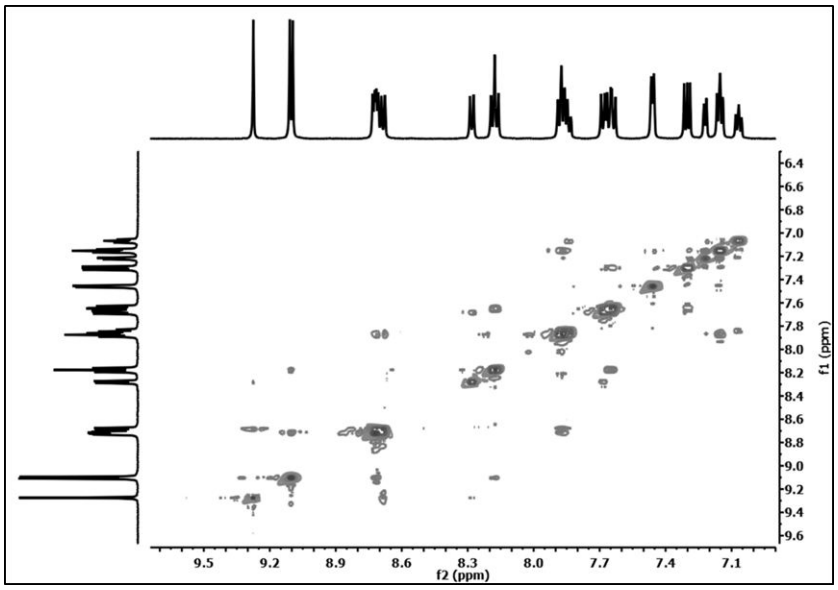

Figure A16: 2D-NOESY spectrum of bimetallic triangle **238**.

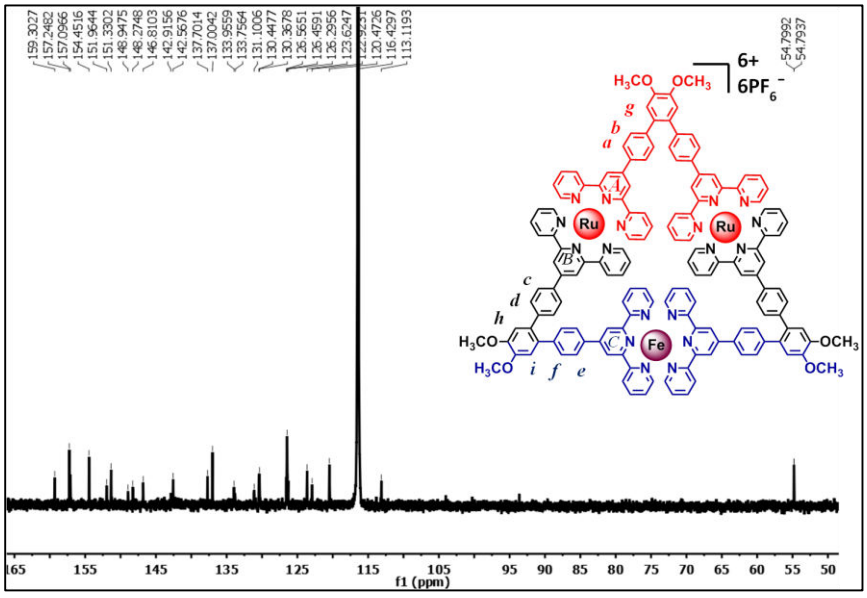

Figure A17: ^{13}C NMR spectrum of bimetallic triangle **238**.

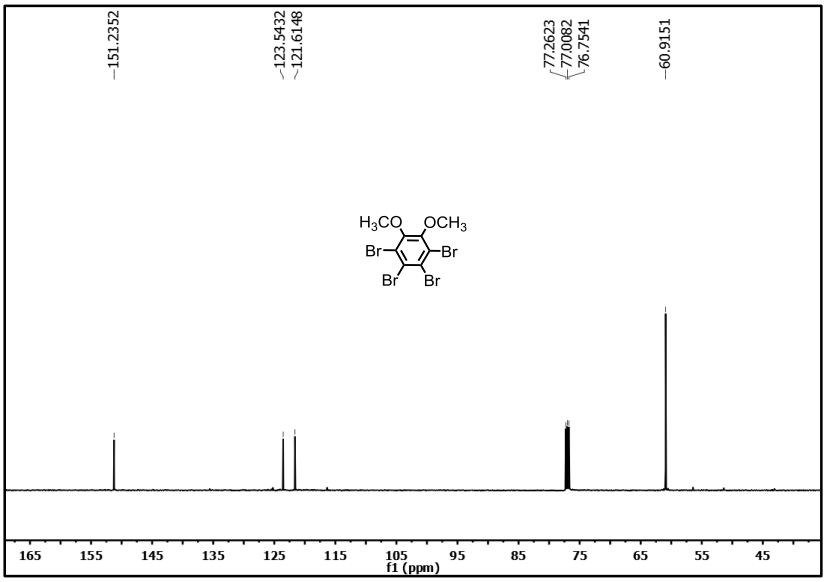

Figure A18: ^{13}C NMR spectrum of 2,3,5,6-Tetrabromoveratrole **240**.

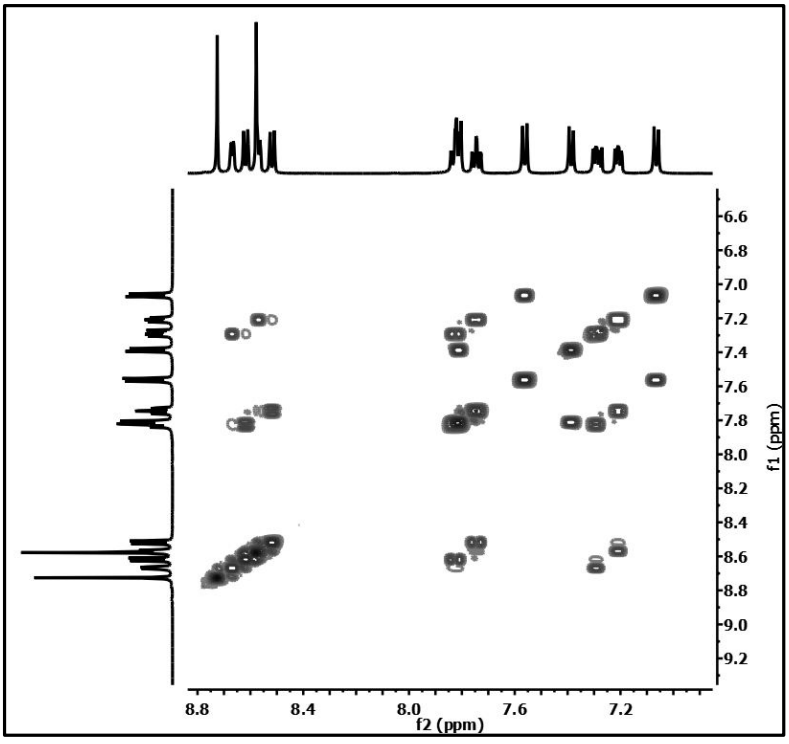

Figure A19: 2D-COSY spectrum of ligand **241**.

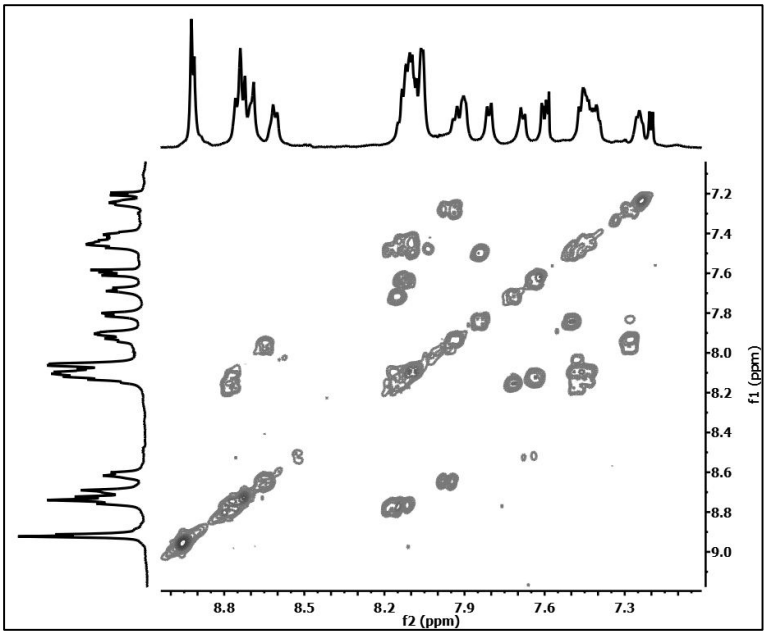

Figure A20: 2D-COSY spectrum of Sierpiński triangle **242**.

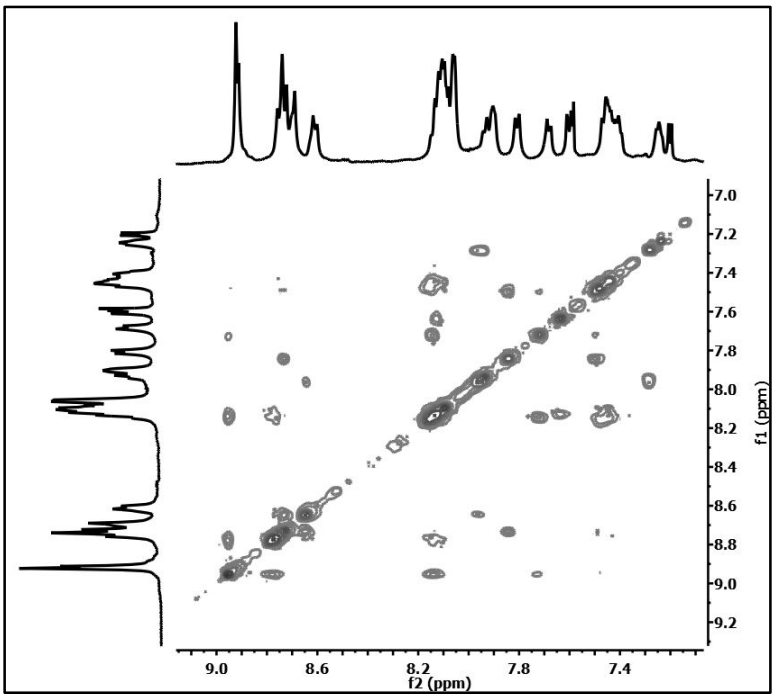

Figure A21: 2D-NOESY spectrum of Sierpiński triangle **242**.